

ECOLE NORMALE SUPÉRIEURE DE LYON
LABORATOIRE DE PHYSIQUE

THÈSE

Présentée par

MAÏTÉ DUPUIS

Pour obtenir le grade de

DOCTEUR DE L'ECOLE NORMALE SUPÉRIEURE DE LYON

Ecole doctorale : Physique et Astrophysique de Lyon

SPIN FOAM MODELS FOR QUANTUM GRAVITY AND SEMI-CLASSICAL LIMIT

Modèles de mousses de spin pour la gravité quantique et leur régime
semi-classique

Soutenue le 16 décembre 2010, devant la commission d'examen composée de

Mr John BARRETT	Membre
Mr Laurent FREIDEL	Membre/Rapporteur
Mr Etera LIVINE	Membre
Mr Jean-Michel MAILLET	Membre
Mr Alejandro PEREZ	Membre/Rapporteur

Remerciements

Merci tout d'abord à Etera, mon directeur de thèse qui m'a fait découvrir le monde de la recherche et la gravité quantique!

Merci à tous les membres du laboratoire de physique de l'ENS (je pense en particulier à mes différents co-bureaux!) qui m'ont si gentilement accueillie puis supportée pendant ces trois années!

Merci aussi à tous les chercheurs qui forment la (encore petite mais si dynamique, jeune et sympathique) communauté de la gravité quantique à boucles! Et un merci particulier à tous ceux qui m'ont invitée dans leur groupe et qui se sont tous montrés très ouverts à la discussion et à la collaboration: Florian à Sydney; Carlo, Alejandro et Simone à Marseille; Thomas à Erlangen; Laurent et Lee à Waterloo; Bianca et Daniele à Berlin; Renate à Utrecht.

Merci aussi à mes deux rapporteurs, Alejandro et Laurent, pour leur lecture attentive de cette thèse, ainsi qu'aux autres membres du jury de ma soutenance, Etera, Jean-Michel et John pour leur intérêt à mon travail. Un merci spécial à André qui a une importance toute spéciale pour moi et qui a pris le temps de relire cette thèse.

Et bien sûr un grand merci à tous ceux qui m'ont entouré pendant ces trois années! Flo pour son soutien quotidien! Ma famille: mes parents, mon frère Xavier et ma soeur Margot ainsi que tous mes super oncles, tantes, cousins, cousines et grands-parents! Mes amis: ceux de Besançon qui me connaissent depuis si longtemps, les amis rencontrés en prépa, les amis de l'ENS, les amis de l'athlétisme ainsi que mes différents entraîneurs.... Je ne donne pas vos noms mais merci à vous tous pour tous les moments partagés ensemble qui ont été si importants!

Résumé

MODÈLES DE MOUSSES DE SPIN POUR LA GRAVITÉ QUANTIQUE ET LEUR RÉGIME SEMI-CLASSIQUE

Les mousses de spin fournissent un formalisme d'intégrale de chemin pour la gravité quantique qui s'inspire de la gravité quantique à boucles. Ils décrivent la structure quantique de l'espace-temps et l'évolution temporelle des états cinématiques de la gravité quantique à boucles. La quantification covariante en terme de mousses de spin est basée sur l'écriture de la relativité générale comme une théorie topologique contrainte.

Les contraintes, appelées contraintes de simplicité, introduisent les degrés de libertés locaux et permettent de passer d'une théorie topologique à une théorie de la géométrie de l'espace-temps. Elles sont donc essentielles. Cependant leur implémentation est encore mal comprise. Dans cette thèse, une manière originale d'imposer les contraintes est proposée: les contraintes de simplicités sont reformulées en utilisant un nouveau formalisme construit à partir d'oscillateurs harmoniques et des états cohérents, solutions des contraintes, sont donnés.

D'autre part, un modèle de mousse de spin pour la gravité quantique est cohérent s'il peut être relié à l'approche canonique à boucles et possède la bonne limite semi-classique.

Un lien entre les états cinématiques de la gravité quantique à boucles et les états frontières d'une mousse de spin est ici explicité reliant ainsi clairement l'approche canonique et l'approche covariante.

Nous proposons aussi de nouvelles techniques pour calculer le développement asymptotique semi-classique des amplitudes de transition de la gravité quantique. En particulier dans le contexte de la gravité 3d, des outils analytiques nécessaires pour calculer toutes les corrections quantiques des corrélations du champs gravitationnel sont présentés. Des calculs explicites, basés sur des méthodes d'approximation et sur l'utilisation de relations de récurrence sur les amplitudes de mousses de spins, ont été effectués. Les résultats sont pertinents pour dériver des corrections quantiques à la dynamique du champ gravitationnel.

Mots clé : relativité générale, théorie des champs topologique, gravité quantique, mousses de spin, réseaux de spins.

SPIN FOAM MODELS FOR QUANTUM GRAVITY AND SEMI-CLASSICAL LIMIT

The spinfoam framework is a proposal for a regularized path integral for quantum gravity. Spinfoams define quantum space-time structures describing the evolution in time of the spin network states for quantum geometry derived from Loop Quantum Gravity (LQG). The construction of this covariant approach is based on the formulation of General Relativity as a topological theory plus the so-called simplicity constraints which introduce local degrees of freedom.

The simplicity constraints are essential in turning the non-physical topological theory into 4d gravity. In this PhD manuscript, an original way to impose the simplicity constraints in 4d Euclidean gravity using harmonic oscillators is proposed and new coherent states, solutions of the constraints, are given.

A consistent spinfoam model for quantum gravity has to be connected to LQG and must have the right semi-classical limit.

An explicit map between the spin network states of LQG and the boundary states of spinfoam models is given connecting the canonical and the covariant approaches.

New techniques to compute semiclassical asymptotic expressions for the transition amplitudes of 3d quantum gravity and to extract semi-classical information from a spinfoam model are introduced. Explicit computations based on approximation methods and on the use of recurrence relations on spinfoam amplitudes have been performed. The results are relevant to derive quantum corrections to the dynamics of the gravitational field.

Keywords: general relativity, topological field theory, quantum gravity, spin networks, spin foams.

Contents

1	Introduction	11
I	From Loop Quantum Gravity to Spin foam models	17
2	Motivations for a quantum theory of gravity	19
3	Hamiltonian formalism of General Relativity	21
3.1	Canonical formulation of General Relativity in ADM variables	21
3.2	Loop quantum gravity variables	26
3.3	Classical framework for a "covariant" loop quantum gravity theory	30
4	Loop Quantum Gravity	33
4.1	The kinematical Hilbert space and cylindrical functions	33
4.2	Gauge-invariant Hilbert space and spin networks	35
4.3	Loop quantum gravity and dynamics	39
4.3.1	Solutions of the diffeomorphism constraint: abstract spin networks	39
4.3.2	The Hamiltonian constraint	40
5	Covariant Loop Quantum Gravity	43
5.1	Cylindrical Functions and Gauge Invariance	43
5.2	The Basis of Projected Spin Networks	45
6	Feynman's path integral approach: Spin Foams	47
6.1	Three-dimensional gravity, the Ponzano-Regge model	50
6.2	Reformulating 4d gravity as a BF theory: Plebanski's action	54
6.3	The spin foam framework	56
6.3.1	Spin foam quantization of the 4d BF theory	57
6.3.2	Some ambiguities in the 4d gravity spin foam quantization procedure	58
II	Spin foam models for 4d gravity	63
7	Simplicity constraints and the Barrett-Crane model	67
7.1	The Euclidean Barrett-Crane model	67
7.2	The Lorentzian Barrett-Crane model	70
8	Simplicity constraints and the EPRL-FK models	73
8.1	A quantization à la Gupta-Bleuler	73
8.1.1	The Euclidean case with a finite Immirzi parameter	77
8.1.2	The Lorentzian, with a finite Immirzi parameter	78
8.2	Using coherent states	79

8.2.1	The $SU(2)$ coherent intertwiners	80
8.2.2	Intertwiner states as weak solutions of the simplicity constraints	80
9	Simplicity constraints and $SU(2)$ spin networks	83
9.1	Back and forth between projected and $SU(2)$ spin networks	83
9.1.1	Projecting down to $SU(2)$ spin networks	83
9.1.2	Lifting back Spin Networks	84
9.2	Simplicity Constraints and the Immirzi Parameter	86
9.2.1	Weak Constraints	86
9.2.2	Strong Constraints	88
9.2.3	Comparing $SU(2)$ and $SL(2, \mathbb{C})$ Scalar Products	88
10	Simplicity constraints and the $U(N)$ framework	91
10.1	$SU(2)$ intertwiners and the $U(N)$ framework	92
10.2	Coherent states and the $U(N)$ framework	95
10.2.1	Revisiting the $SU(2)$ Coherent Intertwiners	95
10.2.2	The $U(N)$ coherent states	97
10.2.3	Relaxing the Closure Conditions	99
10.2.4	The F -action on Coherent Intertwiners	100
10.2.5	Operator Algebra on Coherent Intertwiners	100
10.3	The $U(N)$ setting for $Spin(4)$ intertwiner and a Gupta-Bleuler quantization	103
10.3.1	The Closed Algebra of Simplicity Constraints	104
10.3.2	Highest weight vectors for the $\mathfrak{u}(N)$ -simplicity constraints	105
10.3.3	Using $F^L - F^R$ Constraints	106
10.3.4	Using $F^L - (F^R)^\dagger$ Constraints	107
10.3.5	Including the Immirzi Parameter?	108
10.4	Weakening the constraints and using the $U(N)$ coherent states	109
10.4.1	Back to $SU(2)$ coherent intertwiners	109
10.4.2	The final proposal: using $U(N)$ coherent states	110
III	Spinfoam models and the semi-classical limit	115
11	The graviton propagator	119
12	The asymptotic expansion in 3d	121
12.1	The canonical framework for 3d correlation in gravity/ The boundary states and the kernel for 3d correlation in gravity	121
12.2	How to study the $\{6j\}$ -symbol?	123
13	Group integral techniques and the asymptotic expansion of the $\{6j\}$	125
13.1	The $\{6j\}$ -symbol and the Racah's single sum formula	125
13.2	Perturbative expansion of the $6j$ -symbol	126
13.2.1	General procedure	126
13.2.2	Contributions of the stationary points	129
13.3	Some particular cases	133
13.3.1	The equilateral tetrahedron	133
13.3.2	The isosceles tetrahedron	133

14 Recursion relations and the asymptotic expansion of the $\{6j\}$	137
14.1 Exact and Approximate Recursion Relation for the Isosceles Tetrahedron	137
14.2 Pushing to the Next-to-Leading Order	138
14.3 Consequences of the unitary property of the $\{6j\}$ -symbol	143
14.4 “Ward-Takahashi identities” for the spinfoam graviton propagator	144
14.4.1 Relating Observables	145
14.4.2 Rescaling the Tetrahedron	146
15 Physical boundary state for the quantum 4-simplex	147
15.1 Semi-Classical States: the Decoupled Gaussian Ansatz	148
15.2 The Coupled Gaussian Ansatz	153
16 Conclusion	157
A Quick Overview of $SL(2, \mathbb{C})$ Representations	163
B Coherent States for the Harmonic Oscillator	165
C Commutation Relations Of the E, F, F^\dagger Action on Coherent States	167
D Norm of the $U(N)$-invariant state: $J\rangle$	169
E The $\{6j\}$-symbol - recoupling theory	171
F Factorials	173
G First approximation in the ”brute force” asymptotic expansion of the $\{6j\}$	175
H Third approximation in the ”brute force” asymptotic expansion of the $\{6j\}$	179
I Physical States with a Real Phase	181

Chapter 1

Introduction

One of the deepest questions for physicists is to unravel the essential nature of space and time and how the world came into existence. This quest on the meaning of space and time has a very long history which teaches us that an answer to a question can radically change our view of the world. Although a new theory on the nature of space and time can be the end of a journey, it is often the starting point for more questions. A new theory brings us new frameworks and new technical tools which open new frontiers and enlarge our perception. It improves our understanding of the notions of space and time and gives us access to more and more refined scales of observations. The historical evolution of space-time theories from the Aristotelician world, the Newton's views to Einstein's breakthrough, emphasizes that a final description of our physical world is far from being done.

Three dimensional constants play a fundamental role in the description of our physical world: the speed of light in vacuum¹ $c \sim 3 \times 10^9 m.s^{-1}$, Planck's constant $h \sim 6.6 \times 10^{-34} m^2.kg.s^{-1}$, the Newton universal gravitational constant² $G \sim 6.7 \times 10^{-34} m^3.kg^{-1}.s^{-1}$. Their order of magnitude is much larger (or smaller) than the meter, kilogram and second, which are the units (from the International System of Units) significant to describe direct everyday life experiments. Each of these three constants is associated to a physical regime and corresponds to a particular scale of observation. They are specific to some theories and the links between each constant and the different theories are summarized in Fig. 1.1.

Let us present some of the theories appearing in Fig. 1.1. In the general relativity theory, Einstein makes the revolutionary claim that the geometry of space is not fixed but evolves in time. Quantum mechanics tells us that every dynamical quantity is not continuum but quantized. The size of a "quantum" is characterized by Planck's constant h . At the end of the first half of the twentieth century, Freeman Dyson, Richard Feynman among many others consistently combined quantum theory with special relativity to give the so-called quantum field theory in which both constants, h and c appear. A very useful and experimental successful example of a quantum field theory fixed Minkowski background is the standard model. It describes three of the four fundamental interactions which govern the myriad of phenomena in nature: electromagnetism, the strong nuclear force which holds atomic nuclei together and the weak nuclear force which is responsible for radioactive decay; gravity is however neglected. The standard model is therefore an approximation describing particle physics in the lab and in a variety of astrophysical situations when the gravitational force can be considered weak below a given energy scale which is the so-called Planck scale. It is defined by the combination of the three constants: c , $\hbar = h/2\pi$, G .

The Planck length equals: $l_p = \sqrt{\frac{\hbar G}{c^3}}$ in 4d and its value is then $l_p = 1.616252(81) \times 10^{-35} m$ that corresponds to an energy $E_p = 1.22 \times 10^{28} eV$. E_p can be compared with the energies obtained in our most powerful accelerator, the Large Hardon Collider in Geneva, which are of the order of $10^{12} eV$. Below this Planck scale, the gravity effects can be neglected and the standard model is a good approximation, above a theory of quantum gravity is necessary to describe space and time. Since the 1980s, the problem of understanding what happens to general

¹Its value was fixed to $299\,792\,m.s^{-1}$ in 1983 by the BIPM (Bureau International des Poids et Mesures) and this value does define the meter.

²The fractional uncertainty in G precisely measured in the 1980's (uncertainty of 0.0128%) is thousands of times larger than those of other fundamental constants. Moreover, recently the value of G has been called into question by new measurements which suggest the uncertainty of G could be much larger than originally thought.

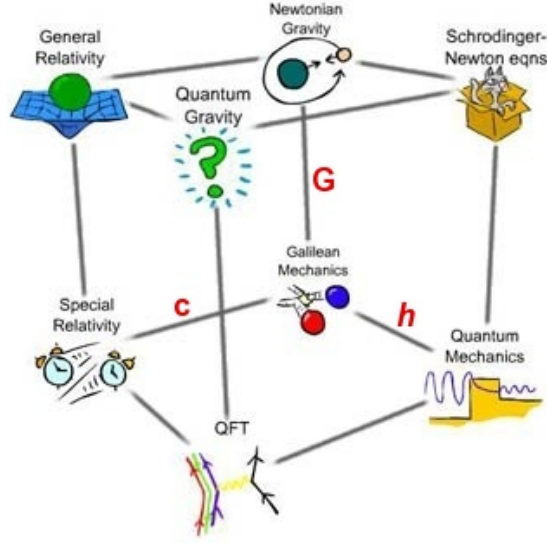


Figure 1.1: Fundamental constants and theories.

relativity at the extreme short-distance Planck scale l_p has been one of the most pressing questions in theoretical physics. Before going on with quantum gravity, let us point out that the regime where both G and h have to be taken into account can be studied thanks to the so-called Schrodinger-Newton equations. Theoretically, this brings nothing really new, however, some experimental results obtained in 2001 are very interesting: physicists have observed quantized states of matter under the influence of gravity for the first time. Ultra-cold neutrons moving in a gravitational field do not move smoothly but jump from one height to another, as predicted by quantum theory [1].

Let us detail the plan of the next three main parts.

In the first part, we will give the reasons why we need a theory of quantum gravity. Several serious answers to this challenge have been proposed. These include non-commutative geometry, string theory, loop quantum gravity, emergent gravity,... This three year work is exclusively based on the so-called loop quantum gravity theory [2, 3] which is a theory focusing on the problem of quantizing gravity with no aim to find a unified description of all interactions. Loop quantum gravity is an attempt to define a quantization of gravity paying great attention to the conceptual lessons of general relativity. For example, general relativity teaches us that the degrees of freedom of the gravitational field are encoded in the geometry of spacetime and in this sense, the gravitational interaction is fundamentally different from all other known forces. The spacetime geometry is fully dynamical and the notion of absolute space on top of which 'things happen' ceases to make sense in gravitational physics (see Fig. 1.2). The idea is therefore to build a theory of quantum gravity which will not be based on a notion of background geometry. In Part II, we will describe loop quantum gravity established as a proposal of background independent and non perturbative quantization of general relativity. This presentation will be done in two steps. We will first recall the Hamiltonian formulation of general relativity starting with the conventional ADM variables and then introduce the variables that are used in the definition of loop quantum gravity. The second step is the quantization: we will give a short review of the canonical approach of quantization of general relativity and then describe the Hilbert space of the quantum states and in particular define the *spin network states*. The spin network states are the building block of loop quantum gravity: they provide a basis of the kinematical Hilbert space and diagonalize some geometric operators, such as surface areas. The kinematics of loop quantum gravity is in fact beautifully under control. However, understanding the dynamics is still in progress. In the last section of Part II, we will present the *spin foam* formalism which can be considered as a possible approach to solve the dynamics of spin networks. Indeed, a spin foam picture emerges when considering

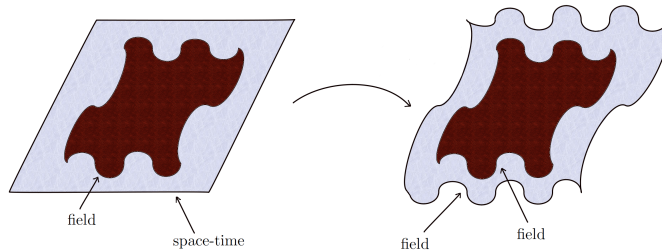


Figure 1.2: Space-time geometry becomes a dynamical object like the other fields.

the evolution in “time” of spin networks. But spin foam models can also be naturally interpreted as a form of path integral approach to quantum gravity, *the covariant approach*. In this approach, one abandons the canonical approach and seeks a functional integral description of transition amplitudes between two quantum gravity states. The states are given by 3-geometries relative to 3d hypersurfaces not necessarily connected and the histories interpolating between them are 4-geometries inducing the given 3-geometries on the hypersurfaces. The different steps – the first order formalism of general relativity, the discretization, the quantification – will be concretely illustrated in Section 6.1 where we will give the technical details of the construction and the derivation of a spin foam amplitude in the case of the Ponzano-Regge model which is a spin foam model for 3d quantum gravity. 3d general relativity has no local degree of freedom: it can be discretized and quantized exactly without losing any of its physical content and consequently offers a simpler laboratory than the physically relevant 4d case.

In Part II and Part III, new results are presented. The spin foam framework is the starting point of all this work. Two of the main issues for this approach are:

- to define a consistent 4d model of quantum gravity,
- to have a low-energy prediction of the theory.

The difficulties of the first point come from the fact that unlike the 3d case, 4d general relativity is not a topological theory but a topological theory plus constraints. The issue is to understand how to impose consistently the constraints – the so-called *simplicity constraints* – at the quantum level in order to turn the topological theory into a geometrical theory and to introduce local degrees of freedom. The second point is essential to test the theory and to make predictions but it is difficult since the starting point is a non-perturbative formalism. That is why it is challenging to define a perturbative expansion in the Planck scale l_p in order to check if the correct semi-classical limit arises. The next step is to explore if loop quantum gravity can provide a UV completion of the perturbative quantization in terms of graviton, which unlike the other interactions in the standard model turns out to be non-renormalizable. This could consequently provide predictions for possible experiments. These two different lines have been explored and our results can bring some elements of response to both issues.

Another important question related to the low-energy limit predictions will be to understand the behavior of spin foam models under renormalization and to study the coarse-graining of such model. This is fundamental in order to truly define the continuum limit of spinfoam models and their semi-classical regime. In fact, we do not expect a unique spin foam model for 4d gravity but a class of models characterized by a renormalization flow. This question to define a renormalization group flow in a background independent context has still to be seriously tackled [4].

Part III will be devoted to the problem of defining a spin foam model for 4d gravity. We will first recall the definition of the Barrett-Crane model which was the first explicit attempt to solve the simplicity constraints. However, the loop quantum gravity point of view or the spin foam graviton calculations seem to indicate that too many degrees of freedom of the 3d space geometry are frozen in this model. We will then introduce the EPRL-FK models which were proposed to address this issue prior to the inception of this work. In these models, the simplicity constraints are imposed weakly either following a procedure inspired from the Gupta-Bleuler

quantization or using coherent states. After a review on these two different approaches, we will present some results, – which we presented in [5] – regarding one aspect of the problematic focusing on the relation between loop quantum gravity and the spin foam formalism. More precisely, we have defined the various ways to map the loop quantum gravity spin networks onto certain subspaces of Lorentz invariant states – *the projected spin networks* – which satisfy the simplicity constraints and would therefore legitimately implement the dynamics and evolution of spin networks for loop quantum gravity.

In the last part of Part III tackling the issue of the definition of a 4d spin foam model for gravity, we will present some results – we presented in [6] – focusing on the implementation of the simplicity constraints at the quantum level using a new framework introduced in [7] and developed more recently in [8, 9]. This framework leads to a better interpretation of the structure of the Hilbert space of $SU(2)$ *intertwiners*³ from $U(N)$ representations. This $U(N)$ framework, based on the Schwinger representations of the $\mathfrak{su}(2)$ Lie algebra in term of a couple of harmonic oscillators, proposes a closed algebra of geometric observables acting on the space of $SU(2)$ intertwiners and a new set of coherent states which are covariant under $U(N)$ transformations. A first part of my work has been to complete the analysis of the $U(N)$ framework for $SU(2)$ intertwiners initiated in [7, 8, 9] in order to have an explicit action of the different newly introduced geometrical observables on the $U(N)$ coherent states. Then, we have shown how these $U(N)$ tools can be applied to the analysis of the simplicity constraints for 4d Euclidean gravity and proposed new sets of constraints. Solving them in term of the $U(N)$ coherent states has yielded weak solutions to all simplicity constraints for arbitrary values of the Immirzi parameter⁴.

In Part III, we will present new results concerning the issue of the low-energy interpretation of the theory from the spin foam formalism and show how they are relevant to derive quantum corrections to the classical dynamics of the gravitational field. This work is based on the “spinfoam graviton” framework proposed by Carlo Rovelli and collaborators who have introduced a technique to study n-point functions within loop quantum gravity [10, 11]. The graviton propagator corresponds to the correlator between excitations of quanta of space or more explicitly to the correlator between geometrical observables such as the areas of elementary surfaces. The two main ingredients to define it are the boundary amplitude that codes the quantum gravity dynamics – the $\{6j\}$ symbol in the Ponzano-Regge model, the $\{10j\}$ symbol in the Barrett-Crane model – and a weighted functional of spin networks. This latter is usually chosen to be a semi-classical state peaked on both the intrinsic and extrinsic geometry of a closed 3d surface, interpreted as the physical boundary of a 4d spacetime region. We have focused on a 3d toy model to explore the properties of the boundary amplitude which is the quantum amplitude associated to a vertex of the spin foam⁵. The 3d case has the advantage that the semi-classical limit is better understood and all the issues of the 4d case can be addressed in this simplified context. In the Ponzano-Regge model, the vertex amplitude is given by the $\{6j\}$ symbol from the recoupling theory of the representations of $SU(2)$. We need to understand the corrections to the asymptotical behavior of the $\{6j\}$ symbol in order to compute the higher order quantum corrections to the classical propagator of the graviton. We have developed two methods to study the asymptotic expansion of the $\{6j\}$ symbol: either performing a brute-force approximation starting from the explicit algebraic formula of the $\{6j\}$ symbol as a sum over some products of factorials [12], or using a recursion relation for the $\{6j\}$ symbol derived from the invariance of the $\{6j\}$ symbol under Pachner moves (Biedenharn-Elliott identity) [13]. The first method has allowed to investigate the asymptotical behavior of the $\{6j\}$ symbol at next-to-leading order and to compute it analytically. With the second method, we have provided explicit formulas for up to the third order correction beyond the leading order for the particular case of a ‘isosceles’ $\{6j\}$ symbol and we have in addition shown how the relation recursions can be used to derive Ward-Takahashi-like identities between the expectation values of graviton-like spin foam correlations.

Another problem we tackled concerns the second key ingredient regarding the graviton propagator, i.e. the

³ $SU(2)$ intertwiners are $SU(2)$ invariant tensors attached to each vertex of a spin network. They are the basic building blocks of spin network states and glued together, they generate the quantum 3d space. The intertwiner space geometrical interpretation is therefore necessary for a better understanding of loop quantum gravity at both kinematical and dynamical levels.

⁴The Immirzi parameter, denoted γ , appears when adding to the classical action for gravity a topological term which is required in order to have a well-defined connection on the boundary. This has no effect on the classical equations of motion but this introduces a quantization ambiguity.

⁵This 3d toy model is a topological model. We thus know how to quantize it exactly as a spin foam model and in addition we know how to introduce defaults such as particles which introduce local degrees of freedom.

boundary state. The original ansatz is to take as boundary state a Gaussian state with a phase factor in the Hilbert space of boundary spin networks. However, this state has to be physical, that is to be a gauge invariant spin network state that solves the quantum gravity constraints. A criterion to select a physical boundary state had already been proposed in [14] in the 3d case. We have extended this approach to determine physical boundary state in the 4d case considering the Barrett-Crane model [15].

Part I

From Loop Quantum Gravity to Spin foam models

Chapter 2

Motivations for a quantum theory of gravity

Nevertheless, due to the inner atomic movement of electrons, atoms would have to radiate not only electromagnetic but also gravitational energy, if only in tiny amounts. As this is hardly true in Nature, it appears that quantum theory would have to modify not only Maxwellian electrodynamics but also the new theory of gravitation.

Albert Einstein,
(*Preussische Akademie Sitzungsberichte*, 1916)

Two of the most exciting developments of XXth century physics were general relativity and quantum theory. Both have modified our understanding of the physical world in depth. General relativity treats gravity, while the 'standard model' – the culminating development of quantum theory – treats the rest of the forces of nature.

General relativity represents the result of a long line of developments that go all the way back to Galileo's thought experiments about relativity of the motion, Mach's arguments about the nature of space and time and finally to Einstein's magnificent conceptual breakthrough. It has provided beautiful insights about the nature of the Universe through astrophysics and cosmology and even led to key technological developments such as the Global Positioning System.

Quantum theory has been developed roughly at the time, triggering new discoveries about the fundamental nature of matter and its interactions, through atomic physics, nuclear and particle physics, condensed matter physics.

Even though both theories had impressive successes in making predictions which were checked with very high precision, they have their own limits.

For example, central objects for astronomers and theoretical physicists are black holes. A black hole is a region of space from which nothing, not even light, can escape. Its defining feature is the appearance of an event horizon – a boundary in spacetime through which matter and light can only pass inward. Although the discovery in the early 1970s by Bekenstein and Hawking among many others of the thermodynamic behavior of black holes (see e.g. [16]) – achieved primarily by classical and semiclassical analyses – has provided a better understanding of this notion of black hole horizon, many important issues remain unresolved. Primary among these are the "black hole information paradox"¹ and the gravitational singularity in the center of the black hole where the spacetime curvature becomes infinite.

In the context of cosmology, the Friedmann, Lemaître, Robertson, Walker models² and perturbations thereof are empirical successes. Indeed, it appears that the rich data that we now have and are likely to accumulate in the near future from astrophysical observations would be adequately described by these models derived

¹It suggests that physical information could "disappear" in a black hole, allowing many physical states to evolve into precisely the same state.

²The Friedmann - Lemaître - Robertson - Walker metric is an exact solution of Einstein's field equations of general relativity; it describes a simply connected, homogeneous, isotropic expanding or contracting universe (see [17, 18]).

from general relativity and quantum field theory. However, these theories are conceptually incomplete since they assume that the universe begins with a “Big Bang” at which matter densities and space-time curvature become infinite, i.e. a singularity. The appearance of singularities in general relativity is commonly perceived as signaling the breakdown of the theory.

At the atomic scale, the gravitational force can be safely neglected and this is also true for the current high energy experiments. Therefore it might be surprising at first sight that gravitational and quantum effects should be taken into account both at the same time. However a simple dimensional analysis shows that at the Planck scale $l_P = \sqrt{\frac{\hbar G}{c^3}} \sim 10^{-35}m$, the gravity effects become important again and cannot be neglected any more. This means that before reaching the singularity in a black hole one has to enter a regime where gravity is quantized. In particular, one can expect that the notion of singularity is blurred and regularized, solving this singularity issue [19]. A similar reasoning applies in cosmology. The Universe should have cooled down from an extreme phase where the gravitational degrees of freedom were quantized. The notion of “Big Bang” should be blurred and regularized by the quantum effects. This justifies, at least theoretically, the necessity to study quantum gravity.

From an experimental point of view, quantum gravity is a theory expected to describe regimes that are so far inaccessible: indeed in the current most powerful accelerator, the Large Hadron Collider, we are able to obtain energies of the order of a few TeV while the Planck energy E_P , the energy scale at which quantum gravity effects are believed to become important, is 10^6 TeV.

It was therefore thought for a long time that one could only see quantum gravitational effects in the cosmological realm, these effects being moreover extremely weak and hard to measure. This situation has changed; different experiments both terrestrial (VERITAS) and spatial (FERMI satellite), using extreme high energy particle physics (essentially gamma-rays bursts) are being set up and hope to measure quantum gravitational effects [20]. A new experimental window is opening, allowing us to explore the fundamental structure of spacetime. The current situation in this field is therefore exciting, one has to make physical predictions to the outcome of these experiments, and make concrete statements about the physics involved in the quantum gravity regime.

We need a working theory of gravity that takes quantum effects into account. This theory of quantum gravity should in particular synthesis the generally relativistic principle of background independence and the uncertainty principle of quantum mechanics. However, it is a non trivial task to assemble the two theories, general relativity and quantum mechanics, into a single coherent picture of the world. Indeed, the “naive” try consisting in applying the standard (perturbative) quantum field theory tools so successful for the standard model, does fail: the perturbative quantization of general relativity is non-renormalizable. Moreover one can argue that this approach is not really respecting the essence of general relativity since one introduces a background around which one quantizes the gravitational fluctuations. Introducing a background does break a fundamental feature of general relativity, the background invariance.

Following the lead of Bergmann and Dirac, physicists (Arnowitt, Deser, Misner) have also tried to apply the Dirac quantization rules to general relativity during the mid 60’s. Quickly enough it was realized that using the metric formulation, this approach was also bound to fail due to the intrinsic complexity of the formulation.

It was not before the mid 80’s that Ashtekar realized that with a clever change of variables the Hamiltonian analysis of general relativity was greatly simplified. The subsequent rediscovery by Rovelli and Smolin of the spin networks introduced in the 70’s by Penrose as the basis for the kinematical Hilbert space sparked the *loop quantum gravity* field. While trying to understand its quantum dynamical aspects, the notion of *spinfoam* was introduced. They can also be viewed as a (discretized) path integral quantization of general relativity. For a 3d space-time case, it was realized those spinfoams were in fact similar to an old model, the Ponzano-Regge model, introduced in the 60’s [21]. Since then the spinfoam approach was developed on its own as a way to regularize the general relativity partition function.

Chapter 3

Hamiltonian formalism of General Relativity

General relativity is a constrained theory. I will first give the Hamiltonian formulation of general relativity in terms of ADM variables (see [22] for a review) which was used by Arnowitt, Deser, Misner (ADM) among many others to apply Dirac's quantization program to general relativity. The Dirac's procedure can be schematically divided in three steps [23, 24, 25]

- Find a representation of the phase space variables of the theory as operators in a kinematical Hilbert space \mathcal{H}_{kin} satisfying the standard commutation relations: $\{ , \} \rightarrow -i/\hbar[,]$.
- Promote the constraints to (self-adjoint) operators in \mathcal{H}_{kin} .
- Characterize the space of solutions of the constraints and define the corresponding inner product. This would define the so-called physical Hilbert space \mathcal{H}_{phys} .

These steps should then be completed with a physical interpretation of the quantum observables – the gauge invariant observables are operators commuting with the constraints. Dirac's procedure applied to the ADM phase space defines a kinematical Hilbert space which is already ill-defined and on which there is no measure theory. Therefore, we will not apply the quantization program proposed by Dirac to the set of ADM variables but we will see how we can define new variables from the ADM ones to reformulate general relativity in a way more amenable to Dirac's quantization procedure. Indeed, all choices of fundamental variables do not work out as well when quantizing a theory and the key to *loop quantum gravity* has precisely been a choice of different variables to describe gravity. From the ADM variables, the definition of the new variables will be done in two steps

$$\begin{array}{ccccc} \text{ADM formulation} & & \text{triad formulation} & & \text{SU(2) Ashtekar-Barbero connection variables} \\ (\pi^{ab}, q_{ab}) & \longrightarrow & (E_i^a, K_b^j) & \longrightarrow & (P_i^a, A_b^j) \end{array}$$

The first change of variables will introduce a new constraint and the second one is a canonical transformation. In the first section, I will recall the definition of the ADM variables. Then, in the second section I give more details on both changes of variables. Finally, in the last section, I will present the classical framework of *covariant loop quantum gravity* which is a program of quantizing gravity *à la loop* starting from a Lorentz covariant canonical formulation. In fact, this covariant loop quantum gravity theory uses the same techniques and tools as loop quantum gravity but in this case the gauge group is the Lorentz group $SL(2, \mathbb{C})$ instead of $SU(2)$.

3.1 Canonical formulation of General Relativity in ADM variables

The Hamiltonian formulation of gravity is the basis of any attempt to canonically quantize gravity. The Hamiltonian treatment of General Relativity is based on a $3+1$ splitting of space-time [26, 27, 28, 29, 30]. This

splitting allows to coordinatize the phase space Γ explicitly. The phase space defined as the space of solutions of the equation of motion is a covariant notion, however the coordinatization we choose for it breaks covariance. Given a four-geometry – a globally (hyperbolic) spacetime \mathcal{M} with metric tensor fields $g_{\mu\nu}$ of Lorentzian signature¹ $(-+++)$ – we consider a one-parameter family of three-dimensional spacelike hypersurfaces Σ_t ($t = \text{constant}$), with spatial coordinates x^a ($a = 1, 2, 3$) [17]. In the following, we shall use latin letters a, b, \dots for space indices and greek letters μ, ν, \dots for space-time indices. Let us consider a nearby pair $(\Sigma_t, \Sigma_{t+dt})$ of spacelike hypersurfaces labelled by the time coordinates t , and $t + dt$. The foliation allows us to identify the function $t \in \mathbb{R}$ as a (unphysical) time parameter. We need to define “moving forward in time” with the parameter time t starting from the surface Σ_t and reaching the surface Σ_{t+dt} . For this, let us choose a vector field t^μ on \mathcal{M} satisfying $t^\mu \nabla_\mu t = 1$. We decompose t^μ into its normal and tangential parts to Σ_t (see Fig. 3.1)

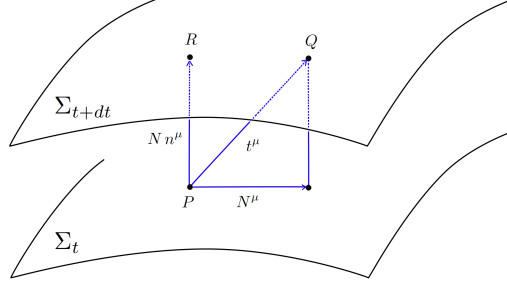


Figure 3.1: Coordinates for two nearby hypersurfaces labelled by t and $t + dt$

by defining the *lapse function* N and the *shift vector* N^μ with respect to t^μ by

$$\begin{aligned} N &= -t^\mu n_\mu, \\ N_\mu &= q_{\mu\nu} t^\nu, \end{aligned}$$

where n^μ is the unit normal vector field to the hypersurfaces Σ and $q_{\mu\nu} = g_{\mu\nu} + n_\mu n_\nu$ is a (3d Riemannian) *spatial metric* induced on each Σ by the space-time metric $g_{\mu\nu}$.

$$t^\mu = N^\mu + N n^\mu. \quad (3.1)$$

We can interpret the vector field t^μ as the “flux of time” across space-time. Moreover, it is then obvious that the lapse function N and the shift vector N^μ are not considered dynamical since they merely prescribe how to “move forward in time”. The metric $q_{\mu\nu}$ is spatial in the sense that $q_{\mu\nu} n^\mu = 0$ and by convention, we now denote the induced spatial metric using only spatial coordinates q_{ab} in the coordinates patch $\{x^a\}$ on the surface Σ .

The ADM formalism characterizes the phase space of general relativity when the degrees of freedom are encoded in the metric. The object of interest is the Einstein-Hilbert action for the metric $g_{\mu\nu}$ which propagates on the manifold \mathcal{M}

$$S_{EH} = \frac{1}{2\kappa} \int_{\mathcal{M}} d^4x \sqrt{|\det(g)|} R, \quad (3.2)$$

where R is the Ricci scalar associated with $g_{\mu\nu}$, and $\kappa = 8\pi G$ in units $c = 1$.

The ten components of the spacetime metric are then replaced by the six components of the induced Riemannian metric q_{ab} of Σ , plus the three components of the shift vector N^a and the lapse function N . Let us now illustrate this by defining the coordinates for two nearby hypersurfaces (see Fig. 3.2) using the ADM variables (q_{ab}, N, N_a) [22].

¹ $(-+++)$ induces a positive definite metric on spacelike metric. In some cases, we will consider a Riemannian manifold, that is the metric will have a $(++++)$ signature.

- The intrinsic metric of each surface Σ is $q_{ab} = g_{ab}$. The metric of the hypersurface Σ_t ,

$$q_{ab} dx^a dx^b = g_{ab}(t, x, y, z) dx^a dx^b, \quad (3.3)$$

tells the square of the distance between two points in Σ_t . The metric on the upper hypersurface, Σ_{t+dt} , is similarly given by

$$g_{ab}(t + dt, x, y, z) dx^a dx^b. \quad (3.4)$$

This formalism thus suggests that the spatial metric on a three-dimensional hypersurface Σ can be viewed as the dynamical variable in general relativity. Indeed, if we identify the hypersurfaces Σ_t, Σ_{t+dt} by the diffeomorphism resulting from following integral curves of t^μ , we may view the effect of “moving forward in time” as that of changing the spatial metric on an *abstract* three-dimensional Σ from $q_{ab}^{(t)}(x, y, z) = g_{ab}(t, x, y, z)$ to $q_{ab}^{(t+dt)}(x, y, z) = g_{ab}(t + dt, x, y, z)$. That is, the space-time $(\mathcal{M}, g_{\mu\nu})$ may be viewed as representing the time development of q_{ab} on a fixed three-dimensional manifold.

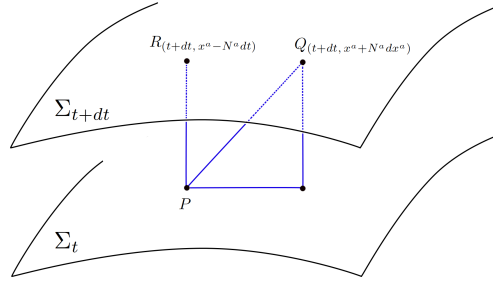


Figure 3.2: Coordinates for two nearby hypersurfaces labelled by t and $t + dt$

- The shift vector $N^a = N^a(t, x^b)$ appears when following the timelike normal vector from a point P with co-ordinates (t, x^a) to a point R on Σ_{t+dt} , the upper surface with coordinates:

$$R = (t + dt, x^a - N^a dt). \quad (3.5)$$

N^a measures therefore the amount of “shift” tangential to Σ_t in the time flow vector field t^μ .

- The proper time elapsed from P (lower surface) to R (upper surface) can be defined from the lapse function $N(t, x^a)$:

$$(\text{lapse of proper time between lower and upper hypersurface}) = N(t, x, y, z) dt. \quad (3.6)$$

That is, N measures the rate of proper time flow with respect to the unphysical coordinate time, t , as one moves normally to Σ_t .

- In Fig. 3.2, let Q be a point on the final surface with coordinates $(t + dt, x^a + dx^a)$, then the squared interval $ds^2 = g_{\mu\nu} dx^\mu dx^\nu$ for the infinitesimal vector dx^μ describing PQ is deduced from the Lorentzian geometry in Fig. 3.2:

$$\begin{aligned} ds^2 &= (\text{proper distance in base 3-geometry})^2 - (\text{proper time from lower to upper 3-geometry})^2 \\ &= q_{ab}(dx^a + N^a dt)(dx^b + N^b dt) - (N dt)^2. \end{aligned} \quad (3.7)$$

From this equation (3.7), the four-metric can be constructed out of the three-metric and the lapse and shift functions:

$$g_{\mu\nu} = \begin{pmatrix} g_{00} & g_{0b} \\ g_{a0} & g_{ab} \end{pmatrix} = \begin{pmatrix} (N_a N^a - N^2) & N_b \\ N_a & q_{ab} \end{pmatrix}, \quad (3.8)$$

where N^a are the components of the shift in its contravariant form, and $N_a = q_{ab}N^b = g_{ab}N^b$ are the covariant components; they are calculated within the three-geometry with the three-metric. The inverted relation $N^b = q^{bc}N_c$ is obtained using the inverse three-metric q^{bc} that has to be distinguished from the inverse four-metric. One can verify that the inverse four-metric is

$$g^{\mu\nu} = \begin{pmatrix} g^{00} & g^{0b} \\ g^{a0} & g^{ab} \end{pmatrix} = \begin{pmatrix} -1/N^2 & N^b/N^2 \\ N^a/N^2 & (h^{ab} - \frac{N^aN^b}{N^2}) \end{pmatrix}, \quad (3.9)$$

by expanding the relation $g_{\mu\nu}g^{\mu\lambda} = \delta_\nu^\lambda$.

- The unit future-directed *normal vector* n^μ to the hypersurface Σ_t points along PR in Fig. 3.2. It corresponds to the one-form which has the value:

$$n_\mu dx^\mu = -Ndt. \quad (3.10)$$

Therefore, in covariant one-form representation, this unit timelike normal vector has the components

$$n_\mu = (-N, 0, 0, 0) \quad (3.11)$$

$$n^\mu = g^{\mu\nu}n_\nu = \left(\frac{1}{N}, -\frac{N^m}{N}\right). \quad (3.12)$$

In terms of these variables, after performing the standard Legendre transformation, the action of general relativity becomes,

$$S_{EH}[q_{ab}, \pi^{ab}, N^a, N] = \frac{1}{2\kappa} \int dt \int_\Sigma d^3x \left[\pi^{ab} \dot{q}_{ab} + 2N_b \nabla_a^{(3)}(q^{-1/2} \pi^{zb}) + N(q^{1/2}[R^{(3)} - q^{-1} \pi_{cd} \pi^{cd} + \frac{1}{2} q^{-1} \pi^2]) \right] \quad (3.13)$$

where $\pi^{ab} = \frac{\partial \mathcal{L}_{EH}}{\partial \dot{q}_{ab}}$ are the momenta canonically conjugated to the space metric q_{ab} , $\pi = \pi^{ab} q_{ab}$, $\nabla_a^{(3)}$ is the covariant derivative compatible with the metric q_{ab} , q is the determinant of the space metric q_{ab} and $R^{(3)}$ is the Ricci tensor of q_{ab} .

We now introduce the concepts of intrinsic and extrinsic curvatures which appear in the language associated to this 3 + 1 space-time split. The intrinsic curvature gives the three-geometry of a spacelike hypersurface Σ . It may be defined and calculated by the same methods known for the calculation of four-dimensional curvature from the induced metric q_{ab} on Σ . The extrinsic curvature, denoted K_{ab} , of a three-dimensional hypersurface embedded in a four-geometry gives the rate of change of the three-metric in the normal direction (see Fig. 3.3).

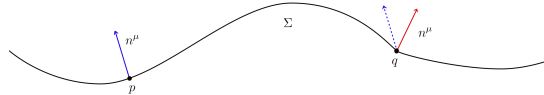


Figure 3.3: This spacetime diagram illustrates the notion of the extrinsic curvature of a hypersurface Σ . The dashed arrow at q represents the parallel transport of the normal vector n^μ at q along a geodesic connecting p to q . The failure of this vector to coincide with n^μ at q corresponds intuitively to the bending of Σ in the space-time in which it is embedded. The extrinsic curvature K_{ab} is a spatial entity; $K_{\mu\nu}$ the 4-dimensional entity is defined such that K_{ab} is the pull-back on Σ of $K_{\mu\nu}$. Then, $K_{\mu\nu} \equiv q_\mu^\rho \nabla_\rho n_\nu$ shows that $K_{\mu\nu}$ directly measures this failure of the two vectors at q to coincide for p near q .

The momenta π_{ab} are related to the extrinsic curvature K_{ab} of Σ since we can check that

$$\pi^{ab} = q^{-1/2}(K^{ab} - Kq^{ab}), \quad (3.14)$$

with $K = K_{ab}q^{ab}$. Variations of the Einstein-Hilbert action with respect to the lapse function and the shift vector produce the following constraints.

$$\text{The vector constraint:} \quad -V^b(q_{ab}, \pi^{ab}) \equiv 2\nabla_a^{(3)}(q^{-1/2} \pi^{ab}) = 0, \quad (3.15)$$

The scalar constraint:
$$-S(q_{ab}, \pi^{ab}) \equiv (q^{1/2}[R^{(3)} - q^{-1}\pi_{cd}\pi^{cd} + 1/2q^{-1/2}\pi^2]) = 0. \quad (3.16)$$

The vector constraint V^b and the scalar constraint are also respectively called the space-diffeomorphism constraint and the Hamiltonian constraint. Physical configurations (also called on-shell configurations) must satisfy these constraints that we can write under the more compact form $H^\mu = (S, V^b)$. H^μ are the generators of the space-time diffeomorphism group $\text{Diff}\mathcal{M}$ on physical configurations. We can now rewrite the action under the form.

$$S_{EH}[q_{ab}, \pi^{ab}, N^a, N] = \frac{1}{2\kappa} \int dt \int_{\Sigma} d^3x [\pi^{ab}\dot{q}_{ab} - N_b V^b(q_{ab}, \pi^{ab}) - NS(q_{ab}, \pi^{ab})]. \quad (3.17)$$

From this, we see that the Hamiltonian density of general relativity is

$$\mathcal{H}(q_{ab}, \pi^{ab}, N_a, N) = N_b V^b(q_{ab}, \pi^{ab}) + NS(q_{ab}, \pi^{ab}).$$

The Hamiltonian

$$\mathbf{H} = \frac{1}{2\kappa} \int d^3x (N_b V^b(q_{ab}, \pi^{ab}) + NS(q_{ab}, \pi^{ab})) \quad (3.18)$$

vanishes on-shell since it is a linear combination of constraints. General relativity is an example of so-called constrained Hamiltonian system with no physical Hamiltonian (for an introduction of this topic see [23, 24]). Classically, the constraints are equivalent to the equations of motion. The fact that the Hamiltonian is zero is a consequence of the diffeomorphisms symmetry of the theory: the “time” t should not be regarded as a physical quantity and there is no proper dynamics with respect to t .

The formulation given by (3.17) allows to study the phase space of general relativity parametrized by the pair (q_{ab}, π^{ab}) with the symplectic structure given by the canonical Poisson brackets:

$$\{\pi^{ab}(t, x), q_{cd}(t, y)\} = 2\kappa\delta_c^a\delta_d^b\delta(x-y), \quad \{\pi^{ab}(t, x), \pi^{cd}(t, y)\} = \{q_{ab}(t, x), q_{cd}(t, y)\} = 0. \quad (3.19)$$

This defines the kinematical phase space. On this space, the constraints (3.15) and (3.16) will define a hypersurface – the constraint surface – where they are satisfied, i.e. the subspace of (q_{ab}, π^{ab}) such that $H^\mu(q, \pi) = 0$. The constraints H^μ have their Poisson brackets which vanish on this constraint surface and are therefore by definition *first class constraints* [23]. There are six configuration variables q_{ab} and four first class constraint equations given by (3.15) and (3.16) so that we have two physical degrees of freedom, which is the usual result. Note that this counting of physical degrees of freedom is correct only because the constraints are first class.

We recall that a first class constraint generates a gauge transformation on the constraint surface [23]. We have illustrated in Fig. 3.4 the concepts of constraint surface and gauge orbits in two cases: the left-hand side represents a generic situation where the Hamiltonian can be decomposed as $\mathbf{H} = H_0 + \text{constraints}$; the right-hand side figure illustrates the case of general relativity where the Hamiltonian is simply given by $\mathbf{H} = \text{constraints}$. We refer to the trajectories generated by the gauge transformations as *gauge orbits*. Points along one gauge orbit correspond to the same physical configuration, only described in different coordinate systems.

The ADM formulation could not be used for a canonical quantization following Dirac’s framework. Indeed, the constraints H^μ are non-polynomial functions of the variables (q_{ab}, π^{ab}) which makes therefore the theory too complicated to quantize. It was therefore thought for many years that it was impossible to quantize gravity by other means than the perturbative quantum field formalism, approach which was itself plagued by important issues such as non-renormalizability or the fact that one only deals with linearized gravity in this context. This was until A. Ashtekar came and found a change of variables to simplify the shape of the constraints H^μ , that sparked the loop quantum gravity revolution.

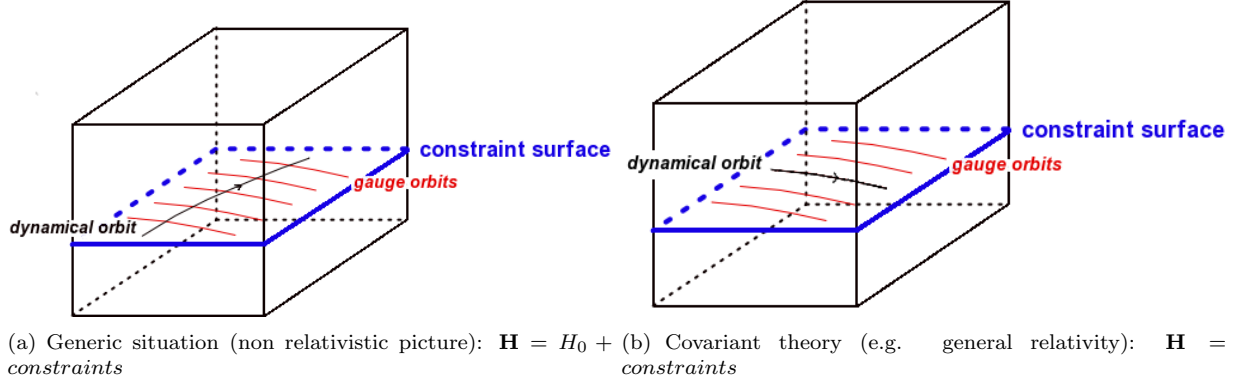


Figure 3.4: Illustration of dynamical orbits generated by \mathbf{H} and gauge orbits generated by first class constraints.

3.2 Loop quantum gravity variables

We will now make a very simple change of variables (see [31, 3, 32, 33] for review articles). A triad² e_a^i is a set of three 1-forms defining a frame at each point in Σ and such that the 3-metric q_{ab} is given by

$$q_{ab} = e_a^i e_b^j \delta_{ij}. \quad (3.20)$$

The crucial change of variables is defined using the densitized triad E_i^a

$$E_i^a \equiv \frac{1}{2} \epsilon_{ijk} \epsilon^{abc} e_b^j e_c^k, \quad (3.21)$$

which is related to the inverse metric q^{ab} as follows

$$qq^{ab} = E_i^a E_j^b \delta^{ij} \quad \text{with } i, j = 1, 2, 3. \quad (3.22)$$

Another relevant 1-form K_a^i can be constructed by combining the extrinsic curvature K_{ab} and the densitized triad E_i^a

$$K_a^i = \frac{1}{\sqrt{\det(E)}} K_{ab} E_j^b \delta^{ij}. \quad (3.23)$$

We can then rewrite (3.17) in terms of the new variables (K_a^i, E_i^a) . Indeed, the canonical term is simply

$$\pi^{ab} \dot{q}_{ab} = -\pi_{ab} \dot{q}^{ab} = 2E_i^a \dot{K}_a^i \quad (3.24)$$

and the constraints (3.15) and (3.16) can also easily be written in terms of these variables $V^a(E_i^a, K_a^i)$ and $S(E_i^a, K_a^i)$. However, the six components of q^{ab} are described from (3.22) using nine E_i^a . The extra three degrees of freedom come from the fact that we have the freedom to perform internal $\text{SO}(3)$ rotations. Indeed two different triads related by a local $\text{SO}(3)$ transformation acting in the internal indices $i = 1, 2, 3$ will define the same 3-metric q_{ab} . Since three degrees of freedom have been added to the configuration variables whereas the physical degrees of freedom have not changed, three new constraints have to be added. In fact, we missed the fact that $K_{(ab)} = K_{ab}$. which is equivalent to

$$G_{jk}(E_j^a, K_a^j) := K_{a[j} E_{k]}^a = 0. \quad (3.25)$$

²The triad e_a^i is the spatial part of the tetrad field $e^I = e_\mu^I dx^\mu$ which defines the space-time metric: $g_{\mu\nu} = e_\mu^I e_\nu^J \eta_{IJ}$. η_{IJ} is the flat metric in the tangent Minkowski space, I, \dots are internal indices living in the tangent Minkowski space. $i = 1 \dots 3$ is an internal index and the spatial component of I . e_μ^I thus represents the gravitational field and indeed, it can be viewed as the field that determines, at each point of space-time, the preferred frame in which motion is inertial.

Therefore, the Einstein-Hilbert action on this extended phase space generated by (K_a^i, E_i^a) becomes

$$S_{EH}[E_j^a, K_a^j, N^a, N, \lambda^{kl}] = \frac{1}{\kappa} \int dt \int_{\Sigma} d^3x \left[E_i^a \dot{K}_a^i - N_b V^b(E_j^a, K_a^j) - NS(E_j^a, K_a^j) - \lambda^{kl} G_{kl}(E_j^a, K_a^j) \right]. \quad (3.26)$$

The symplectic structure is now given by

$$\{E_j^a(t, x), K_b^i(t, y)\} = \kappa \delta_b^a \delta_j^i \delta(x - y), \quad \{E_j^a(t, x), E_i^b(t, y)\} = \{K_a^j(t, x), K_b^i(t, y)\} = 0. \quad (3.27)$$

The vector and scalar constraints (3.15) and (3.16) have not been modified in the transition from the ADM phase space to the extended phase space. The addition of new degrees of freedom does not, by itself, simplify the constraints.

The key-step in the simplification is a canonical transformation on the extended phase space which is performed to construct the Ashtekar-Barbero connection variables (A_a^i, P_i^a) [34, 35, 36].

$$(E_j^a, K_b^i) \longrightarrow \begin{cases} A_a^i \equiv \Gamma_a^i + \gamma K_a^i \\ P_i^a \equiv \frac{1}{\gamma} E_i^a \end{cases} \quad (3.28)$$

where $\gamma \in \mathbb{R}^*$ is a constant called Immirzi parameter [37] and Γ_a^i is a $\mathfrak{so}(3)$ -spin connection which is characterized as the solution of Cartan's structure equations

$$\partial_{[a} e_{b]}^i + \epsilon_{jk}^i \Gamma_{[a}^j e_{b]}^k = 0. \quad (3.29)$$

A spin connection is defined as an extension of the spatial covariant derivative from tensors to generalized tensors with $\mathfrak{so}(3)$ indices. Then, A^i is also a well-defined $\mathfrak{so}(3)$ connection. Indeed, K_a^i is the conjugate momentum of the densitized triad E_j^a which transforms in the vector representation of $\text{SO}(3)$ under the redefinition of the triad ($q_{ab} = e_a^i e_b^j \delta_{ij}$). Consequently, $K_a^i = \frac{1}{\sqrt{\det(E)}} K_{ab} e_j^b \delta^{ij}$ transforms also as a vector. This is why $A_a^i = \Gamma_a^i + \gamma K_a^i$ is also a $\mathfrak{so}(3)$ connection.

Let us emphasize that the constraint structure does not distinguish $\text{SO}(3)$ from $\text{SU}(2)$ as both groups have the same Lie algebra. Thus, from now on we choose to work with the more fundamental (universal covering) group $\text{SU}(2)$. Moreover, from this point, we will rather use the variables E_j^a instead of the variables P_j^a as mostly used in the literature.

Consider now the (rotational) constraint G_{ij} . It can be written as

$$G_i(E_j^a, K_a^j) = \epsilon_{ikl} K_a^k E_l^a, \quad (3.30)$$

then, using the new variables, it simplifies into

$$G_i(E_j^a, A_a^j) = D_a E_i^a \equiv \partial_a E_i^a + \epsilon_{ij}^k A_a^j E_k^a = 0, \quad (3.31)$$

i.e. it is the covariant divergence of the densitized triad. Therefore, written with the Ashtekar-Barbero variables (A_a^i, E_i^a) , this constraint takes the structure of a Gauss law constraint for an $\text{SU}(2)$ gauge theory. G_i is called the Gauss constraint and generates gauge transformations. As we mentioned above, E_i^b and A_a^i transform respectively as an $\text{SU}(2)$ vector and as an $\text{SU}(2)$ connection under this transformation. The other constraints (3.15) and (3.16) which still form with the Gauss constraint a first class algebra, become

$$\begin{aligned} V_a(E_j^a, A_a^j) &= F_{ab}^j E_j^b - (1 + \gamma^2) K_a^i G_i, \\ S(E_j^a, A_a^j) &= \frac{E_i^a E_j^b}{\sqrt{\det(E)}} \left(\epsilon^{ij} F_{ab}^k - 2(1 + \gamma^2) K_{[a}^i K_{b]}^j \right), \end{aligned} \quad (3.32)$$

where $F_{ab}^i = \partial_a A_b^i - \partial_b A_a^i + \epsilon_{jk}^i A_a^j A_b^k$ is the curvature of the connection A_a^i . We can then rewrite the action

$$S_{EH}[E_j^a, A_a^j, N^i, N, \lambda^k] = \frac{1}{\kappa} \int dt \int_{\Sigma} d^3x \left[E_i^a \dot{A}_a^i - N_b V^b(E_j^a, A_a^j) - NS(E_j^a, A_a^j) - \lambda^k G_k(E_j^a, A_a^j) \right], \quad (3.33)$$

and the Poisson brackets of the Ashtekar-Barbero variables are given by the fundamental Poisson brackets:

$$\{A_a^i(t, x), E_j^b(t, y)\} = \kappa\gamma\delta_a^b\delta_j^i\delta(x - y), \quad \{E_j^a(t, x), E_i^b(t, y)\} = \{A_a^j(t, x), A_b^i(t, y)\} = 0. \quad (3.34)$$

The $\kappa\gamma$ factor arises in the first Poisson bracket because the conjugate momentum of the configuration variable A_a^i (obtained as the derivative of the Lagrangian with respect to the velocities) is actually given by $1/\kappa \times P_i^a$. Moreover, the fact that the Immirzi parameter γ can be arbitrary is important because the quantum theories obtained starting with different values of γ will lead to different physical predictions. Furthermore γ enters the spectrum of geometrical observables such as areas and volumes (at the kinematical level) as well as the black hole entropy [38, 39, 40, 41, 42, 43, 44, 45, 46, 47, 48].

The next step is to smear this algebra. This is needed in order to proceed with the quantization. The densitized triad is a 2-form, thus we smear it on a two dimensional surface $S \subset \Sigma$ and define its flux across S :

$$E_i(S) \equiv \int_S n_a E_i^a d^2\sigma, \quad (3.35)$$

where $n_a = \frac{\partial x^b}{\partial \sigma^1} \frac{\partial x^c}{\partial \sigma^2} \epsilon_{abc}$ is the normal to the surface S and σ^1, σ^2 are local coordinates on S . Moreover, E_i^a encodes the full background independent Riemannian geometry of Σ since the inverse metric q^{ab} is related to E_i^a as follows: $qq^{ab} = E_i^a E_j^b \delta^{ij}$.

The connection A_a^i , which is a 1-form, has also a simple geometrical interpretation: it provides a definition of parallel transport of $SU(2)$ spinors on the space manifold Σ . Consider now a path $e \subset \Sigma$, we define the holonomy³ of A along e by

$$h_e[A] \equiv \mathcal{P} \exp \left(\int_e A \right), \quad (3.36)$$

where \mathcal{P} denotes a path-order product.

$$h_e = \sum_{n=0}^{\infty} \iint\limits_{1 > s_n > \dots > s_1 > 0} A(e(s_1)) \cdots A(e(s_n)) ds_1 \cdots ds_n, \quad (3.37)$$

where we parametrized the line with $s \in [0, 1]$ and $A = A_a^i \tau_i \frac{dx^a(s)}{ds}$ with τ_i the $\mathfrak{su}(2)$ generators and $x^a(s) : [0, 1] \rightarrow \Sigma$ a parametrization⁴ of the path e .

The resulting smeared algebra of $h_e[A]$ and $E_i(S)$ is called the *holonomy-flux* algebra. It provides a regular version of the Poisson algebra (3.34), i.e. no delta function appears anymore. This regularization step of the Ashtekar-Barbero variables using paths and surfaces is the last step to prepare general relativity for the loop quantization.

Before giving a description of the implementation of Dirac's program in the case of gravity using the classical variables presented above, we would like to comment on the fact that loop quantum gravity considers $SU(2)$ as gauge group of general relativity instead of the non-compact Lorentz group $SL(2, \mathbb{C})$. In the next section, we will introduce the classical framework which leads to a *covariant* loop quantum gravity theory, based on a $SL(2, \mathbb{C})$ connection.

The initial canonical formulation of loop quantum gravity used the (Ashtekar) variables (A, E) as canonical variables [31]: a self-dual complex connection $A = \Gamma \pm iK$ and its conjugate triad field E . The resulting theory is then invariant under the Lorentz group $SL(2, \mathbb{C})$ (seen as the complexified $SU(2)$ group, and it is the covering

³Some useful properties of the holonomy are:

- The holonomy of the composition of two paths e_1, e_2 is the product of the holonomies of each path: $h_{e_1 e_2} = h_{e_1} h_{e_2}$.
- Under a local gauge transformation, $g(x) \in SU(2)$, the holonomy transforms as $h_e^g = g_{s(e)} h_e g_{t(e)}^{-1}$, where $s(e)$ and $t(e)$ are respectively the source and the target points of the path e .
- Under the action of diffeomorphism, the holonomy transforms as: $h_e[\phi^* A] = h_{\phi \circ e}[A]$.

⁴For a given parametrization of the path e , $x^a(s) : [0, 1] \rightarrow \Sigma$ and for a given connection A_a^i , we integrate $A_a = A_a^i \tau_i$, a $SU(2)$ element, along e as a line integral $\int_e A \equiv \int_0^1 ds A_a^i(x(s)) \frac{dx^a(s)}{ds} \tau_i$.

group of the restricted Lorentz group $SO(1, 3)^+$ and under space-time diffeomorphism. However, a difficulty comes from the reality constraints expressing that the imaginary part of the triad field E vanishes and that the real part of the connection A is actually a function of the E : $A_a^i + \bar{A}_a^i = \Gamma_a^i(E)$.

These constraints rendered the quantization complicated. The standard formulation of loop quantum gravity presented above avoids this reality constraint issue using the *real* Ashtekar-Barbero connection $A = \Gamma + \gamma K$ where $\gamma \in \mathbb{R}$ and its real conjugate triad E . But then, the Ashtekar-Barbero connection A , on the spatial slice, is *not* the pull-back of a space-time connection⁵ and from that point of view, the real connection A cannot be considered as a genuine gauge field: $SU(2)$ can not be viewed as the gauge group of gravity [49]. In fact, deriving the theory from the original first order formalism, considering the Palatini action as starting point,

$$S_{\text{Pal}} = \frac{1}{2\kappa} \epsilon_{IJKL} \int_{\mathcal{M}} e^I \wedge e^J \wedge F^{KL}(\omega) \quad (3.38)$$

we can see that the $SU(2)$ gauge group appears because of a particular (partial) gauge fixing, the time gauge, which breaks the local Lorentz invariance down to a local $SU(2)$ gauge invariance and allows to recover the Ashtekar-Barbero variables. In the previous action (3.38), the tetrad field e_μ^I is defined as $e^I = e_\mu^I dx^\mu$ and $F(\omega) = d\omega + \omega \wedge \omega$ is the curvature tensor of the connection ω with $\omega = \omega_\mu^{IJ} J_{IJ} dx^\mu$ a $\mathfrak{sl}(2, \mathbb{C})$ -valued 1-form, with $J_{IJ} \in \mathfrak{sl}(2, \mathbb{C})$. A tetrad $e_\mu^I(x)$, $I = 0, 1, 2, 3$ is defined such that

$$g_{\mu\nu}(x) = e_\mu^I(x) e_\nu^J(x) \eta_{IJ} \quad (3.39)$$

and thus provide a local isomorphism between a general reference frame and an inertial one, characterized by the flat metric η_{IJ} . A local inertial frame is defined up to a Lorentz transformation: $e_\mu^I(x) \rightarrow \tilde{e}_\mu^I(x) = \Lambda_J^I(x) e_\mu^J(x)$. Notice that the definition (3.39) is well invariant under such a transformation. Thus, the "internal" index I carries a representation of the Lorentz group. Contracting vectors and tensors in spacetime with the tetrad, we get objects that transform under the Lorentz group. For example, we define the "internal time direction" x^I from the unit normal vector field n^μ (3.12) to Σ which appears in the 3+1 splitting of space-time ($\mathcal{M} \cong \mathbb{R} \times \Sigma$) by:

$$x^I = e_\mu^I n^\mu = \left(\frac{e_0^0 - e_a^0 N^a}{N}, \frac{e_0^i - e_a^i N^a}{N} \right) \quad (3.40)$$

We will see that this field is fundamental in the covariant framework presented in the following chapter 3.3. In (3.38), the connection ω is considered as an independent variable and consequently, the action (3.38) is invariant under local Lorentz transformations. When varying the action with respect to e , we obtain the "torsion-free" equation

$$de^I + \omega_J^I \wedge e^J = 0, \quad (3.41)$$

On the other hand, varying with respect to ω , and considering ω as a solution $\omega(e)$ of (3.41) one recovers the solutions of the Einstein equations (plus an additional sector with degenerate metrics in the case of a degenerate (i.e. non-invertible) tetrad), further details can be found in [33].

For the Hamiltonian formulation of the Palatini action, we proceed as before, assuming a 3 + 1 splitting of the space-time ($\mathcal{M} \cong \mathbb{R} \times \Sigma$) and coordinates (t, x) . Using the definition of x^I (3.40), we obtain that a tetrad for the ADM metric (3.7) is given by

$$e_0^I = N x^I + N^a e_a^I, \quad q_{ab} = e_a^i e_b^j \delta_{ij}, \quad i, j = 1, 2, 3. \quad (3.42)$$

where the spatial part of the tetrad, e_a^i is the triad. At this stage, the structure is complicated, in particular because the constraint algebra is second class. Indeed, the fact to use the tetrad and the connection as independent fields implies that the conjugate variables are now functions of both e_a^I and ω_a^{IJ} (and their time derivative) as opposed to be function of the metric q_{ab} only. Furthermore, the canonically conjugated variables to the connection ω_a^{IJ} are not independent and satisfy the so-called *simplicity constraints* which are second class

⁵Whereas in the case where $\gamma = \pm i$, A_a is the pullback of ω_μ^{+IJ} ($I, J = 1, \dots, 4$) with $\omega_\mu^{+IJ} = \frac{1}{2}(\omega_\mu^{IJ} - \frac{i}{2}\epsilon^{IJ}_{KL}\omega_\mu^{KL})$ the self-dual part of a Lorentz connection ω_μ^{IJ} .

constraints (i.e. which Poisson brackets do not vanish weakly). This is why the "time gauge" $x^I = e^I_\mu n^\mu = \delta_0^I$ is used in order to simplify the discussion

$$e_\mu^0 = (N, 0) \longrightarrow e_0^I = (N, N^a e_a^I). \quad (3.43)$$

Working in the time gauge breaks the local Lorentz invariance but allows to define the densitized triad (3.21) and the Ashtekar-Barbero connection⁶ $A_a^i = \frac{1}{2}\epsilon^i_{jk}\omega_a^{jk} + \gamma\omega_a^{0i}$ and to recover the first class constraint algebra with (3.31) and (3.32).

In the following section, we present an alternative classical framework where no gauge is fixed.

3.3 Classical framework for a "covariant" loop quantum gravity theory

We now review the classical framework of a Lorentz covariant approach to loop quantum gravity. The aim is to develop the canonical formalism for gravity with the full Lorentz group as a local symmetry. This was first performed by Alexandrov [50] and was coined *covariant loop quantum gravity*. We will see that the canonical variables are in this approach a Lorentz connection ω and its conjugate triad e valued in the Lorentz algebra. We consider once again a first order formalism of general relativity with Palatini action (3.38) where the connection ω is independent from the tetrad e . It is possible to take into account directly at this level the Immirzi parameter γ which appear in the change of variables (3.28). Indeed, we can add to the Palatini action a second term – the Holst term – which is compatible with all the symmetries and has mass dimension 4 [51]. This leads to the so-called Palatini-Holst action

$$S[\omega, e] = \int_{\mathcal{M}} \left[\frac{1}{2} \epsilon_{IJKL} e^I \wedge e^J \wedge F^{KL}(\omega) - \frac{1}{\gamma} e^I \wedge e^J \wedge F_{IJ}(\omega) \right]. \quad (3.44)$$

As it can be checked directly, the equations of motion are not affected by the Holst term and we recover the Einstein equations when the tetrad is not degenerated. The Immirzi parameter γ appearing in front of the Holst term has no effect on the equations of motion and thus does not matter at the classical level. As we mentioned previously, the difficulty in the canonical analysis comes from the second class nature of the constraints which appear. More precisely, the canonically conjugated variable Ω_{IJ}^a to the connection ω_a^{IJ} is $\Omega_{IJ}^a = \epsilon^{abc} \epsilon_{IJKL} e_b^K e_c^L$. These variables are not independent and they satisfy the *simplicity constraints*

$$\forall a, b, \epsilon^{IJKL} \Omega_{IJ}^a \Omega_{KL}^b = 0. \quad (3.45)$$

These constraints are the non trivial part of the canonical structure. In the "time gauge" $x^I = e^I_\mu n^\mu = \delta_0^I$ we recover the Ashtekar-Barbero variables (E_a^i, A_a^i) , the first class constraint algebra with (3.31) and (3.32), and the simplicity constraints do not appear. However, it is also possible to explicitly solve these constraints and by breaking the Lorentz covariance later, we still recover the Ashtekar-Barbero formalism [52].

Nevertheless, it is possible to write a canonical formulation of general relativity with the Immirzi parameter which preserves the full Lorentz gauge symmetry and to treat it in a covariant way. Such a formulation was constructed in [50]. The internal time direction x^I , defined by (3.40) or equivalently by

$$x^I = e^{I\mu} n_\mu = -N (e^{00}, e^{i0}), \quad (3.46)$$

where we used (3.11) for the definition of n_μ , can now be written under the general form

$$x^I(\mathcal{X}) = \frac{1}{\sqrt{1 - |\vec{\mathcal{X}}|^2}} (1, \mathcal{X}^i). \quad (3.47)$$

⁶The link between the form $A_a^i = \frac{1}{2}\epsilon^i_{jk}\omega_a^{jk} + \gamma\omega_a^{0i}$ of the Ashtekar-Barbero connection and the previous form $A_a^i = \Gamma_a^i + \gamma K_a^i$ is explicitly given in [3].

Therefore, comparing the two previous equations (3.46) and (3.47), we deduce that $\mathcal{X}^i = \frac{e^{i0}}{e^{00}}$.

We now start again with a space-time $\mathcal{M} \cong \mathbb{R} \times \Sigma$ where we distinguish the time direction from the three space dimensions. The lapse function N , the shift vector N^a , the triad e_i^a and the new field \mathcal{X}_i arise from the following decomposition of the tetrad

$$\begin{aligned} e^0 &= Ndt + \mathcal{X}_i \mathcal{E}_a^i dx^a \\ e^i &= \mathcal{E}_a^i N^a dt + \mathcal{E}_a^i dx^a. \end{aligned} \quad (3.48)$$

where \mathcal{E}_a^i is a triad. The field \mathcal{X}_i describes the deviation of the normal to the spacelike hypersurface $\{t = 0\}$ from the time direction⁷.

x defines a subgroup $H_x = \text{SU}_x(2)$ of the gauge group $\text{SL}(2, \mathbb{C})$ which is the isotropy subgroup of x^I with respect to the standard action of $\text{SL}(2, \mathbb{C})$ in \mathbb{R}^4 . The field \mathcal{X} is absent in the Ashtekar-Barbero formalism since the condition $\mathcal{X} = 0$, which corresponds to the time gauge, is imposed from the very beginning.

Let's call $X, Y, \dots = 1..6$ the $\mathfrak{sl}(2, \mathbb{C})$ -indices labeling antisymmetric couples $[IJ]$. The first 3 components correspond to $(0, i)$ and the other 3 are obtained after contraction of the (i, j) components with $\frac{1}{2}\epsilon^{ijk}$. We define new connection and triad variables $(\mathcal{A}^X, \mathcal{R}_X)$ valued in $\mathfrak{sl}(2, \mathbb{C})$ instead of the standard $\mathfrak{su}(2)$ of Ashtekar-Barbero variables (A^i, E_i) . The Lorentz connection \mathcal{A}_a^X is

$$\mathcal{A}^X = \left(\frac{1}{2}\omega^{0i}, \frac{1}{2}\epsilon_{jk}^i \omega^{jk} \right). \quad (3.49)$$

It is just the space components of the spin-connection ω^{IJ} . We define a "rotational" triad and a "boost" triad

$$\mathcal{R}_X^a = \left(-\epsilon_i^{jk} \mathcal{E}_a^i \mathcal{X}_k, \mathcal{E}_a^i \right), \quad \mathcal{B}_X^a = \left(\mathcal{E}_a^i, \epsilon_i^{jk} \mathcal{E}_a^i \mathcal{X}_k \right) = (\star \mathcal{R}^a)_X \quad (3.50)$$

where \star is the Hodge operator on $\mathfrak{sl}(2, \mathbb{C})$ switching the boost and rotation part of the algebra. The action then reads

$$S = \int dt d^3x \left(\left(\mathcal{B}_X^a - \frac{1}{\gamma} \mathcal{R}_X^a \right) \partial_t \mathcal{A}_a^X + \lambda^X G_X + N^a V_a + NS \right). \quad (3.51)$$

The phase space is therefore defined with the Poisson bracket,

$$\left\{ \mathcal{A}_a^X(t, x), \left(\mathcal{B}_Y^b - \frac{1}{\gamma} \mathcal{R}_Y^b \right)(t, y) \right\} = \delta_Y^X \delta_a^b \delta(x - y) \quad (3.52)$$

λ^X, N^a, N are Lagrange multipliers enforcing the ten first class constraints

$$\begin{aligned} G_X &= D_A \left(\mathcal{B}_X - \frac{1}{\gamma} \mathcal{R}_X \right), \\ V_a &= - \left(\mathcal{B}_X^b - \frac{1}{\gamma} \mathcal{R}_X^b \right) F_{ab}^X(\mathcal{A}), \\ S &= \frac{1}{1 + \frac{1}{\gamma^2}} \left(\mathcal{B} - \frac{1}{\gamma} \mathcal{R} \right) \left(\mathcal{B} - \frac{1}{\gamma} \mathcal{R} \right) F(\mathcal{A}) \end{aligned} \quad (3.53)$$

G_X generates the local Lorentz transformation, the analogue for the Gauss constraint (3.31) (there are effectively 6 constraints) and V_a and S generate space-time diffeomorphisms (4 constraints). The constraints have essentially the same form as the ones of the Ashtekar-Barbero formulation (3.31) and (3.32) with E_i^a, A_a^i being replaced by $(\mathcal{B}_X^a - \frac{1}{\gamma} \mathcal{R}_X^a)$ and \mathcal{A}_a^X , the structure constants of $\mathfrak{su}(2)$ being replaced by the structure constants of $\mathfrak{sl}(2, \mathbb{C})$ ⁸ and the last term in the Hamiltonian constraint S involving the intrinsic curvature being dropped.

⁷The slice is respectively spacelike, lightlike or timelike when $|\vec{\mathcal{X}}|^2 = \mathcal{X}^i \mathcal{X}_i$ is respectively less than 1, equal to 1 or bigger than 1. The presentation given here holds for a spacelike foliation but the timelike can also be treated in the same way [53].

⁸i.e. in particular, D_A is defined as D in (3.31) and $F(\mathcal{A})$ as $F(A)$ replacing A by \mathcal{A} and ϵ_{jk}^i by the $\text{SL}(2, \mathbb{C})$ structure constants. The explicit definition of the $\mathfrak{sl}(2, \mathbb{C})$ structure constants f^{XYZ} can be found in appendix of [53, 54].

However, in contrast to the framework for loop quantum gravity, we also have to deal with second class constraints

$$\phi^{ab} = (\star \mathcal{R}^a)^X \mathcal{R}_X^b, \quad \psi^{ab} \equiv \mathcal{R}^a \mathcal{R}^b D_{\mathcal{A}} \mathcal{R}. \quad (3.54)$$

The constraints ϕ are the simplicity constraints. The constraints $\psi = 0$ come from the Poisson bracket $\{S, \phi\}$ and is required in order that the constraint $\phi = 0$ is preserved under gauge transformations (generated by G, V_a, S) and in particular under time evolution. ψ correspond to the reality constraints of complex loop quantum gravity.

The next step to deal with second class constraints is to define the Dirac brackets $\{f, g\}_D = \{f, g\} - \{f, \varphi_r\} \Delta_{rs}^{-1} \{\varphi_s, g\}$ where the Dirac matrix $\Delta_{rs} = \{\varphi_r, \varphi_s\}$ is made of the Poisson brackets of the constraints $\varphi = (\phi, \psi)$. It is in fact at this step that computing the Dirac brackets of the smeared constraints G, V_a, S we can show that the smeared G constraints now generate $\text{SL}(2, \mathbb{C})$ gauge transformations and that the algebra of the first class constraints is not modified [50, 55, 54].

However, a new difficulty emerges from the fact that although the triad field R is still commutative for the Dirac bracket, the properties of the connection \mathcal{A} change drastically: it is not canonically conjugated to the triad and it does not commute with itself. The structure of the commutator which replaces the simple canonical commutation relation of loop quantum gravity (3.34) is now complicated. To define covariant loop quantum gravity variables, the choice is to keep the triad \mathcal{R} and to define a new connection $\tilde{\mathcal{A}}$. Requiring a good behavior of this Lorentz connection under Lorentz gauge transformations and space diffeomorphisms as well as requiring that it is conjugate to the triad⁹ \mathcal{R} allows to isolate a two-parameter family of possible connection variables: $\tilde{\mathcal{A}}(\alpha, \beta)$. Then requiring that the connection further behaves as a one-form under space-time diffeomorphisms (i.e. which transforms as a 1-form under space-time diffeomorphisms generated by the constraints V_a, S) allows to identify a unique covariant connection corresponding to $(\alpha, \beta) = (0, 1)$ [56, 57] that we will simply denote $\tilde{\mathcal{A}}$ in the following parts. The problem with this connection is that it is non-commutative. Indeed, the bracket $\{\tilde{\mathcal{A}}^X, \tilde{\mathcal{A}}^Y\}_D$ does not vanish and turns out to be complicated. This comes from the fact that the rotational part of $\tilde{\mathcal{A}}^{10}$ is not independent of the triad field \mathcal{R} whereas the boost part of $\tilde{\mathcal{A}}$ is canonically conjugate to the boost triad $\mathcal{B} = \star \mathcal{R}$. The explicit relation between $\tilde{\mathcal{A}}$ and \mathcal{R} which can be found in [57, 53] is reminiscent of the reality constraint $A_a^i + \bar{A}_a^i = \Gamma_a^i(E)$ of the complex loop quantum gravity formulation. On the other hand, both the rotation and the boost parts of $\tilde{\mathcal{A}}$ are commutative. Therefore, the geometrical interpretation of $\tilde{\mathcal{A}}$ in quantum theory is not straightforward. However, we will see in the chapter 5 that it is possible to precisely define the Hilbert and quantum states of space(-time) geometry at least at the kinematical level.

⁹This is required in order that the states resulting from a loop quantization using the connection $\tilde{\mathcal{A}}$ diagonalize the area operators $A_S = \int_S d^2x \sqrt{n_a n_b \mathcal{R}_X^a \mathcal{R}^{bX}}$ with n_a the normal to the surface S .

¹⁰We can define $(P_{\mathcal{R}})_Y^X = \mathcal{R}_a^X \mathcal{R}_Y^a$, $(P_{\mathcal{B}})_Y^X = \mathcal{B}_a^X \mathcal{B}_Y^a$ which are respectively the projector on the Lie subalgebra of H_x (rotations) and on its orthogonal complement (boosts). The rotational part of $\tilde{\mathcal{A}}$ is then given by $P_{\mathcal{R}} \tilde{\mathcal{A}}$ and its boost part by $P_{\mathcal{B}} \tilde{\mathcal{A}}$.

Chapter 4

Loop Quantum Gravity

We now come back to the time gauge fixed 'triad-connection' formulation of general relativity which was the key to reformulate general relativity in a more amenable way to Dirac's quantization than the ADM formulation. The general aim is now to construct a Hilbert space of dynamical (physical) states which are annihilated by the quantum version of the constraints we derived earlier, using the $SU(2)$ Ashtekar-Barbero variables. To recapitulate the classical Hamiltonian analysis we have recalled, we have formulated general relativity as a $SU(2)$ gauge theory, with Poisson brackets (3.34) and the three sets of constraints

$$\begin{array}{ll} G_i = 0 & \text{Gauss law,} \\ V_a = 0 & \text{Spatial diffeomorphism,} \\ S = 0 & \text{Hamiltonian constraint.} \end{array}$$

Note however that there is a key difference between general relativity and a gauge theory. Indeed, in a standard gauge theory like Yang-Mills, after imposing the Gauss law, the dynamics is determined by a physical Hamiltonian whereas in general relativity the whole dynamics content is in the four left constraints (V_a, S) .

The loop quantum gravity program starts with the definition of the kinematical Hilbert space \mathcal{H}_{kin} . Once a well-behaved kinematical Hilbert space is constructed, we can follow Dirac's procedure and we will have a well-posed problem of reduction by the constraints

$$\begin{array}{ccccccc} \mathcal{H}_{\text{kin}} & \xrightarrow{\hat{G}_i=0} & \mathcal{H}_{\text{kin}}^G & \xrightarrow{\hat{V}_a=0} & \mathcal{H}_{\text{Diff}} & \xrightarrow{\hat{S}=0} & \mathcal{H}_{\text{phys}} \\ \text{cylindrical functions} & & \text{spin networks} & & \text{abstract spin networks} & & ? \end{array} \quad (4.1)$$

4.1 The kinematical Hilbert space and cylindrical functions

We regard the connection as the configuration variable. The kinematical Hilbert space consists of a suitable set of functionals $\Psi[A]$ of the connection which have to be square integrable with respect to a suitable gauge invariant and diffeomorphism invariant measure $d\mu_{AL}[A]$. The kinematical inner product will then be given by:

$$\langle \Psi, \Phi \rangle = \mu_{AL}[\bar{\Psi}\Phi] = \int d\mu_{AL}[A] \bar{\Psi}[A] \Phi[A]. \quad (4.2)$$

The difficulty at this stage comes from the fully dynamical feature of the metric. We do not have a background metric at disposal to define the integration measure. We need to define a measure on the space of connections without relying on any fixed background metric. The key to do this relies on the notion of cylindrical functions. We have already seen that a natural quantity associated with a connection consists in the holonomy along a path (3.36). We recall that geometrically the holonomy $h_e[A]$ is a functional of the connection that provides a rule for the parallel transport of $SU(2)$ spinors along the path e . If we think of it as a functional of the path e it is clear that it captures all the information about the field A_a^i . In addition, it has a very simple behavior under the transformations generated by six of the constraints.

- Under the gauge transformation generated by the Gauss constraint G_i , the holonomy transforms as

$$h_e^g = g_{s(e)} h_e g_{t(e)}^{-1} \quad (4.3)$$

where $s(e)$ and $t(e)$ are respectively the source and the target points of the path e .

- Under the diffeomorphism action generated by the vector constraint V_a , the holonomy transforms given $\phi \in \text{Diff}(\Sigma)$

$$h_e[\phi^* A] = h_{\phi \circ e}[A], \quad (4.4)$$

where $\phi^* A$ denotes the action of ϕ on A . Transforming the connection with a diffeomorphism is therefore equivalent to simply 'moving' the path with ϕ .

For these reasons, the holonomy is a natural choice of basic functional of the connection.

We call *cylindrical functions* the functionals that depend on the connection only through the holonomies $h_e[A] = \mathcal{P}(\int_e A)$ along some finite set of paths e . Given a graph $\Gamma \subset \Sigma$, defined as a collection of oriented paths $e \subset \Sigma$ meeting at most at their endpoints, we denote by E the total number of edges it contains. A cylindrical function $\psi_{(\Gamma, f)}[A]$ is a functional of the connection A , labelled by a graph Γ and a smooth function $f : \text{SU}(2)^E \rightarrow \mathbb{C}$

$$\psi_{(\Gamma, f)}[A] = f(h_{e_1}[A], \dots, h_{e_E}[A]) \quad (4.5)$$

where e_i with $i = 1, \dots, E$ are the edges of the corresponding graph Γ . Given a graph Γ , we denote by Cyl_Γ the space of cylindrical functions associated to Γ .

The next step is to equip Cyl_Γ with a scalar product in order to turn it into an Hilbert space. The switch from the connection to the holonomy which is an $\text{SU}(2)$ element, is here crucial since there exists a unique gauge-invariant and normalized measure dg of $\text{SU}(2)$, called the Haar measure¹. Using E copies of the Haar measure, we define on Cyl_Γ the following scalar product

$$\langle \psi_{(\Gamma, f)} | \psi_{(\Gamma, g)} \rangle \equiv \int \left[\prod_{e \in \Gamma} dh_e \right] \overline{f(h_{e_1}[A], \dots, h_{e_E}[A])} g(h_{e_1}[A], \dots, h_{e_E}[A]). \quad (4.6)$$

This turns Cyl_Γ into an Hilbert space \mathcal{H}_Γ associated to a given graph Γ . Next, we need to consider Cyl the algebra of the cylindrical functions of the connection A which can be defined as

$$Cyl(A) = \bigcup_{\gamma} Cyl_\gamma \quad (4.7)$$

where \bigcup_{γ} denotes the union on all graphs γ in Σ . We can then deduced from (4.6) a scalar product between two cylindrical functions in $Cyl(A)$. Indeed, any cylindrical function $\psi_{(\Gamma', f')}$ based on a graph Γ' can be viewed as a cylindrical function $\psi_{(\Gamma, f)}$ based on a larger graph Γ containing Γ' by simply choosing f to be independent from the links in Γ but not in Γ' . Moreover, any edge of a graph can be broken in two edges, separated by a (bivalent) node. As a consequence the scalar product for two cylindrical functions $\psi^{(1)}, \psi^{(2)}$ with graphs Γ_1 and Γ_2 is constructed as follows.

- If $\psi^{(1)}, \psi^{(2)}$ share the same graph, the definition of the scalar product (4.6) immediately applies.
- If they have different graphs, say Γ_1, Γ_2 , they can be viewed as having the same graph Γ_3 formed by the union of the two graphs $\Gamma_3 \equiv \Gamma_1 \cup \Gamma_2$ (f_1 and f_2 are trivially extended on Γ_3) and we define the scalar product on Γ_3 as (4.6).

$$\langle \psi_{(\Gamma_1, f_1)}^{(1)} | \psi_{(\Gamma_2, f_2)}^{(2)} \rangle \equiv \langle \psi_{(\Gamma_3, f_1)}^{(1)} | \psi_{(\Gamma_3, f_2)}^{(2)} \rangle. \quad (4.8)$$

¹The Haar measure of $\text{SU}(2)$ is defined by the following properties:

$$\int_{\text{SU}(2)} dg = 1, \quad \text{and} \quad dg = d(\alpha g) = d(g\alpha) = dg^{-1} \quad \forall \alpha \in \text{SU}(2).$$

This last definition can be interpreted as a scalar product between cylindrical functionals of the connection:

$$\int d\mu_{AL}[A] \overline{\psi_{(\Gamma_1, f_1)}^{(1)}[A]} \psi_{(\Gamma_2, f_2)}^{(2)}[A] \equiv \langle \psi_{(\Gamma_1, f_1)}^{(1)} | \psi_{(\Gamma_2, f_2)}^{(2)} \rangle \quad (4.9)$$

with respect to $d\mu_{AL}$, the so-called Ashtekar-Lewandowski measure, which is an integration measure over the space of connections [58]. This key result, due to Ashtekar and Lewandowski, can be reformulated as follows. The measure $d\mu_{AL}$ allows us to define an Hilbert space \mathcal{H}_{kin} as the Cauchy completion of the space of cylindrical functions \mathcal{Cyl} in the Ashtekar-Lewandowski measure $d\mu_{AL}$

$$\mathcal{H}_{\text{kin}} = \overline{\mathcal{Cyl}(A)}, \quad (4.10)$$

that is in addition to cylindrical functions we add to \mathcal{H}_{kin} the limits of all the Cauchy convergent sequences in the μ_{AL} norm.

It is convenient to introduce an orthonormal basis for \mathcal{H}_{kin} . This can be easily done thanks to the Peter-Weyl theorem. This theorem can be viewed as a generalization of Fourier theorem for functions on \mathcal{S}^1 . It states that, given a function $f \in L_2[\text{SU}(2)]$, it can be expressed as a sum over irreducible representations of $\text{SU}(2)$, namely

$$f(g) = \sum_j d_j \hat{f}_{mn}^j D_{mn}^{(j)}(g), \quad j \in \mathbb{N}/2, \quad m = -j, \dots, j, \quad d_j = 2j + 1, \quad (4.11)$$

where

$$\hat{f}_{mn}^j = d_j \int_{\text{SU}(2)} dg D_{mn}^{(j)}(g) f(g), \quad (4.12)$$

with dg is the Haar measure of $\text{SU}(2)$ and the Wigner matrices $D_{mn}^{(j)}(g)$ give the spin- j irreducible matrix representation of the group element g . The Peter-Weyl theorem can be applied to any cylindrical function $\psi_{(\Gamma, f)} \in \mathcal{H}_{\Gamma}$, since \mathcal{H}_{Γ} is just a tensor product of $L_2(\text{SU}(2), d\mu_{\text{Haar}})$

$$\begin{aligned} \psi_{(\Gamma, f)}[A] &= f(h_{e_1}[A], \dots, h_{e_E}[A]) \\ &= \sum_{j_e, m_e, n_e} \hat{f}_{m_1, \dots, m_E, n_1, \dots, n_E}^{j_1, \dots, j_E} \tilde{D}_{m_1 n_1}^{(j_1)}(h_{e_1}[A]) \dots \tilde{D}_{m_E n_E}^{(j_E)}(h_{e_E}[A]), \end{aligned} \quad (4.13)$$

where we have introduced the normalized representation matrices $\tilde{D}_{mn}^{(j)} := \sqrt{d_j} D_{mn}^{(j)}$. According to (4.12), $\hat{f}_{m_1, \dots, m_E, n_1, \dots, n_E}^{j_1, \dots, j_E}$ is given by the kinematical inner product of the cylindrical function $\psi_{(\Gamma, f)}$ with the tensor product of irreducible representations $\tilde{D}_{m_1 n_1}^{(j_1)} \dots \tilde{D}_{m_E n_E}^{(j_E)}$

$$\hat{f}_{m_1, \dots, m_E, n_1, \dots, n_E}^{j_1, \dots, j_E} = \langle \tilde{D}_{m_1 n_1}^{(j_1)} \dots \tilde{D}_{m_E n_E}^{(j_E)} | \psi_{(\Gamma, f)} \rangle, \quad (4.14)$$

where $\langle | \rangle$ is the kinematical inner product defined by (4.6). Moreover, the Wigner matrix elements, matrix elements of the unitary irreducible representation of $\text{SU}(2)$, form a complete set of orthogonal functions of $\text{SU}(2)$

$$\int dg D_{m_1 n_1}^{(j_1)}(g) D_{m_2 n_2}^{(j_2)}(g) = \frac{1}{2j_1 + 1} \delta_{j_1 j_2} \delta_{m_1 m_2} \delta_{n_1 n_2}. \quad (4.15)$$

Thus, the product of components of irreducible representations $\prod_{i=1}^E D_{m_i n_i}^{(j_i)}[h_{e_i}]$ associated with the E edges $e \in \Gamma$ (for any graph Γ , for all values of the spin j , and $-j \leq m, n \leq j$) is a complete orthonormal basis of \mathcal{H}_{kin} .

4.2 Gauge-invariant Hilbert space and spin networks

We are now interested in the solutions of the quantum Gauss constraint. They are characterized by the states in \mathcal{H}_{kin} which are $\text{SU}(2)$ gauge invariant. They define a new Hilbert space $\mathcal{H}_{\text{kin}}^G$ and an orthonormal basis in $\mathcal{H}_{\text{kin}}^G$ is the so-called *spin network* basis which is a very important tool in the theory [59, 60, 61, 62, 63].

The simplest example of a $SU(2)$ gauge invariant cylindrical function is given by the Wilson loop $W_\gamma[A]$. Given a closed loop γ , the Wilson loop is defined as the trace of the holonomy $h_\gamma[A]$ around the loop, namely

$$W_\gamma[A] := \text{tr}[h_\gamma[A]]. \quad (4.16)$$

The gauge invariance of a Wilson loop is straightforward from the behavior of the holonomy under $SU(2)$ gauge transformation (4.3) and the invariance of the trace. Using $SU(2)$ unitary irreducible representation matrices of spin $j \in \mathbb{N}/2$ for $-j \leq m, n \leq j$, the cylindrical function $W_\gamma^j[A]$ is the simplest example of spin network function.

$$W_\gamma^j[A] := \sum_m D_{mm}^j(h_\gamma[A]) \quad (4.17)$$

As already mentioned, spin network functions, which are $SU(2)$ gauge invariant functionals of the connection, form a complete set of orthogonal solutions of the Gauss constraints. To construct a spin network, let us impose the gauge-invariance to a generic cylindrical function. This requires the spin network to be invariant under the gauge transformations that act on the nodes n of the graph Γ :

$$\begin{aligned} \psi_{(\Gamma, f)} &= f(h_{e_1}, \dots, h_{e_E}) \\ &= f(g_{s_1} h_{e_1} g_{t_1}^{-1}, \dots, g_{s_E} h_{e_E} g_{t_E}^{-1}). \end{aligned} \quad (4.18)$$

This property can be easily implemented via group averaging. Given an arbitrary $F \in Cyl_\gamma$,

$$\psi_{(\Gamma, f)} = \int \prod_n dg_n F(g_{s_1} h_{e_1} g_{t_1}^{-1}, \dots, g_{s_E} h_{e_E} g_{t_E}^{-1}) \quad (4.19)$$

clearly satisfies (4.18).

Let us first illustrate this procedure to construct a more sophisticated example of spin network function than the Wilson loop. We consider a theta graph represented by the graph in Fig. 4.1. We associate to this graph a

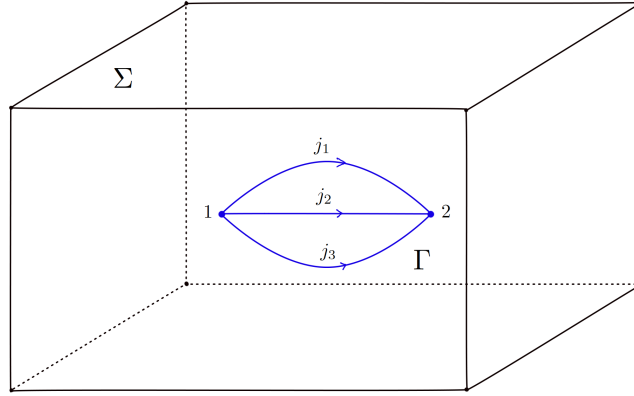


Figure 4.1: An embedded theta graph

generic cylindrical function that we decompose in Fourier modes as in (4.11). Since the gauge transformations act only on the group elements, the gauge-invariant part is obtained by looking at the gauge-invariant part of the product of Wigner matrices,

$$\psi_{(\Gamma, f)}^{\text{inv}}[A] = \sum_{j_e, m_e, n_e} \hat{f}_{m_1, m_2, m_3, n_1, n_2, n_3}^{j_1, j_2, j_3} \left[D_{m_1 n_1}^{(j_1)}(h_1[A]) D_{m_2 n_2}^{(j_2)}(h_2[A]) D_{m_3 n_3}^{(j_3)}(h_3[A]) \right]_{\text{inv}}.$$

The invariant part of the basis is selected thanks to the group averaging

$$\left[D_{m_1 n_1}^{(j_1)}(h_1) D_{m_2 n_2}^{(j_2)}(h_2) D_{m_3 n_3}^{(j_3)}(h_3) \right]_{\text{inv}} = \int dg_1 dg_2 D_{m_1 n_1}^{(j_1)}(g_1 h_1 g_2^{-1}) D_{m_2 n_2}^{(j_2)}(g_1 h_2 g_2^{-1}) D_{m_3 n_3}^{(j_3)}(g_1 h_3 g_2^{-1}),$$

where the projector on the gauge invariant space can be isolated

$$\mathcal{P}_{m_1 m_2 m_3 \alpha_1 \alpha_2 \alpha_3} = \int dg_1 D_{m_1 \alpha_1}^{(j_1)}(g_1) D_{m_2 \alpha_2}^{(j_2)}(g_1) D_{m_3 \alpha_3}^{(j_3)}(g_1).$$

We obtain therefore that

$$\left[D_{m_1 n_1}^{(j_1)}(h_1) D_{m_2 n_2}^{(j_2)}(h_2) D_{m_3 n_3}^{(j_3)}(h_3) \right]_{\text{inv}} = \mathcal{P}_{m_1 m_2 m_3 \alpha_1 \alpha_2 \alpha_3} \mathcal{P}_{\beta_1 \beta_2 \beta_3 n_1 n_2 n_3} D_{\alpha_1 \beta_1}^{(j_1)}(h_1) D_{\alpha_2 \beta_2}^{(j_2)}(h_2) D_{\alpha_3 \beta_3}^{(j_3)}(h_3).$$

The projector \mathcal{P} can be written in terms of the Wigner's 3j-symbols (which are normalized Clebsch-Gordan coefficients²) when the triangular conditions $|j_2 - j_3| \leq j_1 \leq j_2 + j_3$ (also called Clebsch-Gordan conditions) hold,

$$\int dg_1 D_{m_1 \alpha_1}^{(j_1)}(g_1) D_{m_2 \alpha_2}^{(j_2)}(g_1) D_{m_3 \alpha_3}^{(j_3)}(g_1) = \begin{pmatrix} j_1 & j_2 & j_3 \\ m_1 & m_2 & m_3 \end{pmatrix} \overline{\begin{pmatrix} j_1 & j_2 & j_3 \\ \alpha_1 & \alpha_2 & \alpha_3 \end{pmatrix}}. \quad (4.20)$$

With this notation,

$$\left[D_{m_1 n_1}^{(j_1)}(h_1) D_{m_2 n_2}^{(j_2)}(h_2) D_{m_3 n_3}^{(j_3)}(h_3) \right]_{\text{inv}} = \begin{pmatrix} j_1 & j_2 & j_3 \\ m_1 & m_2 & m_3 \end{pmatrix} \overline{\begin{pmatrix} j_1 & j_2 & j_3 \\ n_1 & n_2 & n_3 \end{pmatrix}} \prod_e D^{(j_e)}(h_e) \prod_n i_n,$$

where i_n is here a short-hand notation for the 3j-symbols. More generally, it will also denote the invariant tensor in the space of $\otimes_{e \in n} j_e$ of all spins j_e that enter in the node n . i_n is called an *intertwiner*. Finally, we have

$$\psi_{(\Gamma, f)}^{\text{inv}} = \sum_{j_e} \hat{f}^{j_1, j_2, j_3} \prod_e D^{(j_e)} \prod_n i_n, \quad (4.21)$$

where $\hat{f}^{j_1, j_2, j_3} = \sum_{m_e n_e} \hat{f}_{m_1, m_2, m_3, n_1, n_2, n_3}^{j_1, j_2, j_3} \begin{pmatrix} j_1 & j_2 & j_3 \\ m_1 & m_2 & m_3 \end{pmatrix}$. In this theta graph example, we have seen that the projector on the gauge invariant space acts non trivially only at both the 3-valent nodes and it can be written as

$$\mathcal{P} = i i^*, \quad (4.22)$$

with i an intertwiner which is unique and given by Wigner's 3j-symbols in that 3-valent node case and i^* its dual. This formula of the projector (4.22) can be generalized to a N -valent vertex:

$$\mathcal{P} : \begin{cases} \bigotimes_{e=1}^N V^{(j_e)} = \bigoplus_i V^{(j_i)} \longrightarrow \text{Inv}[\bigotimes_e V^{(j_e)}] = V^{(0)} \\ \prod_e D_{m_e n_e}^{(j_e)}(g) \mapsto \mathcal{P}_{m_1 \dots m_N, n_1 \dots n_N} \equiv \int dg \prod_e D_{m_e n_e}^{(j_e)}(g) = \sum_{\alpha=1}^{\dim V^{(0)}} i_{m_1 \dots m_N}^{\alpha} i_{n_1 \dots n_N}^{\alpha*}, \end{cases} \quad (4.23)$$

with $\bigotimes_{e=1}^N V^{(j_e)}$ the tensor product of $\text{SU}(2)$ irreducible representations. The integration in the definition (4.23) of the projector \mathcal{P} selects the gauge invariant part of $\bigotimes_e V^{(j_e)}$, namely the singlet space $V^{(0)}$, if the latter exists. $i_{m_1 \dots m_N}^{\alpha}$ is an orthonormal set of invariant vectors (where α labels the basis elements and α^* labels the dual basis elements), i.e. an orthonormal basis for $\text{Inv}[\bigotimes_e V^{(j_e)}] = V^{(0)}$. These invariants are the so-called *intertwiners*. In fact, any intertwiner in the tensor product of an arbitrary number of irreducible representations can be expressed in terms of basic intertwiners between three irreducible representations uniquely defined by the Wigner's 3j-symbols (see Fig. 4.2).

²The explicit relation between the Wigner's 3j-symbol and the Clebsch-Gordan coefficient is given by

$$\begin{pmatrix} j_1 & j_2 & j_3 \\ m_1 & m_2 & m_3 \end{pmatrix} = \frac{(-1)^{j_1 - j_2 - m_3}}{\sqrt{2j_3 + 1}} \langle j_1 m_1 j_2 m_2 | j_3 - m_3 \rangle.$$

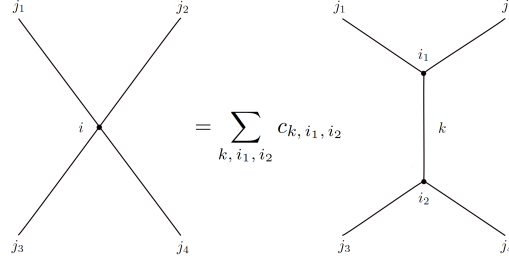


Figure 4.2: Example of decomposition of an intertwiner: any intertwiner between four irreducible representations can be split into two intertwiners between three irreducible representations.

The result (4.21) can be generalized: any solution of the Gauss constraint can be written as a linear combination of products of representation matrices $D^{(j_e)}(h_e)$ contracted with intertwiners.

To summarize, these states labeled with a graph Γ , an irreducible representation $D^{(j)}(h)$ of spin j of the holonomy h along each link and an element i_n of the intertwiner space $\text{Inv}[\bigotimes_e V^{(j_e)}]$ in each node, are called *spin network states*, and are given by

$$\psi_{\Gamma, j_e, i_n}[h_e] \equiv \bigotimes_e D^{(j_e)}(h_e) \bigotimes_n i_n \quad (4.24)$$

where the indices of representation matrices and intertwiners are left implicit in order to simplify the notation (see Fig. 4.3).

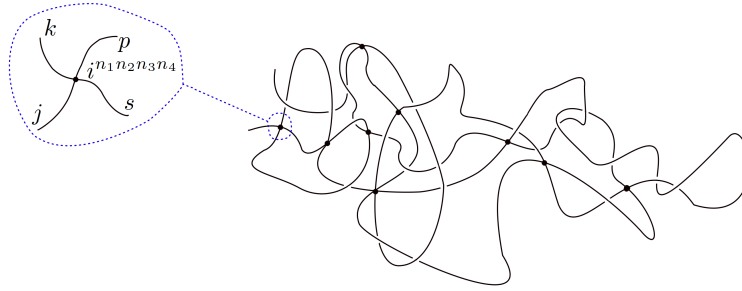


Figure 4.3: Schematic representation of the construction of a spin network. To each node, we associated an invariant vector in the tensor product of irreducible representations converging at the node. For the node magnified on the left, we take $i^{n_1 n_2 n_3 n_4} \in j \otimes k \otimes p \otimes s$ and the relevant piece of spin network function is $D^j(h_{e_1}[A])_{m_1 n_1} D^k(h_{e_2}[A])_{m_2 n_2} D^p(h_{e_3}[A])_{m_3 n_3} D^s(h_{e_4}[A])_{m_4 n_4} i^{n_1 n_2 n_3 n_4}$.

Spin network states form a complete basis of the Hilbert space of solutions of the quantum Gauss law $\mathcal{H}_{\text{kin}}^G$ [61].

The geometrical interpretation of spin network states is provided by the properties of the area and volume operators.

The area operator $\hat{A}(\mathcal{S})$ [38, 39, 40] is a self-adjoint operator well-defined on $\mathcal{H}_{\text{kin}}^G$, such that its classical limit is the geometrical area of the two-dimensional surface $\mathcal{S} \subset \Sigma$. It is diagonalized by a basis of spin network states [40, 40], more explicitly, its action on a spin network ψ_Γ is given by

$$\hat{A}(\mathcal{S}) \psi_\Gamma = 8\pi l_P^2 \gamma \sum_{p \in \mathcal{S} \cap \Gamma} \sqrt{j_p(j_p + 1)} \psi_\Gamma. \quad (4.25)$$

where p are the intersection points between the spin network ψ_Γ and the surface \mathcal{S} (see Fig. 4.4).

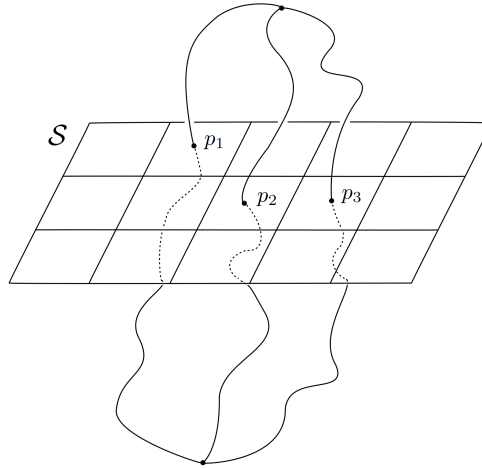


Figure 4.4: A simple spin network intersecting a surface \mathcal{S} . We have considered a partition of the surface \mathcal{S} sufficiently fine for which each puncture p_k falls on a different small surface \mathcal{S}_k ($k \in \{1, 2, 3\}$). The punctures p_k are the intersection points between the spin network ψ_Γ and the surface \mathcal{S} (for further details, see [64]).

Notice that the spectrum of the area operator depends on the value of the Immirzi parameter γ . Moreover, the spectrum of the area operator is discrete. It can be said that edges of spin networks carry a quanta of area. We will not give any details concerning the volume operator but the same kind of procedure can be applied to construct a quantum operator corresponding to the volume of a 3-hypersurface [38, 39, 65, 66] and to find that the eigenspectrum is again discrete. Two distinct mathematically well-defined volume operators have been proposed in the literature [38, 39, 66]. Both of them act not trivially only at the nodes of a spin network state and the volume is given by the nodes (plus some additional labels to resolve degeneracy when needed) of the spin network inside the hypersurface [38, 39, 65, 67, 68, 69, 70].

Therefore, all the information about the degrees of freedom of geometry (hence the gravitational field) is contained in the combinatorial aspects of the graph (what is connected to what) and in the discrete quantum numbers labeling area quanta (spin labels of edges) and volume quanta (linear combinations of intertwiners at nodes).

4.3 Loop quantum gravity and dynamics

4.3.1 Solutions of the diffeomorphism constraint: abstract spin networks

From now on, we note S the (embedded) spin network given by the triplet (Γ, j_e, i_n) . It is essentially a colored graph as illustrated in Fig. 4.1. It defines a quantum state $|S\rangle$, represented in terms of the connection by a functional, a spin network state $\psi_S[A]$ such that $\psi_S[A]$ is in $\mathcal{H}_{\text{kin}}^G$, i.e. $\hat{G}_i \psi_S[A] = 0$. The next step in the Dirac program is to implement the spatial diffeomorphisms, namely to find gauge-invariant states such that $\hat{V}^a \psi_S[A] = 0$. We will not give the details of the construction of $\mathcal{H}_{\text{Diff}}$, the Hilbert space of diffeomorphism invariant states. An analogous technique to the one used to obtain $\mathcal{H}_{\text{kin}}^G$ can be applied. We will only emphasize the fact that the orbits of the diffeomorphisms are not compact (contrary to the orbits of the Gauss constraint). Consequently, diffeomorphism invariant states are not contained in the original \mathcal{H}_{kin} . They have to be regarded as distributional states³. The diffeomorphism-invariant Hilbert space $\mathcal{H}_{\text{Diff}}$ which can be considered as the space

³Diffeomorphism invariant states are therefore in the dual of the cylindrical functions Cyl . The Gelfand triple of interest is $Cyl \subset \mathcal{H}_{\text{kin}} \subset Cyl^*$ and diffeomorphism invariant states have a well defined meaning as linear forms in Cyl^* . We denote $U(\phi)$ the operator representing the action of a diffeomorphism $\phi \in \text{Diff}(\Sigma)$ on $\psi_\Gamma, f[A]$. It is induced by the action of ϕ on the holonomy given

$\mathcal{H}_{\text{kin}}/\text{Diff}(\Sigma)$ turns out to have a natural basis labeled by knots, or more precisely by “ s -knots” (also called *abstract spin network states*). A s -knots is an equivalence class s of embedded spin networks S under the action of diffeomorphisms $\text{Diff}(\Sigma)$, i.e. $S, S' \in s$ if there exists a $\phi \in \text{Diff}(\Sigma)$ such that $S' = \phi \cdot S$ (see Fig. 4.5).

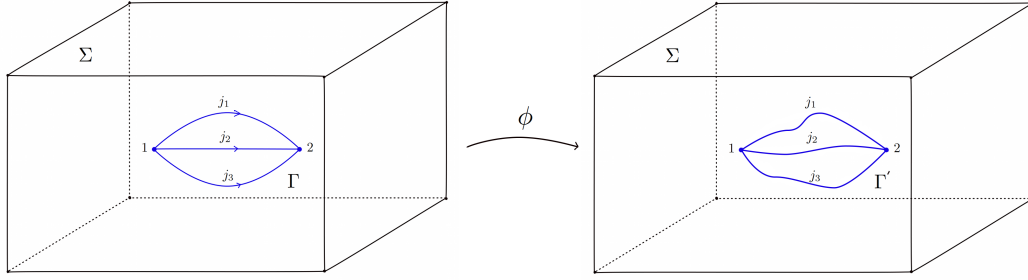


Figure 4.5: $\phi \in \text{Diff}(\Sigma)$: $\phi \circ \Gamma = \Gamma'$ therefore $\{\Gamma'\} \approx \{\Gamma\}$

A s -knot is characterized by its “abstract” graph (defined only by the adjacency relations between links and nodes), by the coloring, and by its knotting and linking properties, as in knot theory. To be more explicit, we still know how loops in the graph wind around holes in the manifold for example, or how edges intersect each other; but “where” the graph sits inside the manifold, its location and its metric properties (e.g. length of edges,...) are no more well-defined concepts. Therefore, each s -knot defines a gauge and diffeomorphism invariant state $|s\rangle$ of the gravitational field. It can be proven that the states $(1/\sqrt{is(s)})|s\rangle$, where $is(s)$ is the number of isomorphisms of the s -knot into itself, preserving the coloring and generated by a diffeomorphism of Σ , form an orthonormal basis for $\mathcal{H}_{\text{Diff}}$. Although s -knots are labelled by discrete quantum numbers, the picture is not truly entirely discrete. It was pointed out in [71] that if the nodes of the s -knots have a valence higher than five, s -knots are labelled also by certain continuous moduli parameters (see [71] for details). These moduli do not seem to play any significant role in the theory (they are virtually undetectable by the hamiltonian operator that governs the dynamics and they do not seem to affect the physics of the theory) but they spoil the discreteness of the picture. In fact they change the structure of $\mathcal{H}_{\text{Diff}}$, rather drastically, making it nonseparable. It has been shown that by using the notion of “extended” diffeomorphisms, the moduli disappear and the knot class become countable. The kinematical Hilbert space of loop quantum gravity, “the extended $\mathcal{H}_{\text{Diff}}$ ”, becomes then separable. For further details see [71].

A s -knot is a purely algebraic kinematical quantum state of the gravitational field: each link of the graph can be seen as carrying a quantum of area and the nodes carrying quanta of volume. A s -knot can therefore be seen as an elementary quantum excitation of space formed by “chunks” of space (the nodes) with quantized volume, separated by sheets of surface (corresponding to the links), with quantized area. The key point is that a s -knot does not live on a manifold. The quantized space does not reside “somewhere” but it defines the “where” by itself. It appears as the dual picture of the quantum geometry of a s -knot state (see Fig. 4.6).

This is the picture of quantum space-time that emerges from loop quantum gravity.

4.3.2 The Hamiltonian constraint

The structure that gives the quantum states of the gravitational field at the kinematical level is therefore well understood. We still have to consider the scalar (Hamiltonian) constraint which encodes the dynamics. Indeed, the physical state of the theory should lie in the kernel of the quantum Hamiltonian constraint operator \hat{S} . I will give here neither any details concerning the well posed definition of this constraint nor a strategy to compute its kernel (for details see [3, 72, 73, 74]). I will only give the action of the Thiemann’s Hamiltonian operator, \hat{S} , on a spin network $|S\rangle$ [73].

by (4.4). This operator maps Cyl_{Γ} to $Cyl_{\phi \circ \Gamma}$, that is $U(\phi)\psi_{\Gamma, f}[A] = \psi_{\phi \circ \Gamma, f}[A]$. Its action is well-defined and unitary, thanks to the fact that the Ashtekar-Lewandowski measure is diffeomorphism invariant. To explicitly obtain states which are invariant under U , one has to solve $U\psi = \psi$ for (distributional states) $\psi \in Cyl^*$. For details on the resolution, see [58, 32].

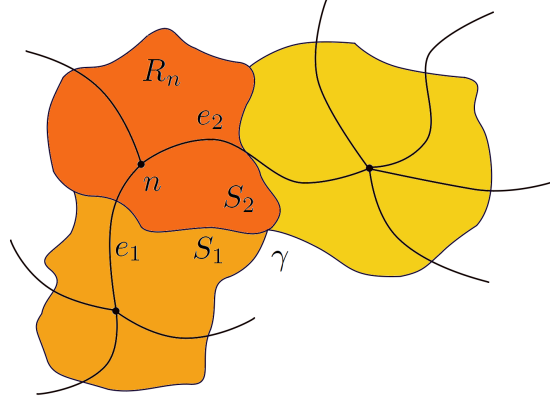


Figure 4.6: A portion of a s -knot graph and the associated dual picture of quantum geometry. The region R_n is dual to the node n . Two adjacent regions are shown. The surface S_1 and S_2 are dual to the links e_1 and e_2 . They identify a curve γ on the boundary of R_n .

It acts only on the nodes of the spin network. The result turns out to be given by

$$\hat{S}[N]|S\rangle = \sum_{\text{nodes } n \text{ of } S} A_n N(x_n) \hat{D}_n |S\rangle, \quad (4.26)$$

where x_n refers to the point in which the node n is located and we used $\hat{S}[N]$ the Hamiltonian constraint smeared with a scalar function $N(x)$ given by $\hat{S}[N] = \int d^3x N(x) \hat{S}(x)$. The action of the operator \hat{D}_n is illustrated in the figure on the left-hand side of equation (4.26): an extra link with color one connecting two points v_1 and v_3 lying on distinct links adjacent to the node v is created when acting on a single node. The color of the link between v and v_1 , as well as between v and v_3 is altered and the state is multiplied by a coefficient A_n (explicit expressions are computed in [75]). The action of this Hamiltonian operator has been criticized to be too local [76] in the sense that the modifications performed by this Hamiltonian constraint operator at a given node of a spin network do not propagate over the whole graph but are confined to a neighborhood of the node. Repeated actions of this Hamiltonian operator generate more and more new edges ever closer to the node, never intersecting each other and thus producing a fractal structure⁴. Another criticism regarding this Hamiltonian operator is that it is highly ambiguous; several sources of ambiguities can be distinguished (factor ordering ambiguities, representation ambiguities, loop assignment ambiguities,...) [3].

To conclude this chapter, the kinematics of loop quantum gravity seems to be beautifully under control. One key result of loop quantum gravity, derived using kinematical states given by the spin network states, is that the space is discrete. However, the resolution of the dynamics is still an open question. The effort to gain control over this issue has flourished into two main lines of research. The first one that we will not review here, is the idea of the Master Constraint [77]. One defines a unique constraint implementing simultaneously the vector (diffeomorphism) and scalar (Hamiltonian) constraints. The second one is the spin foam formalism [78].

⁴Let us notice that there is no action of the Hamiltonian operator at the new created nodes and this is quite different from what happens in lattice gauge theory where no new links are created.

This framework will be introduced in details in the last chapter since it is the basis of all my research results presented in the third and fourth parts. However, before reviewing the spin foam formalism, I will recall some important features concerning the kinematics of covariant loop quantum gravity, following the the classical set up which was presented in the section 3.3.

Chapter 5

Covariant Loop Quantum Gravity

Loop quantum gravity as presented above seems to be a promising approach for quantizing general relativity. It gives some interesting results like discrete quanta of area and volume. However, several problems appear (in addition to the implementation of the dynamics). First of all, it is based on the use of space triad and an $SU(2)$ connection where $SU(2)$ is the gauge group for the three dimensional space. Therefore, as we have previously pointed it out, this particular choice of variables loses the explicit covariance of the theory and a space-time geometrical interpretation. Moreover, there exists an additional puzzle: a free parameter in the theory, γ , the Immirzi parameter. This parameter comes out of the canonical transformation (3.28) but creates a full one-parameter family of quantizations which are not unitarily equivalent [79]. Moreover, this unphysical parameter appears in the spectra of the area operator $\hat{A}(\mathcal{S})$.

One way to avoid this ambiguity is to consider the *covariant loop quantum gravity framework*. One main difference with the standard loop quantum gravity is that the area operator has now (at the kinematical level) a continuous spectrum which is now independent of the Immirzi parameter. However, it involves the variable \mathcal{X} , the time normal introduced in 3.3. One of the main advantages of the formalism is that the covariance of the theory is kept; the main drawback of the approach is a non-compact gauge group and a non-commutative connection.

We are going now to review the definition of the kinematical Hilbert space of covariant loop quantum gravity. We recall that the canonical variables are a Lorentz connection $\tilde{\mathcal{A}}$, its conjugated triad \mathcal{R} (a one-form valued in the Lorentz algebra) and the time normal $\chi \in SL(2, \mathbb{C})/SU(2)$. These variables have been defined in the section 3.3.

5.1 Cylindrical Functions and Gauge Invariance

Let us now define the quantum states of space-(time) geometry. Let us consider an arbitrary oriented graph Γ with E edges and V vertices. Since geometric observables (such as area) involve \mathcal{X} and that \mathcal{X} commutes with the connection $\tilde{\mathcal{A}}$ [57, 53], the full configuration space is spanned by functionals dependent on both $\tilde{\mathcal{A}}$ and \mathcal{X} . To define the Hilbert space structure, one considers generalized cylindrical functions which as the usual ones, are associated with graphs and whose dependence on the connection is supposed to be through the Lorentz group elements represented by holonomies $G_e \in SL(2, \mathbb{C})$. In addition, they also depend on the values of the field \mathcal{X} at the vertices¹. Note that \mathcal{X} is naturally encoded in the unit vector $x^I = (1, \mathcal{X}^i)$ as defined in (3.47). Since x is normalized² $|x|^2 = -1$, it is an element of the (upper) hyperboloid $\mathcal{H}_+ = \{x^\mu \in \mathbb{R}^4, |x|^2 = -1, x^0 > 0\}$, which is an homogenous space $\mathcal{H}_+ \sim SL(2, \mathbb{C})/SU(2) \sim SO(3, 1)/SO(3)$. This implies that the generalized cylindrical functions $\varphi(G_e, x_v)$, the functionals of the Lorentz connection and the time-normal field, live on the homogenous space $SL(2, \mathbb{C})^E \times \mathcal{H}_+^V$.

¹Let emphasize that it is possible to chose any Lorentz connection as “configuration” variable. However, we will have to be careful to define operators. For example, in the considered case, since the $SL(2, \mathbb{C})$ connection $\tilde{\mathcal{A}}$ does not commute with itself, the holonomy operators will not simply act by multiplication on the generalized quantum states – the projected spin networks – as it is the case for the action of loop quantum gravity holonomy operators on $SU(2)$ spin networks.

²We are using the signature $(-+++)$

We further require that our functionals $\varphi(G_e, x_v)$ are invariant under the action of the Lorentz group to solve the analogue of the Gauss law $G_X \varphi(G_e, x_v) = 0$.

$$\varphi(G_e, x_v) = \varphi(\Lambda_{s(e)} G_e \Lambda_{t(e)}^{-1}, \Lambda_v \triangleright x_v), \quad \forall \Lambda_v \in \text{SL}(2, \mathbb{C})^{\times V}, \quad (5.1)$$

where $G_e \in \text{SL}(2, \mathbb{C})$, $x_v \in \mathcal{H}_+$. $s(e)$ and $t(e)$ are respectively the source and target vertices of the edge e .

The 4-vector $\Lambda \triangleright x$ is obtained by acting on x by the $\text{SO}(3, 1)$ transformation corresponding to $\Lambda \in \text{SL}(2, \mathbb{C})$. The easiest way to write this action is to represent 4-vectors as 2×2 Hermitian matrices:

$$x = (x_0, x_1, x_2, x_3) \rightarrow X = \begin{pmatrix} x_0 + x_3 & x_1 + ix_2 \\ x_1 - ix_2 & x_0 - x_3 \end{pmatrix}, \quad (5.2)$$

with $\text{tr} X = 2x_0$ and $\det X = -|x|^2$. Then $\text{SL}(2, \mathbb{C})$ group elements act by conjugation, $\Lambda \triangleright X \equiv \Lambda X \Lambda^\dagger$. From there, we can act on the 4-vector $\omega = (1, 0, 0, 0)$, or equivalently on its corresponding matrix $\Omega = \mathbb{I}$, to generate all elements in \mathcal{H}_+ :

$$x = B \triangleright \omega, \quad X = B \mathbb{I} B^\dagger = B B^\dagger, \quad B \in \text{SL}(2, \mathbb{C}). \quad (5.3)$$

It is clear that this expression is invariant under the right $\text{SU}(2)$ action $B \rightarrow B h$ with $h \in \text{SU}(2)$. This actually shows the fact that \mathcal{H}_+ is the coset $\text{SL}(2, \mathbb{C})/\text{SU}(2)$. From these various representations, we can equivalently see our functionals as depending on 4-vectors, 2×2 Hermitian matrices or $\text{SL}(2, \mathbb{C})$ group elements (with an extra $\text{SU}(2)$ invariance), i.e respectively $\varphi(G_e, x_v)$ or $\varphi(G_e, X_v)$ or $\varphi(G_e, B_v)$.

A first important remark on these Lorentz invariant functions is that they are entirely determined by their section at $x_v = \omega$ for all v . Indeed, let us define this section:

$$\phi(G_e) \equiv \varphi(G_e, x_v = \omega). \quad (5.4)$$

Effectively, these functions still satisfy a remaining $\text{SU}(2)$ -invariance, inherited from the full $\text{SL}(2, \mathbb{C})$ -invariance:

$$\phi(G_e) = \phi(h_{s(e)} G_e h_{t(e)}^{-1}), \quad \forall h_v \in \text{SU}(2)^{\times V}. \quad (5.5)$$

And we can reconstruct the full functional from that particular section:

$$\varphi(G_e, x_v) = \varphi(G_e, B_v B_v^\dagger) = \phi(B_{s(e)}^{-1} G_e B_{t(e)}). \quad (5.6)$$

The second remark is that if we integrate over the time-normals, then we recover the standard $\text{SL}(2, \mathbb{C})$ -invariant cylindrical functions, whose basis are $\text{SL}(2, \mathbb{C})$ spin networks. More precisely, we define the group-averaged functional

$$\varphi_g(G_e) = \int_{\mathcal{H}_+^V} [dx_v] \varphi(G_e, x_v) = \int_{\text{SL}(2, \mathbb{C})^V} [d\Lambda_v] \varphi(G_e, \Lambda_v \triangleright \omega), \quad (5.7)$$

where $[dx]$ is the translation-invariant measure on \mathcal{H}_+ inherited from the Haar measure $[d\Lambda]$ on $\text{SL}(2, \mathbb{C})$. This new function satisfy a simple $\text{SL}(2, \mathbb{C})$ -invariance at the vertices:

$$\varphi_g(G_e) = \varphi_g(\Lambda_{s(e)} G_e \Lambda_{t(e)}^{-1}), \quad \forall \Lambda_v \in \text{SL}(2, \mathbb{C})^{\times V}, \quad (5.8)$$

We now have all the tools to endow our space of cylindrical functions with a scalar product, following [80].

$$\langle \varphi | \varphi' \rangle \equiv \int [dG_e] \bar{\varphi}(G_e, x_v) \varphi'(G_e, x_v). \quad (5.9)$$

Due to the $\text{SL}(2, \mathbb{C})$ gauge invariance satisfied by the functionals, it is easy to see that this definition holds for any arbitrary choice of time-normals x_v as long as both functionals are evaluated on the same set of x_v 's. Therefore, this scalar product can be entirely computed by setting all time-normals to the origin ω :

$$\langle \varphi | \varphi' \rangle = \int [dG_e] \bar{\phi}(G_e) \phi'(G_e). \quad (5.10)$$

We call the corresponding L^2 space of functions as the Hilbert space of projected cylindrical functionals on the graph Γ , following the terminology introduced in [80], and we will simply write H for it (leaving implicit the dependence on the underlying graph Γ , since our whole analysis does not involve changing graph).

5.2 The Basis of Projected Spin Networks

The next step is to introduce the basis of the Hilbert space H of Lorentz invariant functions $\varphi(G_e, x_v)$. To this purpose, a few facts about the unitary representations of the Lorentz group $\text{SL}(2, \mathbb{C})$ are recalled in appendix A.

Following the original work [80], we start with the section $\phi(G_e) = \varphi(G_e, \omega)$, which fully determines the whole function $\varphi(G_e, x_v)$. We apply the Plancherel decomposition formula to $\phi(G_e)$ (see appendix A for details), thus attaching an irreducible representation (n_e, ρ_e) and the corresponding matrix $D^{(n_e, \rho_e)}(G_e)$ to each edge e of the graph. Then we glue these matrices at each vertex v of the graph with vectors in the tensor product of the irreps attached to the incoming/outgoing edges. These tensors are not chosen entirely arbitrarily since the functions $\phi(G_e)$ are required to be $\text{SU}(2)$ -invariant at each vertex.

The final result of this procedure are the *projected spin networks*. A projected spin network on the graph Γ is defined by the choice of a $\text{SL}(2, \mathbb{C})$ irrep $\mathcal{I}_e = (n_e, \rho_e)$ for each edge, a choice of couple of $\text{SU}(2)$ irrep (j_e^s, j_e^t) attached to the source and target vertices of each edge, and finally a $\text{SU}(2)$ -intertwiner (or equivalently $\text{SU}(2)$ -invariant tensor, or a singlet state in layman terminology) i_v for each vertex v . The intertwiner i_v lives in the tensor product of the $\text{SU}(2)$ irreps coming in and going out the vertex v , or more precisely:

$$i_v : \bigotimes_{e|s(e)=v} V^{j_e^s} \longrightarrow \bigotimes_{e|t(e)=v} V^{j_e^t}.$$

Then the functions is defined as:

$$\varphi_{\mathcal{I}_e, j_e^s, j_e^t, i_v}(G_e, x_v) \equiv \text{tr} \prod_e \langle \mathcal{I}_e, j_e^s, m_e^s | B_{s(e)}^{-1} G_e B_{t(e)} | \mathcal{I}_e, j_e^t, m_e^t \rangle \prod_v \langle \bigotimes_{e|t(e)=v} \mathcal{I}_e, j_e^t, m_e^t | i_v | \bigotimes_{e|s(e)=v} \mathcal{I}_e, j_e^s, m_e^s \rangle. \quad (5.11)$$

The trace is taken over the $\text{SU}(2)$ representations i.e it amounts to summing over the basis labels $m_e^{s,t}$. We must require that the choice of spins $j_e^{s,t}$ be compatible with the choice of the $\text{SL}(2, \mathbb{C})$ irreps $\mathcal{I}_e = (n_e, \rho_e)$, i.e that $j_e^{s,t} \geq n_e$, else the projected spin network functional would simply vanish.

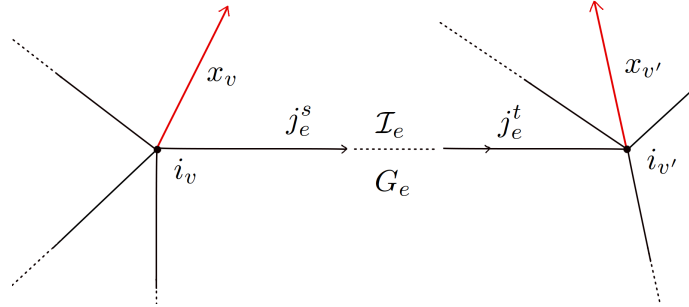


Figure 5.1: An edge of a projected spin network.

First, to check that this function is well-defined, one must make sure that its definition is invariant under the right $\text{SU}(2)$ -action on the group elements B_v . It is actually the requirement of having $\text{SU}(2)$ -invariant intertwiners i_v which ensures that the expression above is correctly invariant under the transformation $B_v \rightarrow B_v h_v$ for all $h_v \in \text{SU}(2)^{\times V}$.

Then, we would like to check that these projected spin networks are properly $\text{SL}(2, \mathbb{C})$ -invariant. The Lorentz action at the vertices reads as:

$$\begin{vmatrix} G_e \\ x_v \\ B_v \end{vmatrix} \longrightarrow \begin{vmatrix} \Lambda_{s(e)} G_e \Lambda_{t(e)}^{-1} \\ \Lambda_v \triangleright x_v \\ \Lambda_v B_v \end{vmatrix}.$$

It is clear that the functions defined above are invariant under such transformations.

Finally, the Plancherel decomposition formula ensures that these projected spin network functionals cover the whole Hilbert space H and provide us with an orthonormal basis. Indeed we can compute the scalar product between two such spin networks:

$$\langle \varphi_{\mathcal{I}_e, j_e^{s,t}, i_v} | \varphi_{\tilde{\mathcal{I}}_e, \tilde{j}_e^{s,t}, \tilde{i}_v} \rangle = \int [dG_e] \bar{\phi}_{\mathcal{I}_e, j_e^{s,t}, i_v}(G_e) \phi_{\tilde{\mathcal{I}}_e, \tilde{j}_e^{s,t}, \tilde{i}_v}(G_e) = \prod_e \frac{\delta_{n_e, \tilde{n}_e} \delta(\rho_e - \tilde{\rho}_e)}{\mu(n_e, \rho_e)} \delta_{j_e^{s,t}, \tilde{j}_e^{s,t}} \prod_v \langle i_v | \tilde{i}_v \rangle. \quad (5.12)$$

Thus a choice of orthonormal basis is given by a choice of an orthonormal basis of $SU(2)$ intertwiners, just as for the standard $SU(2)$ spin networks of Loop Quantum Gravity.

Using these projected spin networks allow to project the Lorentz structures on specific fixed $SU(2)$ representations. This allows to diagonalize the area operators. Considering a surface \mathcal{S} intersecting the graph Γ only on one edge e , its area operator $A[\mathcal{S}]$ will be diagonalized by the projected spin network basis:

$$A[\mathcal{S}] | \varphi_{\mathcal{I}_e, j_e, i_v} \rangle = l_P^2 \sqrt{j_e(j_e + 1) - n_e^2 + \rho_e^2 + 1} | \varphi_{\mathcal{I}_e, j_e, i_v} \rangle \quad (5.13)$$

Interestingly, this spectrum contains a term coming from the Lorentz symmetry which makes it continuous and this spectrum does not depend on the Immirzi parameter which thus remains unphysical (at least at this kinematical level) as it was at the classical level. .

Therefore, we now have described the kinematical structure of covariant loop quantum gravity. We still need to tackle the issue of defining the dynamics of the theory. On one hand, one can try to regularize and quantize *à la Thiemann* the action of the Hamiltonian constraint on the covariant connection $\tilde{\mathcal{A}}$. On the other hand, one can turn to the spin foam formalism.

Chapter 6

Feynman's path integral approach: Spin Foams

The concept of spin foam going from one spin network to another was introduced in order to address the problem of dynamics of loop quantum gravity [81, 82, 32]. We have seen how spin networks describe the (quantum) geometry of space, we now introduce the spin foams which will describe the (quantum) geometry of space-time. The definition of a spin foam is very analogous to a spin network, but everything is one dimension higher. The same algebraic and combinatorial structures as loop quantum gravity are used. Just as a spin network is a graph with edges labeled by representations and vertices labeled by intertwiners, a spin foam is a 2-dimensional piecewise linear cell complex – roughly a finite collection of polygons attached to each other along their edges – with faces labeled by representations and edges labeled by intertwiners.

The spin foam formalism attempts the construction of the path integral representation of the theory in order to provide an explicit tool to compute transition amplitudes in quantum gravity.

The solutions of the scalar constraint can be characterized by the definition of the generalized projection operator P from the kinematical Hilbert space $\mathcal{H}_{\text{Diff}}$ into the kernel of the scalar constraint $\mathcal{H}_{\text{phys}}$. Formally, one can write P as

$$P = \int [dN] e^{i\hat{S}[N]} = \int [dN] e^{i \int N \hat{S}}. \quad (6.1)$$

P can also be defined in a manifestly covariant manner [83, 84], that amounts to giving sense to the path integral of gravity

$$P := \int D[e] D[\omega] \mu[\omega, e] \exp[iS_{\text{GR}}(e, \omega)], \quad (6.2)$$

where we used the first order formulation of gravity given by (3.38): e is the tetrad field, ω is the space time connection and $\mu[\omega, e]$ denotes the appropriate measure.

The matrix elements of P define the physical scalar product $\langle \cdot, \cdot \rangle_P$ providing the vector space of solutions $|\tilde{\psi}\rangle$ of the quantum Einstein's equations $\hat{G}_i|\tilde{\psi}\rangle = 0$, $\hat{V}_a|\tilde{\psi}\rangle = 0$, $\hat{S}|\tilde{\psi}\rangle = 0$ with the Hilbert space structure that defines $\mathcal{H}_{\text{phys}}$.

$$\langle \psi, \psi' \rangle_P := \langle P\psi, \psi' \rangle, \quad \psi, \psi' \in \mathcal{H}_{\text{Diff}}. \quad (6.3)$$

When these matrix are computed in the spin network basis, they can be expressed as a sum over amplitudes of “spin network histories”, i.e. spin foams. They are defined as colored 2-complexes. A 2-complex C is a set of elements called “vertices” v , “edges” e and “faces” f , and a boundary relation among these, such that an edge is bounded by two vertices, and a face is bounded by a cyclic sequence of continuous edges (edges sharing a vertex). A spin foam (see Fig. 6.1) is a 2-complex plus a “coloring” c , that is an assignment of an irreducible representation j_f of $\text{SU}(2)$ (or more generally of any given group G) to each face f and of an intertwiner i_e to each edge e .

More generally, let us give the generic features of the spinfoam framework for an arbitrary gauge group G . We have seen that the Hilbert space of quantum geometry states for loop quantum gravity $\mathcal{H}_{\text{Diff}}$ is spanned by spin network states $|\psi\rangle$ where in $\psi = (\gamma, j_l, i_n)$: γ is a graph, j_l is a “spin” labeling an irreducible representation

of the gauge group G associated to the link l of the graph, and i_n is associated to the node n of γ and labels intertwiners. We consider a 4d space-time region \mathcal{M} with a 3d boundary Σ . The spin network state $|\psi\rangle$ defines the quantum state of geometry of the boundary Σ , then the spin foam amplitudes define the dynamical probability amplitude of that state and encode the whole quantum gravity dynamical content. More precisely, the standard ansatz for local spinfoam amplitudes can be presented in the following general form

$$K[\psi] = \sum_{C|\partial C=\gamma_\psi} w(C) \sum_{j_f, i_e} \prod_f A_f(j_f) \prod_e A_e(j_f, i_e) \prod_v A_v(j_f, i_e), \quad (6.4)$$

where the sum is taken over two-complexes C and their “coloring” $c \equiv \{j_f, i_e\}$. The 2-complexes are constraint to fit the graph γ_ψ of the spin network ψ at the boundary. The representations j_f are associated to the faces f of C and the intertwiners i_e to its edges e . They are also constrained to fit the representation j_l and intertwiners i_n of the state ψ living on the boundary. A spinfoam is then defined as a colored two-complex, namely a couple (C, c) . Finally, the spinfoam amplitude is made of four types of factors. First, $w(C)$ is a statistical weight that depends only on the two-complex C (similar to the symmetry factor for Feynman diagrams in standard quantum field theory). A_f are weight factors associated to the faces and A_e are amplitudes associated to the edges of the 2-complex. These three types of factors can be interpreted as measure factors of the discrete path integral defined by $K[\psi]$. All the dynamical information is encoded in the vertex amplitude, $A_v(j_f, i_e)$, which is an amplitude associated with each vertex v of the two-complex C and depends on the spins j_f and intertwiners i_e living on the faces and edges around that vertex.

The amplitudes are usually assumed to be local, i.e. they depend only on the coloring of adjacent simplicial elements. Thus, A_f is a function of the representations located on the face f , A_e is a function of the intertwiner assigned to e and the representations on the faces containing e , whereas A_v depends on the representations on the faces and on the intertwiners on the edges containing the vertex v . Generally speaking, the choice of the vertex amplitude A_v corresponds to the choice of a specific form of the hamiltonian operator in the canonical theory. Since a spin network state defines a quantum state for the boundary geometry, spin foams are thus interpreted as representing the states of the bulk defining the quantum space-time interpolating between given boundary data.

Let us now focus on the special case where the boundary is made of two disconnected pieces an initial spin network ψ and a final spin network ψ' , which we can interpret as the initial boundary and the final boundary in order to make a clearer connection with the canonical framework, whose goal is to define transition amplitudes between initial and final states. A spin foam $\mathcal{F} : \psi \rightarrow \psi'$ defined by the 2-complex C bordered by the supporting graphs of ψ and ψ' , respectively γ and γ' , represents then a transition from the spin network state $\psi = (\gamma, j_l, i_n)$ into $\psi' = (\gamma', j'_l, i'_n)$. Nodes and links in the initial spin network $|\psi\rangle$ evolve into 1-dimensional edges and faces. New links are created and spins are reassigned at vertexes. This defines a foam-like structure whose components inherit the spin representations from the initial spin network ψ and are at the end compatible with the spin representations of the final spin network ψ' (see Fig. 6.1). The propagator kernel $K[\psi, \psi']$ obtained by summing over all the spinfoams compatible with the boundary data can be then interpreted as the physical inner product between $|\psi\rangle$ and $|\psi'\rangle$

$$\langle \psi, \psi' \rangle_p = \langle P\psi, \psi' \rangle = K[\psi, \psi'] = \sum_{\mathcal{F}|\partial\mathcal{F}=\psi\cup\psi'} \mathcal{A}_{\mathcal{F}}[\psi, \psi'], \quad (6.5)$$

where we have introduced a more compact notation than in (6.4): the sum over the compatible spin foam \mathcal{F} gathers the sum over the two-complexes C compatible with the graphs γ and γ' and the sums over the G-representations compatible with the representations j_l and j'_l and over the intertwiners compatible with i_n and i'_n . $\mathcal{A}_{\mathcal{F}}[\psi, \psi']$ is the spin foam amplitude associated to the spin foam $\mathcal{F} : \psi \rightarrow \psi'$ interpolating between the initial and final states. It is given as above as a product of vertex, edge and face amplitudes: A_v, A_e, A_f . A spin foam thus represents a possible history of the gravitational field and can be interpreted as a set of transitions through different quantum states of space.

In quantum theory, the probability for any fundamental event is given by the absolute square of a complex amplitude; the amplitude for some event is given by adding together all the histories which include that event. In order to find the overall probability amplitude for a given process, one adds up, or integrates, the amplitude

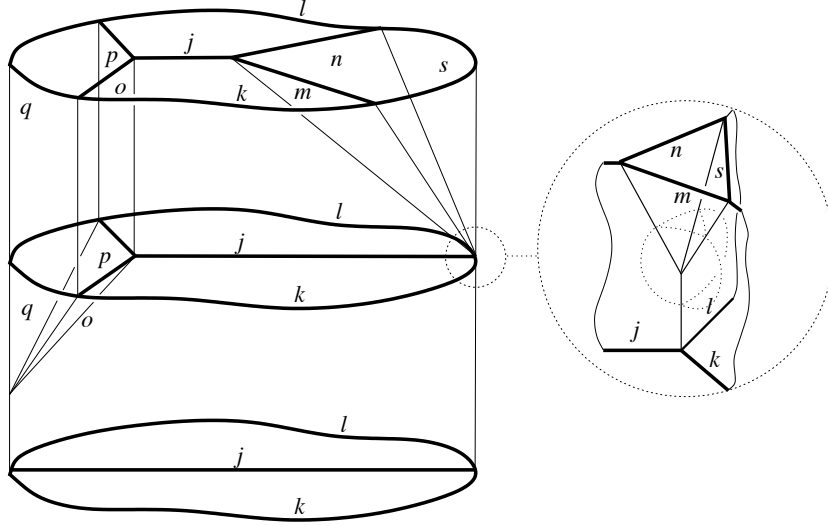


Figure 6.1: A spin foam as a colored 2-complex representing the transition between three different spin network states. The vertex amplitude of the vertex magnified on the right is $A_v(j, k, l, m, n, s)$ [32].

of each possible history over the space of all possible histories of the system in between the initial and final states. In the spinfoam formalism, the *paths* summed over are the 4-geometries represented by the *spin foam* $\mathcal{F} = (C, c)$. The model is defined by the partition function

$$Z = \sum_C w(C) \sum_{j_f, i_e} \prod_f A_f(j_f, i_e) \prod_e A_e(j_f, i_e) \prod_v A_v(j_f, i_e), \quad (6.6)$$

with again A_f , A_e and A_v the amplitude associated to faces, edges, vertices respectively and $w(C)$ a normalization factor for each 2-complex C . We will see in the next sections that this partition function can be derived directly as a regularization of the covariant path integral

$$Z = \int D[e] D[\omega] \mu[\omega, e] \exp[iS_{\text{GR}}(e, \omega)] \quad (6.7)$$

To summarize, quantum gravity formulated as a 'spin foam' consists of a rule for computing amplitudes from spin foam vertices, faces, and edges.

Before going further, we have to emphasize that the sum over spinfoam $\mathcal{F} = (C, c)$ is not exactly well-defined. Usually, for fixed C , the sum over colorings c is well-controlled. On the other hand, controlling the full sum over two-complexes is a much more subtle issue. It is nevertheless non-perturbatively defined as quantum field correlations in the context of *group field theory* (GFT) [85, 86], which are non-local scalar field theories defined over some group manifolds. In this context, $\mathcal{A}_{\mathcal{F}}$ actually depends on the GFT coupling constant λ . Indeed the statistical weight $w(C)$ for a two-complex C is given by the symmetry factor of the two-complex (considered as a Feynman diagram for the GFT) times a factor λ^V where V is the number of vertices of the two-complex. The sum over 4-geometries in $K[\psi]$ can be written as a power series in λ .

$$K[\psi] = \sum_{V=0}^{\infty} \lambda^V K_V[\psi], \quad (6.8)$$

where $K_V[\psi] = \sum_{\mathcal{F}^V |_{\partial \mathcal{F}^V = \psi}} \mathcal{A}_{\mathcal{F}^V}[\psi]$ is the sum over spinfoams \mathcal{F}^V with V vertices. Spin foams appear then naturally as higher-dimensional analogs of Feynman diagrams of the GFT.

Spin foam models were initially constructed as a history formalism for loop quantum gravity describing the evolution of spin network states. However since then, they have been developed as a discretization of the path

integral of general relativity. The more standard procedure is now to start with the path integral of general relativity reformulated as a topological BF gauge theory plus constraints. In three dimensions, general relativity is simply given by the BF theory whereas in 4 dimensions, general relativity can be viewed as a BF theory with extra constraints. We will present this point of view in the following.

Since BF theory is topological, it does not have any local degree of freedom and can be discretized and quantized exactly as a spin foam model without losing any of its physical content. In the first following section, we will illustrate the quantization of a BF theory by deriving the spin foam model for 3d Euclidean gravity, the so-called Ponzano-Regge model.

In four dimensions, we attempt to impose consistently the constraints turning the BF theory into a geometrical theory and introducing local degrees of freedom directly at the quantum level in the spin foam framework. One approach is based on the MacDowell-Mansouri action, which writes general relativity as a BF theory for the gauge group $SO(4, 1)$ (or $SO(5)$ in the Euclidean case) with a non-trivial potential in the B -field which breaks the symmetry down back to the Lorentz group [87]. Although this is a very interesting proposition, it has not yet led to a definite proposal for a spinfoam model. Therefore we will focus on the reformulation using the Plebanski's action which is at the heart of the spinfoam models developed up to now. This will be presented in the second and third following sections.

6.1 Three-dimensional gravity, the Ponzano-Regge model

As we have already mentioned it, in three space-time dimensions, gravity is a topological theory which can be exactly quantized as a spin foam model, the well-known Ponzano-Regge model [21]. We review here the construction of the model for a 3d Riemannian theory of gravity without cosmological constant (see [88] for a review). We consider the general relativity action in first order formalism, which is simply a BF action, on \mathcal{M} a closed manifold.

$$S[B, \omega] = \int_{\mathcal{M}} \text{tr} (B \wedge F[\omega]), \quad (6.9)$$

The triad B is a $\mathfrak{su}(2)$ -valued 1-form, from which the metric is reconstructed as $g_{\mu\nu} = B_{\mu}^I B_{\nu}^J \eta_{IJ}$. The parallel transport on the manifold is given by the $\mathfrak{su}(2)$ -valued connection ω and its curvature $F[\omega] = d\omega + \omega \wedge \omega$ is an $\mathfrak{su}(2)$ -valued 2-form. tr is the trace over the Lie algebra $\mathfrak{su}(2)$. The classical equations of motion impose that the connection is torsion-free and flat

$$d_{\omega} B \equiv dB + [\omega, B] = 0, \quad F[\omega] = 0, \quad (6.10)$$

where $[\cdot, \cdot]$ is the $\mathfrak{su}(2)$ Lie bracket. A simple counting of the degrees of freedom shows that there are no local degrees of freedom. This theory has three types of symmetries: local Lorentz gauge symmetries, diffeomorphisms and translations [89].

The formal path integral for 3d gravity is

$$Z_{\mathcal{M}} = \int \mathcal{D}B \mathcal{D}\omega e^{iS[B, \omega]}. \quad (6.11)$$

Heuristically speaking, since BF theory is topological and does not have any local degree of freedom, we do not expect to lose any information by replacing the manifold \mathcal{M} by a simplicial manifold Δ_3 , with similar topology. More precisely, we consider a triangulation Δ_3 built from gluing tetrahedra together along their respective triangles and edges. The different elements of the triangulation Δ_3 are recalled in Table 6.1. We also need the notion of *dual 2-complex* of Δ_3 , denoted by Δ_3^* , which is a combinatorial object defined by a set of vertices $v^* \subset \Delta_3^*$ (dual to tetrahedra t in Δ_3), edges $e^* \subset \Delta_3^*$ (dual to triangles f in Δ_3) and faces $f^* \subset \Delta_3^*$ (dual to segments e in Δ_3).

The fields B and ω are replaced by configurations which are distributional with support on subsimplices of Δ_3 and its topological dual Δ_3^* respectively. The triad B is a 1-form and as such it is naturally integrated on one dimensional structures. We integrate it along the segments $e \in \Delta_3$ of the triangulation, and replace it by the collection of Lie-algebra elements X_e obtained in this way. To discretize the connection field, one considers the dual 2-complex Δ_3^* . One can naturally consider the holonomy of the connection along the edges

Δ_3	Δ_3^*
tetrahedron	<i>vertex</i> (4 edges, 6 faces)
triangle	<i>edge</i> (3 faces)
segment	<i>face</i>
point	3d region

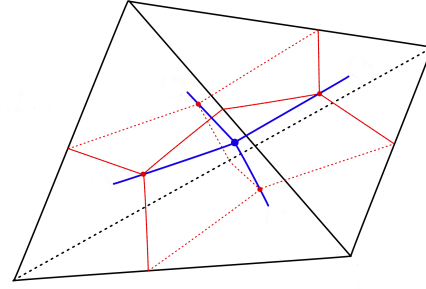
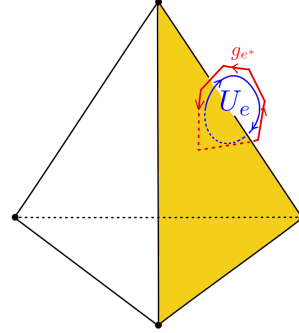


Table 6.1: Relation between a triangulation Δ_3 and its dual Δ_3^* in 3 dimensions. In *italic*, the two-complex. In parentheses: adjacent elements. The figure represents the dual two-complex (blue edges) dual to a tetrahedron (black segments): to each tetrahedron a dual vertex is associated $v^* \sim t$, to each triangle a dual edge is associated $e^* \sim f$ and to each segment a dual face is associated $f^* \sim e$.

e^* of the dual two complex. This assigns a group element g_{e^*} to each dual edge e^* . The discretized curvature is obtained as the holonomy of the connection around an edge e of Δ_3 , which is defined as the ordered product of corresponding group elements living on the dual edges e^* forming the dual face $f^* \sim e$.

$$\begin{aligned}
 B &\rightarrow X_e = \int_e B && \in \mathfrak{su}(2), \\
 \omega &\rightarrow g_{e^*} = \mathcal{P}e^{\int_{e^*} \omega} && \in \text{SU}(2), \\
 F[\omega] &\rightarrow U_e = \prod_{e^* \subset e}^{\rightarrow} g_{e^*}^{\epsilon(e, e^*)} && \in \text{SU}(2).
 \end{aligned}$$



The flatness constraint $F[\omega] = 0$ translates into the triviality of holonomies $U_e = \mathbb{I}$ (around closed loops, for trivial homotopy). After this discretization, the action on the triangulation reads

$$S[X_e, g_{e^*}] = \sum_{e \in \Delta_3} \text{tr}(X_e U_e). \quad (6.12)$$

Actually the original path integral derivation of the Ponzano-Regge model introduced the Lie algebra element $Z_e = \log(U_e) \in \mathfrak{su}(2)$ and considered the action $\sum_e \text{tr}(B_e Z_e)$ [90]. Nevertheless, one faces the issue of the non-continuity of the log map (and the choice of a particular branch and so on). Therefore, we prefer to work with the now more usual formulation presented in [89] which uses directly the group element U_e . The discrete path integral is then given by

$$Z_{\Delta_3} = \left(\prod_{e \in \Delta_3} \int_{\mathfrak{su}(2)} d^3 X_e \right) \left(\prod_{e^* \in \Delta_3^*} \int_{\text{SU}(2)} dg_{e^*} \right) e^{iS[X_e, g_{e^*}]}, \quad (6.13)$$

where the Lebesgue measure $d^3 X_e$ on $\mathfrak{su}(2) \sim \mathbb{R}^3$ and the Haar measure dg_{e^*} on $\text{SU}(2)$ are the natural choices for the discretized path integral measures. Integrating over the X_e variables and using

$$\int dX_e \exp(i \text{tr}(X_e U_e)) = \delta(U_e) = \sum_j d_j \text{tr}(D^j(U_e)), \quad d_j = 2j + 1 \quad (6.14)$$

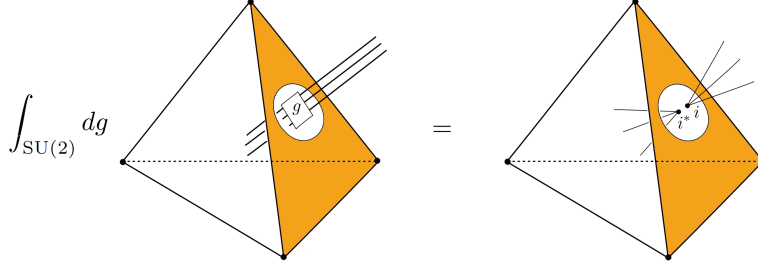
where we used the Peter-Weyl theorem in the last equality, one obtains

$$Z_{\Delta_3} = \sum_{\{j\}} \left(\prod_{e^* \in \Delta_3^*} \int_{\text{SU}(2)} dg_{e^*} \right) \prod_{e \in \Delta_3} d_{j_e} \text{tr} [D^{j_e}(U_e)]. \quad (6.15)$$

Notice that the delta function $\delta(U_e)$ in (6.14) is the delta function on the group $\text{SO}(3)$ and not $\text{SU}(2)$, i.e. it is the distribution localizing the group element U on the identity in $\text{SO}(3)$ and it thus does not distinguish \mathbb{I} and $-\mathbb{I}$ as $\text{SU}(2)$ group elements ($\delta_{\text{SO}(3)}(U) = \delta_{\text{SU}(2)}(U) + \delta_{\text{SU}(2)}(-U)$). Consequently, the sum of the Pancherel decomposition in (6.14) is over integer spin representations $j_e \in \mathbb{N}$. To recover the $\text{SU}(2)$ Ponzano-Regge model with a sum over both integer and half-integer representations $j_e \in \mathbb{N}/2$, the amplitude in the path integral has to be slightly modified [89, 91] in order to kill the $\delta_{\text{SU}(2)}(-U)$ term in the $\delta_{\text{SO}(3)}(U)$ distribution.

We consider that the sum over j_e in (6.15) is now a sum over $j_e \in \mathbb{N}/2$. It remains to integrate over the lattice connection $\{g_{e^*}\}$. Each edge $e^* \subset \Delta_3^*$ bounds 3 faces $f^* \subset \Delta_3^*$, therefore they will be 3 traces of the form $\text{tr} [D^{j_e}(\cdots g_{e^*} \cdots)]$ in (6.15) containing g_{e^*} in argument. In order to integrate over g_{e^*} , we can use the identity (4.20) recalled here

$$\begin{aligned} \int_{\text{SU}(2)} dg D_{m_1 n_1}^{j_1}(g) D_{m_2 n_2}^{j_2}(g) D_{m_3 n_3}^{j_3}(g) &= (-1)^{j_1+j_2+j_3} \begin{pmatrix} j_1 & j_2 & j_3 \\ m_1 & m_2 & m_3 \end{pmatrix} \begin{pmatrix} j_1 & j_2 & j_3 \\ n_1 & n_2 & n_3 \end{pmatrix} \\ &= i i^* \end{aligned} \quad (6.16)$$



where we can recognize the Wigner's 3j-symbol, which is the unique (up to normalization) three valent $\text{SU}(2)$ intertwiner denoted by i . The figure below the equation (6.16) illustrates that each 3j-symbol is in fact associated to a triangle $f \subset \Delta_3$ of a tetrahedron $t \subset \Delta_3$, i.e. in the spin foam quantization procedure, a triangle becomes an intertwiner. The triangles of a given tetrahedron glued together form the boundary of the tetrahedron which is the key kinematical object. An intertwiner i lives on the dual 1-skeleton of the triangle: the intertwiner vertex corresponds to the inside of the triangle while each leg crosses on edge of the triangle (it consequently inherits the same representation j_e). Then, the intertwiners associated to the four triangles of the tetrahedron are glued together into one spin network which defines the quantum state of the boundary of the tetrahedron.

In the case of a tetrahedron, the spin network dual to this original tetrahedron is also a tetrahedron. By combining the four normalized Clebsh-Gordan coefficients ι_1, \dots, ι_4 corresponding to these four triangles, we then get a well-known object in recoupling theory of $\text{SU}(2)$ given by the six variables j_1, \dots, j_6 , irreducible representations of the group, associated to the segments of the tetrahedron (or equivalently to the edges of the dual tetrahedral spin network (see Fig. 6.2)).

$$\begin{aligned} \left\{ \begin{matrix} j_1 & j_2 & j_3 \\ j_4 & j_5 & j_6 \end{matrix} \right\} &= \sum_{m_1, \dots, m_6} (-1)^{j_4+j_5+j_6+m_4+m_5+m_6} \begin{pmatrix} j_1 & j_2 & j_3 \\ m_1 & m_2 & m_3 \end{pmatrix} \begin{pmatrix} j_3 & j_5 & j_4 \\ m_3 & -m_5 & m_4 \end{pmatrix} \\ &\quad \begin{pmatrix} j_4 & j_2 & j_6 \\ -m_4 & m_2 & m_6 \end{pmatrix} \begin{pmatrix} j_6 & j_5 & j_1 \\ -m_6 & m_5 & m_1 \end{pmatrix}, \end{aligned}$$

where $\left\{ \begin{matrix} j_1 & j_2 & j_3 \\ j_4 & j_5 & j_6 \end{matrix} \right\}$ is the so-called $\{6j\}$ -symbol. Finally, the Ponzano-Regge amplitude for a given colored

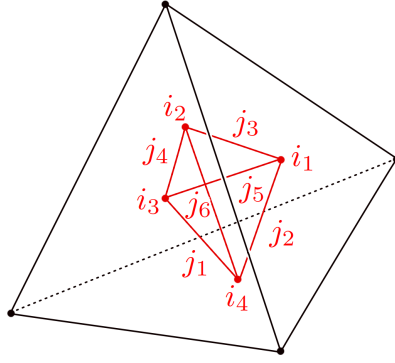


Figure 6.2: Tetrahedron

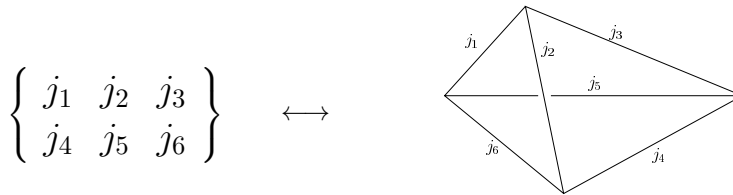
triangulation is simply given by the product of the $\{6j\}$ -symbol

$$Z_{\Delta_3} = \sum_{\{j_e\}} \prod_e d_{j_e} \prod_t \left\{ \begin{matrix} j_1^{(t)} & j_2^{(t)} & j_3^{(t)} \\ j_4^{(t)} & j_5^{(t)} & j_6^{(t)} \end{matrix} \right\}_N, \quad (6.17)$$

where the index N means that it is the normalized $\{6j\}$ symbol which appears¹. Moreover, let us recall that the starting point (6.13) of the construction presented above gives the Ponzano-Regge model for $\text{SO}(3)$ and not $\text{SU}(2)$. In (6.15), the sum over half-integer representations $j_e \in \mathbb{N}/2$ instead of the sum over integer representations $j_e \in \mathbb{N}$ was introduced by hand. In this last formula (6.17) a sign factor only visible for the half-integer representations is still missing [92] and the Ponzano-Regge model is actually given by

$$Z_{\Delta_3} = \sum_{\{j_e\}} \prod_e (-1)^{2j_e} d_{j_e} \prod_t \left\{ \begin{matrix} j_1^{(t)} & j_2^{(t)} & j_3^{(t)} \\ j_4^{(t)} & j_5^{(t)} & j_6^{(t)} \end{matrix} \right\}_N. \quad (6.18)$$

Historically, this model is the first spin foam model ever built. It was proposed by Ponzano and Regge in 1968 [21]. The simple quantization ansatz was that the edge lengths are quantized as $l_e = (j_e + 1/2)l_P$ (with l_P the Planck length) and that the $\{6j\}$ -symbol, which is thus the basic building block of their model, is associated to each “quantized” tetrahedron.



This ansatz was justified by the asymptotic of the $\{6j\}$ symbol.

$$\left\{ \begin{matrix} j_1 & j_2 & j_3 \\ j_4 & j_5 & j_6 \end{matrix} \right\} \sim_{j \rightarrow \infty} \frac{1}{\sqrt{12\pi V}} \cos \left(S_R + \frac{\pi}{4} \right), \quad (6.19)$$

where V is the volume of the tetrahedon and $S_R = \sum_e \frac{d_{j_e}}{2} \theta_e$ is the Regge action for discrete gravity, with the sum being over the edges of the tetrahedron, the θ_e being the dihedral angle of the edge e , i.e. the angle

$$1 \left\{ \begin{matrix} j_1 & j_2 & j_3 \\ j_4 & j_5 & j_6 \end{matrix} \right\}_N = (-1)^{j_1+j_2+j_3+j_4+j_5+j_6} \left\{ \begin{matrix} j_1 & j_2 & j_3 \\ j_4 & j_5 & j_6 \end{matrix} \right\}.$$

between the two outward normals of the two faces incident on that edge. The large spin limit is a semi-classical limit. Indeed, since the $SU(2)$ irreducible representations are interpreted as lengths

$$l_e = (j_e + \frac{1}{2})l_p = (j_e + \frac{1}{2})G\hbar, \quad (6.20)$$

the large spin limit for a fixed length l_e is equivalent to make \hbar (or l_p) approaching 0. This justifies that the Ponzano-Regge model is a quantum gravity model. More details concerning the $\{6j\}$ -symbol and the recoupling theory of $SU(2)$ can be found in appendix E and a detailed study of some of its properties and its asymptotical behavior has been done in [12] and [13]. The results which are relevant to extracting the semi-classical information from the spin foam formalism will be presented in Chapters 13 and 14.

Let us now consider the 4 dimensional case and see how we can write general relativity as a BF theory plus some additional constraints.

6.2 Reformulating 4d gravity as a BF theory: Plebanski's action

The Plebanski action (without cosmological constant)² reformulates general relativity as a constrained BF gauge theory for the Lorentz group, $SO(3,1)$ (or $SO(4)$ in the Euclidean case)

$$S_{\text{Plebanski}}[B, \omega, \lambda] = \int_{\mathcal{M}} B^{IJ} \wedge F_{IJ}[\omega] - \frac{1}{2} \lambda_{IJKL} B^{KL} \wedge B^{IJ}, \quad (6.21)$$

where we recall that \mathcal{M} is the space-time manifold, I, J are Lorentz indices running from 0 to 3, ω is a $\mathfrak{so}(3,1)$ -valued 1-form (or $\mathfrak{so}(4)$ -valued in the Euclidean theory), $\omega = \omega_{\mu}^{IJ} J_{IJ} dx^{\mu}$, J_{IJ} are the Lorentz generators and $F[\omega]$ is its strength tensor. The B field is a $\mathfrak{so}(3,1)$ valued 2-form, $B = B_{\mu\nu}^{IJ} J_{IJ} dx^{\mu} \wedge dx^{\nu}$. The constraints $\mathcal{C}_{IJKL}[B] \equiv B^{IJ} \wedge B^{KL}$ are enforced by the Lagrange multipliers λ_{IJKL} which satisfy $\lambda_{IJKL} = -\lambda_{JIKL} = -\lambda_{IJLK} = \lambda_{KLIJ}$ and $\lambda_{IJKL} \epsilon^{IJKL} = 0$. The B field is thus constrained in a such way that we recover general relativity in its first order formalism as given in (3.38). Indeed, the associated equations of motion are

$$\frac{\delta S}{\delta \omega} \longrightarrow \mathcal{D}B = dB + [\omega, B] = 0 \quad (6.22)$$

$$\frac{\delta S}{\delta B} \longrightarrow F^{IJ}(\omega) = \lambda^{IJKL} B_{KL} \quad (6.23)$$

$$\frac{\delta S}{\delta \lambda} \longrightarrow B^{IJ} \wedge B^{KL} = e \epsilon^{IJKL} \quad (6.24)$$

where $e = \frac{1}{4!} \epsilon_{IJKL} B^{IJ} \wedge B^{KL}$. The relation with gravity arises because of this last constraint. When $\tilde{e} = \frac{1}{4!} \epsilon_{IJKL} \epsilon^{\mu\nu\rho\delta} B_{\mu\nu}^{IJ} B_{\rho\delta}^{KL} \neq 0$, the last constraint is equivalent to

$$\epsilon_{IJKL} B_{\mu\nu}^{IJ} B_{\rho\delta}^{KL} = \epsilon_{\mu\nu\rho\delta} \tilde{e}, \quad (6.25)$$

which can be decomposed in three parts

$$\begin{aligned} a) \quad & \epsilon_{IJKL} B_{\mu\nu}^{KL} B_{\mu\nu}^{IJ} = 0 \\ b) \quad & \epsilon_{IJKL} B_{\mu\nu}^{KL} B_{\mu\rho}^{IJ} = 0 \\ c) \quad & \epsilon_{IJKL} B_{\mu\nu}^{KL} B_{\rho\delta}^{IJ} = \pm \tilde{e} \end{aligned} \quad (6.26)$$

where the indices μ, ν, ρ, δ are all different and the sign in the last equation is determined by the sign of their permutation. It is usually this system which is referred as the simplicity constraints. $\epsilon_{IJKL} B_{\mu\nu}^{IJ} B^{KL\mu\nu} = 0$

²The cosmological constant can be added to the Plebanski action which thus becomes

$$S_{\text{Plebanski}}[B, \omega, \lambda] = \int_{\mathcal{M}} B^{IJ} \wedge F_{IJ}[\omega] - \frac{\Lambda}{4} \epsilon_{IJKL} B^{IJ} \wedge B^{KL} - \frac{1}{2} \lambda_{IJKL} B^{KL} \wedge B^{IJ}$$

is equivalent to say that $B_{\mu\nu}$ is a simple bivector (i.e. of the form $B = u \wedge v$). Moreover, the constraint $B^{IJ} \wedge B^{KL} = e \epsilon^{IJKL}$ (with $e \neq 0$) is satisfied if and only if there exists a real tetrad field $e^I = e^I_\mu dx^\mu$ so that one of the following equations holds:

$$(\star) \quad B^{IJ} = \pm e^I \wedge e^J \quad (6.27)$$

$$(s) \quad B^{IJ} = \pm \epsilon^{IJ}_{KL} e^K \wedge e^L. \quad (6.28)$$

The action (3.38) is obtained if we restrict the field B to be always in the sector (s) (with the plus sign), and substitute the expression for B in terms of the tetrad field into (6.21). We denote by $(\star B)^{IJ} \equiv \frac{1}{2} \epsilon^{IJ}_{KL} B^{KL}$ the Hodge duality operation. Therefore, the Plebanski model is not exactly pure gravity. The restriction on the B field is always possible classically, so the two theories do not differ at the classical level, but they are different at the quantum level, since in the quantum theory one cannot avoid interference between different sectors. Indeed, this interference is due to the existence in the Plebanski action of a $\mathbb{Z}_2 \times \mathbb{Z}_2$ symmetry:

$$B \rightarrow -B, \quad B \rightarrow \star B. \quad (6.29)$$

Before considering the spin foam level, let us emphasize that the simplicity constraints $(\star B) \cdot B = 0$ correspond to the simplicity constraints (3.54) of the canonical analysis.

$$(\star B) \cdot B = 0 \longleftrightarrow \phi = (\star \mathcal{R}) \cdot \mathcal{R} = 0.$$

They are thus second class constraints. Furthermore, there is no analogue here of the other second class constraints we have given in (3.54), i.e. $\psi = \mathcal{R} \mathcal{R} D_{\mathcal{A}} \mathcal{R} = 0$ since the spin foam formalism is fully covariant. Indeed, the ψ are secondary constraints, coming from the Poisson bracket $\{S, \phi\}$. In the canonical approach, $\phi = 0$ is only imposed on the initial hypersurface and $\psi = 0$ is then needed to ensure $\phi = 0$ under the Hamiltonian evolution (given by the Hamiltonian constraint) whereas in the spin foam formalism approach $\phi = 0$ is directly imposed on all space-time structures. That is that we have projected on $\phi = 0$ at all stages of the evolution (i.e. on all hypersurfaces) and therefore we do not need the secondary constraints ψ .

Another important point which appears in the canonical approach for quantum gravity is the Immirzi parameter. A way to introduce it in the spin foam formalism is to consider a generalized BF-type action for gravity instead of the Plebanski action (6.21) as starting point of the quantization procedure. Indeed, it is possible to recover the Palatini-Holst action (3.44) for general relativity with Immirzi parameter considering a more general constraint on the λ field [93],

$$a \lambda_{IJ}^{IJ} + b \lambda_{IJKL} \epsilon^{IJKL} = 0. \quad (6.30)$$

This constraint $H \equiv a \lambda_{IJ}^{IJ} + b \lambda_{IJKL} \epsilon^{IJKL}$ can be taken into account in a generalized BF-type action for gravity given by

$$S[B, \omega, \lambda, \mu] = \int_{\mathcal{M}} B^{IJ} \wedge F_{IJ}[\omega] - \frac{1}{2} \lambda_{IJKL} B^{KL} \wedge B^{IJ} + \mu H, \quad (6.31)$$

where the condition $H = 0$ is enforced by the Lagrange multiplier μ while λ_{IJKL} still enforces the constraints on the B -field. The equations of motion for ω and B are the same as those coming from the Plebanski action, but the constraints on the B -field are now:

$$B^{IJ} \wedge B^{KL} = \frac{1}{6} (B^{MN} \wedge B_{MN}) \eta^{[I|K|} \eta^{J]L} + \frac{\epsilon}{12} (B^{MN} \wedge (\star B)_{MN}) \epsilon^{IJKL}, \quad (6.32)$$

$$2a B^{IJ} \wedge B_{IJ} - \epsilon b B^{IJ} \wedge (\star B)_{IJ} = 0, \quad (6.33)$$

where η^{IJ} is the flat metric and the constant ϵ is 1 in the Euclidean case and -1 in the Lorentzian case.

Let us note that we are back to the Plebanski action in the case $a = 0$. By choosing $a = 4\gamma$ and $b = -(\epsilon + \gamma^2)$ with γ a non-zero parameter, the solution of (6.32) and (6.33), for non-degenerate B ($B^{IJ} \wedge (\star B)_{IJ} \neq 0$), is then

$$(\star) \quad B^{IJ} = \pm \frac{1}{\gamma} (\star(e^I \wedge e^J) - \epsilon \gamma e^I \wedge e^J) \quad (6.34)$$

$$(s) \quad B^{IJ} = \pm \star (e^I \wedge e^J) - \frac{1}{\gamma} e^I \wedge e^J. \quad (6.35)$$

The same symmetry (6.29) as in the Plebanski case, brings us four sectors. Both positive sectors (6.34) and (6.35) yield to general relativity with different Immirzi parameters. Indeed, we get the Palatini-Holst action (3.44) inserting any of the two positive solutions (6.34), (6.35), into (6.31). In the (s) sector, the Immirzi parameter is as usual γ whereas in the (\star) sector the Immirzi parameter is instead ϵ/γ . In the following, we will work with a *finite* (non-zero) Immirzi parameter, unless specified otherwise.

6.3 The spin foam framework

The starting point of the spin foam framework is a BF-like action

$$S = \int_{\mathcal{M}} [\text{tr}(B \wedge F) + \Phi(B)]. \quad (6.36)$$

A general prescription for the definition of constrained BF theories on the lattice has been studied in [90]. The three dimensional case, with $\Phi(B \equiv 0)$, has been discussed in the previous Section 6.1. In the following we shall study the four dimensional case where $\Phi(B)$ is a quadratic function which also depends on some Lagrange multipliers ($\Phi(B) = -\frac{1}{2} \lambda_{IJKL} B^{KL} \wedge B^{IJ} + \mu H$). We will also discuss in details the implementation of the simplicity constraints encoded in $\Phi(B)$.

The strategy usually followed in four dimensions can be sketched in three main stages

1. discretize the classical theory by putting it on a cellular decomposition;
2. quantize the topological BF part of the discretized theory;
3. impose the simplicity constraints at the quantum level.

In this sense, the classical relation between BF theory and gravity is directly translated to the quantum level.

As we have seen in the three dimensional case, the first step is the discretization of the manifold \mathcal{M} . We start with a cellular decomposition Δ_4 of the 4d space-time manifold \mathcal{M} built from gluing 4-cells together.

The 4-cells are 4-simplices, the 3-cells are tetrahedra and the other elements of Δ_4 are recalled in Table 6.2. Since BF theory is topological, it does not have any local degree of freedom. It can be discretized on the cellular decomposition of \mathcal{M} and quantized exactly as a spinfoam model without losing any of its physical content. Then one works directly at the quantum level in the spinfoam framework and attempts to impose consistently the constraints turning the BF theory into a geometrical theory and introducing local degrees of freedom. We will see that there exists ambiguities in the way constraints can be imposed. Up to now, several theories (such as the EPRL-FK models [94, 95, 96, 97, 98]) have been proposed and any of these theory can at this moment be considered as a quantum theory of gravity. I will give a short review focusing only on the models relevant for the next parts.

Before going on to the specific quantization, let us remark that it is quite possible that one should construct in a different way, following a different strategy, the relevant spinfoam to encode 4d quantum gravity. Two recent results point to this direction. Firstly, B. Dittrich and J. Ryan have recently proposed an interesting new procedure[99] – that we will not explain here – which seems to give even at the discretized level a different model than the EPRL-FK models constructed using the usual strategy and which we shall describe in the next section. Secondly, this strategy we have recalled above to construct spinfoam models in 4d – firstly quantize, secondly implement the constraints – has been criticized in details recently in [100]. An alternative method would thus be to discretize the simplicity constraints and include them at the classical level in a discrete BF action. I will not give more details on this procedure used in [101] which however seems cleaner but which leads to spin foam amplitudes much more complicated and not always local.

Δ_4	Δ_4^*
4-simplex	<i>vertex</i> (5 edges, 10 faces)
tetrahedron	<i>edge</i> (4 faces)
triangle	<i>face</i>
segment	3d region
point	4d region

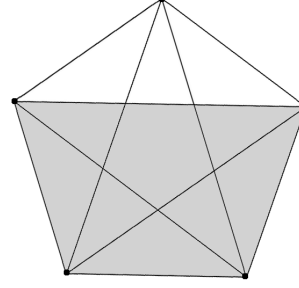


Table 6.2: Relation between a triangulation Δ_4 and its dual Δ_4^* in 4 dimensions. In *italic*, the two-complex. In parentheses: adjacent elements. The figure represents a 4-simplex. In grey, a tetrahedron of the 4-simplex.

6.3.1 Spin foam quantization of the 4d BF theory

The Euclidean case. In this case, we use $\text{Spin}(4)$ as gauge group. The action of the BF theory is given by the first term of the action (6.36)

$$S_{BF}[B, \omega] = \int_{\mathcal{M}} B^{IJ} \wedge F_{IJ}[\omega] = \int_{\mathcal{M}} \text{tr}(B \wedge F[\omega]) \quad (6.37)$$

where $B_{\mu\nu}^{IJ}$ is a $\mathfrak{spin}(4)$ Lie algebra valued 2-form, ω_μ^{IJ} is a connection on a $\text{Spin}(4)$ principle bundle over \mathcal{M} . The theory has no local excitations and its properties are analogous to the case of three dimensional gravity studied in Section 6.1. For simplicity, we will work with the discretization of \mathcal{M} given by a triangulation Δ_4 (instead of a general cellular decomposition).

The next step is to discretize the fields, the B -field and the Lorentz gauge connection ω . The connection curvature $F[\omega]$ is associated to the dual surfaces. Indeed, if we introduce a dual link variable $g_{e^*} = e^{i\omega_{e^*}}$ for each dual link e^* , through the holonomy of the $\mathfrak{spin}(4)$ -connection ω along the link, then consequently, the product of dual link variables along the boundary ∂f^* of a dual plaquette f^* leads to a curvature located at the center of the dual plaquette: $\prod_{e^* \in \partial f^*} g_{e^*} \equiv U_{f^*}$. The B -field is a 2-form and is naturally discretized on the faces Δ of the cellular decomposition

$$B_{\Delta}^{IJ} = \int_{\Delta} B_{\mu\nu}^{IJ} dx^\mu \wedge dx^\nu. \quad (6.38)$$

The faces Δ of the cellular decomposition in the case of a triangulation Δ_4 are triangles and in 4 dimensions triangles $\in \Delta_4$ are dual to faces $f^* \in \Delta_4^*$. This one-to-one correspondence allows us to denote the discrete B by either a triangle B_{Δ} or a face B_{f^*} subindex respectively. B_{f^*} can be interpreted as the smearing of the continuous 2-form B on triangles in Δ_4 . Using these discretized variables, the path integral becomes

$$Z_{\Delta_4}^{\text{BF}} = \int \prod_{e^* \in \Delta_4^*} dg_{e^*} \prod_{f^* \in \Delta_4^*} dB_{f^*} e^{iB_{f^*} U_{f^*}}, \quad (6.39)$$

which is analogous to (6.13) in the 3 dimensional case. The result of the B integration is given by

$$Z_{\Delta_4}^{\text{BF}} = \int \prod_{e^* \in \Delta_4^*} dg_{e^*} \prod_{f^* \in \Delta_4^*} \delta(U_{f^*}), \quad (6.40)$$

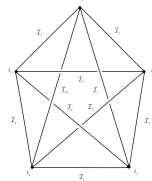
where δ is the delta distribution defined on $L^2(\text{Spin}(4))$. This interpretation of this result is simple: we have to sum over the flat connection. We can use the Peter-Weyl theorem as in (6.14), to obtain

$$Z_{\Delta_4}^{\text{BF}} = \sum_{\mathcal{I}_1 \dots \mathcal{I}_P} \int \prod_{e^* \in \Delta_4^*} dg_{e^*} \prod_{f^* \in \Delta_4^*} d_{\mathcal{I}_{f^*}} \text{tr}[D^{\mathcal{I}_{f^*}}(g_{e^*}^1 \dots g_{e^*}^n)] \quad (6.41)$$

where $\mathcal{I}_1 \cdots \mathcal{I}_P$ are the quantum numbers associated to the P faces of Δ_4^* . \mathcal{I} denotes an arbitrary unitary irreducible representation appearing in the Plancherel measure of the group $\text{Spin}(4)$ and $d_{\mathcal{I}}$ is its dimension. There is an integration for each g_{e^*} . In Δ_4^* , each $e^* \in \Delta_4^*$ bounds precisely four different faces; therefore, the g_{e^*} in (6.41) appears in four different traces. We can then introduce the intertwiners as in (4.23) using

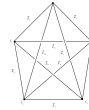
$$\int dg \prod_{e=1}^N D_{m_e n_e}^{j_e} = \sum_i i_{m_1 \cdots m_N} i_{n_1 \cdots n_N}^*,$$

to obtain that the partition function is equal to

$$Z_{\Delta_4}^{\text{BF}} = \sum_{\{\mathcal{I}_{f^*}\}, \{i_{e^*}\}} \prod_{f^*} d_{\mathcal{I}_{f^*}} \prod_{v^*} \text{[Diagram]} \quad (6.42)$$


The 4-simplex in the formula is dual to the 4-simplex in the original triangulation that contains $v^* \subset \Delta_4^*$. Its edges are labelled by the representations labeling the ten dual faces incident to v^* and its vertices are labelled by the intertwiners labeling the dual edges incident to v^* . We can rewrite this formula for the partition function by splitting each 4-valent vertex into two trivalent vertices using the relation described in Fig. 4.2. The resulting equation involves a trivalent spin network with 15 edges: $(\mathcal{I}_{f^*}, \mathcal{I}_{e^*})$ where \mathcal{I}_{e^*} is the spin coming from the splitting of the 4-valent intertwiner i_{e^*} . This trivalent spin network is called a $\{15\}$ -symbol since it depends on 15 spins.

Let us notice that $\text{Spin}(4) \sim \text{SU}_L(2) \times \text{SU}_R(2)$. An irreducible representation \mathcal{I}_{f^*} of $\text{Spin}(4)$ is thus labeled by a couple $(j_{f^*}^L, j_{f^*}^R)$. Consequently, an intertwiner $i_{e^*} = i_{j_{e^*}^L} \otimes i_{j_{e^*}^R}$ where $(j_{e^*}^L, j_{e^*}^R) \equiv \mathcal{I}_{e^*}$ and the different weights

$$A_v^{\text{Spin}(4)}(\mathcal{I}_{f^*}, \mathcal{I}_{e^*}) \equiv \text{[Diagram]} = \{15j\}_{\text{SU}_L(2)} \{15j\}_{\text{SU}_R(2)} = A_v^{\text{SU}(2)}(j_{f^*}^L, j_{e^*}^L) A_v^{\text{SU}(2)}(j_{f^*}^R, j_{e^*}^R). \quad (6.43)$$


As in the 3-dimensional case, due to the absence of local degrees of freedom in the topological theory, the partition function is invariant under changes of triangulation keeping the topology fixed (i.e. invariant under the Pachner moves).

The Lorentzian case. The gauge group is now $\text{SL}(2, \mathbb{C})$. The resulting partition function constructed in this case is formally the same as in (6.42). The principal series of unitary, irreducible representations of $\text{SL}(2, \mathbb{C})$ are labelled by two parameters (n, ρ) , with n a half-integer and ρ a real number. To describe explicitly the partition function in this Lorentzian case, we consider the partition function obtained in (6.42). We associate the couple $2j^L + 1 = n + i\rho$, $2j^R + 1 = n - i\rho$ to each unitary principal representation (n, ρ) and use the factorized formula from the Euclidean case (6.43).

6.3.2 Some ambiguities in the 4d gravity spin foam quantization procedure

The idea is now to provide a definition of the path integral of gravity formally written as

$$\int \mathcal{D}B \mathcal{D}\omega \delta[B \rightarrow \star(e \wedge e)] \exp \left[i \int \text{tr}[B \wedge F] \right] \quad (6.44)$$

where the measure $\mathcal{D}B \mathcal{D}\omega \delta[B \rightarrow \star(e \wedge e)]$ restricts the sum of the BF theory path integral

$$Z^{\text{BF}} = \int \mathcal{D}B \mathcal{D}\omega \exp \left[i \int \text{tr}[B \wedge F] \right]$$

to those configurations of the topological theory satisfying the constraints $B = \star(e \wedge e)$ for some tetrad e . The constraints $B = \star(e \wedge e)$ are going to be directly implemented on the spin foam configurations of $Z_{\Delta_4}^{\text{BF}}$ by the appropriate restriction on the allowed spin labels and intertwiners.

In the spinfoam quantization process a number of ambiguities appear. The most severe ones are related to the discretization process, while another appears due to Immirzi parameter dependence in the action.

The discretization ambiguities arise in the different steps of the spinfoam quantization. The first important one, and most obvious, is the choice of cellular decomposition of the manifold. There is a very large number of decompositions available – a triangulation, a square lattice or an arbitrary irregular cellular decomposition – and we have to pick up one. One proposal to solve this issue is the use of GFT which provides automatically the sum over the relevant complexes [85, 86]. The most common approach to this issue, which we will adopt here, consists in simply postponing this issue and working either with a triangulation to allow to write explicitly the spin foam amplitudes or when possible with an arbitrary cellular decomposition in order to remain as general as possible.

Once such a manifold discretization as been chosen, another key ambiguity appears since there is no unique prescription to discretize the curvature F . We will not discuss this point here. We will mostly focus on the simplicity constraints which only concern the discretized B field, B_Δ , and which are not affected by the definition of the discretized curvature. We will only specify for each approach how the Lorentz gauge connection is discretized and if some constraints are consequently added.

The third discretization ambiguity appears when discretizing the dynamical content of the theory, i.e. the constraints. We will address this issue at length in Part II.

Finally, we recall that the classical Palatini-Holst action contains some ambiguity in the Immirzi parameter choice. This parameter is important to have the spin connection as a well-defined configuration variable [31]. To relate the spinfoam formalism with the loop quantum gravity approach, it is therefore important to take this parameter into account in the spinfoam quantization. However, just as in loop quantum gravity, it then generates some ambiguities in the formalism: we have a free parameter dependent theory. We consider the action (6.31) as the starting point of the procedure. We have seen that the continuum constraints on the B -fields are then modified compared to the Plebanski constraints (6.25). For clarity we denote B^{IJ} the bivector $\star(e^I \wedge e^J)$ and Σ^{IJ} the bivector $\star(e^I \wedge e^J) - \frac{1}{\gamma} e^I \wedge e^J = B^{IJ} - \frac{1}{\gamma} \star B^{IJ}$, which depends on the Immirzi parameter γ , and is solution to the constraints (6.32) and (6.33).

Two different procedures of quantization are usually followed.

- The first approach consists in taking directly into account the Immirzi parameter at the discretized level. We focus on the variables Σ^{IJ} constrained by (6.32) and (6.33). Then, noticing that the constraints (6.32) and (6.33) (with $a = 4\gamma$, $b = -(\epsilon + \gamma^2)$) can be recast in an equivalent form

$$\left(\epsilon_{IJKL} + \frac{4\gamma}{\epsilon + \gamma^2} \eta_{[I|K|} \eta_{J|L]} \right) \Sigma_{cd}^{KL} \Sigma_{ab}^{IJ} = \epsilon \epsilon_{abcd} \left(1 - \epsilon \frac{4\gamma^2}{(\epsilon + \gamma^2)^2} \right), \quad (6.45)$$

with $e = \frac{1}{4!} \epsilon_{IJKL} B^{IJ} \wedge \Sigma^{KL}$, we consider the discretized version of this new constraint. The quantization step is simply to replace Σ_Δ^{IJ} with the canonical generators J_Δ^{IJ} of $\mathfrak{spin}(4)$. Finally, writing the simplicity constraints for the generators J_Δ^{IJ} translates into a condition on the Casimirs of $\mathfrak{spin}(4)$ or $\mathfrak{sl}(2, \mathbb{C})$.

- The second approach consists in considering as discretized variable the B -field constrained to be a simple bivector. Contrary to the previous case, the Immirzi parameter will be taken into account only at the quantized level. This is the procedure that we are going to detail in the following.

Let us first review the discretized setting. The simplicity constraints of the 2-form, $\epsilon_{IJKL} B_{\mu\nu}^{IJ} B_{\rho\delta}^{KL} = \epsilon \epsilon_{\mu\nu\rho\delta}$ ensure that B comes from a tetrad field e . We want to translate this constraint to the discrete setting. We

recall that the B -field is a 2-form and is naturally discretized on the faces Δ of the cellular decomposition

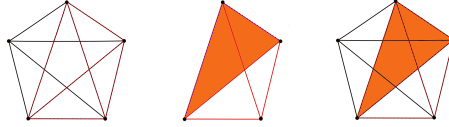
$$B_{\Delta}^{IJ} = \int_{\Delta} B_{\mu\nu}^{IJ} dx^{\mu} \wedge dx^{\nu}. \quad (6.46)$$

Let us look in details at the simplicity constraints within a 4-cell. For any two faces $\Delta, \tilde{\Delta}$, we have:

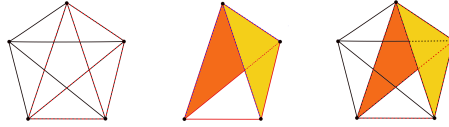
$$\epsilon_{IJKL} B_{\Delta}^{IJ} B_{\tilde{\Delta}}^{KL} = \int_{\Delta, \tilde{\Delta}} e d^2\sigma \wedge d^2\sigma' = V(\Delta, \tilde{\Delta}), \quad (6.47)$$

where $V(\Delta, \tilde{\Delta})$ is the 4-volume spanned by the two faces. Like for the continuum constraints appearing in the Plebanski action (6.26), we can again distinguish three different cases.

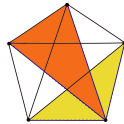
1. The faces are the same $\Delta = \tilde{\Delta}$, then $\epsilon_{IJKL} B_{\Delta}^{IJ} B_{\Delta}^{KL} = 0, \forall \Delta$, i.e. the associated bivector B_{Δ} must be simple. In the case of a triangulation Δ_4 , within a 4-simplex, this constraint imposes to each bivector associated to a triangle to be simple.



2. Δ and $\tilde{\Delta}$ belong to the same 3-cell, then $\epsilon_{IJKL} B_{\Delta}^{IJ} B_{\tilde{\Delta}}^{KL} = 0, \forall \Delta \neq \tilde{\Delta}$, therefore the sum $B_{\Delta} + B_{\tilde{\Delta}}$ must be simple. In the case of a triangulation Δ_4 , this constraint acts on two bivectors associated to two different triangles belonging to the same tetrahedron, i.e. sharing a common edge and imposes to the sum to be simple.



3. Δ and $\tilde{\Delta}$ do not belong to the same 3-cell, then $\epsilon_{IJKL} B_{\Delta}^{IJ} B_{\tilde{\Delta}}^{KL} = V(\Delta, \tilde{\Delta})$. In the case of a triangulation Δ_4 , this constraint acts on two bivectors associated to two different triangles which only share a common vertex and consequently do not belong to the same tetrahedron. It imposes that the quantity $\epsilon_{IJKL} B_{\Delta}^{IJ} B_{\tilde{\Delta}}^{KL}$ is equal to the 4-simplex volume (up to a factor).



Moreover, the discrete B -fields are constraints to satisfy a closure constraint for each 3-cell

$$\sum_{\Delta \in 3\text{-cell}} B_{\Delta}^{IJ} = 0. \quad (6.48)$$

This is the discrete equivalent of the Gauss law ensuring the $G = \text{Spin}(4)$ or $\text{SL}(2, \mathbb{C})$ gauge invariance.

Let us now discuss the simplicity constraints. We are going to see that the constraints 1. are straightforward to deal with while discussing the other two. As we pointed out in the previous section, the simplicity constraints 2. $(\star B_{\Delta}) \cdot B_{\tilde{\Delta}} = 0$ correspond to the continuum simplicity constraint (3.54), i.e. $\phi = (\star \mathcal{R}) \cdot \mathcal{R} = 0$ of the canonical analysis. Hence they are primary constraints.

We also recalled that the other second class constraints (3.54), i.e. $\psi = \mathcal{R}RD_A\mathcal{R} = 0$, the secondary constraints are not needed here since the spin foam formalism is fully covariant.

At this discrete level, this can be justified by noticing that the simplicity constraints 3. $(\star B_\Delta) \cdot B_{\tilde{\Delta}} = V$ give the secondary constraints. Indeed, assuming that the constraints 2. $(\star B_\Delta) \cdot B_{\tilde{\Delta}} = 0$ hold on the initial hypersurface (e.g. one a 3-cell of the 4-cell) and that the simplicity constraints 3. are satisfied, then using the closure constraints (10.28), it is possible to show that $(\star B_\Delta) \cdot B_{\tilde{\Delta}} = 0$ is also true on the final hypersurface (e.g. all remaining 3-cells). Therefore the simplicity constraints 3. ensure that the spatial constraints 2. are satisfied under time evolution and are the secondary constraints analogue. Furthermore, still using the closure constraints (10.28), it is possible to show that when the constraints 2. hold for all 3-cells of the 4-cell, the constraints 3. are true. That is why we only need to solve the constraints 2., the primary constraints, in the spin foam formalism. Moreover, these constraints will usually be solved separately on each 3-cells of the cellular decomposition.

Let us therefore focus on one 3-cell, which we denote v , for the vertex the dual element of the 3-cell of interest. The bivectors B_Δ^{IJ} associated to each face Δ on the (3d) polyhedron boundary define the geometry of the polyhedron. We distinguish two sectors: the normal bivector to the face (the normal to a plane embedded in a 4d manifold is indeed a bivector) is either B_Δ^{IJ} , which we call the standard sector (s), or it is given by its Hodge dual $(\star B)_\Delta^{IJ} \equiv \frac{1}{2}\epsilon^{IJ}{}_{KL}B_\Delta^{KL}$, which we call the dual sector (\star). In both cases, the norm of the bivector $|B_\Delta^{IJ}|$ gives the area of the face Δ and the bivectors satisfy the closure constraint (6.48). These two sectors correspond, at the discrete level, to the two sectors of solutions (6.27) and (6.28) of the simplicity constraints of the Plebanski action. A discussion on how these two sectors correspond to gravity or not has been given in the previous section. We have seen that the usual discrete *quadratic simplicity constraints* (the discretized version of the Plebanski constraints (6.26))

$$\forall \Delta, \tilde{\Delta} \in \partial v, \quad \epsilon_{IJKL} B_\Delta^{IJ} B_{\tilde{\Delta}}^{KL} = 0 \quad (6.49)$$

do not distinguish the two sectors (s) and (\star) since they are invariant under taking the Hodge dual $B \rightarrow \star B$. This means that we have to recognize the two sectors by hand when solving these simplicity constraints.

However, it is possible to rewrite the quadratic simplicity constraints in such a way that they distinguish the two different sectors [95]. Indeed, geometrically, the simplicity constraints come from the fact that all the faces of a given 3-cell v lay in the same hypersurface. Let us call x_I the 4-vector normal to that hypersurface. This leads to very simple constraints on the bivectors B_Δ^{IJ} . We will call them the *linear simplicity constraints*³

$$(s) \quad x_I \cdot B_\Delta^{IJ} = 0, \forall \Delta \in \partial v, \quad (\star) \quad \epsilon^{IJ}{}_{KL} x_J \cdot B_\Delta^{KL} = 0, \forall \Delta \in \partial v. \quad (6.50)$$

We will see in the next part that these linear simplicity constraints are at the root of the construction of the recent EPRL-FK model and other new spinfoam models [95, 98, 96, 97, 102]. A clear link between the quadratic and the linear simplicity constraints has been given in [95]. These linear simplicity constraints involve explicitly the time normal x_I , which is an extra field. We have seen that this field variable appears also in the definition of the projected spin network (see chapter 5). This is therefore the first evidence of the possible relationship between the projected spin networks and the spinfoam models.

Let us now go on with the last step of the spin foam quantization procedure which is the quantization itself. The key kinematical ingredient is the boundary of the 4-cell. More precisely, the boundary of a given 4-cell is made of 3-cells glued together. We have seen that we can solve the simplicity constraints within a 3-cell. We thus consider the discretized B -field, the bivectors B_Δ associated to each face of a given boundary 3-cell. The bivectors are then translated as elements of $\mathfrak{spin}(4)^*$ or $\mathfrak{sl}(2, C)^*$. There exists an ambiguity at this level. Indeed, there exists a family of isomorphisms between bivectors and Lie algebra elements.

$$B \leftrightarrow \tilde{J}^{IJ} = \alpha J^{IJ} + \beta \star J^{IJ}. \quad (6.51)$$

³The quadratic constraints (6.45) can also be replaced, at the discrete level, by some linear simplicity constraints where in order to take into account the Immirzi parameter, we consider a linear combination of these two sectors, (s) and (\star), thus leading to a linear simplicity constraint of the type $x_I \cdot (\Sigma_\Delta^{IJ} + \gamma \epsilon^{IJ}{}_{KL} \Sigma_\Delta^{KL}) = 0$. We have chosen not to follow this procedure because the geometrical interpretation of the B_Δ variable is not as obvious as in the presented case.

We will actually discuss this ambiguity in the next part II. The rest of the quantization procedure for the 3-cell is very simple: we associate an irreducible representation of our gauge group $\text{Spin}(4)$ or $\text{SL}(2, \mathbb{C})$ to each face Δ and we quantize the bivectors B_{Δ}^{IJ} as the Lie algebra generators J_{Δ}^{IJ} (or more generally as $\alpha J_{\Delta}^{IJ} + \beta \star J_{\Delta}^{IJ}$) acting in that representation. The states of the 3-cell v live then in the tensor product of the representations of all its faces. Moreover, taking into account the closure constraint,

$$\sum_{\Delta \in \partial v} B_{\Delta}^{IJ} = 0 \quad \longrightarrow \quad \sum_{\Delta \in \partial v} J_{\Delta}^{IJ} = 0,$$

we require that the states associated to the 3-cell must be invariant under the global $\text{Spin}(4)$ or $\text{SL}(2, \mathbb{C})$ action which acts simultaneously on all faces. Thus, the Hilbert space of quantum states of the 3-cell is the space of $\text{Spin}(4)$ or $\text{SL}(2, \mathbb{C})$ intertwiners between the representations attached to its faces. We still need to implement the simplicity constraints. It is one of the key issue of the spin foam program to implement them at the quantum level in the regularized path integral. For example when using the quadratic simplicity constraints, we have to implement the constraints

$$\forall \Delta, \tilde{\Delta} \in \partial v, \quad \epsilon_{IJKL} \tilde{J}_{\Delta}^{IJ} \tilde{J}_{\tilde{\Delta}}^{KL} = 0, \quad (6.52)$$

which translate into conditions on the Casimir operators on the intertwiners states. The next chapter is devoted to this issue of imposing consistently the simplicity constraints at this quantum level.

Part II

Spin foam models for 4d gravity

In the previous Part, we ended the presentation of the spin foam quantization procedure just before the last step which is the implementation of the simplicity constraints at the quantized level. At this penultimate step of the procedure, the Hilbert space of quantum states of a 3-cell is the space of $\text{Spin}(4)$ or $\text{SL}(2, \mathbb{C})$ intertwiners between the representations attached to its faces. The last step consists in imposing the simplicity constraints on these intertwiners. This last step is still a topic of discussion, no final consensus has been reached on the "correct" way to proceed.

The two projects presented in this part (Chapter 9 and Chapter 10) aimed at understanding better these simplicity constraints and in particular focused on the two specific questions:

- What is a consistent implementation of the simplicity constraints at the quantum level?
- What are the consequences of their implementation on the boundary Hilbert space of the 3-cell (or more generally of the whole boundary space)?

The main difficulty comes from the fact that the algebra of these simplicity constraints – which translate into conditions on the Casimir operators – does not close at the quantized level. This reflects that they correspond to second class constraints.

We will distinguish the diagonal simplicity constraints that we will denote $\hat{\mathcal{C}}_\Delta$ or \mathcal{C}_i where i refers to the intertwiner's leg dual to the face Δ and the cross simplicity constraints that we will denote $\hat{\mathcal{C}}_{\Delta\tilde{\Delta}}$ or \mathcal{C}_{ij} with $\Delta \neq \tilde{\Delta}$ (or $i \neq j$). We recall that there is a one-to-one correspondence between a 3-cell and its dual vertex v and between a face Δ of the 3-cell and its dual link, the leg i of the vertex, which explains that we can equivalently use the face subindex $\Delta, \tilde{\Delta}, \dots$ or the leg subindex i, j, \dots .

In the Euclidean case, the quantum version of the quadratic simplicity constraints (6.49) is simply given by

$$\mathcal{C}_{\Delta\tilde{\Delta}} \equiv \bar{J}_\Delta^L \cdot \bar{J}_{\tilde{\Delta}}^L - \bar{J}_\Delta^R \cdot \bar{J}_{\tilde{\Delta}}^R = 0, \quad (6.53)$$

where \bar{J}^L, \bar{J}^R are the $\mathfrak{su}(2)$ generators of the two commuting $\mathfrak{su}(2)$ algebra of the $\mathfrak{spin}(4)$ algebra decomposition $\mathfrak{spin}(4) = \mathfrak{su}_L(2) \oplus \mathfrak{su}_R(2)$. Looking at the cross simplicity constraints, it is fairly easy to check that the Lie algebra of the quadratic simplicity constraints does not close

$$\left[\bar{J}_{\Delta_1}^L \cdot \bar{J}_{\Delta_2}^L - \bar{J}_{\Delta_1}^R \cdot \bar{J}_{\Delta_2}^R, \bar{J}_{\Delta_1}^L \cdot \bar{J}_{\Delta_3}^L - \bar{J}_{\Delta_1}^R \cdot \bar{J}_{\Delta_3}^R \right] = \bar{J}_{\Delta_1}^L \cdot \left(\bar{J}_{\Delta_2}^L \wedge \bar{J}_{\Delta_3}^L \right) + \bar{J}_{\Delta_1}^R \cdot \left(\bar{J}_{\Delta_2}^R \wedge \bar{J}_{\Delta_3}^R \right). \quad (6.54)$$

In this way, we generate higher and higher order constraints by computing further commutators.

Naturally, the first attempt was to impose these constraints strongly to obtain intertwiner states $|\psi\rangle$ vanishing under the simplicity constraints

$$\mathcal{C}_{\Delta\tilde{\Delta}} |\psi\rangle = 0 \quad \forall \Delta, \tilde{\Delta}. \quad (6.55)$$

The resolution to this system of equations led to the first spin foam model for 4 dimensional gravity, the Barrett-Crane spin foam model, which was actually initially built as a geometrical quantization of individual 4-simplices [103, 104]. Both Euclidean and Lorentzian versions of this model – which remained the leading proposal during 10 years – will be detailed in the next Chapter. It was shown (at least in the 4-valent case corresponding to a tetrahedron) in [105] that these equations have a unique solution once the representations associated to each Δ are specified. This unique or "frozen" intertwiner property leads to several problems in the interpretation of the Barrett-Crane model, especially when looking at its relation with the canonical loop quantum gravity framework and when studying the graviton propagator derived in the asymptotical semi-classical regime of the model. The uniqueness of the intertwiner state can be traced back to the fact that the Lie algebra of the quadratic simplicity constraints does not close. Indeed, since the commutators between two different cross simplicity constraints (6.54) generate higher order constraints, when we impose strongly the quadratic simplicity constraints on the intertwiner state $|\psi\rangle$, we are actually also imposing all these higher order constraints. Then it is not surprising to find a unique solution, although it could actually be considered surprising to find at least one solution.

To remedy this issue, it was proposed to solve the crossed simplicity constraints weakly, either by some coherent state techniques [106] or by some Gupta-Bleuler-like method using the linear simplicity constraints [94, 95, 98].

In the coherent state approach, one seeks semi-classical states such that the simplicity constraint is solved in average [106, 96],

$$\langle \psi | \mathcal{C}_{\Delta\bar{\Delta}} | \psi \rangle = 0, \quad (6.56)$$

while minimizing the uncertainty of these operators.

In the Gupta-Bleuler-like approach⁴, one looks for a Hilbert space \mathcal{H}_s such that the matrix elements of the simplicity constraints on this Hilbert space all vanish [94, 97]

$$\forall \phi, \psi \in \mathcal{H}_s, \quad \langle \phi | \mathcal{C}_{\Delta\bar{\Delta}} | \psi \rangle = 0. \quad (6.57)$$

These two approaches were shown to lead to the same spinfoam amplitudes [96, 97] apart from some subtle cases [107].

Before detailing these different ways of implementing the simplicity constraints, let us emphasize that a true Gupta-Bleuler method would involve decomposing the constraints $\mathcal{C}_{\Delta\bar{\Delta}}$ under a sum of holomorphic and anti-holomorphic factors (or equivalently of creation and annihilation operators), i.e. $\mathcal{C}_{\Delta\bar{\Delta}} = \sum_{\alpha} (\mathcal{F}_{\Delta\bar{\Delta}}^{\alpha})^{\dagger} \mathcal{F}_{\Delta\bar{\Delta}}^{\alpha}$. Then, from this decomposition, the next step would be to extract algebraic constraints \mathcal{F}^{α} which are strongly solved in the sense: $\mathcal{F}_{\Delta\bar{\Delta}}^{\alpha} | \psi \rangle = 0$. And finally, (6.57) would appear as the consequence of the resolution of the algebraic constraints $\mathcal{F}_{\Delta\bar{\Delta}}^{\alpha}$. Indeed, $\forall | \psi \rangle, | \phi \rangle \in \mathcal{H}_s$ such that $\mathcal{F}_{\Delta\bar{\Delta}}^{\alpha} | \psi \rangle = 0$ and $\mathcal{F}_{\Delta\bar{\Delta}}^{\alpha} | \phi \rangle = 0$, then $\langle \phi | (\mathcal{F}_{\Delta\bar{\Delta}}^{\alpha})^{\dagger} \mathcal{F}_{\Delta\bar{\Delta}}^{\alpha} | \psi \rangle = 0$ and $\langle \phi | \mathcal{C}_{\Delta\bar{\Delta}} | \psi \rangle = 0$.

In the next two Chapters of this part, the different approaches, [103, 104], [106, 96], [94, 97] are presented. In Chapter 10, we will present the right Gupta-Bleuler method to implement the second class simplicity constraints at the quantum level [6].

⁴We will review in the section 8.1 that in fact in this procedure (followed in [94, 95, 98]) the simplicity constraints are imposed prior to the imposition of the closure constraint (6.48), and that consequently the Hilbert space of the 3-cell on which the simplicity constraints will be imposed is not an intertwiner space yet.

Chapter 7

Simplicity constraints and the Barrett-Crane model

7.1 The Euclidean Barrett-Crane model

We are now going to review the construction of the Barrett-Crane model of 4d Euclidean quantum gravity without Immirzi parameter [103]. The manifold \mathcal{M} is replaced by a cellular decomposition. Explicit results will be mostly given in the simplest case of a triangulation Δ_4 (see Table 6.2) since it is the framework for the results exposed in the next part, Chapter 15, regarding the physical boundary state for the quantum 4-simplex. However, as often as possible the definitions will be given for the general case of a cellular decomposition.

Going from the continuum theory to the Barrett-Crane model is achieved in three main steps. We recall that the first step is the discretization of the two-form into bivectors associated to each face to the cellular decomposition. Bivectors are then translated as elements of $\mathfrak{so}(4)^*$. The last step is the quantization itself, using techniques from geometric quantization. It gives representation labels to the faces of the cellular decomposition and gives the Barrett-Crane model (to some normalisation factors). It is this last step that we are going to detail now.

Since $\text{Spin}(4) \sim \text{SU}_L(2) \times \text{SU}_R(2)$, the irreducible representations of $\text{Spin}(4)$ are labeled by a couple of half-integers (j^L, j^R) . Hence, we attach a pair of spin to every face Δ and the intertwiner space for the 3-cell is the tensor product of the space of $\text{SU}_L(2)$ intertwiners between the spins j_Δ^L and the space of $\text{SU}_R(2)$ intertwiners between the spins j_Δ^R

$$H_{j_\Delta^L, j_\Delta^R} \equiv \text{Inv} \left[\bigotimes_{\Delta} V^{j_\Delta^L} \right] \otimes \text{Inv} \left[\bigotimes_{\Delta} V^{j_\Delta^R} \right]. \quad (7.1)$$

Finally, we now come to the crucial step of implementing the simplicity constraints (6.49) at the level of the spin foam model of BF theory. In the Barrett-Crane model, the quantum version of these constraints is given by

$$\begin{aligned} \widehat{\mathcal{C}}_\Delta &= \epsilon_{IJKL} J_\Delta^{IJ} J_\Delta^{KL} = 0 & \forall \Delta & \quad \text{diagonal simplicity constraints,} \\ \widehat{\mathcal{C}}_{\Delta\tilde{\Delta}} &= \epsilon_{IJKL} J_\Delta^{IJ} J_{\tilde{\Delta}}^{KL} = 0 & \forall \Delta \neq \tilde{\Delta} \in \partial v & \quad \text{cross simplicity constraints.} \end{aligned} \quad (7.2)$$

That is the bivectors B_Δ^{IJ} of the discretized constraints (6.49) have been replaced by generators J^{IJ} of the $\mathfrak{spin}(4)$ Lie algebra in the representation $\mathcal{I}_\Delta = (j_\Delta^L, j_\Delta^R)$. In the expression of the diagonal simplicity constraints, $\frac{1}{4} \star J \cdot J$ is the pseudo-scalar quadratic Casimirs of $\mathfrak{spin}(4)$ and it is equal to the difference of the quadratic Casimir of $\mathfrak{su}_L(2)$ and $\mathfrak{su}_R(2)$. This gives a restriction on the representations $\mathcal{I}_\Delta = (j_\Delta^L, j_\Delta^R)$ of $\text{Spin}(4)$

$$2j_\Delta^L(j_\Delta^L + 1) - 2j_\Delta^R(j_\Delta^R + 1) = 0 \quad \forall \Delta, \quad (7.3)$$

leading to $j^L = j^R$. The irreducible representations satisfying this condition are called *simple representations*. The strong imposition of the diagonal simplicity constraints implies that only simple representations are associated to faces Δ of the 3-cell [81, 108].

The cross simplicity constraint is already imposed at the level of a 3-cell and induces a restriction on possible intertwiners. In the simple case where the cellular decomposition is a triangulation Δ_4 , a 3-cell is a tetrahedron and taking into account that the intertwiners couple simple representations, it is easy to conclude that the restriction means that, given a decomposition of any two \mathcal{I}_Δ 's, the intertwiner has support only on simple intermediate representations. Indeed, we have four simple representations (j_α, j_α) for the four triangles $\Delta_{\alpha=1\dots 4}$ on the tetrahedron boundary. In $H_{j_\alpha} \equiv \text{Inv} \left[\bigotimes_{\alpha=1}^4 V^{j_\alpha} \right] \otimes \text{Inv} \left[\bigotimes_{\alpha=1}^4 V^{j_\alpha} \right]$ with $j_\alpha \equiv j_\alpha^L = j_\alpha^R$, we have to

Figure 7.1: The label (j_{12}^L, j_{12}^R) stands for the representation $(J_1 + J_2)$.

impose the three independent cross simplicity constraints $\mathcal{C}_{\alpha\beta} = \epsilon J_\alpha J_\beta = 0$ for all couples of triangles $(\Delta_\alpha, \Delta_\beta)$. These constraints mean that the sum $(J_\alpha + J_\beta)$ is required to remain simple. Using the standard recoupling basis of intertwiner as in Fig. 7.1, we denote the representation of $J_\alpha + J_\beta$, $(j_{\alpha\beta}^+, j_{\alpha\beta}^-)$. Strongly imposing the simplicity conditions $\mathcal{C}_{1,2}$ forces the recoupled representation to be simple, $j_{12}^L = j_{12}^R$. Further imposing $\mathcal{C}_{1,3}$ and $\mathcal{C}_{1,4}$ then leads to a single intertwiner [105]: the Barrett-Crane intertwiner, i_{BC} . One can now implement these restrictions at the level of the partition function. For this it is sufficient to take the spin foam representation of the BF partition function (6.42) and restrict the sum over j_Δ to only simple representations and to remove the sum over intertwiners substituting for them i_{BC} . We recall that the volume simplicity constraint (quantized version of the third equation in 6.26) can be ignored because it is a consequence of the other simplicity constraints (6.49) supplemented by the closure (6.48) and that the latter is already satisfied since we have started from the state space of BF theory.

Once we have determined the state space, the spin foam amplitude for the Euclidean Barrett-Crane model (valid also for an arbitrary cellular decomposition) is explicitly given by the evaluation of a spin network ψ with group $\text{Spin}(4)$ such that each node n of the graph γ of ψ is associated to a $\text{Spin}(4)$ group element G_n and each link l is labelled by a simple irreps of $\text{Spin}(4)$ $\mathcal{I}_l = (j_l, j_l)$. Using the homomorphism $\text{Spin}(4) = \text{SU}(2)_L \times \text{SU}(2)_R$, $\text{Spin}(4)$ group elements decompose as the product of two left and right rotations $G = g_L g_R$. The evaluation then reads [109]

$$\mathcal{A}[\psi] \equiv \int_{\text{Spin}(4)} \prod_n [dG_n] \prod_i \mathcal{K}_{\mathcal{I}_i}(G_{s(i)}^{-1} G_{t(i)}), \quad (7.4)$$

where we use the Haar measure $dG = dg_L dg_R$. The kernel $\mathcal{K}_{\mathcal{I}}(G)$ is the matrix element of G on the $\text{SU}(2)$ -invariant vector $|\mathcal{I}, 0\rangle$ in the \mathcal{I} representation with $\mathcal{I} = (j, j)$ a simple representation of $\text{Spin}(4)$. Here $\text{SU}(2)$ is the diagonal rotation group, corresponding to the subgroup of 3d rotations. Expressing the invariant vector in term of left/right components

$$|\mathcal{I}, 0\rangle = \frac{1}{\sqrt{d_j}} \sum_m (-1)^{j-m} |j, m\rangle_L |j, -m\rangle_R, \quad (7.5)$$

where $d_j = 2j + 1$ is the dimension of the $\text{SU}(2)$ representation of spin j . It is straightforward to show that the kernel $\mathcal{K}_{\mathcal{I}}$ is simply given by the $\text{SU}(2)$ character $\chi_j(g)$, defined as the trace of the group element in the j -representation of $\text{SU}(2)$. Parameterizing the $\text{SU}(2)$ group elements as

$$g(\theta, \hat{n}) = \cos \theta \mathbb{I} + i \sin \theta \hat{n} \cdot \vec{\sigma}, \quad \theta \in [0, \pi], \quad (7.6)$$

the characters depend entirely on the class angle θ (half the rotation angle) and are expressed as

$$\chi_j(g) = \frac{\sin d_j \theta}{\sin \theta}. \quad (7.7)$$

Using the properties of invariance of the Haar measure, it can then be proved that the relativistic spin network evaluation is actually a 3d object involving only integrals over $SU(2)$ [110]

$$\mathcal{A} = \int_{SU(2)} \prod_n dg_n \prod_i \frac{1}{d_{j_i}} \chi_{j_i}(g_{s(i)}^{-1} g_{t(i)}). \quad (7.8)$$

The Barrett-Crane model was originally derived for specific two-complexes C , which are the dual 2-skeleton of 4-dimensional triangulations Δ_4 (see Table 6.2). Starting with the triangulation Δ_4 , the dual two-skeleton C is constructed by associating to each simplex a point in its interior. An edge of the skeleton connects two points, which corresponds to two 4-simplices having a common tetrahedron. Then, a triangle of the triangulation Δ_4 correspond to a face of the two-complex C formed by the edges of the dual tetrahedra having this triangle in common. This duality allows to derive the spin foam amplitudes from a quantization of the geometry of a 4-simplex. Indeed, the amplitude for a single 4-simplex defines the vertex amplitude of the spinfoam model. Arbitrary 2-complexes are constructed by gluing 4-simplices together and the corresponding spinfoam amplitudes are given by the product of these vertex amplitudes corresponding to each 4-simplex.

Considering a single 4-simplex, the vertex amplitude is constructed as the evaluation of its boundary spin network. The boundary graph is constructed as the dual of the boundary of the 4-simplex: each tetrahedron is mapped on a node of the graph and each triangle shared by two tetrahedra is mapped to a link between these nodes. This gives a graph s with 5 nodes $n \in \{1, \dots, 5\}$ and 10 links between them, as represented in Fig. 7.2.

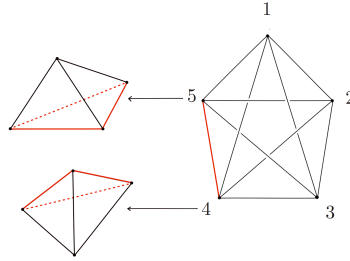


Figure 7.2: The 4-simplex (or pentahedral) boundary spin network. We label the nodes $a = 1, \dots, 5$. In the dual picture, they are in correspondence with tetrahedra of the boundary triangulation. Two of them are represented. The ten links ab , on the other hand, are dual to triangles. Consider for instance the link 45: this is dual to the triangle shared by the tetrahedra 4 and 5. The dihedral angle θ_{45} between the tetrahedra 4 and 5 is associated with the link 45.

The vertex amplitude $\mathcal{A}[s]$ is the given – up to normalization factors – by the evaluation of the boundary spin network s and defines the Barrett-Crane $\{10j\}$ -symbol, following (7.8).

$$\{10j\} \equiv \int_{SU(2)} \prod_{n=1}^5 dg_n \prod_{i=1}^{10} \chi_{j_i}(g_{s(i)}^{-1} g_{t(i)}), \quad (7.9)$$

The normalization ambiguity leads to an ambiguity in the definition of the Barrett-Crane model. It corresponds to arbitrary gluing factors between 4-simplices, or equivalently to ambiguity in defining the spinfoam edge amplitude \mathcal{A}_e . We will come back to this issue in the last part, Chapter 15.

Moreover, the $\{10j\}$ symbol will be the central object of the discussion about the physical boundary state for the quantum 4-simplex in the context of the Barrett-Crane model presented in the Chapter 15.

This symbol admits a geometrical interpretation associated to a 4-simplex which we explain now. We introduce the notation (ab) for i linking the nodes a and b . The indices $a, b = 1 \dots 5$ label the five nodes of the pentahedral; in the triangulation picture, there are in correspondence with tetrahedra of the boundary 4-simplex and links $i \equiv (ab)$ are dual to triangles (see Fig. 7.2). Thus, in the triangulation picture, while the five group elements $g_a \in SU(2)$ are associated to the 5 tetrahedra of the 4-simplex, the ten representations

$j_i \equiv j_{ab}$ for $a \neq b$ can be seen as attached to the triangles of the 4-simplex. The key fact is that it can be written as an integral over ten class angles $\theta_{ab} \in [0, \pi]$ of the group elements $g_a^{-1}g_b$: θ_{ab} is the dihedral angle and we use the convention $\theta_{aa} = 0$. In the triangulation picture, it is the angle between the outward normals to the tetrahedron a and the tetrahedron b of the 4-simplex. The $\{10j\}$ symbol then reads

$$\{10j\} = \int d\mu[\theta_{ab}] \prod_{a < b} \chi_{j_{ab}}(\theta_{ab}), \quad (7.10)$$

where the measure on the ten class angles $d\mu[\theta_{ab}]$ takes into account that the group elements $g_a^{-1}g_b$ are obviously not independent. The measure is in fact simply given by a constraint [111]

$$d\mu[\theta_{ab}] = \prod_{a < b} d\theta_{ab} \sin \theta_{ab} \delta(\det G_{ab}), \quad (7.11)$$

where G is the Gram matrix, a symmetric 5×5 matrix defined as $G_{ab} = \cos \theta_{ab}$. The constraint $\delta(G)$ contains all the geometric information and allows to relate the $\{10j\}$ -symbol to the Regge amplitude (which describes discretized gravity) for a Euclidean 4-simplex in the large j asymptotics [111, 110].

The independent variables are the areas of the triangles of the 4-simplex representing the triangulation or equivalently the dimension of the representation j_{ab} , $d_{j_{ab}} = 2j_{ab} + 1$, since $A_{ab} = l_P^2 d_{j_{ab}}$. The geometry of the 4-simplex is fixed by giving the ten areas $A_{ab} = d_{j_{ab}}$ and the dihedral angles can be considered as functions $\theta_{ab}(d_{j_{cd}})$ of the areas. Actually, we scale the area $d_{j_{ab}}$ instead of the spins j_{ab} , then the asymptotic behaviour on a single 4-simplex at the leading order¹ is given by [111]

$$\{10j\} \sim P(d_{j_{ab}}) \cos \left(\frac{1}{l_P^2} S_R[d_{j_{ab}}] \right) + D(d_{j_{ab}}), \quad (7.12)$$

where $S_R[d_{j_{ab}}] = \sum_{a < b} d_{j_{ab}} \theta_{ab}$. S_R is the action derived by Regge as a discretization of general relativity [112]. The function $P(d_{j_{ab}})$ is a slowly varying factor, that grows as $\zeta^{-9/2}$ when scaling all triangle areas $d_{j_{ab}}$ by ζ . $D(d_{j_{ab}})$ is a contribution coming from degenerate configurations of the 4-simplex. This is a non-oscillating term which has no interpretation in term of geometrical 4-simplices [113]. It was found to scale like $1/\zeta^2$ and thus dominate the large spin limit of the \tilde{j} -symbol. Moreover, it was shown in a recent paper [114] that even after having removing the dominating contribution of order $1/\zeta^2$, there are additional non-oscillating contributions still hiding the Regge term. This result indicates that the connection between this Barrett-Crane model and general relativity is not so simple.

7.2 The Lorentzian Barrett-Crane model

Let us now introduce the Lorentzian Barrett-Crane model [104, 115]. In the Lorentzian case, we need to start with the $\text{SL}(2, \mathbb{C})$ BF theory where $\text{SL}(2, \mathbb{C})$, regarded as a real Lie group, is the spin cover of the Lorentz group. We recall that the principal series of unitary, irreducible representations of $\text{SL}(2, \mathbb{C})$ are labelled by two parameters (n, ρ) , with n a half-integer and ρ a real number. As for the Euclidean case, the diagonal simplicity constraints impose a restriction on representations $\mathcal{I}_\Delta = (n_\Delta, \rho_\Delta)$,

$$2n_\Delta \rho_\Delta = 0 \quad \forall \Delta, \quad (7.13)$$

leading to² $n_\Delta = 0 \quad \forall \Delta$. The cross simplicity constraints are also imposed strongly at the level of a tetrahedron and induce a restriction on possible intertwiners. The analysis done in the Euclidean case is valid and the Lorentzian model is based on a vertex amplitude given by a $\{10j\}$ symbol, labelled by ten numbers ρ_i , one per edge of the 4-simplex boundary spin network. Let us introduce again the notation (ab) for the edge i linking the nodes a and b ($a, b = 1, \dots, 5$). The vertex amplitude is then explicitly given by

$$\{10j\}(\rho_{ab}) \equiv \int_{\mathcal{H}_+^4} \prod_{a=1}^4 dx_a \prod_{ab} K_{\rho_{ab}}(x_a, x_b). \quad (7.14)$$

¹To scale $d_{j_{ab}}$ instead of j_{ab} has no effect on the leading order.

²The solutions $\rho_\Delta = 0$ have been disregarded in the initial model [104], but incorporated later in [116].

$\mathcal{H}_+ = \{x_\mu \in \mathbb{R}^4, x^2 = -1, x_0 > 0\}$ is the unit upper hyperboloid in Minkowski space and the propagator $K_{\rho ab}(x_a, x_b)$ is defined by

$$K_\rho(x, y) \equiv \frac{\sin(\rho r(x, y))}{\rho \sinh(r(x, y))}, \quad (7.15)$$

where $r(x, y)$ is the hyperbolic distance between x and y . To integrate over $\mathcal{H}_+^{\times 4}$ instead of $\mathcal{H}_+^{\times 5}$ allows to regularize the amplitude which is otherwise divergent [104].

Let us now introduce the Immirzi parameter in this model. Indeed we will see in chapter 9 that a canonical basis of quantum states of geometry for the Lorentzian Barrett-Crane spinfoam model for quantum gravity can be given by projected spin networks (introduced in Chapter 5). In Chapter 9, we will define in particular a map from these projected spin networks to the standard $SU(2)$ spin networks of loop quantum gravity. We will show that this map is not one-to-one and that the corresponding ambiguity is parameterized by the Immirzi parameter [5].

In both the Euclidean and Lorentzian Barrett-Crane models, the Immirzi parameter γ can be taken into account by modifying the correspondence relation between the bivector B and the element of the Lie algebra

$$B \leftrightarrow \tilde{J}^{IJ} = \alpha J^{IJ} + \beta \star J^{IJ}, \quad (7.16)$$

with α and β functions of γ [93]. It has been shown in [93] that the Barrett-Crane spin foam amplitude remains valid for all constructions taking as correspondence relation any relation of the form (7.16). Therefore, the fact to take into account the Immirzi parameter does not modify the final Barrett-Crane spinfoam model defined by (7.9) in the Euclidean case and by (7.15) in the Lorentzian case.

Chapter 8

Simplicity constraints and the EPRL-FK models

It seems that the Barrett-Crane presented above is not able to capture the dynamics of general relativity. In the Euclidean case, the vertex amplitude given by a $\{10j\}$ symbol does not reproduce the semi-classical Regge action. This important property was identified in [117] where it was shown that the Barrett-Crane model is not able to reproduce the structure of the graviton propagator. This result is linked to the fact that each 4-simplex contribution in the partition function is independent because of the uniqueness of the Barrett-Crane intertwiner. Hence, such unique intertwiner seems to be inadequate to carry information from one 4-simplex to another. Considered from the point of view of loop quantum gravity, this intertwiner also has the drawback that it seems to freeze too many degrees of freedom of the 3d space geometry. Since the uniqueness of the Barrett-Crane intertwiner is a consequence of the imposition of the simplicity constraints, it became clear that one should modify the way these constraints are imposed. It was then proposed to solve the crossed simplicity constraints *weakly*, either by using some coherent state techniques [106] or by using a Gupta-Bleuler-like method involving the linear simplicity constraints [94, 95, 98]. The "weak" sense means in this context that one only requires that $\langle \phi | \mathcal{C}_{\Delta\tilde{\Delta}} | \psi \rangle = 0$ for any allowed boundary spin network states. These two approaches were shown to lead to the same spinfoam amplitudes [96, 97] apart from some subtle cases [107]. The weak imposition is justified by noting that after identification of the bivectors B_{Δ} with the generators J of the gauge group (or a linear combination of the generators and of its Hodge dual due to the ambiguity in the correspondence step, see Section 6.3.2), the simplicity constraints become non-commutative and imposing them strongly leads to inconsistencies.

The EPRL-FK models rely on a linear reformulation of the simplicity constraints (6.50) which distinguishes the two sectors (\star given in (6.27)) and (s given in (6.28)).

$$(s) \quad x_I \cdot B_{\Delta}^{IJ} = 0, \quad \forall \Delta \in \partial v, \quad (\star) \quad \epsilon^{IJ}{}_{KL} x_J \cdot B_{\Delta}^{KL} = 0, \quad \forall \Delta \in \partial v, \quad (8.1)$$

which replace the off simplicity constraints, i.e. the quadratic simplicity constraints (6.49) for the case where the two faces Δ, Δ' are involved. The diagonal simplicity constraints remain under their quadratic form

$$\epsilon_{IJKL} B_{\Delta}^{IJ} B_{\Delta}^{KL} = 0. \quad (8.2)$$

8.1 A quantization à la Gupta-Bleuler

We will review the derivation of the EPRL model both in the Euclidean case and the Lorentzian case with a finite Immirzi parameter. In these models, the Immirzi parameter is incorporated in the Plebanski formulation by modifying the BF part of the action. We will see that this will imply a modification of the correspondence rule used in the Barrett-Crane model above. We will not simply have $B \rightarrow J$ with J the generators of $\mathfrak{g} = \mathfrak{spin}(4)$ in the Euclidean case and $\mathfrak{g} = \mathfrak{sl}(2, \mathbb{C})$ in the Lorentzian case but a relation of the type (7.16) where the parameters α, β can be determined studying the symplectic structure of the boundary space [95, 98].

We review here the construction of [98] done in the case of a triangulation Δ_4 and for a group $G = \text{Spin}(4)$, $\text{SL}(2, \mathbb{C})$. We will specialize the analysis in the Euclidian and Lorentzian cases to identify their specific features after introducing the general procedure to quantize the model à la Gupta-Bleuler. The model has been then generalized to the case of an arbitrary cellular decomposition in [118]. Furthermore, we will present the model defined for a cellular decomposition in the next section 8.2 where we will build the model using coherent states.

In order to translate the simplicity constraints (8.1) at the quantum level, we first need to fix the ambiguity in the correspondence relation,

$$B \leftrightarrow \tilde{J}^{IJ} = \alpha J^{IJ} + \beta \star J^{IJ}, \quad (8.3)$$

that is we need to determine α , β and we shall proceed using the symplectic structure of the boundary space. Let us first precise the boundary variables [95]. As in the BF theory or in the Barrett-Crane model, the B -fields are discretized on the triangles Δ of the triangulation Δ_4 . We are now going to explain the way the curvature is discretized. Geometry is assumed to be flat on each 4-simplex, therefore a cartesian coordinate patch can be chosen in order to cover the whole 4-simplex. However, the triangulation is usually not flat and this patch cannot be extended to cover several 4-simplexes $\{v_{f^*}^1, v_{f^*}^2, \dots, v_{f^*}^n\}$ which surround the dual face $f^* \in \Delta_4^*$. The curvature is thus concentrated on the dual faces f^* in the dual 2-complex of Δ_4 and is coded in the holonomy around the link of each f^* .

The variables to describe this geometry are chosen as follows. We denote by

$$e(t) = e_\mu^I(t) v_I dx^\mu, \quad (8.4)$$

an orthonormal basis for the tetrahedron t where v_I is a basis in \mathbb{R}^4 chosen once and for all and

$$e(v) = e_\mu^I(v) v_I dx^\mu, \quad (8.5)$$

an orthonormal basis describing the geometry in the 4-simplex v . We denote by t_a , $a = 1, \dots, 5$, the five tetrahedra that bound the single 4-simplex v , then there exists five matrices $V_{vt_a} \in G$ such that each $e(t_a)$ is related to $e(v)$ by

$$e(v)_\mu^I = (V_{vt_a})_J^I e(t_a)_\mu^J, \quad (8.6)$$

in the common coordinate patch. We can also define the elements $U_{t_a t_b} \in G$ which describe the parallel transport between two tetrahedra t_a , t_b belonging to the 4-simplex v .

$$e(t_a) = U_v(t_a t_b) e(t_b) \quad \text{with} \quad U_v(t_a t_b) = (V_{vt_a})^{-1} V_{vt_b} = V_{t_a v} V_{vt_b}, \quad (8.7)$$

the last equality reflecting the fact that the 4-simplices are supposed to be flat. If we consider now two tetrahedra t and t' sharing a face Δ but not necessarily at the same 4-simplex, we can also define the parallel transport between t and t' by $U_\Delta(t, t') \in G$ such that

$$U_\Delta(t, t') \equiv V_{tv_1} V_{v_1 t_1} V_{t_1 v_2} \dots V_{v_n t'}, \quad (8.8)$$

where the product is around the link of Δ in the clock-wise direction from t' to t . We can then write for each tetrahedron t

$$B_\Delta(t)^{IJ} \equiv \int_\Delta \star (e(t)^I \wedge e(t)^J). \quad (8.9)$$

Two bivectors $B_\Delta(t)$, $B_\Delta(t')$ associated to the same triangle Δ represent the triangle Δ in two different internal frames associated to two distinct tetrahedra t and t' . These two bivectors are different but related by

$$U_\Delta(t, t') B_\Delta(t') = B_\Delta(t) U_\Delta(t, t'). \quad (8.10)$$

For a given triangle Δ , we denote $t_1 \dots t_n$ the set of the tetrahedra in the link around Δ and $v_{12}, v_{23}, \dots, v_{n1}$ the corresponding set of simplicies in this link, where t_2 bounds v_{12} and v_{23} and so on cyclically. We call the link around the face Δ , the cyclic sequence of 4-simplices separated by the tetrahedra that meet at the triangle Δ . The curvature associated to Δ is then defined by

$$U_\Delta(t_1) = U_{v_{12}}(t_1, t_2) \dots U_{v_{n1}}(t_n, t_1) = V_{t_1 v_{12}} V_{v_{12} t_2} \dots V_{t_n v_{n1}} V_{v_{n1} t_1} \quad (8.11)$$

that is by the product of the matrices obtained turning along the link of the triangle Δ , beginning with the tetrahedron t_1 . The V matrices are associated to the tetrahedra or equivalently to the dual edges $e^* \in \Delta_4^*$, $U_\Delta(t) \equiv U_\Delta(t, t)$ is the holonomy around the triangle Δ and the V matrices are the analogous of the group elements g_{e^*} , defined in the discrete BF theory (see Section 6.3.1), which also appear in the derivation of the Barrett-Crane model (see Chapter 7).

The classical discrete action is [98, 119]

$$S = - \sum_{\Delta \in \text{int} \Delta_4} \text{tr} \left[B_\Delta(t) U_\Delta(t) + \frac{1}{\gamma} \star B_\Delta(t) U_\Delta(t) \right] - \sum_{\Delta \in \partial \Delta_4} \text{tr} \left[B_\Delta(t) U_\Delta(t, t') + \frac{1}{\gamma} \star B_\Delta(t) U_\Delta(t, t') \right]. \quad (8.12)$$

This action with the simplicity constraints (8.1) and closure constraint (10.28) defines a discretization of general relativity [95, 98]. The boundary variables are in this formulation $B_\Delta(t) \in \mathfrak{g}$ and $U_\Delta(t, t') \in G$. The conjugated variable¹ to $U_\Delta(t, t')$ is

$$J_\Delta(t) = B_\Delta(t) + \frac{1}{\gamma} \star B_\Delta(t) \quad \Rightarrow \quad B_\Delta(t) = \frac{\gamma^2}{\gamma^2 - s} \left(J_\Delta(t) - \frac{1}{\gamma} \star J_\Delta(t) \right), \quad (8.13)$$

where $s = 1$ for $G = \text{Spin}(4)$ and $s = -1$ for $G = \text{SL}(2, \mathbb{C})$ and where we have assumed γ finite and $\gamma \neq 0, 1$. Thus a group element $U_\Delta \in G$ and as conjugated variable element $J_\Delta \in \mathfrak{g}$ are associated to each boundary triangle Δ in the boundary Δ_∂ of the triangulation Δ_4 .

$$G \times \mathfrak{g} \ni (U_\Delta, J_\Delta) \longrightarrow \Delta \subset \Delta_\partial.$$

It has been shown in [95] that this choice of variables (U_Δ, J_Δ) defines the same boundary phase space as for a lattice Yang-Mills theory with gauge group G . The explicit expression of the symplectic structure can be found in [95].

Before quantizing the theory, let us express the constraints for the J field. Indeed, the constraints (8.1) and (8.2) as well as the closure constraint (6.48) on the B field translate into constraints on the J field.

The closure for the B is equivalent to the closure for the J and this constraint will be imposed automatically by the dynamics. The simplicity constraints (8.2) and (8.1) become respectively

$$C_{\Delta\Delta} \equiv \star J_\Delta \cdot J_\Delta \left(1 + \frac{s}{\gamma^2} \right) - s \frac{2}{\gamma} J_\Delta \cdot J_\Delta = 0, \quad (8.14)$$

$$C_\Delta^J \equiv x_I \left((\star J)^{IJ} - \frac{s}{\gamma} J_\Delta^{IJ} \right) = 0, \quad (8.15)$$

where in the first equation, the dot stands for the scalar product in the algebra. To solve the second, we fix the gauge to $x_I = \delta_I^0$

$$C_\Delta^j = L_\Delta^j - \frac{s}{\gamma} K_\Delta^j = 0, \quad (8.16)$$

where

$$L_\Delta^j \equiv \frac{1}{2} \epsilon_{kl}^j J_\Delta^{kl} \quad \text{and} \quad K_\Delta^j \equiv J_\Delta^{0j} \quad (8.17)$$

are respectively the generators of the $\text{SU}(2)$ subgroup that leave x_I invariant and the generators of the corresponding boosts. The choice of this gauge corresponds in the Lorentzian case to the restriction of spacelike tetrahedra. The general case is recovered thanks to gauge invariance.

Let us now focus on the quantization step. We first need to write the Hilbert space associated with the boundary state space. For a given boundary, a 3-surface denoted by Σ , the associated Hilbert space is

$$\mathcal{H}_\Sigma = L^2 \left(G^L, d\mu_{\text{Haar}} \right),$$

¹Note that this not the conjugated variables in the 3+1 canonical sense. They are conjugated in the general sense where J and U are conjugated means that the action can be written as $S = \int U J$ [108].

where L is the number of links of the graph of the dual 2-complex Δ_∂^* of the boundary triangulation Δ_∂ (see Table 6.1 for the precise relation between a three-dimensional triangulation and its dual two-complex) and $d\mu_{\text{Haar}}$ is the Haar measure on the group G . In fact, we can write \mathcal{H}_Σ under the form

$$\mathcal{H}_\Sigma = \bigoplus_{\mathcal{I}_\Delta} \bigotimes_t \mathcal{H}_t, \quad (8.18)$$

where \mathcal{H}_t is the associated Hilbert space to the tetrahedron t .

Let us focus on a single tetrahedron t of the boundary triangulation Δ_∂ and on its associated Hilbert space \mathcal{H}_t . We associate an irreducible representation of G , \mathcal{I}_Δ , to each triangle Δ of the tetrahedron. We denote $\Delta_{\alpha=1\dots 4}$ the four triangles associated to t , then

$$\mathcal{H}_t \equiv \bigotimes_{\alpha=1}^4 \mathcal{H}_{\mathcal{I}_\alpha}, \quad (8.19)$$

where $\mathcal{H}_{\mathcal{I}}$ is the carrier space of the representation \mathcal{I} . It is the bivector conjugated to the curvature, J_Δ in our case, that is quantized being replaced by the generator of the symmetry algebra \mathfrak{g} in this representation². We denote \hat{J} the \mathfrak{g} generators. The closure constraint on the J -fields associated to the faces of the tetrahedron translates into a closure constraint on the \mathfrak{g} -generators \hat{J}_Δ . However, contrary to the Barrett-Crane model (see section 7) in which the simplicity constraints were imposed on the G -intertwiner space – i.e. the closure constraint was imposed before the simplicity constraints – the procedure followed in [94, 95, 98] consists in imposing firstly the simplicity constraints and in imposing the closure constraint secondly.

Let us precise the procedure followed to impose the different constraints in this context.

The quadratic diagonal simplicity constraints (8.14) imposed strongly translates into an equation on the Casimirs \tilde{C}_G and C_G .

$$\left(1 + \frac{s}{\gamma^2}\right) \tilde{C}_G(\mathcal{I}_\Delta) - \frac{2s}{\gamma} C_G(\mathcal{I}_\Delta) = 0, \quad (8.20)$$

where

$$\tilde{C}_G(\mathcal{I}_\Delta) = \frac{1}{2} \epsilon^{IJKL} \hat{J}_{IJ}^{\mathcal{I}_\Delta} \hat{J}_{KL}^{\mathcal{I}_\Delta} = 4sL^j K_j, \quad (8.21)$$

is the pseudo-scalar Casimir of the group G , and

$$C_G(\mathcal{I}_\Delta) = (\hat{J}^{\mathcal{I}_\Delta})^{IJ} \hat{J}_{IJ}^{\mathcal{I}_\Delta} = 2(L^2 + sK^2) \quad (8.22)$$

is the scalar Casimir of G . We have respectively $s = 1, -1$ for $G = \text{Spin}(4), \text{SL}(2, \mathbb{C})$. This strong constraint will restrict the allowed G -representations to γ -simple representations. The definition of a γ -simple representation for the group G will be explicitly given in the two next sections where we will distinguish the Euclidean case $G = \text{Spin}(4)$ and the Lorentzian case $G = \text{SL}(2, \mathbb{C})$.

Regarding the gauge-fixed cross simplicity constraints (8.16), we look for a Hilbert space \mathcal{H}_s , a subspace of \mathcal{H}_t , such that the matrix elements of the cross simplicity constraints (8.16) on this smaller Hilbert space all vanish

$$\forall \phi, \psi \in \mathcal{H}_s, \quad \langle \phi | \mathcal{C}_\Delta^j | \psi \rangle = 0. \quad (8.23)$$

The strategy followed in [119, 98] is inspired by [77, 120, 121, 122]. The set of constraints (8.16) is replaced by the single "master" constraint

$$\mathcal{M}_\Delta \equiv \sum_j \left(\mathcal{C}_\Delta^j \right)^2 = \sum_j \left(L^j - \frac{s}{\gamma} K^j \right)^2 = 0. \quad (8.24)$$

This new constraint can be written in terms of the Casimir operators \tilde{C}_G and C_G respectively given by (8.21) and (8.22)

$$\mathcal{M}_\Delta = L^2 \left(1 - \frac{s}{\gamma} \right) + \frac{s}{2\gamma^2} \tilde{C}_G - \frac{1}{2\gamma} C_G = 0, \quad (8.25)$$

²This is justified in [95, 98] by the symplectic structure of the boundary phase space which reproduces the one of a lattice Yang-Mills theory with gauge group G .

which combined with (8.20) simplifies into

$$C_G - 4\gamma L^2 = 0. \quad (8.26)$$

This new equation will select one subspace of the Hilbert space associated to the tetrahedron. This subspace corresponds to \mathcal{H}_s – this is explicitly shown in [123] for the Euclidean case and in [124] for the Lorentzian case. Finally, once the simplicity has been implemented, the closure constraint (6.48) is imposed on \mathcal{H}_s turning it into an intertwiner space. In terms of the SU(2) rotation and boost generators, L and K , this constraint (6.48) becomes

$$\sum_{\Delta \in t} L_{\Delta}^i = 0 \quad \forall i, \quad (8.27)$$

$$\sum_{\Delta \in t} K_{\Delta}^i = 0 \quad \forall i. \quad (8.28)$$

In fact, these closure constraints are imposed only weakly turning \mathcal{H}_s into a SU(2) intertwiner space, denoted by

$$\mathcal{K}_s \equiv \text{Inv}_{\text{SU}(2)}[\mathcal{H}_s]. \quad (8.29)$$

More precisely, by definition of \mathcal{K}_s , the left-hand-side of (8.27) which is the generator of global SU(2) transformations vanishes strongly on \mathcal{K}_s whereas the left-hand-side of (8.28) is weakly proportional to $\sum_{\Delta \in t} L_{\Delta}^i$ due to the weak relation (8.23) and therefore vanishes weakly.

The total physical boundary space \mathcal{H}_{ph} of the theory is finally obtained as the span of spin networks in $L^2[G^L/G^V, d\mu_{\text{Haar}}] - V$ is the number of vertices of the graph of the dual 2-complex Δ_{∂}^* of the boundary triangulation Δ_{∂} – with γ -simple representations on edges and with intertwiners in the spaces \mathcal{K}_s at each vertex. Thus, by definition, the boundary states correspond to projected spin networks $|\varphi_{\mathcal{I}_e, j_e^s, i_v}\rangle$ defined in (5.11) with $\mathcal{I}_e \equiv \mathcal{I}_{\Delta}$ γ -simple representations of G for any triangulation³ Δ and $j_e^s = j_e^t \equiv j_{\Delta}$ a SU(2) irreducible representations such that $(\vec{L}_{\Delta})^2 = j_{\Delta}(j_{\Delta} + 1)$. The embedding of the irreducible representations j_{Δ} into the G irreducible representations \mathcal{I}_{Δ} given by the relation (8.25) is explicitly detailed in the two next sections, respectively for $G = \text{Spin}(4)$ and $G = \text{SL}(2, \mathbb{C})$. Moreover, i_v is the SU(2) intertwiner chosen in \mathcal{K}_s associated to each vertex v . We will see in the Chapter 9 that the projected spin networks are in addition very easily related to the SU(2) spin networks of loop quantum gravity.

Finally, to recover G spin networks the last step is a group averaging (as defined in (5.7)).

The EPRL-FK vertex amplitude can then be defined using the BF amplitude (6.43). The explicit expressions, which depends on the considered group G , are given in the two following sections: let us identify now the different aspects of the model according to the choice of group $G = \text{Spin}(4)$ or $G = \text{SL}(2, \mathbb{C})$.

8.1.1 The Euclidean case with a finite Immirzi parameter

We recall that unitary representations of Spin(4) are labelled by a couple of half integers $\mathcal{I} = (k^L, k^R)$.

- The diagonal simplicity constraints (8.20) impose then the following restriction on the representations associated to each face Δ

$$k_{\Delta}^L = \left| \frac{\gamma + 1}{\gamma - 1} \right| k_{\Delta}^R. \quad (8.30)$$

Let us notice that in order to obtain this solution – more precisely in order that (8.20) for the Spin(4) Casimir does have solutions – the authors of [98] had to choose a different ordering than the usual one used to define Casimirs operators⁴ of Spin(4).

³We recall that edges $e \in \Delta_{\partial}^*$ in the dual picture are dual to triangles $\Delta \in \Delta_{\partial}$ and this one-to-one correspondence allows us to denote the discrete variables by either a triangle Δ or an edge e subindex respectively.

⁴With the usual ordering, we have

$$\tilde{C}_{\text{Spin}(4)} = 4k^L(k^L + 1) + 4k^R(k^R + 1) \quad \text{and} \quad C_{\text{Spin}(4)} = 4k^L(k^L + 1) - 4k^R(k^R + 1).$$

- Let us restrict to the case $\gamma > 0$ which implies $k^L > k^R$. Inserting (8.30) into the "master" constraint (8.26) constraints the quantum number j associated to the $SU(2)$ Casimir L^2 (again up to an ordering ambiguity) to

$$j^2 = \left(\frac{2k^L}{1+\gamma} \right)^2 = \left(\frac{2k^R}{1-\gamma} \right)^2 \quad \Rightarrow \quad j = \begin{cases} k^L + k^R & 0 < \gamma < 1 \\ k^L - k^R & \gamma > 1 \end{cases}. \quad (8.31)$$

This constraint selects a subspace \mathcal{H}_s of $\mathcal{H}_t = \bigotimes_{\alpha=1}^4 \mathcal{H}_{\mathcal{I}_\alpha}$. Indeed, for each triangle $\Delta_{\alpha=1\dots 4}$, the Clebsch-Gordan decomposition of $\mathcal{H}_{\mathcal{I}_\alpha}$ gives

$$\mathcal{H}_{\mathcal{I}_\alpha} = \mathcal{H}_{k_\alpha^L \otimes k_\alpha^R} = \bigoplus_{j_\alpha = |k_\alpha^L - k_\alpha^R|}^{k_\alpha^L + k_\alpha^R} \mathcal{H}_{j_\alpha}, \quad (8.32)$$

and the constraint (8.31) selects in $\mathcal{H}_{\mathcal{I}_\alpha}$ the "extremum" subspace leading to

$$\mathcal{H}_s = \begin{cases} \bigotimes_{\alpha=1}^4 \mathcal{H}_{k_\alpha^L + k_\alpha^R}, & \text{for } \gamma < 1, \\ \bigotimes_{\alpha=1}^4 \mathcal{H}_{k_\alpha^L - k_\alpha^R}, & \text{for } \gamma > 1. \end{cases} \quad (8.33)$$

The simplicity constraints (8.15), when (8.30) is holding, is then satisfied weakly in \mathcal{H}_s [123]. That is, the action of the constraints on the states in \mathcal{H}_s (8.23) results in states orthogonal to \mathcal{H}_s .

- The last step is to solve weakly the closure constraints given by (8.27) and (8.28) in the space \mathcal{H}_s in order to get an intertwiner space \mathcal{K}_s . We get that

$$\mathcal{K}_s = \text{Inv}_{SU(2)} [\mathcal{H}_s]. \quad (8.34)$$

- Then, to get a $\text{Spin}(4)$ spin network a group averaging on $\text{Spin}(4)$ is performed. We can now define the vertex amplitude. We will not give any details on its construction which can be obtained starting from the $\text{Spin}(4)$ BF vertex amplitude (6.43), see [95, 98].

$$A_v^{\text{Spin}(4) \text{ EPRL-FK}}(j_{f^*}, i_{v^*}) = \sum_{i_{e^*}^L, i_{e^*}^R} 15j \left(\frac{(1+\gamma)}{2} j_{f^*}, i_{v^*}^L \right) 15j \left(\frac{|1-\gamma|}{2} j_{f^*}, i_{v^*}^R \right) \bigotimes_{v^*} f_{i_{v^*}^L i_{v^*}^R}^{i_{v^*}} \quad (8.35)$$

where the $15j$ are the standard $SU(2)$ Wigner symbols and $f_{i_{v^*}^L i_{v^*}^R}^{i_{v^*}}$ are the fusion coefficient obtained contracting $SU(2)$ intertwiners i_{v^*} and $\text{Spin}(4)$ intertwiners $(i_{v^*}^L, i_{v^*}^R)$ (for further details see [98]).

8.1.2 The Lorentzian, with a finite Immirzi parameter

We recall that the principal series of unitary representations of $SL(2, \mathbb{C})$ are labelled by two parameters $\mathcal{I} = (n, \rho)$ with n a half-integer and ρ a real number.

- The diagonal simplicity constraints (8.20) impose the following restriction on the representations associated to each face Δ

$$\rho = \gamma(n+1). \quad (8.36)$$

Let us notice that this solution first proposed in [124] differs from the usual solution $\rho = \gamma n$ found in the literature but it is this ansatz we use in the Chapter 9. Moreover, there exists a second branch of solutions to these constraints (8.20) given by $\rho = -n/\gamma$ but it is eliminated by the master constraint (8.26).

- Inserting this relation (8.36) into the "master" constraint (8.26) constraints the quantum number j associated to the $SU(2)$ Casimir L^2 to

$$j = n. \quad (8.37)$$

This constraint selects a subspace \mathcal{H}_s of $\mathcal{H}_t = \bigotimes_{\alpha=1}^4 \mathcal{H}_{\mathcal{I}_\alpha}$. Indeed, for each triangle $\Delta_{\alpha=1\dots 4}$, $\mathcal{H}_{\mathcal{I}_\alpha}$ splits into the irreducible representations \mathcal{H}_{j_α} of the $SU(2)$ subgroup as

$$\mathcal{H}_{\mathcal{I}_\alpha} = \mathcal{H}_{(n_\alpha, \rho_\alpha)} = \bigoplus_{j_\alpha=n_\alpha}^{\infty} \mathcal{H}_{j_\alpha}, \quad (8.38)$$

with j_α increasing in steps of 1 and the constraint (8.37) selects in $\mathcal{H}_{\mathcal{I}_\alpha}$ the "minimal" subspace leading to

$$\mathcal{H}_s = \bigotimes_{\alpha=1}^4 \mathcal{H}_{n_\alpha}. \quad (8.39)$$

The simplicity constraints (8.15), when (8.36) is holding, is then satisfied weakly in \mathcal{H}_s [124]. That is, the action of the constraints on the states in \mathcal{H}_s (8.23) results in states orthogonal to \mathcal{H}_s .

- The last step is to solve weakly the closure constraints given by (8.27) and (8.28) in the space \mathcal{H}_s in order to get an intertwiner space \mathcal{K}_s . We get that

$$\mathcal{K}_s = \text{Inv}_{SU(2)}[\mathcal{H}_s]. \quad (8.40)$$

- As in the Euclidean case, the last step is a group averaging over $SL(2, \mathbb{C})$ in order to obtain $SL(2, \mathbb{C})$ spin networks and the vertex amplitude is given by [98, 124]

$$A_v^{\text{SL}(2, \mathbb{C}) \text{ EPRL-FK}}(j_{f^*}, i_{v^*}) = \sum_{n_{e^*}} \int d\rho_{e^*} (\rho_{e^*}^2 + n_{e^*}^2) 15j_{\text{SL}(2, \mathbb{C})}(j_{f^*}, \gamma(j_{f^*} + 1); (n_{e^*}, \rho_{e^*})) \left(\prod_{e^* \text{ st}} f_{n_{e^*}, \rho_{e^*}}^{i_{e^*}}(j_{f^*}) \right) \quad (8.41)$$

where we now use the $15j$ of $SL(2, \mathbb{C})$ and $f_{n_{e^*}, \rho_{e^*}}^{i_{e^*}}$ are fusion coefficients obtained contracting $SU(2)$ intertwiners i_{v^*} and $SL(2, \mathbb{C})$ intertwiners (n_{e^*}, ρ_{e^*}) .

This concludes our overview of the way introduced in [94, 95, 98] to deal with the simplicity constraints.

8.2 Using coherent states

We will now introduce the coherent intertwiners used to solve weakly the cross simplicity constraints in the EPRL-FK models. The problem of defining "coherent states" for loop quantum gravity has raised an increasing interest over the last few years. Indeed, although the fact that spin network states, the building block of loop quantum gravity, provide a basis of the kinematical Hilbert space and diagonalize some geometric operators, they lack a low-energy interpretation. We need to bridge the Planck scale quantum geometry to a smooth and classical three dimensional geometry, which is why the construction of coherent states is very important. These semi-classical states should be the analogue of wave packets or coherent states that approximate classical configurations in ordinary quantum theory. We recall that the phase space of general relativity can be described by the triad and $SU(2)$ connection (E_i^a, A_a^i) used in loop gravity. Consequently, a coherent state for loop gravity should be a superposition of spin networks peaked on (E_i^a, A_a^i) , with small fluctuations. This approach has been developed by T. Thiemann and collaborators [72, 125, 126, 127, 128].

In the context of spin foam models, the approach to find semi-classical quantum states that approximate a given classical geometry is different. In the spin foam framework, a classical phase space point is described in terms of quantities referring to discrete geometries, e.g. areas and dihedral angles, as opposed to holonomies and fluxes. The precise connection between the loop quantum variables associated to a given graph Γ and labels describing the spin foam discrete geometry has been done using twisted geometries [129, 130]. Twisted geometries are quantities describing the intrinsic and extrinsic geometry of the cellular decomposition dual to the graph Γ .

We now define the $SU(2)$ coherent states introduced by E. Livine and S. Speziale in [106]. These coherent intertwiners, labelled by N unit vectors in \mathbb{R}^3 satisfying a closure condition – in the case of a N valent vertex –, have very interesting semi-classical properties and allow to peak intertwiners on specific classical convex polyhedra [131, 132, 8].

8.2.1 The $SU(2)$ coherent intertwiners

The $SU(2)$ coherent states are derived by acting with $SU(2)$ rotations on the highest weight vectors $|j, j\rangle$

$$\forall g \in SU(2), \quad |j, g\rangle \equiv g |j, j\rangle. \quad (8.42)$$

These states are coherent states à la Perelomov and transform consistently under the $SU(2)$ action

$$h |j, g\rangle = |j, hg\rangle. \quad (8.43)$$

They also satisfy a very simple tensorial property

$$|j, g\rangle \otimes |\tilde{j}, g\rangle = g(|j, j\rangle \otimes |\tilde{j}, \tilde{j}\rangle) = g |j + \tilde{j}, j + \tilde{j}\rangle = |j + \tilde{j}, g\rangle. \quad (8.44)$$

It is easy to compute their expectation values

$$\langle j, g | \vec{J} | j, g \rangle = j \hat{n}, \quad \hat{n} = g \hat{z}, \quad (8.45)$$

where the unit vector $\hat{n} \in \mathcal{S}^2$ is obtained by rotating the z axis by the $SU(2)$ group element g . They are actually coherent states on the 2-sphere $\mathcal{S}^2 \sim SU(2)/U(1)$ since \hat{n} only depends on g up to a $U(1)$ phase. Actually, the standard definition of the $SU(2)$ coherent states involves a choice of section and we usually choose the unique group element $g(\hat{n})$ for a given unit vector \hat{n} such that the rotation axis lays in the (xy) plane. Then the coherent state is defined as $|j, \hat{n}\rangle \equiv g(\hat{n}) |j, j\rangle = |j, g(\hat{n})\rangle$. Finally, these states minimize the uncertainty relation

$$\langle j, g | \vec{J}^2 | j, g \rangle - \langle j, g | \vec{J} | j, g \rangle^2 = j(j+1) - j^2 = j. \quad (8.46)$$

Then N -valent coherent intertwiners are defined following [106] by tensoring N such $SU(2)$ coherent states and group averaging this tensor product in order to get an intertwiner. More precisely, we choose N representations of $SU(2)$ labeled by the spins j_1, \dots, j_N and N unit 3-vectors $\hat{n}_1, \dots, \hat{n}_N$, then we define

$$|j_i, \hat{n}_i\rangle \equiv \int_{SU(2)} dg g \triangleright \bigotimes_{i=1}^N |j_i, \hat{n}_i\rangle = \int_{SU(2)} dg \bigotimes_{i=1}^N gg(\hat{n}_i) |j_i, j_i\rangle. \quad (8.47)$$

8.2.2 Intertwiner states as weak solutions of the simplicity constraints

Now coming back to the $\text{Spin}(4) \sim SU_L(2) \times SU_R(2)$ and the simplicity constraints, we use simple $\text{Spin}(4)$ representations with $j_i^L = j_i^R$ and double the labels of the coherent states introducing unit 3-vectors $\hat{n}_1^{L,R}, \dots, \hat{n}_N^{L,R}$. Considering the tensor product of $SU(2)$ coherent states $|j, \hat{n}^L\rangle \otimes |j, \hat{n}^R\rangle$, the expectation values of the $\mathfrak{spin}(4)$ generators $\vec{J}_i^{L,R}$ are $j \hat{n}^{L,R}$. These two 3-vectors with equal norm define a single bivector $B \in \wedge^2 \mathbb{R}^4$ being its self-dual and anti-self dual components. Then considering N such coherent states $|j_i, \hat{n}_i^L\rangle \otimes |j_i, \hat{n}_i^R\rangle$, their expectation values give N bivectors B_i . We now impose the simplicity constraints on these classical bivectors.

First looking at the sector (s) (defined by (6.27), the fact that the bivectors B_i all share a same time normal x translates to the existence of a $SU(2)$ transformation mapping simultaneously all the self-dual part (left) onto the anti-self-dual part (right). Moreover, this $SU(2)$ group element defines uniquely the normal 4-vector,

$$\forall i, x \cdot B_i = 0 \quad \Leftrightarrow \quad \exists g \in SU(2), \quad \forall i, \hat{n}_i^L = g \hat{n}_i^R, \quad x = (g, \mathbb{I}) \triangleright \omega, \quad (8.48)$$

where $\omega = (1, 0, 0, 0)$ is the reference unit time vector and the $\text{Spin}(4)$ group element (g, \mathbb{I}) is defined through its left/right factors. Imposing this constraint on the labels of the coherent states, we define a $\text{Spin}(4)$ coherent

intertwiner by group averaging. This coherent intertwiner is labeled by the representation label, plus the unit 3-vectors \hat{n}_i^R , plus the group element g which gives the time normal and the rotation which defines the components \hat{n}_i^L from the \hat{n}_i^R

$$\begin{aligned} ||j_i, \hat{n}_i, g\rangle_s &= \int_{\text{SU}_L(2) \times \text{SU}_R(2)} dg_L dg_R \left[g_L \triangleright \bigotimes_{i=1}^N g |j_i, \hat{n}_i\rangle \right] \otimes \left[g_R \triangleright \bigotimes_{i=1}^N |j_i, \hat{n}_i\rangle \right] \\ &= \left[\int_{\text{SU}(2)} dg_L g_L \triangleright \bigotimes_{i=1}^N |j_i, \hat{n}_i\rangle \right] \otimes \left[\int_{\text{SU}(2)} dg_R g_R \triangleright \bigotimes_{i=1}^N |j_i, \hat{n}_i\rangle \right]. \end{aligned} \quad (8.49)$$

Two things are obvious from this expression.

- The Spin(4) group averaging erases the group element g and thus all the data about the precise time normal x . In particular, we can drop the label g and call these states simply $||j_i, \hat{n}_i\rangle_s$.
- This states $||j_i, \hat{n}_i\rangle_s$ are the tensor product of two identical SU(2) intertwiners for the left and right parts. In particular, they obvious satisfy the quadratic simplicity constraints

$$\forall i, j, \quad \langle \vec{J}_i^L \cdot \vec{J}_j^L \rangle = \langle \vec{J}_i^R \cdot \vec{J}_j^R \rangle. \quad (8.50)$$

Moreover, they minimize the uncertainty by definition.

We can go one step further by re-writing these states,

$$||j_i, \hat{n}_i\rangle_s = \int_{\text{Spin}(4)} dG G \triangleright \bigotimes_{i=1}^N |j_i, \hat{n}_i\rangle_L \otimes |j_i, \hat{n}_i\rangle_R = \int_{\text{Spin}(4)} dG G \triangleright \bigotimes_{i=1}^N |2j_i, \hat{n}_i\rangle, \quad (8.51)$$

where we used the tensorial property of the SU(2) coherent states $|j, \hat{n}\rangle \otimes |\tilde{j}, \tilde{\hat{n}}\rangle = |j + \tilde{j}, \hat{n}\rangle$. This shows that the coherent states are exactly the EPR states [94, 95] which form a Hilbert space $H_s[j_\Delta]$ solving weakly the simplicity constraints [96, 97].

Second, we consider the dual sector (\star) (defined by (6.28)) and we follow the same procedure. The only difference is a sign in solving the corresponding linear simplicity constraints.

$$\forall i, \epsilon x B_i = 0 \quad \Leftrightarrow \quad \exists g \in \text{SU}(2), \quad \forall i, \hat{n}_i^L = -g \hat{n}_i^R. \quad (8.52)$$

This leads to similar coherent states [96, 97].

$$||j_i, \hat{n}_i\rangle_\star = \left[\int_{\text{SU}(2)} dg_L g_L \triangleright \bigotimes_{i=1}^N |j_i, -\hat{n}_i\rangle \right] \otimes \left[\int_{\text{SU}(2)} dg_R g_R \triangleright \bigotimes_{i=1}^N |j_i, \hat{n}_i\rangle \right], \quad (8.53)$$

$$= \left[\int_{\text{SU}(2)} dg_L g_L \triangleright \bigotimes_{i=1}^N \overline{|j_i, \hat{n}_i\rangle} \right] \otimes \left[\int_{\text{SU}(2)} dg_R g_R \triangleright \bigotimes_{i=1}^N |j_i, \hat{n}_i\rangle \right]. \quad (8.54)$$

Once again, it is obvious to check that these states satisfy the quadratic simplicity constraints in expectation value. Also, the information about the time normal is completely erased by the group averaging. Finally, the key difference with the previous sector (s) is that these intertwiner states generate the whole intertwiner space and do not form a subspace. This ansatz looks more like a fuzzy version of the Barrett-Crane intertwiner.

This concludes our quick overview of the standard way to deal with the crossed simplicity constraints using the SU(2) coherent intertwiners.

Chapter 9

Simplicity constraints and $SU(2)$ spin networks

9.1 Back and forth between projected and $SU(2)$ spin networks

We focus in this Chapter on the Lorentzian case, i.e. $G = SL(2, \mathbb{C})$. Let us consider an arbitrary oriented graph Γ with E edges and V vertices. We denote again $H = L^2_{SU(2) \text{ inv.}}[dG^L]$ where dG is the $SL(2, \mathbb{C})$ Haar measure, the Hilbert space of projected cylindrical functionals on the graph Γ introduced in Section 5. We have left implicit the underlying graph Γ since the whole following analysis is done for the fixed graph Γ . The projected spin networks

$$\varphi_{\mathcal{I}_e, j_e^s, i_v}(G_e, x_v) \equiv \text{tr} \prod_e \langle \mathcal{I}_e, j_e^s, m_e^s | B_{s(e)}^{-1} G_e B_{t(e)} | \mathcal{I}_e, j_e^t, m_e^t \rangle \prod_v \langle \otimes_{e|t(e)=v} \mathcal{I}_e, j_e^t, m_e^t | i_v | \otimes_{e|s(e)=v} \mathcal{I}_e, j_e^s, m_e^s \rangle, \quad (9.1)$$

form an orthonormal basis of H and are the natural boundary states for Spin Foam models (as explained in Section 8.1 for the EPRL-FK spin foam models and in [80] for the Barrett-Crane model). In the previous formula, we recall that $\mathcal{I} = (n, \rho)$ are $SL(2, \mathbb{C})$ irreducible representations, j are $SU(2)$ irreducible representations and i are $SU(2)$ intertwiners. Our goal is to compare the projected spin networks with the $SU(2)$ spin network basis of loop quantum gravity. As we have seen, the projected spin networks are Lorentz-invariant functionals of the $SL(2, \mathbb{C})$ connection and of the time-normal field. Nevertheless, as soon as we fix the value of the time-normal field (at the vertices of the graph used to construct the spin network), they are only required to satisfy an effective $SU(2)$ invariance and thus they are built using $SU(2)$ -intertwiners and not $SL(2, \mathbb{C})$ -intertwiners. Since $SU(2)$ spin networks are also built from $SU(2)$ -intertwiners, this hints towards a direct path between the two sets of states. From this perspective, projected spin networks seems to be extensions of $SU(2)$ spin networks, allowing to evaluate them on the whole Lorentz group $SL(2, \mathbb{C})$ and not only on the $SU(2)$ subgroup.

9.1.1 Projecting down to $SU(2)$ spin networks

Let us start by reminding the definition of $SU(2)$ cylindrical functions on the graph Γ introduced in Section 4.1. They are functions of E group elements in $SU(2)$ living on the edges of the graph and satisfying a $SU(2)$ invariance at every vertex

$$\psi(g_e) = \psi(h_{s(e)} g_e h_{t(e)}^{-1}), \quad \forall h_v \in SU(2)^{\times V}. \quad (9.2)$$

The natural scalar product on this space of functions is

$$\langle \psi | \psi' \rangle_{SU(2)} = \int_{SU(2)} [dg_e] \bar{\psi}(g_e) \psi'(g_e), \quad (9.3)$$

where dg is the Haar measure on the $SU(2)$ Lie group. Let us call H_S the L^2 space of such $SU(2)$ invariant cylindrical functions. Then this Hilbert space H_S is spanned by the usual spin network states defined in Section

4.3. A spin network is labeled by a set of spins j_e for each edge and SU(2)-intertwiners i_v for every vertex. Then we define

$$\psi_{j_e, i_v}(g_e) \equiv \text{tr} \prod_e \langle j_e, m_e^s | g_e | j_e, m_e^t \rangle \prod_v \langle \otimes_{e|t(e)=v} j_e, m_e^t | i_v | \otimes_{e|s(e)=v} j_e, m_e^s \rangle, \quad (9.4)$$

which simply amounts to contracting the Wigner matrices $D_{m^s m^t}^j(g) = \langle j, m^s | g | j, m^t \rangle$ along every edge e with the intertwiners sitting at the vertices. We point out that this definition is almost the same as the one of projected spin networks: the difference is that we evaluate projected spin networks on the whole $\text{SL}(2, \mathbb{C})$ group and this requires the choice of an extra $\text{SL}(2, \mathbb{C})$ irrep \mathcal{I}_e for each edge of the graph.

The scalar product between two such SU(2) spin networks is easily computed

$$\langle \psi_{j_e, i_v} | \psi_{\tilde{j}_e, \tilde{i}_v} \rangle_{\text{SU}(2)} = \prod_e \frac{\delta_{j_e, \tilde{j}_e}}{d_{j_e}} \prod_v \langle i_v | \tilde{i}_v \rangle, \quad (9.5)$$

where we remind that $d_j = (2j + 1)$ is the dimension of the SU(2)-irrep of spin j .

Since the projected cylindrical functions and the SU(2) cylindrical functions share the same SU(2) invariance, it is natural to introduce the following projection

$$\begin{aligned} \mathcal{M}: \quad H &\rightarrow H_S \\ \varphi(G_e, x_v) &\mapsto \psi(g_e) = \varphi(g_e, \omega) = \phi(g_e), \end{aligned} \quad (9.6)$$

which is simply the restriction of the projected cylindrical function to the SU(2) subgroup. Considering the invariance property of the function φ and its section ϕ at $x_v = \omega$, $\forall v$, the map \mathcal{M} is well-defined and the resulting function ψ is correctly SU(2)-invariant as wanted.

It is straightforward to compute the image of the projected spin network by the map \mathcal{M} . First, considering the case of functions with $j_e^s \neq j_e^t$, the corresponding SU(2) function vanishes:

$$\forall j_e^s \neq j_e^t, \quad \mathcal{M} \varphi_{\mathcal{I}_e, j_e^s, t, i_v} = 0, \quad (9.7)$$

since a SU(2) group element could never trigger a transition between two different SU(2) irreps (by definition). On the other hand, now assuming that the two spins are equal for all edges so that we can drop the index s, t , $j_e^s = j_e^t = j_e$, then the image of the corresponding projected spin network is as expected simply a SU(2) spin network:

$$\forall j_e^s = j_e^t = j_e, \quad \mathcal{M} \varphi_{\mathcal{I}_e, j_e, i_v} = \psi_{j_e, i_v}, \quad (9.8)$$

as long as the spin j_e is compatible with the $\text{SL}(2, \mathbb{C})$ irrep, i.e $j_e \geq n_e$ (or more exactly $j_e \in n_e + \mathbb{N}$).

In the next sections, we investigate the inverse map(s) to \mathcal{M} , that is how to lift SU(2) cylindrical functions to functions on the whole Lorentz group $\text{SL}(2, \mathbb{C})$. Understanding in details how this lifting is achieved is crucial to the construction of the EPR-FK class of spin foam models and their interpretation as an ansatz for the dynamics of Loop Quantum Gravity.

In the following, we will focus on projected spin networks satisfying the “matching” constraints $j_e^s = j_e^t$. We call H_p the Hilbert spanned by these “proper” projected spin network functionals (whose evaluation on the SU(2) subgroup does not trivially vanish). As seen from the last equation above, inverting the map \mathcal{M} would more or less simply amount to choosing a $\text{SL}(2, \mathbb{C})$ irrep \mathcal{I}_e into which to embed the SU(2) irrep j_e . We analyze this in details below.

9.1.2 Lifting back Spin Networks

Starting with a SU(2) cylindrical function $\psi(g_e)$ invariant under the SU(2) action at every vertex, the goal is to construct a Lorentz invariant extension for it. Following the insight of the previous section, the simplest way to proceed would be to decompose the function ψ in SU(2) irrep j_e and to choose a $\text{SL}(2, \mathbb{C})$ irrep for every spin. At the level of the groups, these operations are done through convolutions with SU(2) and $\text{SL}(2, \mathbb{C})$ characters.

More precisely, starting with $\psi(g_e)$, we construct the following projected cylindrical function:

$$\varphi(G_e, B_v) \equiv \sum_{\{j_e\}} \Delta_{j_e} \int_{\text{SU}(2)} [dh_e dk_e] \psi(k_e) \chi^{j_e}(h_e k_e) \Theta^{\mathcal{I}_e}(B_{s(e)}^{-1} G_e B_{t(e)} h_e). \quad (9.9)$$

Δ_j is a weight depending on the spin j that we will uniquely fix below by requiring that $\mathcal{M}\varphi = \psi$ or more explicitly $\varphi(g_e, \mathbb{I}) = \psi(g_e)$. The label \mathcal{I}_e is an arbitrary function of the spin j_e and it does not need to be the same for all the edges e of the graph. The only constraint is that the SU(2)-irrep j_e needs to be in the $\text{SL}(2, \mathbb{C})$ -irrep \mathcal{I}_e , i.e we require that $n_e \leq j_e$ always (more exactly, $j_e \in n_e + \mathbb{N}$).

First, we check that the constructed function is invariant under SU(2) shifts $B_v \rightarrow B_v h_v$. This is true thanks to the SU(2) invariance of the original function ψ . Then, we easily see that this function is invariant under Lorentz transformations acting simultaneously on both G_e and B_v . Finally, we would like to ensure that φ is a proper lifting of ψ , i.e that $\mathcal{M}\varphi = \psi$. To check this, we compute straightforwardly the value of φ for $G_e = g_e \in \text{SU}(2)$ and $B_v = \mathbb{I}$:

$$\varphi(g_e, \mathbb{I}) \equiv \sum_{\{j_e\}} \Delta_{j_e} \int_{\text{SU}(2)} [dh_e dk_e] \psi(k_e) \chi^{j_e}(h_e k_e) \Theta^{\mathcal{I}_e}(g_e h_e). \quad (9.10)$$

As we reviewed earlier, we can express the $\text{SL}(2, \mathbb{C})$ -character in term of the SU(2) characters when evaluated on SU(2) group elements:

$$\Theta^{(n_e, \rho_e)}(g_e h_e) = \sum_{l_e \in n_e + \mathbb{N}} \chi^{l_e}(g_e h_e).$$

We can then proceed to the integration over h_e using the known convolution formula¹ for SU(2)-characters :

$$\varphi(g_e, \mathbb{I}) = \int_{\text{SU}(2)} [dk_e] \psi(k_e) \prod_e \sum_{j_e} \frac{\Delta_{j_e}}{d_{j_e}} \chi^{j_e}(g_e k_e^{-1}) = \psi(g_e),$$

as long as we fix the weights $\Delta_j \equiv d_j^2 = (2j+1)^2$ in order to recover the δ -distribution, $\sum_j d_j \chi^j(g k^{-1}) = \delta(g k^{-1})$.

Finally, we have checked that our formula (9.9) correctly defines a lift of SU(2) cylindrical functions to Lorentz-invariant projected cylindrical functions and properly inverts the projection map \mathcal{M} . The parameters of this lifting are a choice of \mathcal{I}_e irrep label for each spin j_e on each edge e . There have been two typical choices for this parameter in the spin foam literature reviewed in Sections 7.2 and 8.1:

- **The Barrett-Crane ansatz:** $n_e = 0$ for all spins j_e on all edges

This restricts to irreps of the type $(0, \rho)$ used in the (Lorentzian) Barrett-Crane model [104, 115]. Let us emphasize that the label of the $\text{SL}(2, \mathbb{C})$ n_e is not the spin j_e , which can still vary freely. If we further fix $j_e = 0$, then we recover the simple spin networks usually used as boundary states of the Barrett-Crane model. Nevertheless, our analysis here suggests that we should *not* proceed to such a restriction and we would have a Hilbert space of projected spin networks for the BC model which would be isomorphic to the space of SU(2) spin networks. This interpretation of the BC model in term of projected spin networks and time-normals was already pushed forward in [80, 133, 134]. In particular, in [134], it was speculated that spins $j_e \neq 0$ would correspond to particle insertions in the Barrett-Crane model, but we will not pursue in this direction.

¹The convolution formula for SU(2)-characters is:

$$\int_{\text{SU}(2)} dh \chi^j(hk) \chi^l(gh) = \frac{\delta_{j,l}}{d_j} \chi^j(gk^{-1}),$$

where $d_j = (2j+1)$ is the dimension of the SU(2)-irrep of spin j . This follows from the orthonormality of matrix elements with respect to the Haar measure. When $g = k$ in particular, we recover the usual orthonormalization condition for characters $\int \chi^j \chi^l = \delta_{j,l}$.

- **The EPRL-FK ansatz:** $n_e = j_e$ for all spins j_e on all edges

This is the condition to build $\text{SL}(2, \mathbb{C})$ coherent states used in the construction of the Lorentzian spinfoam models of the EPRL-FK type [98, 96, 135]. We will study this case in details in the next section, and see how the Immirzi parameter enters our definition of the inverse lift.

9.2 Simplicity Constraints and the Immirzi Parameter

9.2.1 Weak Constraints

Following the approach used for constructing the EPRL-FK spinfoam models, we look at weak constraints that are satisfied by the projected spin network states [95, 98, 96, 97]. More precisely, we compare the matrix elements of the $\text{SU}(2)$ rotation generators \vec{J} and of the boost generators \vec{K} [95, 98, 124]. The simplicity constraints amounts to requiring that the matrix elements of these two operators are the same up to a global factor, which would be identified as the Immirzi parameter.

We start with $\text{SU}(2)$ spin network states ψ and $\tilde{\psi}$, which we lift to projected spin networks φ and $\tilde{\varphi}$ using the same mapping i.e the same choice of $\text{SL}(2, \mathbb{C})$ irreps. Then considering a fixed edge e , let us start by looking at the matrix elements of the left action of the boost generators \vec{K}_e on these projected spin networks:

$$\begin{aligned} \langle \varphi | \vec{K}_e^{(L)} | \tilde{\varphi} \rangle &\equiv \int [dG_e] \bar{\varphi}(G_e) \vec{K}_e \triangleright_L \tilde{\varphi}(G_e) \\ &= \int [dG_e] [dh_e d\tilde{h}_e dk_e d\tilde{k}_e] \bar{\psi}(k_e) \tilde{\varphi}(\tilde{k}_e) \prod_e \sum_{j_e} d_{j_e}^2 d_{j_e}^2 \chi^{j_e}(h_e k_e) \chi^{\tilde{j}_e}(\tilde{h}_e \tilde{k}_e) \overline{\Theta^{(n_e, \rho_e)}}(G_e h_e) \Theta^{(n_e, \rho_e)}(\vec{K}_e G_e \tilde{h}_e). \end{aligned} \quad (9.11)$$

The integral over the $\text{SL}(2, \mathbb{C})$ group elements G_e can be done using the orthonormality of the $\text{SL}(2, \mathbb{C})$ matrix elements with respect to the Haar measure and give $\Theta^{(n_e, \rho_e)}(\vec{K}_e h_e^{-1} \tilde{h}_e)$ up to a measure factor depending solely on (n, ρ) . Let us have a closer look at this term:

$$\Theta^{(n_e, \rho_e)}(\vec{K}_e h_e^{-1} \tilde{h}_e) = \sum_{l_e, m_e} \langle (n_e, \rho_e) l_e m_e | \vec{K}_e h_e^{-1} \tilde{h}_e | (n_e, \rho_e) l_e m_e \rangle.$$

First, the group variable $h_e^{-1} \tilde{h}_e$ is in the $\text{SU}(2)$ subgroup and therefore doesn't change the spin l_e . Thus only the matrix elements of the boost generators \vec{K}_e in the $\text{SU}(2)$ -irrep of spin l_e matter. Next, due to the integration over h_e and the insertion of the character $\chi^{j_e}(h_e k_e)$, only the component $l_e = j_e$ enters the calculation of the expectation value above. Similarly, the integration over \tilde{h}_e and the insertion of the character $\chi^{\tilde{j}_e}(\tilde{h}_e \tilde{k}_e)$ forces $l_e = \tilde{j}_e = j_e$. Finally, we refer to the explicit action of the boost and rotation generators in a (n, ρ) -irrep given in (A.4) and (A.5),

$$\forall l, m, m', \quad \langle (n, \rho) l, m | \vec{K} | (n, \rho) l, m' \rangle = \beta_j^{(n, \rho)} \langle (n, \rho) l, m | \vec{J} | (n, \rho) l, m' \rangle, \quad (9.12)$$

where the coefficient β_j is given in (A.6). This was already noticed in [133, 98, 124]. We would like to use this fact in order to relate the values of the expectation values $\langle \varphi | \vec{K}_e^{(L)} | \tilde{\varphi} \rangle$ and $\langle \varphi | \vec{J}_e^{(L)} | \tilde{\varphi} \rangle$. The obvious issue is that $\beta_{j_e}^{(n_e, \rho_e)}$ depends on j_e and the precise choice of embedding (n_e, ρ_e) chosen for each value of j_e .

Considering the Barrett-Crane ansatz $n_e = 0$ for all values of j_e , we get the trivial value of the proportionality coefficients, $\beta_{j_e}^{(0, \rho_e)} = 0$. This leads to the identity:

$$\text{Barrett-Crane ansatz } n_e = 0 \quad \Rightarrow \quad \langle \varphi | \vec{K}_e^{(L)} | \tilde{\varphi} \rangle = 0. \quad (9.13)$$

We do not consider this ansatz particularly useful, but at least worth mentioning considering the attention that the Barrett-Crane model has received over the past decade.

The case of the EPRL-FK ansatz is much more interesting. We choose the maximal value for the label of the $\text{SL}(2, \mathbb{C})$ irrep, $n_e = j_e$. Then we would like to fix the value of the coefficients β_{j_e} to a fixed value β_e which does not depend on the value of the spin j_e but only on the considered edge e . This leads to a unique solution for ρ_e as a function of the spin j_e :

$$n_e(j_e) = j_e, \quad \rho_e(j_e) = \beta_e(j_e + 1), \quad \Rightarrow \quad \beta_{j_e}^{(n_e, \rho_e)} = \frac{n_e \rho_e}{j_e(j_e + 1)} = \beta_e. \quad (9.14)$$

This leads to the final equality:

$$\textbf{EPRL-FK ansatz } (n_e, \rho_e) = (j_e, \beta_e(j_e + 1)) \quad \Rightarrow \quad \langle \varphi | \vec{K}_e^{(L)} | \tilde{\varphi} \rangle = \beta_e \langle \varphi | \vec{J}_e^{(L)} | \tilde{\varphi} \rangle. \quad (9.15)$$

The same equality holds if considering the right action of the boost and rotation generators. This is exactly the (linear) simplicity constraints that are imposed in the EPRL-FK spinfoam model with Immirzi parameter β_e . Let us underline that we do not need to choose the same proportionality coefficient β_e for all edges e .

This is what is usually assumed in the EPRL-FK spinfoam model. However, in our framework, we are free to choose a different value β_e for each edge of the graph, i.e a different value of the Immirzi parameter along the edges of the projected spin networks. This makes it more like an Immirzi field than an Immirzi parameter.

Finally, we introduce the precise lift inverting the projection map \mathcal{M} in the EPRL-FK ansatz. This lift is parameterized by a choice of coefficients $\{\beta_e\} \in \mathbb{R}^E$ for all edges of the graph. Then we define:

$$\begin{aligned} \mathcal{L}_{\{\beta_e\}} : \quad H_S &\rightarrow H_p \\ \psi(g_e) &\mapsto \varphi(G_e, B_v) = \int_{\text{SU}(2)} [dh_e dk_e] \psi(k_e) \sum_{j_e} d_{j_e}^2 \chi^{j_e}(h_e k_e) \Theta^{(j_e, \beta_e(j_e+1))} (B_{s(e)}^{-1} G_e B_{t(e)} h_e). \end{aligned} \quad (9.16)$$

As already shown in section 9.1.2, this provides us with a proper inverse for the map \mathcal{M} :

$$\forall \{\beta_e\}, \quad \forall \psi \in H, \quad \mathcal{M} \mathcal{L}_{\{\beta_e\}} \psi = \psi. \quad (9.17)$$

We can even go further by noticing by all possible values for $(n_e, \rho_e) \in \mathbb{N}/2 \times \mathbb{R}$ are reached as j_e and β_e vary respectively in $\mathbb{N}/2$ and \mathbb{R} . Indeed, we can inverse the relations given above to get:

$$j_e = n_e, \quad \beta_e = \frac{\rho_e}{j_e + 1}. \quad (9.18)$$

This means that we can use the maps $\mathcal{L}_{\{\beta_e\}}$ to obtain a full foliation of the Hilbert of (proper) projected spin network:

$$H_p = \bigoplus_{\{\beta_e\} \in \mathbb{R}^E} \mathcal{L}_{\{\beta_e\}} H. \quad (9.19)$$

In words, this means that choosing arbitrary values of the Immirzi parameter β_e for each edge of the graph, we will cover the whole space of proper projected spin networks by applying the lifting map $\mathcal{L}_{\{\beta_e\}}$ to the standard $\text{SU}(2)$ spin networks. We underline that we are restricted to *proper* projected spin networks since we always require that $j_e^s = j_e^t$ on all edges of the graph.

From the point of view of Loop Quantum Gravity's dynamics, we believe that the dynamical LQG operators would act on the Hilbert space H of standard $\text{SU}(2)$ spin networks. This hints towards considering each subspace $\mathcal{L}_{\{\beta_e\}} H$ of projected spin networks as *super-selection sectors* for the dynamics. A spinfoam model would then work in a given $\mathcal{L}_{\{\beta_e\}} H$ subspace with all the parameters β_e fixed, and would not mix these different sectors. Since spinfoam models are usually built for arbitrary graphs Γ , the simplest restriction would be to require that the Immirzi parameter be fixed and the same for all edges on all graphs, i.e $\beta_e = \beta, \forall e, \Gamma$. This can be obtained by imposing in addition the closure constraints (8.27) and (8.28) on the projected spin network $|\varphi\rangle, |\tilde{\varphi}\rangle$. (8.27) holds strongly by definition of a projected spin network and (8.28) can only be satisfied weakly because of (9.15) as it is the case on the EPRL-FK boundary Hilbert space. This additional condition imposes that

$$\beta_e = \beta \quad \forall e. \quad (9.20)$$

Then we recover the boundary states for the usual (Lorentzian) EPRL-FK spinfoam models with fixed Immirzi parameter.

Nevertheless, our framework leaves us the freedom of attributing a different value of the Immirzi parameter for each edge of the graph. Let us speculate on the possibility that the Immirzi parameter provides us with a (length/area) scale which we would vary when coarse-graining or renormalizing LQG's transition amplitudes and dynamics. Then our framework for boundary states would allow to coarse-grain various regions of space independently.

9.2.2 Strong Constraints

From the perspective of the construction of spinfoam models, the weak constraints can be translated to strong constraints in the spirit of “master constraints”. The logic is to replace the weak constraints $\langle \varphi | \vec{K}_e - \beta_e \vec{J}_e | \tilde{\varphi} \rangle = 0$ by strong constraints using the SU(2) and SL(2, \mathbb{C}) Casimir operators [95, 98].

Considering the EPRL-FK ansatz, $n(j) = j$ and $\rho(j) = \beta(j+1)$, we can easily express the values of the SL(2, \mathbb{C}) Casimir operators in term of the SU(2) Casimir operator:

$$\begin{aligned} C_2 &= \vec{J} \cdot \vec{K} = 2n\rho = 2\beta j(j+1) = 2\beta \vec{J}^2 \\ C_1 &= \vec{K}^2 - \vec{J}^2 = \rho^2 - n^2 + 1 = (\beta^2 - 1)j(j+1) + (\beta^2 + 1)(j+1) = (\beta^2 - 1)\vec{J}^2 + (\beta^2 + 1)(\sqrt{\vec{J}^2 + \frac{1}{4}} + \frac{1}{2}). \end{aligned} \quad (9.21)$$

The expression of the second quadratic Casimir looks much simpler and it is straightforward to check that the explicit definition that the projected spin networks $\varphi = \mathcal{L}_{\{\beta_e\}}\psi$ indeed satisfy strong (simplicity) constraints:

$$\forall \varphi = \mathcal{L}_{\{\beta_e\}}\psi, \quad \left(\vec{J}_e \cdot \vec{K}_e - 2\beta_e \vec{J}_e^2 \right) \phi = 0. \quad (9.22)$$

Here, it does not matter whether we consider the left or right action of the boost and rotation operators as long as we take them all as acting on the same side of the group variable G_e . Moreover, we wrote the constraint as acting on the section $\phi(G_e) = \varphi(G_e, \omega)$. This constraint can be rotated by the suitable Lorentz transformations to apply it on the whole function $\varphi(G_e, B_v)$.

As long as we require by hand that $n_e = j_e$, this strong constraint is sufficient to impose that $\rho_e = \beta_e(j_e + 1)$. However, in order to impose $n_e = j_e$ through an operator constraint as well, we need to impose the other constraint involving the first Casimir operator. The drawback is that this constraint involve a rather ugly “quantum correction” term in $\sqrt{\vec{J}^2}$ operator, which is nevertheless necessary if we want an exact constraint at the quantum level.

9.2.3 Comparing SU(2) and SL(2, \mathbb{C}) Scalar Products

Since we have constructed a map between SU(2) spin networks and projected spin networks, it is natural to wonder if these lifts are unitary and preserve the scalar products. It is straightforward to see that this is a priori not the case. Indeed, considering two projected cylindrical functions, φ and $\tilde{\varphi}$, and their projections $\psi = \mathcal{M}\varphi$, $\tilde{\psi} = \mathcal{M}\tilde{\varphi}$, the scalar products are best expressed in term of the sections $\phi, \tilde{\phi}$:

$$\begin{aligned} \langle \varphi | \tilde{\varphi} \rangle &= \int_{\text{SL}(2, \mathbb{C})} \bar{\phi}(G_e) \tilde{\phi}(G_e), \\ \langle \psi | \tilde{\psi} \rangle_{\text{SU}(2)} &= \int_{\text{SU}(2)} \bar{\phi}(g_e) \tilde{\phi}(g_e). \end{aligned} \quad (9.23)$$

These two evaluations are a priori very different. This can be seen also from the scalar product between the basis states (5.12) and (9.5):

$$\langle \varphi_{\mathcal{I}_e, j_e^{s,t}, i_v} | \varphi_{\tilde{\mathcal{I}}_e, \tilde{j}_e^{s,t}, \tilde{i}_v} \rangle = \prod_e \frac{\delta_{n_e, \tilde{n}_e} \delta(\rho_e - \tilde{\rho}_e)}{\mu(n_e, \rho_e)} \delta_{j_e^{s,t}, \tilde{j}_e^{s,t}} \prod_v \langle i_v | \tilde{i}_v \rangle, \quad \langle \psi_{j_e, i_v} | \psi_{\tilde{j}_e, \tilde{i}_v} \rangle_{\text{SU}(2)} = \prod_e \frac{\delta_{j_e, \tilde{j}_e}}{d_{j_e}} \prod_v \langle i_v | \tilde{i}_v \rangle,$$

which differ in their measure and normalization. The key difference is due to the extra δ -functions due to the $\text{SL}(2, \mathbb{C})$ -irrep label, more specifically $\delta(\rho_e - \tilde{\rho}_e)$ which potentially could lead to divergences.

To illustrate this, we start with two $\text{SU}(2)$ cylindrical functions $\psi, \tilde{\psi}$ and respectively apply the generalized lifts $\mathcal{L}_{\{\beta_e\}}$ and $\mathcal{L}_{\{\tilde{\beta}_e\}}$ (the following analysis remains the same for two lifts \mathcal{L}_β and $\mathcal{L}_{\tilde{\beta}}$). Then a straightforward calculation leads to:

$$\begin{aligned} \langle \mathcal{L}_{\{\beta_e\}} \psi | \mathcal{L}_{\{\tilde{\beta}_e\}} \tilde{\psi} \rangle &= \int_{\text{SU}(2)} [dk_e d\tilde{k}_e] \bar{\psi}(k_e) \tilde{\psi}(\tilde{k}_e) \prod_e \sum_{j_e} \frac{\Delta_{j_e}^2}{d_{j_e}^2} \frac{\delta(\rho_e - \tilde{\rho}_e)}{(\rho_e^2 + j_e^2)} \chi^{j_e}(k_e^{-1} \tilde{k}_e) \\ &= \prod_e \delta(\beta_e - \tilde{\beta}_e) \int_{\text{SU}(2)} [dk_e d\tilde{k}_e] \bar{\psi}(k_e) \tilde{\psi}(\tilde{k}_e) \prod_e \sum_{j_e} \frac{\Delta_{j_e}^2}{d_{j_e}^2 (j_e + 1)(\beta_e^2 (j_e + 1)^2 + j_e^2)} \chi^{j_e}(k_e^{-1} \tilde{k}_e) \end{aligned}$$

Assuming the standard definition $\Delta_{j_e} = d_{j_e}^2$ ensuring that the lifts $\mathcal{L}_{\{\beta_e\}}$ correctly invert the projection map \mathcal{M} , then it is clear that the two scalar products do not match. Then the natural question is which scalar product (between the Lorentz scalar product and the $\text{SU}(2)$ scalar product) should we use on our kinematical Hilbert space of boundary states? This question should ultimately not matter so much since the final physical scalar should a priori be neither of them. Nevertheless, it is a crucial issue when building spinfoam amplitudes.

An alternative would be to give up the requirement that a lift should be the inverse of the projection map \mathcal{M} , i.e give up the idea that the restriction of the projected cylindrical function to the $\text{SU}(2)$ subgroup be equal to the original $\text{SU}(2)$ cylindrical function. Then we can modify the definition of the weight Δ_{j_e} and choose the new renormalized value, which now depends on the value of the Immirzi parameter β_e :

$$\Delta_{j_e}^{\beta_e} \equiv d_{j_e}^2 \sqrt{(j_e + 1)(\beta_e^2 (j_e + 1)^2 + j_e^2)}. \quad (9.25)$$

This would define modified lifting maps, which would still send $\text{SU}(2)$ cylindrical functions onto projected cylindrical functions, but that would conserve scalar products. Indeed, explicitly defining the new maps,

$$\begin{aligned} L_{\{\beta_e\}} : H_S &\rightarrow H_P \\ \psi(g_e) &\mapsto \varphi(G_e, B_v) = \int_{\text{SU}(2)} [dh_e dk_e] \psi(k_e) \sum_{j_e} \Delta_{j_e}^{\beta_e} \chi^{j_e}(h_e k_e) \Theta^{(j_e, \beta_e(j_e+1))}(B_{s(e)}^{-1} G_e B_{t(e)} h_e). \end{aligned} \quad (9.26)$$

using the new definition of the weight $\Delta_{j_e}^{\beta_e}$ given above, we will have the exact equality:

$$\langle L_{\{\beta_e\}} \psi | L_{\{\tilde{\beta}_e\}} \tilde{\psi} \rangle = \langle \psi | \tilde{\psi} \rangle_{\text{SU}(2)} \prod_e \delta(\beta_e - \tilde{\beta}_e). \quad (9.27)$$

Let us insist on the fact that this lifting map will still send the basis of $\text{SU}(2)$ spin networks on projected spin network states satisfying the EPRL-FK ansatz, but with a different normalization that the lifting maps $\mathcal{L}_{\{\beta_e\}}$ inverting \mathcal{M} .

Finally, the natural issue is which lifting maps should we use to send LQG's $\text{SU}(2)$ cylindrical functions onto the projected cylindrical functions of spinfoam models: should we enforce the matching condition that the restriction of projected cylindrical function to the $\text{SU}(2)$ subgroup be equal to the $\text{SU}(2)$ cylindrical function or should we simply require the matching of the two scalar products and the unitarity of the lifting?

Chapter 10

Simplicity constraints and the $U(N)$ framework

Let us now tackle another open problem in the spin foam quantization procedure which is how to decide the "strength" with which the simplicity constraints turning BF theory into 4d gravity are imposed. In short, the first try has been to impose all the simplicity constraints strongly, leading to the Barrett-Crane model (see chapter 7) which seems to be an over-constrained model. A more recent proposal has been to impose the cross simplicity constraints weakly whereas the diagonal simplicity constraints are still imposed strongly, which had led to the EPRL-FK models (see chapter 8). In this chapter, we present results published in [6] obtained using the $U(N)$ framework initially developed for $SU(2)$ intertwiners [7, 8, 9]. One major interest of this new point of view is that within this $U(N)$ framework one can achieve a precise control on the "strength" with which we decide to impose the simplicity constraints.

In the next section, we start by giving a short review on the $U(N)$ framework. Then, using these $U(N)$ tools, we recall an alternative definition of the $SU(2)$ coherent states used in the section 8.2 as well as the definition of the $U(N)$ coherent states and their link with the usual $SU(2)$ coherent states. The end of the second section is devoted to technical results summarizing a first part of work regarding the analysis of the action of geometrical observables on some $U(N)$ coherent states, elements of the space of $SU(2)$ intertwiners.

The second part of this work consisted in recasting the simplicity constraints for 4d gravity within the $U(N)$ framework. The first idea has been to follow the line of the EPRL-FK model, that is to impose weakly the cross simplicity constraints but to keep strong diagonal simplicity constraints. Different closed algebra of simplicity constraints used to solve weakly the cross simplicity constraints are identified. Details as well as the analysis of their advantages and disadvantages can be found in the third section of this chapter.

The final proposition is exposed in the last section of this chapter. It emphasizes the fact that all simplicity constraints should be treated on the same footing and give a solution in terms of $U(N)$ coherent states in this case. Moreover, this result takes into account the Immirzi parameter γ . The different results are therefore relevant for the definition of a spin foam model for 4 dimensional Euclidean gravity with an arbitrary value of the Immirzi parameter. The investigation of this approach has been done only for the Euclidean case, i.e. constrained BF theory with gauge group $\text{Spin}(4)$ and the corresponding intertwiners.

We recall that in the case of Euclidean 4d gravity, the Hilbert space of quantum states of a 3-cell of the boundary cellular decomposition, before having implemented the simplicity constraints, is the space of $\text{Spin}(4)$ intertwiners between the representations attached to its faces or equivalently to the legs of the dual vertex of this 3-cell. Since $\text{Spin}(4) \sim SU_L(2) \times SU_R(2)$ is the direct product of its two $SU(2)$ subgroups, the irreducible representations of $\text{Spin}(4)$ are labeled by a couple of half-integers (j^L, j^R) . So a pair of spin to every leg i is attached and the intertwiner space for the vertex is the tensor product of the space of $SU_L(2)$ intertwiners between the spins j_i^L and the space of $SU_R(2)$ intertwiners between the spins j_i^R

$$H_{j_i^L, j_i^R} \equiv \text{Inv} \left[\bigotimes_{\Delta} V^{j_i^L} \right] \otimes \text{Inv} \left[\bigotimes_{\Delta} V^{j_i^R} \right]. \quad (10.1)$$

We still need to implement the simplicity constraints

- The *diagonal simplicity constraints* obtained when the legs are the same $i = j$,

$$\forall i, \quad (\vec{J}_i^L)^2 = \rho^2 (\vec{J}_i^R)^2, \quad (10.2)$$

with $\rho = \frac{\gamma+1}{|\gamma-1|}$ the proportionality coefficient between the left and the right parts of the scalar products and γ ($\gamma > 0, \gamma \neq 1$) the Immirzi parameter.

- The *crossed simplicity constraints* in the case that the two legs are different $i \neq j$,

$$\forall i \neq j, \quad (\vec{J}_i^L \cdot \vec{J}_j^L) = \rho^2 (\vec{J}_i^R \cdot \vec{J}_j^R). \quad (10.3)$$

10.1 $SU(2)$ intertwiners and the $U(N)$ framework

As recalled above, the discrete simplicity constraints are usually formulated in term of the scalar product of $SU(2)$ generators. These scalar product operators, $\vec{J}_i \cdot \vec{J}_j$, are the standard invariant operators on the space of $SU(2)$ intertwiner. They act on pairs of legs (i, j) of a $SU(2)$ intertwiner. An important issue is that the algebra of the scalar product operators does not close. More precisely, the commutator of two scalar product operators gives a operator of order 3 in the \vec{J} 's:

$$[\vec{J}_i \cdot \vec{J}_j, \vec{J}_i \cdot \vec{J}_k] = i \vec{J}_i \cdot (\vec{J}_j \wedge \vec{J}_k), \quad (10.4)$$

and so on generating higher and higher order operators. This leads directly to problems when one tries to define coherent intertwiner states minimizing the corresponding uncertainty relations or when one attempts to solve constraints such as the simplicity constraints. The approach followed in [7] was to use Schwinger's representation of the $\mathfrak{su}(2)$ algebra in term of harmonic oscillators to identify a new family of invariant operators, whose Lie algebra closes and which would still generate the full algebra of invariant operators acting on the intertwiner space. This leads to the $U(N)$ framework for $SU(2)$ intertwiners [7, 8, 9], which actually goes beyond this initial objective and offers a whole new perspective on the intertwiner space. It shows that the intertwiner space carries a natural representation of the $U(N)$ unitary group and allows to build semi-classical coherent states transforming consistently under the $U(N)$ action. It also uncovers a deep relation between the intertwiner space and the Grassmannian spaces, which could prove very useful to understand the geometry of the intertwiner space and its (semi-)classical interpretation. We review this formalism below.

Let us consider the Hilbert spaces of intertwiners between N irreducible $SU(2)$ -representations of spin j_1, \dots, j_N :

$$\mathcal{H}_{j_1, \dots, j_N} \equiv \text{Inv}[V^{j_1} \otimes \dots \otimes V^{j_N}]. \quad (10.5)$$

We further introduce the space of intertwiners with N legs and fixed total area $J = \sum_i j_i$:

$$\mathcal{H}_N^{(J)} \equiv \bigoplus_{\sum_i j_i = J} \mathcal{H}_{j_1, \dots, j_N}, \quad (10.6)$$

and the full Hilbert space of N -valent intertwiners:

$$\mathcal{H}_N \equiv \bigoplus_{\{j_i\}} \mathcal{H}_{j_1, \dots, j_N} = \bigoplus_{J \in \mathbb{N}} \mathcal{H}_N^{(J)}. \quad (10.7)$$

The key result of the $U(N)$ formalism is that there is a natural action of $U(N)$ on the intertwiner space \mathcal{H}_N [7]. More precisely the intertwiner spaces $\mathcal{H}_N^{(J)}$ carry irreducible representations of $U(N)$ [8]. Finally the full space \mathcal{H}_N can be endowed with a Fock space structure with creation and annihilation operators compatible with the $U(N)$ action [9].

This $U(N)$ formalism is based on the Schwinger representation of the $\mathfrak{su}(2)$ Lie algebra in term of harmonic oscillators. Let us introduce $2N$ oscillators with creation operators a_i, b_i with i running from 1 to N :

$$[a_i, a_j^\dagger] = [b_i, b_j^\dagger] = \delta_{ij}, \quad [a_i, b_j] = 0.$$

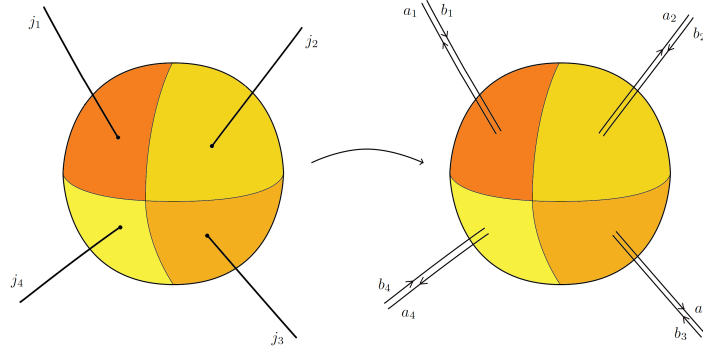


Figure 10.1: Four legs intertwiner and harmonic oscillators.

The generators of the SU(2) transformations acting on each leg of the intertwiner are realized as quadratic operators in term of the oscillators:

$$J_i^z = \frac{1}{2}(a_i^\dagger a_i - b_i^\dagger b_i), \quad J_i^+ = a_i^\dagger b_i, \quad J_i^- = a_i b_i^\dagger, \quad E_i = (a_i^\dagger a_i + b_i^\dagger b_i). \quad (10.8)$$

The J_i 's satisfy the standard commutation algebra while the total energy E_i is a Casimir operator:

$$[J_i^z, J_i^\pm] = \pm J_i^\pm, \quad [J_i^+, J_i^-] = 2J_i^z, \quad [E_i, \vec{J}_i] = 0. \quad (10.9)$$

The correspondence with the standard $|j, m\rangle$ basis of $\mathfrak{su}(2)$ representations is simple:

$$|n_a, n_b\rangle_{HO} = |\frac{1}{2}(n_a + n_b), \frac{1}{2}(n_a - n_b)\rangle, \quad |j, m\rangle = |j + m, j - m\rangle_{HO} \quad (10.10)$$

where m is the eigenvalue of J^z defined as the half-difference of the energies between the two oscillators, while the total energy E_i gives twice the spin, $2j_i$, living on the i -th leg of the intertwiner.

Intertwiner states are by definition invariant under the global SU(2) action, generated by:

$$J^z = \sum_{i=1}^N J_i^z, \quad J^\pm = \sum_i J_i^\pm. \quad (10.11)$$

Then operators acting on the intertwiner space need to commute with these operators too. The simplest family of invariant operators was identified in [7] and are quadratic operators acting on couples of legs:

$$E_{ij} = a_i^\dagger a_j + b_i^\dagger b_j, \quad E_{ij}^\dagger = E_{ji}. \quad (10.12)$$

The main result is that these operators are invariant under global SU(2) transformations and form a $\mathfrak{u}(N)$ algebra:

$$[\vec{J}, E_{ij}] = 0, \quad [E_{ij}, E_{kl}] = \delta_{jk} E_{il} - \delta_{il} E_{kj}. \quad (10.13)$$

The diagonal operators $E_i \equiv E_{ii}$ form the Cartan sub-algebra of $\mathfrak{u}(N)$, while the off-diagonal operators E_{ij} with $i \neq j$ are the raising and lowering operators. As said earlier, the generators E_i give twice the spin $2j_i$ while the U(1) Casimir $E = \sum_i E_i$ will give twice the total area, $2J \equiv \sum_i 2j_i$. Then all operators E_{ij} commute with the U(1) Casimir, thus leaving the total area J invariant:

$$[E_{ij}, E] = 0. \quad (10.14)$$

The usual SU(2) Casimir operators have a simple expression in term of these $\mathfrak{u}(N)$ generators:

$$(\vec{J}_i)^2 = \frac{1}{2} E_i \left(\frac{E_i}{2} + 1 \right), \quad \forall i \neq j, \quad (\vec{J}_i \cdot \vec{J}_j) = \frac{1}{2} E_{ij} E_{ji} - \frac{1}{4} E_i E_j - \frac{1}{2} E_i. \quad (10.15)$$

Let us point out that case $i = j$ of $(\vec{J}_i \cdot \vec{J}_j)$ does not give back exactly the formula for $(\vec{J}_i)^2$ due to the ordering of the oscillator operators. The two formula agree on the leading order quadratic in E_i but disagree on the correction linear in E_i .

The next point is that explicit definition of the E_{ij} 's in term of harmonic oscillators leads to quadratic constraints on these operators as shown in [8] :

$$\forall i, \quad \sum_j E_{ij} E_{ji} = E_i \left(\frac{E}{2} + N - 2 \right), \quad (10.16)$$

where we have assumed that the global $SU(2)$ generators \vec{J} vanish. These quadratic constraints on the E_{ij} operators lead to non-trivial restrictions on the representations of $u(N)$ obtained from this construction. To solve them, the method used in [8] is to apply them to a highest weight vector. This allows to identify the representations corresponding to the intertwiner spaces $\mathcal{H}_N^{(J)}$ at fixed total area $J = \sum_i j_i$. The highest weight vector $v_N^{(J)}$ diagonalizes the generators of the Cartan sub-algebra E_i and vanishes under the action of the raising operators $E_{ij} v = 0$ for all $i < j$. The N eigenvalues depend very simply on the area J :

$$E_1 v_N^{(J)} = E_2 v_N^{(J)} = J v_N^{(J)}, \quad E_k v_N^{(J)} = 0, \quad \forall k \geq 3. \quad (10.17)$$

This highest weight vector corresponds to a bivalent intertwiner between two legs both carrying the spin $\frac{J}{2}$. One can compute the corresponding value of the quadratic $U(N)$ Casimir using the previous quadratic constraints:

$$\sum_{i,j} E_{ij} E_{ji} = E \left(\frac{E}{2} + N - 2 \right) = 2J(J + N - 2), \quad (10.18)$$

and the dimension of $\mathcal{H}_N^{(J)}$ in term of binomial coefficients using the standard formula for $U(N)$ representations:

$$D_{N,J} \equiv \dim \mathcal{H}_N^{(J)} = \frac{1}{J+1} \binom{N+J-1}{J} \binom{N+J-2}{J} = \frac{(N+J-1)!(N+J-2)!}{J!(J+1)!(N-1)!(N-2)!}. \quad (10.19)$$

Next, we introduce annihilation and creation operators to move between the spaces $\mathcal{H}_N^{(J)}$ with different areas J within the bigger Hilbert space of all intertwiners with N legs [9]. We define the new operators:

$$F_{ij} = (a_i b_j - a_j b_i), \quad F_{ji} = -F_{ij}. \quad (10.20)$$

These are still invariant under global $SU(2)$ transformations, but they do not commute anymore with the total area operator E . They nevertheless form a closed algebra together with the operators E_{ij} :

$$\begin{aligned} [E_{ij}, E_{kl}] &= \delta_{jk} E_{il} - \delta_{il} E_{kj} \\ [E_{ij}, F_{kl}] &= \delta_{il} F_{jk} - \delta_{ik} F_{jl}, \quad [E_{ij}, F_{kl}^\dagger] = \delta_{jk} F_{il}^\dagger - \delta_{jl} F_{ik}^\dagger, \\ [F_{ij}, F_{kl}^\dagger] &= \delta_{ik} E_{lj} - \delta_{il} E_{kj} - \delta_{jk} E_{li} + \delta_{jl} E_{ki} + 2(\delta_{ik} \delta_{jl} - \delta_{il} \delta_{jk}), \\ [F_{ij}, F_{kl}] &= 0, \quad [F_{ij}^\dagger, F_{kl}^\dagger] = 0. \end{aligned} \quad (10.21)$$

The annihilation operators F_{ij} allow to go from $\mathcal{H}_N^{(J)}$ to $\mathcal{H}_N^{(J-1)}$ while the creation operators F_{ij}^\dagger raise the area and go from $\mathcal{H}_N^{(J)}$ to $\mathcal{H}_N^{(J+1)}$. We can re-express the scalar product operators in term of this new set of operators:

$$\begin{aligned} \vec{J}_i \cdot \vec{J}_j &= -\frac{1}{2} F_{ij}^\dagger F_{ij} + \frac{1}{4} E_i E_j, \\ &= -\frac{1}{2} F_{ij} F_{ij}^\dagger + \frac{1}{4} (E_i + 2)(E_j + 2). \end{aligned} \quad (10.22)$$

This formula is explicitly symmetric in the edge labels $i \leftrightarrow j$ contrary to the previous formula (10.15) in terms of the E_{ij} -operators. Finally, as shown in [9] and as we review below, these operators can be used to construct coherent states transforming consistently under $U(N)$ transformations. These $U(N)$ coherent states will turn out very convenient in order to re-express and solve the simplicity constraints.

10.2 Coherent states and the $U(N)$ framework

10.2.1 Revisiting the $SU(2)$ Coherent Intertwiners

To define coherent intertwiner states, we attach a spinor z_i to each leg of the intertwiner:

$$z_i = \begin{pmatrix} z_i^0 \\ z_i^1 \end{pmatrix}.$$

Basically, the first component z_i^0 is the label of the coherent state for the oscillator a_i while the second component z_i^1 corresponds to the oscillator b_i . Let us first clear up the geometrical meaning of the spinors z_i . Considering a spinor z , the matrix $|z\rangle\langle z|$ is a 2×2 matrix which can be decomposed on the Pauli matrices σ_a (taken Hermitian and normalized so that $(\sigma_a)^2 = \mathbb{I}$). This defines a 3-vector $\vec{V}(z)$:

$$|z\rangle\langle z| = \frac{1}{2} \left(\langle z|z\rangle \mathbb{I} + \vec{V}(z) \cdot \vec{\sigma} \right), \quad (10.23)$$

where the norm of the vector is $|\vec{V}(z)| = \langle z|z\rangle = |z^0|^2 + |z^1|^2$ and its components are given explicitly as ¹:

$$V^z = |z^0|^2 - |z^1|^2, \quad V^x = 2 \Re(z^0 z^1), \quad V^y = 2 \Im(z^0 z^1). \quad (10.24)$$

The spinor z is entirely determined by the corresponding 3-vector $\vec{V}(z)$ up to a global phase. Following [9], we also introduce the map ς between spinors:

$$\varsigma \begin{pmatrix} z^0 \\ z^1 \end{pmatrix} = \begin{pmatrix} -\bar{z}^1 \\ \bar{z}^0 \end{pmatrix}, \quad \varsigma^2 = -1. \quad (10.25)$$

This is an anti-unitary map, $\langle \varsigma z | \varsigma w \rangle = \langle w | z \rangle = \overline{\langle z | w \rangle}$, and we will write the related state as

$$|z] \equiv \varsigma |z\rangle.$$

This map ς maps the 3-vector $\vec{V}(z)$ onto its opposite:

$$|z][z| = \frac{1}{2} \left(\langle z|z\rangle \mathbb{I} - \vec{V}(z) \cdot \vec{\sigma} \right). \quad (10.26)$$

Finally coming back to the intertwiner with N legs, we have N spinors and their corresponding 3-vectors $\vec{V}(z_i)$. Typically, we can require that the N spinors satisfy a closure constraint, $\sum_i \vec{V}(z_i) = 0$. This can be written in term of 2×2 matrices:

$$\sum_i |z_i\rangle\langle z_i| = A(z) \mathbb{I}, \quad \text{with} \quad A(z) \equiv \frac{1}{2} \sum_i \langle z_i | z_i \rangle = \frac{1}{2} \sum_i |\vec{V}(z_i)|. \quad (10.27)$$

It translates into quadratic constraints on the spinors:

$$\sum_i z_i^0 \bar{z}_i^1 = 0, \quad \sum_i |z_i^0|^2 = \sum_i |z_i^1|^2 = A(z), \quad (10.28)$$

which means that the two components of the spinors, z_i^0 and z_i^1 , are orthogonal N -vectors of equal norm.

Then we can define coherent intertwiner states [106, 131, 132]. First, for a given leg, we define the $SU(2)$ coherent states labeled by the spin j_i and the spinor z_i :

$$|j_i, z_i\rangle \equiv \frac{(z_i^0 a_i^\dagger + z_i^1 b_i^\dagger)^{2j_i}}{\sqrt{(2j_i)!}} |0\rangle. \quad (10.29)$$

¹Remember the convention for the \pm generators:

$$\sigma_\pm = \sigma_x \pm i\sigma_y, \quad \sigma_x = \frac{1}{2}(\sigma_+ + \sigma_-), \quad \sigma_y = -i\frac{1}{2}(\sigma_+ - \sigma_-).$$

This vector clearly lives in the irreducible $SU(2)$ -representation of spin j_i since it's an eigenvector of the energy E_i with value $2j_i$. To show that it transforms coherently under $SU(2)$, we compute the $SU(2)$ action. Dropping the index i , $SU(2)$ rotations are parameterized by an angle θ and a unit 3-vector $\hat{v} \in \mathcal{S}_2$:

$$g(\theta, \hat{v}) \equiv e^{i\theta \hat{v} \cdot \vec{J}} = e^{i\theta(v_z J_z + \frac{v_x}{2} J_+ + \frac{v_y}{2} J_-)}, \quad |\vec{v}|^2 = v_z^2 + |\mathbf{v}|^2 = 1, \quad v_z = \cos \phi, \quad \mathbf{v} = e^{i\psi} \sin \phi. \quad (10.30)$$

It is represented by a 2×2 matrix in the fundamental spin- $\frac{1}{2}$ representation:

$$g(\theta, \hat{v}) = e^{i\theta \hat{v} \cdot \frac{\vec{\sigma}}{2}} = \begin{pmatrix} \cos \frac{\theta}{2} + i \cos \phi \sin \frac{\theta}{2} & i e^{i\psi} \sin \phi \sin \frac{\theta}{2} \\ i e^{-i\psi} \sin \phi \sin \frac{\theta}{2} & \cos \frac{\theta}{2} - i \cos \phi \sin \frac{\theta}{2} \end{pmatrix} \in SU(2). \quad (10.31)$$

To compute the action of $SU(2)$, we first compute the following commutator:

$$\left[\vec{v} \cdot \vec{J}, (z^0 a^\dagger + z^1 b^\dagger) \right] = \left((\vec{v} \cdot \frac{\vec{\sigma}}{2}) z \right)^0 a^\dagger + \left((\vec{v} \cdot \frac{\vec{\sigma}}{2}) z \right)^1 b^\dagger, \quad (10.32)$$

which gets easily exponentiated:

$$e^{i\theta \hat{v} \cdot \vec{J}} (z^0 a^\dagger + z^1 b^\dagger) e^{-i\theta \hat{v} \cdot \vec{J}} = e^{[i\theta \hat{v} \cdot \vec{J}, \cdot]} (z^0 a^\dagger + z^1 b^\dagger) = (\tilde{z}^0 a^\dagger + \tilde{z}^1 b^\dagger), \quad \text{with} \quad \tilde{z} = e^{i\theta \hat{v} \cdot \frac{\vec{\sigma}}{2}} z = g(\theta, \hat{v}) z. \quad (10.33)$$

This shows that the states introduced above are proper $SU(2)$ coherent states:

$$g(\theta, \hat{v}) |j, z\rangle = |j, g(\theta, \hat{v}) z\rangle \quad (10.34)$$

This means that these are the standard $SU(2)$ coherent states à la Perelomov. Indeed, one can always set \tilde{z}^1 to 0, or reversely get any arbitrary state from the initial state without any b -excitation. Such an initial state actually corresponds to the highest weight vector $|j, j\rangle$ of the $SU(2)$ -representation of spin j . More precisely, we act on that highest weight vector with a $SU(2)$ transformation parameterized by α and β satisfying $|\alpha|^2 + |\beta|^2 = 1$:

$$|j, j\rangle = |2j, 0\rangle_{HO} = \frac{(a^\dagger)^{2j}}{\sqrt{(2j)!}} |0\rangle \rightarrow \begin{pmatrix} \alpha & \beta \\ -\bar{\beta} & \bar{\alpha} \end{pmatrix} |j, j\rangle = |j, \begin{pmatrix} \alpha \\ -\bar{\beta} \end{pmatrix}\rangle, \quad (10.35)$$

$$|j, z\rangle = \langle z|z\rangle^j \begin{pmatrix} \frac{z^0}{\sqrt{\langle z|z\rangle}} & \frac{-\bar{z}^1}{\sqrt{\langle z|z\rangle}} \\ \frac{z^1}{\sqrt{\langle z|z\rangle}} & \frac{\bar{z}^0}{\sqrt{\langle z|z\rangle}} \end{pmatrix} |j, j\rangle. \quad (10.36)$$

We also give the scalar product between two such $SU(2)$ coherent states:

$$\langle j, w|j, z\rangle = \langle w|z\rangle^{2j}, \quad (10.37)$$

and the expectation values of the $\mathfrak{su}(2)$ generators:

$$\langle J_z \rangle \equiv \frac{\langle j, z|J_z|j, z\rangle}{\langle j, z|j, z\rangle} = j \frac{|z^0|^2 - |z^1|^2}{|z^0|^2 + |z^1|^2}, \quad \langle J_+ \rangle = 2j \frac{\bar{z}^0 z^1}{|z^0|^2 + |z^1|^2}, \quad \Rightarrow \quad \langle \vec{J} \rangle = j \frac{\vec{V}}{|\vec{V}|}, \quad (10.38)$$

as expected. Finally, expanding these states explicitly on the standard basis for harmonic oscillators,

$$|j, z\rangle = \sum_{n=0}^{2j} \sqrt{\binom{2j}{n}} (z^0)^n (z^1)^{2j-n} |n, 2j-n\rangle_{HO},$$

and following the usual calculation done with oscillator coherent states (as shown in appendix B), we can decompose the identity on the Hilbert space V^j in term of these $SU(2)$ coherent states:

$$\mathbb{I}_j = \sum_{n=0}^{2j} |n, 2j-n\rangle_{HO} {}_{HO}\langle n, 2j-n| = \frac{1}{(2j)!} \int [d^2 z^0 d^2 z^1] \frac{e^{-\langle z|z\rangle}}{\pi^2} |j, z\rangle \langle j, z|. \quad (10.39)$$

One can check that taking the trace of this expression and using the formula for the scalar product between coherent states give back as expected $\text{tr} \mathbb{L}_j = (2j+1)$. Let us emphasize a last point that the projector $|j, z\rangle\langle j, z|$ does not depend on the overall phase of the spinor z but only on the corresponding 3-vector $\vec{V}(z)$.

Coherent intertwiners are then defined following [106] by group averaging the tensor product of $SU(2)$ coherent states attached to every leg of the intertwiner:

$$|\{j_i, z_i\}\rangle \equiv \int_{SU(2)} dg \, g \triangleright \bigotimes_{i=1}^N |j_i, z_i\rangle. \quad (10.40)$$

These are the standard coherent intertwiners used in the construction of the EPRL-FK spinfoam models and their boundary states [96, 97]. Following the logic of [106], we can write the identity on the intertwiner space $\mathcal{H}_{j_1, \dots, j_N}$ in term of these coherent intertwiners:

$$\mathbb{I}_{\mathcal{H}_{j_1, \dots, j_N}} = \int \prod_i \frac{e^{-\langle z_i | z_i \rangle} d^4 z_i}{(2j_i)! \pi^2} |\{j_i, z_i\}\rangle \langle \{j_i, z_i\}|, \quad (10.41)$$

where we used the fact that the spinor norm $\langle z | z \rangle$ is invariant under the $SU(2)$ action. Finally, the main point shown in [106] is that this integral is dominated by intertwiners satisfying the closure constraint $\sum_i j_i \vec{V}(z_i) / |\vec{V}(z_i)| = 0$ while the norm of intertwiners not satisfying this closure constraint is exponentially suppressed. It is also possible to write a decomposition of the identity on the intertwiner space restricting the integral to intertwiners satisfying exactly the closure constraint by modifying slightly the measure [131, 132]. This is achieved through considering and gauging out the $SL(2, \mathbb{C})$ action on spinors complexifying the previous $SU(2)$ action.

10.2.2 The $U(N)$ coherent states

We are now ready to define the $U(N)$ coherent states. Their definition is slightly more complicated. Following [9], we define the following antisymmetric matrix Z_{ij} , which is holomorphic in the spinors z_i and anti-symmetric in $i \leftrightarrow j$:

$$Z_{ij} \equiv [z_i | z_j] = (z_i^0 z_j^1 - z_j^0 z_i^1), \quad (10.42)$$

and the corresponding creation operator:

$$F_Z^\dagger \equiv \frac{1}{2} \sum Z_{ij} F_{ij}^\dagger = \frac{1}{2} \sum (z_i^0 z_j^1 - z_j^0 z_i^1) F_{ij}^\dagger, \quad (10.43)$$

which is also holomorphic in z . A crucial property of this matrix Z is the Plücker relation $Z_{ik} Z_{jl} - Z_{il} Z_{jk} = Z_{ij} Z_{kl}$ which holds for any indices i, j, k, l . The $U(N)$ coherent states are then labeled by the total area J and the N spinors z_i :

$$|J, \{z_i\}\rangle \equiv \frac{1}{\sqrt{J!(J+1)!}} (F_Z^\dagger)^J |0\rangle. \quad (10.44)$$

This state clearly lives in $\mathcal{H}_N^{(J)}$ since it is an intertwiner (invariant under global $SU(2)$ transformation) and is an eigenvector of the total area operator E with value $2J$. Notice that the behavior under rescaling of this coherent state is very simple:

$$z_i \rightarrow \lambda z_i, \quad Z_{ij} \rightarrow \lambda^2 Z_{ij}, \quad |J, \{\lambda z_i\}\rangle = \lambda^{2J} |J, \{z_i\}\rangle. \quad (10.45)$$

Now we assume that the spinors z_i satisfy exactly the closure condition $\sum_i \vec{V}(z_i) = 0$ introduced earlier in (10.28). We can compute the norm of these states:

$$\langle J, \{z_i\} | J, \{z_i\} \rangle = (A(z))^{2J} = \left(\frac{1}{2} \sum_i \langle z_i | z_i \rangle \right)^{2J} = \left(\frac{1}{2} \sum_i |\vec{V}(z_i)| \right)^{2J}. \quad (10.46)$$

Then, as shown in [9], these states are coherent under the action of $U(N)$:

$$\forall u \in U(N), \quad \hat{u} |J, \{z_i\}\rangle = |J, \{(uz)_i\}\rangle, \quad (10.47)$$

where \hat{u} is the operator representing the unitary transformation u , that is for an arbitrary anti-Hermitian matrix α :

$$u = e^\alpha \quad \rightarrow \quad \hat{u} \equiv e^{E_\alpha} \equiv e^{\sum_{ij} \alpha_{ij} E_{ij}}. \quad (10.48)$$

The $U(N)$ action on the N spinors is the natural one:

$$z_i \rightarrow (uz)_i = \sum_j u_{ij} z_j, \quad z \rightarrow uz, \quad Z \rightarrow uZu^t. \quad (10.49)$$

This $U(N)$ -action is proved by computing explicitly the action of \hat{u} on the F^\dagger -operators [9]:

$$[E_\alpha, F_Z^\dagger] = F_{\alpha Z + Z \alpha^t}^\dagger \quad \Rightarrow \quad e^{E_\alpha} F_Z^\dagger e^{-E_\alpha} = F_{e^\alpha Z e^{\alpha^t}}^\dagger. \quad (10.50)$$

Here is a summary of the properties of these $U(N)$ coherent states already proved in [9]:

- They transform simply under $U(N)$ -transformations: $u |J, \{z_i\}\rangle = |J, \{(uz)_i\}\rangle$. This key property actually holds also if the spinors do not satisfy the closure condition.
- They are coherent states *à la* Perelomov and are obtained by the action of $U(N)$ on highest weight states. These highest weight vectors correspond to bivalent intertwiners such as the state defined by the spinors $z_1 = (z^0, z^1)$, $z_2 = \varsigma z_1 = (-\bar{z}^1, \bar{z}^0)$ and $z_k = 0$ for $k \geq 3$. This only holds if one assumes that the spinors satisfy the closure constraint. Indeed, $U(N)$ transformations conserve the closure condition and the spinors defining the bivalent intertwiner satisfy it.
- For large areas J , they are semi-classical states peaked around the expectation values for the $u(N)$ generators and the scalar product operators:

$$\langle E_{ij} \rangle = 2J \frac{\langle z_i | z_j \rangle}{\sum_k \langle z_k | z_k \rangle} = \frac{J}{A(z)} \langle z_i | z_j \rangle, \quad (10.51)$$

$$\forall i \neq j, \quad 4 \langle \vec{J}_i \cdot \vec{J}_j \rangle = \frac{J^2}{A(z)^2} \vec{V}(z_i) \cdot \vec{V}(z_j) + \frac{J}{2A(z)^2} \left(\vec{V}(z_i) \cdot \vec{V}(z_j) - 3|\vec{V}(z_i)| |\vec{V}(z_j)| \right). \quad (10.52)$$

- The scalar product between two coherent states is easily computed:

$$\langle J, \{z_i\} | J, \{w_i\} \rangle = \det \left(\sum_i |z_i\rangle \langle w_i| \right)^J = \left(\frac{1}{2} \text{tr} Z^\dagger W \right)^J.$$

- They minimize the uncertainties on the E_{ij} operators. The interested reader can find the various uncertainties computed in [9]. The simplest is the $U(N)$ -invariant uncertainty:

$$\Delta \equiv \sum_{ij} \langle E_{ij} E_{ji} \rangle - \langle E_{ij} \rangle \langle E_{ji} \rangle = 2J(J + N - 2) - 2J^2 = 2J(N - 2). \quad (10.53)$$

- They are related to the coherent intertwiners discussed above:

$$\frac{1}{\sqrt{J!(J+1)!}} |J, \{z_i\}\rangle = \sum_{\sum j_i = J} \frac{1}{\sqrt{(2j_1)! \cdots (2j_N)!}} ||\{j_i, z_i\}\rangle. \quad (10.54)$$

- The coherent states $|J, \{z_i\}\rangle$ at fixed J provide an over-complete basis on the space $\mathcal{H}_N^{(J)}$. This gives a new decomposition of the identity on that space $\mathbb{I}_N^{(J)} = \int [d\mu(z_i)] |J, \{z_i\}\rangle \langle J, \{z_i\}|$ where $[d\mu(z_i)]$ is a $U(N)$ -invariant measure (on \mathbb{CP}_{2N-1}). For more details, the interested reader can refer to [9].

10.2.3 Relaxing the Closure Conditions

Discussing the $U(N)$ coherent states in the previous section, we have assumed that the spinor labels satisfy the closure condition (10.28) that requires that $\sum_i \vec{V}(z_i) = 0$ or equivalently that $\sum_i |z_i\rangle\langle z_i| \propto \mathbb{I}$, or even equivalently that the two components of the spinors z_i^0 and z_i^1 are orthonormal N -vectors. It has been shown in [9] how to relax this closure condition using the $SL(2, \mathbb{C})$ invariance of the coherent states. Let us review this procedure.

We consider the $GL(2, \mathbb{C})$ action acting simultaneously on all spinors z_i . It has a simple rescaling action on the Z_{ij} matrix, which means that the $U(N)$ coherent states also get simply rescaled:

$$\forall \Lambda \in GL(2, \mathbb{C}), \quad z_i \rightarrow \Lambda z_i, \quad Z_{ij} \rightarrow \det \Lambda Z_{ij}, \quad |J, \{z_i\}\rangle \rightarrow (\det \Lambda)^J |J, \{z_i\}\rangle. \quad (10.55)$$

Thus two coherent states labeled by spinors related through a $GL(2, \mathbb{C})$ action define the same quantum state, up to normalization. In particular, if the transformation Λ lies in $SL(2, \mathbb{C})$ then the coherent state is exactly the same. The moot point is that $GL(2, \mathbb{C})$ transformations allow to go in and out of the closure constraint. Indeed, following [9], given an arbitrary set of N spinors, we consider the matrix:

$$X(z) \equiv \sum_i |z_i\rangle\langle z_i|. \quad (10.56)$$

Since $X(z)$ is obvious a positive Hermitian matrix, there exists a matrix $\Lambda \in SL(2, \mathbb{C})$ which takes its square-root, $X = \sqrt{\det X} \Lambda \Lambda^\dagger$. This matrix is unique up to $SU(2)$ transformations. It allows to define a new set of spinors $\tilde{z}_i \equiv \Lambda^{-1} z_i$ which induce the same coherent state but also satisfy the closure condition:

$$\tilde{X} = \sum_i |\tilde{z}_i\rangle\langle \tilde{z}_i| = \Lambda^{-1} X (\Lambda^\dagger)^{-1} = \sqrt{\det X} \mathbb{I}, \quad \det \tilde{X} = \det X. \quad (10.57)$$

This is the exact same $SL(2, \mathbb{C})$ action used in [131, 132] to take the standard coherent intertwiners in and out of the closure constraint. Let us point out that the $SL(2, \mathbb{C})$ action is simply the complexified $SU(2)$ -action still generated by the operators $J^{z, \pm}$ quadratic in the harmonic oscillators. In the $U(N)$ framework, this simply mean that we can drop the closure condition on the spinor label, when defining $U(N)$ coherent states and integrating over spinor labels, e.g. in the decomposition of the identity. Moreover, the coherent states $|J, \{z_i\}\rangle$ still transform covariantly under $U(N)$ whether they satisfy the closure condition or not, and their norm is easily computed:

$$\langle J, \{z_i\} | J, \{z_i\} \rangle = (\det X)^J. \quad (10.58)$$

Since the projectors $|z_i\rangle\langle z_i|$ are easily expressed in term of the classical 3-vectors $\vec{V}(z_i)$, we give similar expressions for the matrix X and its determinant:

$$X = \frac{1}{2} \left(\sum_i |\vec{V}(z_i)| \mathbb{I} + \sum_i \vec{V}(z_i) \cdot \vec{\sigma} \right) \Rightarrow \det X = \frac{1}{4} \left(\left(\sum_i |\vec{V}(z_i)| \right)^2 - \left| \sum_i \vec{V}(z_i) \right|^2 \right), \quad (10.59)$$

so that $(\det X)^J = A(z)^{2J}$ as before when the closure condition $\sum_i \vec{V}(z_i) = 0$ is satisfied. Let us underline that $\det X \geq 0$ can be interpreted as a measure of how far from the closure condition we are: the larger the total 3-vector $\sum_i \vec{V}(z_i)$ is, the smaller $\det X$ gets.

Finally, we can write a decomposition of the identity on the intertwiner space $\mathcal{H}_N^{(J)}$ as an integral over \mathbb{C}^{2N} :

$$\mathbb{I}_{\mathcal{H}_N^{(J)}} = D_{N,J} \int_{\mathbb{C}^{2N}} \prod_i \frac{e^{-\langle z_i | z_i \rangle} d^4 z_i}{\pi} \frac{|J, \{z_i\}\rangle \langle J, \{z_i\}|}{(\det X(z))^J}. \quad (10.60)$$

This is to be compared with the decomposition of the identity on $\mathcal{H}_{j_1, \dots, j_N}$ in term of coherent intertwiners (10.41). To check this identity, it is enough to check that this integral commutes with the $U(N)$ -action and that its trace is equal to the dimension $D_{N,J}$ of the Hilbert space $\mathcal{H}_N^{(J)}$. As explained in more details in [9], we can gauge-fix this integral by the $GL(2, \mathbb{C})$ -action and restrict it to an integral over the Grassmanian space $\text{Gr}_{2,N} = \mathbb{C}^{2N}/GL(2, \mathbb{C}) = U(N)/U(N-2) \times U(2)$. The $SL(2, \mathbb{C})$ -action allows to gauge-fix to spinors satisfying the closure condition; then rescaling the state allows to fix the matrix $X(z) = \mathbb{I}$ and the total area $A(z) = 1$ thus to restrict the integral to coherent states of unit norm.

10.2.4 The F -action on Coherent Intertwiners

In order to discuss the simplicity constraints in the $U(N)$ framework, we need the explicit action of the operators $E_{ij}, F_{ij}, F_{ij}^\dagger$ on the coherent states. This technical result has been a first part of my work. Let us start by looking closer at the F annihilation operators. We first compute the action of F_{ij} on coherent intertwiners:

$$F_{ij} ||\{j_k, z_k\}\rangle = \int_{\text{SU}(2)} dg g \triangleright F_{ij} \otimes_k \frac{(z_k^0 a_k^\dagger + z_k^1 b_k^\dagger)^{2j_k}}{\sqrt{(2j_k)!}} |0\rangle, \quad (10.61)$$

since the operator F_{ij} is invariant under global $\text{SU}(2)$ transformations and thus commutes with the action of group elements $g \in \text{SU}(2)$. Making $F_{ij} = (a_i b_j - a_j b_i)$ commute through the creation operators, we obtain after a straightforward calculation:

$$F_{ij} ||\{j_k, z_k\}\rangle = Z_{ij} \sqrt{(2j_i)(2j_j)} ||\{j_i - \frac{1}{2}, \dots, j_j - \frac{1}{2}, j_k, z_k\}\rangle, \quad (10.62)$$

where we remind the reader that $Z_{ij} = (z_i^0 z_j^1 - z_i^1 z_j^0)$. Then using the formula (10.54) of $U(N)$ coherent states in term of coherent intertwiners, we easily get:

$$F_{ij} |J, \{z_k\}\rangle = F_{ij} \sum_{\sum j_k = J} \frac{\sqrt{J!(J+1)!}}{\sqrt{(2j_k)!}} ||\{j_k, z_k\}\rangle = Z_{ij} \sqrt{J(J+1)} |J-1, \{z_k\}\rangle. \quad (10.63)$$

This fits with the F -action on $U(N)$ coherent states derived in [9]. Moreover we can use these relations to diagonalize the F_{ij} operators. We introduce the vectors $|\beta, \{z_k\}\rangle$ for $\beta \in \mathbb{C}$:

$$|\beta, \{z_k\}\rangle \equiv \sum_{J \in \mathbb{N}} \frac{\beta^{2J}}{\sqrt{J!(J+1)!}} |J, \{z_k\}\rangle \Rightarrow F_{ij} |\beta, \{z_k\}\rangle = \beta^2 Z_{ij} |\beta, \{z_k\}\rangle. \quad (10.64)$$

These new intertwiners $|\beta, \{z_k\}\rangle$ diagonalize all F_{ij} operators simultaneously. This is normal since the F_{ij} 's all commute with each other. We can also give other convenient expressions for these vectors in term of creation operators acting on the vacuum:

$$|\beta, \{z_k\}\rangle = \sum_J \frac{(\beta^2 F_Z^\dagger)^J}{J!(J+1)!} |0\rangle \quad (10.65)$$

$$= \int dg g \triangleright \otimes_k e^{\beta(z_k^0 a_k^\dagger + z_k^1 b_k^\dagger)} |0\rangle, \quad (10.66)$$

which makes a clear link between these vectors and coherent states for the harmonic oscillator. Finally, we can compute the norm of these states, which is easily expressed as a Bessel function:

$$\langle \beta, \{z_k\} | \beta, \{z_k\} \rangle = \sum_J \frac{(|\beta|^2)^{2J}}{J!(J+1)!} \langle J, \{z_k\} | J, \{z_k\} \rangle = \sum_J \frac{(|\beta|^2 A(z))^{2J}}{J!(J+1)!} = \frac{I_1(2|\beta|^2 A(z))}{|\beta|^2 A(z)}, \quad (10.67)$$

where we assumed the closure condition on the spinors so that the norm of the $U(N)$ coherent state is given directly by $A(z)^{2J}$ (else we should in general replace $A(z)$ by the determinant $\sqrt{\det X(z)}$). Here I_1 is the first modified Bessel function of the first kind. This clears up the action of the F -operators. Below, we further investigate the actions of the E and F^\dagger operators on the $U(N)$ coherent states.

10.2.5 Operator Algebra on Coherent Intertwiners

We already have the action of the annihilation operators F_{ij} on the $U(N)$ coherent states. Now we need to complete the algebra to derive the action of the operators F_{ij}^\dagger and E_{ij} . To this purpose, we use the standard

action as differential operators of the creation and annihilation operators for the harmonic oscillator (see in appendix for some details):

$$a_i \rightarrow z_i^0, \quad a_i^\dagger \rightarrow \frac{\partial}{\partial z_i^0}, \quad b_i \rightarrow z_i^1, \quad b_i^\dagger \rightarrow \frac{\partial}{\partial z_i^1}.$$

Using this on the definition of the operators E and F , we guess the following action of these operators on the $U(N)$ coherent states:

$$F_{ij}|J, \{z_k\}\rangle = \sqrt{(J+1)J} Z_{ij}|J-1, \{z_k\}\rangle, \quad (10.68)$$

$$F_{ij}^\dagger|J, \{z_k\}\rangle = \frac{1}{\sqrt{(J+2)(J+1)}} \Delta_{ij}^z|J+1, \{z_k\}\rangle, \quad (10.69)$$

$$E_{ij}|J, \{z_k\}\rangle = \delta_{ij}^z|J, \{z_k\}\rangle, \quad (10.70)$$

where $Z_{ij} = (z_i^0 z_j^1 - z_i^1 z_j^0)$ as before and where we have defined the following differential operators with respect to the spinor z_i :

$$\Delta_{ij}^z = \frac{\partial^2}{\partial z_i^0 \partial z_j^1} - \frac{\partial^2}{\partial z_i^1 \partial z_j^0}, \quad (10.71)$$

$$\delta_{ij}^z = z_j^0 \frac{\partial}{\partial z_i^0} + z_j^1 \frac{\partial}{\partial z_i^1}. \quad (10.72)$$

The J -factors in front of the actions of F and F^\dagger come from the normalization factor $\sqrt{J!(J+1)!}$ of the coherent states.

The multiplication action of F on the $U(N)$ coherent states can be derived by using the commutation relation between the creation and annihilation operators:

$$[F_{ij}, F_Z^\dagger] = \mathcal{E}_{ij}^Z + 2Z_{ij}, \quad (10.73)$$

$$[\mathcal{E}_{ij}^Z, F_Z^\dagger] = 2Z_{ij} F_Z^\dagger. \quad (10.74)$$

where we have defined the auxiliary operator $\mathcal{E}_{ij}^Z = \sum_m (Z_{im} E_{mj} - Z_{jm} E_{mi})$. To show the second commutator, we have used that the antisymmetric matrix Z satisfies that $Z_{ik} Z_{jl} - Z_{il} Z_{jk} = Z_{ij} Z_{kl}$. This allows the straightforward calculation:

$$\begin{aligned} F_{ij} (F_Z^\dagger)^J |0\rangle &= \sum_{k=0}^{J-1} (F_Z^\dagger)^{J-1-k} \mathcal{E}_{ij}^Z (F_Z^\dagger)^k |0\rangle + 2J Z_{ij} (F_Z^\dagger)^{J-1} |0\rangle, \\ &= \left(\sum_{k=0}^{J-1} 2k + 2J \right) Z_{ij} (F_Z^\dagger)^{J-1} |0\rangle, \\ &= J(J+1) Z_{ij} (F_Z^\dagger)^{J-1} |0\rangle, \end{aligned} \quad (10.75)$$

which gives the expected result. Moreover, we recover the same action for the F_{ij} operators that we had already computed in the previous section using that the $U(N)$ coherent states are superpositions of coherent intertwiners.

As for the F^\dagger -action, it is straightforward to compute the action of the differential operator Δ_{ij}^z on the coherent state taking into account that:

$$\Delta_{ij}^z (Z_{kl}) = 2(\delta_{ik} \delta_{jl} - \delta_{il} \delta_{jk}), \quad \Delta_{ij}^z (F_Z^\dagger)^J = \Delta_{ij}^z \left(\frac{1}{2} \sum_{kl} Z_{kl} F_{kl}^\dagger \right)^J = J(J+1) F_{ij}^\dagger (F_Z^\dagger)^{J-1}. \quad (10.76)$$

This leads to the following action for the creation operator F_{ij}^\dagger

$$\Delta_{ij}^z |J+1, \{z_k\}\rangle = \sqrt{(J+1)(J+2)} F_{ij}^\dagger |J, \{z_k\}\rangle, \quad (10.77)$$

since F_{ij}^\dagger commutes with F_Z^\dagger because they only involve oscillator creation operators a^\dagger and b^\dagger . At this stage, we can also check that the differential F^\dagger -action is indeed the adjoint of the multiplicative F -action on the $U(N)$ coherent state. That is straightforward to show. First, considering the matrix element $\langle K, \{w_k\} | F_{ij} | J, \{z_k\} \rangle$, it doesn't vanish iff $K = (J-1)$. Then, on the one hand, we can compute:

$$\langle J-1, \{z_k\} | F_{ij} | J, \{w_k\} \rangle = \sqrt{J(J+1)} W_{ij} \langle J-1, \{z_k\} | J-1, \{w_k\} \rangle = \sqrt{J(J+1)} W_{ij} \left(\frac{1}{2} \text{tr } Z^\dagger W \right)^{J-1}. \quad (10.78)$$

On the other hand, we have:

$$\langle J, \{w_k\} | F_{ij}^\dagger | J-1, \{z_k\} \rangle = \frac{1}{\sqrt{J(J+1)}} \Delta_{ij}^z \langle J, \{w_k\} | F_{ij}^\dagger | J, \{z_k\} \rangle = \frac{1}{\sqrt{J(J+1)}} \Delta_{ij}^z \left(\frac{1}{2} \text{tr } W^\dagger Z \right)^J. \quad (10.79)$$

To evaluate this expression, we calculate explicitly the action of the differential operator on the J -power of the trace:

$$\Delta_{ij}^z (\text{tr } W^\dagger Z)^J = 2J(J+1) \bar{W}_{ij} (\text{tr } W^\dagger Z)^{J-1}. \quad (10.80)$$

This allows to conclude that we have as expected:

$$\overline{\langle J-1, \{z_k\} | F_{ij} | J, \{w_k\} \rangle} = \langle J, \{w_k\} | F_{ij}^\dagger | J-1, \{z_k\} \rangle. \quad (10.81)$$

Finally, let us now compute the action of the E -operators on the $U(N)$ coherent states. First we compute the commutator $[E_{ij}, F_Z^\dagger] = \sum_m Z_{jm} F_{im}^\dagger$, which easily gets generalized to arbitrary power of the creation operator:

$$[E_{ij}, (F_Z^\dagger)^J] = \sum_{k=0}^{J-1} (F_Z^\dagger)^{J-1-k} [E_{ij}, F_Z^\dagger] (F_Z^\dagger)^k = J \left(\sum_m Z_{jm} F_{im}^\dagger \right) (F_Z^\dagger)^{J-1}, \quad (10.82)$$

since all F^\dagger commute with each other. This proves directly that the E -action on $U(N)$ coherent states is simply related to the F^\dagger -action:

$$E_{ij} (F_Z^\dagger)^J |0\rangle = J \left(\sum_m Z_{jm} F_{im}^\dagger \right) (F_Z^\dagger)^{J-1} |0\rangle. \quad (10.83)$$

Then we can easily compute the action of the differential operator:

$$\begin{aligned} \delta_{ij}^z (F_Z^\dagger)^J &= \left(z_j^0 \frac{\partial}{\partial z_i^0} + z_j^1 \frac{\partial}{\partial z_i^1} \right) \left(\frac{1}{2} \sum_{kl} Z_{kl} F_{kl}^\dagger \right)^J \\ &= J \sum_m \left(Z_{jm} F_{im}^\dagger \right) (F_Z^\dagger)^{J-1} \end{aligned} \quad (10.84)$$

This allows us to deduce the actions of the E -operators and of the differential operators δ_{ij}^z match on the $U(N)$ coherent states:

$$E_{ij} |J, \{z_k\}\rangle = \delta_{ij}^z |J, \{z_k\}\rangle. \quad (10.85)$$

It is possible to check directly that these differential operators actually generate the correct $U(N)$ action on the spinors. Let us for instance consider the infinitesimal unitary transformation $u = \exp(\epsilon(E_{ij} - E_{ji}))$ where i, j are arbitrary but fixed indices. It acts at first order on the spinors as:

$$(u z)_k \sim z_k + \epsilon \delta_{ik} z_j - \epsilon \delta_{jk} z_i.$$

It is very easy to check that this fits with the action of the previous differential operator:

$$\epsilon(\delta_{ij}^z - \delta_{ji}^z) z_k = i\epsilon\delta_{ik}z_j - \epsilon\delta_{jk}z_i \sim (uz)_k - z_k.$$

Following the same steps with the unitary transformations $u = \exp(i\epsilon(E_{ij} + E_{ji}))$ allows to prove completely that the differential operators δ_{ij}^z generate as expected the $U(N)$ action on our coherent states.

Finally, it is also possible to check that the commutation relation between the differential operators corresponding to E , F and F^\dagger satisfy the correct commutation relations (see in appendix).

10.3 The $U(N)$ setting for $\text{Spin}(4)$ intertwiner and a Gupta-Bleuler quantization

We have reviewed the whole $U(N)$ formalism for $SU(2)$ intertwiners and we gave the explicit action of the operators $E_{ij}, F_{ij}, F_{ij}^\dagger$ on the $U(N)$ coherent states. I now present the main part of my work concerning the issue of the way the simplicity constraints can be implemented on a $\text{Spin}(4)$ intertwiner within the $U(N)$ framework. The results obtained show that there is a lot of freedom in the way the simplicity constraints can be implemented. Since the Lie algebra $\mathfrak{spin}(4) = \mathfrak{su}_L(2) \oplus \mathfrak{su}_R(2)$ simply splits into two copies of the $\mathfrak{su}(2)$ algebra, it is straightforward to adapt the whole $U(N)$ framework to $\mathfrak{spin}(4)$. We double all the operators, introduce harmonic oscillators a_i^L, b_i^L and a_i^R, b_i^R and build two sets of $\mathfrak{u}(N)$ operators $E_{ij}^L, F_{ij}^L, F_{ij}^{L\dagger}$ and $E_{ij}^R, F_{ij}^R, F_{ij}^{R\dagger}$. These two $\mathfrak{u}(N)$ sectors don't speak to each other and are a priori decoupled. It is the simplicity constraints that will couple them.

Several ways of imposing the constraints are explored and their advantages and disadvantages are analyzed. The idea presented in this section is to replace the simplicity constraint algebra which does not close by a new equivalent constraint algebra which does close defined using the $\mathfrak{u}(N)$ operators keeping a strong imposition of the diagonal simplicity constraint and imposing weakly the cross simplicity constraints as it is done in the EPRL-FK model. In this section, we only treat the case without Immirzi parameter ($\rho = 1$ in (10.2) and (10.3)). The issue of the extension to the case with a finite Immirzi parameter ($\rho \neq 1$ in (10.2) and (10.3)) is discussed in the next part of this section as well as in the last section of this chapter.

Let us start with the diagonal simplicity constraints: $\forall i, (\vec{J}_i^L)^2 = (\vec{J}_i^R)^2$. Imposed strongly, they constraint the $\mathfrak{spin}(4)$ living on the legs of the intertwiners to be simple. This means that the spins in the left and right sectors match: $j_i^L = j_i^R$. This translates into very simple constraints in the $\mathfrak{u}(N)$ framework:

$$C_i \equiv E_i^L - E_i^R. \quad (10.86)$$

This diagonal simplicity definitively couples the two sectors. This constraint is actually the same than the matching conditions for spin networks on the 2-vertex graph and the whole construction will be very similar [136]. Every (constraint) operator that we will now introduce to solve the simplicity constraints will have to commute (at least weakly) with these diagonal simplicity constraints C_i .

Now moving to the crossed simplicity constraints, $\forall i \neq j, (\vec{J}_i^L \cdot \vec{J}_j^L) = (\vec{J}_i^R \cdot \vec{J}_j^R)$, they refer to couples of legs of the intertwiners and to their scalar product. They amount to impose strongly, weakly or semi-classically, the equality between the scalar products of the left and right sectors, $\vec{J}_i^L \cdot \vec{J}_j^L = \vec{J}_i^R \cdot \vec{J}_j^R$. Dropping the L/R index, we remind the expression for the scalar product operator in term of $\mathfrak{u}(N)$ operators for $i \neq j$:

$$\begin{aligned} \vec{J}_i \cdot \vec{J}_j &= \frac{1}{2}E_{ij}E_{ji} - \frac{1}{4}E_iE_j - \frac{1}{2}E_i, \\ &= \frac{1}{2}E_{ji}E_{ij} - \frac{1}{4}E_iE_j - \frac{1}{2}E_j, \\ &= -\frac{1}{2}F_{ij}^\dagger F_{ij} + \frac{1}{4}E_iE_j, \\ &= -\frac{1}{2}F_{ij}F_{ij}^\dagger + \frac{1}{4}(E_i + 2)(E_j + 2). \end{aligned} \quad (10.87)$$

This expression clearly suggests two things. First, we could replace the $\vec{J}_i^L \cdot \vec{J}_j^L = \vec{J}_i^R \cdot \vec{J}_j^R$ constraints by some constraints of the type $E^L = E^R$ or $F^L = F^R$. We will explore these various possibilities below. Second, we

then expect that the equality $\vec{J}_i^L \cdot \vec{J}_j^L = \vec{J}_i^R \cdot \vec{J}_j^R$ will only hold semi-classically at first order and will usually have corrections linear in the j_i 's (terms in E_i and E_j).

10.3.1 The Closed Algebra of Simplicity Constraints

One big issue about the standard crossed simplicity constraints $\vec{J}_i^L \cdot \vec{J}_j^L - \vec{J}_i^R \cdot \vec{J}_j^R = 0$ for all couples of legs $i \neq j$ is that their algebra doesn't close. The $U(N)$ framework was precisely introduced to close the algebra of scalar product operators and provide an alternative algebra for invariant observables on the space of intertwiners. Indeed, considering the operators E_{ij} instead of $\vec{J}_i \cdot \vec{J}_j$ allowed to have a closed algebra of invariant observables and to build coherent intertwiner states á la Perelomov that transforms nicely under the operators of that algebra. This naturally suggests to replace the simplicity constraints $\vec{J}_i^L \cdot \vec{J}_j^L - \vec{J}_i^R \cdot \vec{J}_j^R = 0$ by a simpler constraint expressed in term of the operators $E_{ij}^{L,R}$. We propose to consider a new set of constraints, that we name the $u(N)$ simplicity constraints:

$$\mathcal{C}_{ij} \equiv E_{ij}^L - E_{ji}^R = E_{ij}^L - (E_{ij}^R)^\dagger, \quad \mathcal{C}_{ij}^\dagger = \mathcal{C}_{ji}. \quad (10.88)$$

The two important facts about these new proposed constraints are:

- They naturally include the diagonal simplicity constraints:

$$\mathcal{C}_{ii} = \mathcal{C}_i = E_i^L - E_i^R.$$

- They form a closed $u(N)$ algebra:

$$[\mathcal{C}_{ij}, \mathcal{C}_{kl}] = \delta_{jk} \mathcal{C}_{il} - \delta_{il} \mathcal{C}_{kj}. \quad (10.89)$$

Moreover, let us \mathcal{H}_C be the Hilbert space of states satisfying these $u(N)$ simplicity constraints:

$$\mathcal{H}_C \equiv \{|\psi\rangle \text{ such that } \mathcal{C}_{ij}|\psi\rangle = 0, \forall i, j\}. \quad (10.90)$$

Then this solves weakly the crossed simplicity constraints at leading order (i.e for large spins). Indeed, for all solution states $\phi, \psi \in \mathcal{H}_C$, we have for $i \neq j$:

$$\begin{aligned} \langle \phi | \vec{J}_i^L \cdot \vec{J}_j^L | \psi \rangle &= \langle \phi | \frac{1}{2} E_{ij}^L E_{ji}^L - \frac{1}{4} E_i^L E_j^L - \frac{1}{2} E_i^L | \psi \rangle = \langle \phi | \frac{1}{2} E_{ji}^R E_{ij}^R - \frac{1}{4} E_i^R E_j^R - \frac{1}{2} E_i^R | \psi \rangle, \\ &= \langle \phi | \vec{J}_i^R \cdot \vec{J}_j^R | \psi \rangle + \langle \phi | \frac{1}{2} (E_j^R - E_i^R) | \psi \rangle. \end{aligned} \quad (10.91)$$

Therefore, the crossed simplicity constraints are solved approximatively at first order. Indeed the expectation values $\langle \vec{J}_i^L \cdot \vec{J}_j^L \rangle$ are of order $\mathcal{O}(j^2)$ while the correction term is of order $(j_j - j_i) \sim \mathcal{O}(j)$. This is not a very big obstacle since we only expect the simplicity constraints to be satisfied semi-classically in the large spin regime. Let us still point out that the diagonal simplicity constraints are still strongly and exactly enforced on all invariant states in \mathcal{H}_C .

As we said above, the operators \mathcal{C}_{ij} generate a $u(N)$ Lie algebra: they actually generate the $U(N)$ action (u, \bar{u}) on the coupled L, R system such that the $U(N)$ transformation acting on the right sector is the complex conjugate of the transformation acting on the left sector. Indeed, a finite transformation generated by the constraints \mathcal{C}_{ij} will read, for a anti-Hermitian matrix $\alpha_{ij} = -\bar{\alpha}_{ji}$:

$$U \equiv e^{\sum_{ij} \alpha_{ij} \mathcal{C}_{ij}} = e^{\sum_{ij} \alpha_{ij} E_{ij}^L} e^{-\sum_{ij} \alpha_{ij} E_{ji}^R} = e^{\sum_{ij} \alpha_{ij} E_{ij}^L} e^{\sum_{ij} \bar{\alpha}_{ij} E_{ij}^R}.$$

Thus, states which are solution to the \mathcal{C}_{ij} -constraints are $U(N)$ -invariant and the Hilbert space \mathcal{H}_C can be obtained by performing a $U(N)$ group averaging on the space of intertwiners $\bigoplus_J \mathcal{H}_N^{(J),L} \otimes \mathcal{H}_N^{(J),R}$. An over-complete basis of solutions can be obtained by group averaging the $U(N)$ coherent states $|J, \{z_k^L\}\rangle \otimes |J, \{z_k^R\}\rangle$. However, we can give a more precise description of the $U(N)$ -invariant space. Indeed, since the spaces $\mathcal{H}_N^{(J)}$ are irreducible $U(N)$ -representations, the Schur's lemma implies that there exists a unique invariant vector in the

tensor product $\mathcal{H}_N^{(J),L} \otimes \mathcal{H}_N^{(J),R}$. Calling $|J\rangle$ this unique state solution to the $\mathfrak{u}(N)$ -constraints for every total spin J , we have a complete basis of our solution space:

$$\mathcal{H}_C = \bigoplus_J \mathbb{C} |J\rangle. \quad (10.92)$$

This construction is exactly the same than the definition of isotropic states in the 2-vertex loop quantum gravity model constructed in [136] using the $U(N)$ formalism. Thus following that approach, we won't perform the $U(N)$ -group averaging to construct our $U(N)$ -invariant states but we will use using the following symmetric operator :

$$f^\dagger \equiv \sum_{kl} F_{kl}^{L\dagger} F_{kl}^{R\dagger}. \quad (10.93)$$

Indeed, this operator commute with all generators \mathcal{C}_{ij} :

$$[\mathcal{C}_{ij}, f^\dagger] = \sum_{kl} \left([E_{ij}^L, F_{kl}^{L\dagger}] F_{kl}^{R\dagger} - F_{kl}^{L\dagger} [E_{ji}^R, F_{kl}^{R\dagger}] \right) = 0, \quad (10.94)$$

therefore, the operator f^\dagger is $U(N)$ -invariant. Since the vacuum state is also $U(N)$ -invariant, we can define the invariant states by applying this creation operator f^\dagger to the vacuum state $|0\rangle$:

$$|J\rangle \equiv (f^\dagger)^J |0\rangle \quad (10.95)$$

is obviously $U(N)$ -invariant. We also check that $|J\rangle \in \mathcal{H}_N^{(J),L} \otimes \mathcal{H}_N^{(J),R}$. Indeed, a straightforward calculation of the action of the total spin operator $E \equiv \sum_i E_i^L = \sum_i E_i^R$ (the left and right total spin operators are obviously equal on the invariant space \mathcal{H}_C) gives :

$$E|J\rangle = 2J|J\rangle. \quad (10.96)$$

Finally, following the computations done in [136], we also give the norm of these invariant vectors:

$$\langle J|J\rangle = 2^{2J} J!(J+1)! \frac{(N+J-1)!(N+J-2)!}{(N-1)!(N-2)!} = 2^{2J} (J!(J+1)!)^2 D_{N,J} \quad (10.97)$$

where $D_{N,J}$ is the dimension of the intertwiner space $\mathcal{H}_N^{(J)}$ given by (10.19). The details of this calculation can be found in the appendix.

The fact that we get a single state for each total spin means that we are imposing constraints which are too strong. In the next parts, we will try to impose less constraints using the E operators then different constraints in terms of the F and F^\dagger operators in order to get a bigger set of solutions to the simplicity constraints. Finally, we will see in the last section how we can use the $U(N)$ coherent states in order to solve weakly all the simplicity constraints.

10.3.2 Highest weight vectors for the $\mathfrak{u}(N)$ -simplicity constraints

As we said in the previous section, it seems that the $\mathfrak{u}(N)$ -simplicity constraints are too strong. Following the idea that we might have imposed too many constraints, we propose a new restricted set of $\mathfrak{u}(N)$ constraints and consider only the raising operators of our $\mathfrak{u}(N)$ algebra. This is also consistent with the line of thoughts that such a procedure usually leads to the construction of proper coherent states with the expected semi-classical properties. Thus we try with the following new set of constraints:

$$\{\mathcal{C}_{i<j} \equiv \mathcal{C}_{ij} \text{ for } i < j \text{ and } \mathcal{C}_i^\sigma = \mathcal{C}_i - \sigma_i\} \quad (10.98)$$

where we have chosen to require that only the raising operators² vanish $\mathcal{C}_{ij} |\psi\rangle = 0$ for $i < j$. We have also relaxed the diagonal simplicity constraints: $\mathcal{C}_i |\psi\rangle = \sigma_i |\psi\rangle$ where the parameters $\sigma_i \in \mathbb{Z}/2$ are arbitrary but

fixed. In general, we will require that $|\sigma_i| \ll j_i$, so that the diagonal simplicity constraint are still satisfied at leading order.

Even we do not impose the full $\mathfrak{u}(N)$ simplicity constraints, the cross simplicity constraints are still weakly satisfied. Indeed, let us define the Hilbert space $\mathcal{H}_{\mathcal{C}_\sigma^\leq}$ of states which satisfy the restricted set of constraints (10.98). For all states $\phi, \psi \in \mathcal{H}_{\mathcal{C}_\sigma^\leq}$, we have:

$$\forall i < j, \quad \langle \phi | \vec{J}_i^L \cdot \vec{J}_j^L | \psi \rangle = \langle \phi | \vec{J}_i^R \cdot \vec{J}_j^R | \psi \rangle + \langle \phi | \frac{1}{2}(E_i^R - E_j^R) - \frac{1}{4}(\sigma_i E_j^R + \sigma_j E_i^R + \sigma_i \sigma_j) - \frac{1}{2}\sigma_j | \psi \rangle \quad (10.100)$$

Therefore, the weak cross simplicity constraints are still satisfied approximatively at leading order: the matrix elements $\langle \phi | \vec{J}_i^R \cdot \vec{J}_j^R | \psi \rangle$ are of order $\mathcal{O}(j^2)$ while the correction terms are of order $\mathcal{O}(j)$.

The meaning of the Hilbert space $\mathcal{H}_{\mathcal{C}_\sigma^\leq}$ is straightforward in term of the theory of representations of the $\mathfrak{u}(N)$ Lie algebra: it is the space of highest weight vectors. More precisely, let us consider the full space of $\mathfrak{spin}(4)$ intertwiners defined as the tensor product of the uncoupled intertwiner spaces for $\mathfrak{su}(2)_L$ and $\mathfrak{su}(2)_R$. It is given by the direct sum over possible total area labels J_L, J_R of the corresponding irreducible $\mathfrak{u}(N)$ representations:

$$\mathcal{H}_N^{\mathfrak{spin}(4)} = \bigoplus_{J_L, J_R} \mathcal{H}_N^{J_L} \otimes \mathcal{H}_N^{J_R}. \quad (10.101)$$

Now our constraint algebra generates the diagonal $\mathfrak{u}(N)$ action which acts simultaneously on both the left and right sectors. Then we decompose the tensor products $\mathcal{H}_N^{J_L} \otimes \mathcal{H}_N^{J_R}$ into irreducible representations of this diagonal $U(N)$ action and the vectors that are annihilated by the raising operators $\mathcal{C}_{i < j}$ are the highest weight vectors of these irreducible representations. The parameters σ_i are the eigenvalues of the diagonal $\mathfrak{u}(N)$ generators, they are the values of the highest weight and select the relevant representations.

For instance, the most natural case, $\sigma_i = 0, \forall i$, corresponds to $U(N)$ -invariant representations and we recover the space \mathcal{H}_C considered in the previous section. Then for a generic choice of σ_i , we do not necessarily require that $J_L = J_R$ as before, but this condition is slightly shifted to $J_L = J_R + \sum_i \sigma_i$. The next step would be to decompose the product tensor of the two $U(N)$ representations $\mathcal{H}_N^{J_L} \otimes \mathcal{H}_N^{J_R}$ into $U(N)$ irreducible representations and then to extract the highest weight vector of this decomposition which correspond to our choice of σ_i 's. This can be done using the Gelfand-Zetlin basis and the Gelfand patterns [137]. I have not investigated further in this direction yet.

10.3.3 Using $F^L - F^R$ Constraints

Another possibility to identify new simplicity constraints within the $U(N)$ framework is to use the F_{ij} -operators instead of the E_{ij} operators. Moreover, introducing simplicity constraints defined in terms of the $F_{ij}^{L,R}$ would be more in the spirit of the Gupta-Bleuler procedure since the F 's are indeed the annihilation operators. Following this intuition, we define F -constraints:

$$f_{ij} \equiv F_{ij}^L - F_{ij}^R. \quad (10.102)$$

First, these constraints all commute with each other, $[f_{ij}, f_{kl}] = 0$. Moreover, these constraints are straightforward to solve since we know how to diagonalize explicitly and simultaneously the operators F_{ij} using the superposition of coherent states $|\beta, \{z_i\}\rangle$.

Furthermore, solving these constraints seem to allow to solve weakly the exact original quadratic simplicity constraints (without correction terms). Indeed, for all states ϕ, ψ in the kernel of f_{ij} for all $i \neq j$, we have

$$\begin{aligned} \langle \phi | \vec{J}_i^L \cdot \vec{J}_j^L | \psi \rangle &= \langle \phi | -\frac{1}{2}F_{ij}^{L\dagger}F_{ij}^L + \frac{1}{4}E_i^L E_j^L | \psi \rangle \\ &= \langle \phi | \vec{J}_i^R \cdot \vec{J}_j^R | \psi \rangle + \langle \phi | \frac{1}{4}(E_i^L E_j^L - E_i^R E_j^R) | \psi \rangle. \end{aligned} \quad (10.103)$$

²This new set of constraints 10.98 still forms a closed algebra. Indeed, let be $i \leq j$ and $k \leq l$ then:

$$[\mathcal{C}_{ij}, \mathcal{C}_{kl}] = \delta_{jk}\mathcal{C}_{il} - \delta_{il}\mathcal{C}_{kj} \quad (10.99)$$

where $i \leq j, k \leq l$ and $j = k$ imply $i \leq l$ or $k \leq l, i \leq j$ and $i = l$ imply $k \leq l$. Therefore, \mathcal{C}_{il} and \mathcal{C}_{kj} are also raising operators.

If we also assume that the diagonal simplicity constraints hold, i.e that the operators $E_i^L - E_i^R$ vanish on both states ψ, ϕ , then the second term vanishes and it all works out. Unfortunately, the F -constraints do not form a closed algebra with the diagonal constraints \mathcal{C}_i :

$$[\mathcal{C}_i, f_{kl}] = [E_i^L, F_{kl}^L] + [E_i^R, F_{kl}^R] = \delta_{il}(F_{ik}^L + F_{ik}^R) - \delta_{ik}(F_{il}^L + F_{il}^R). \quad (10.104)$$

Thus, if we require both $\mathcal{C}_i = 0$ and $F_{kl}^L - F_{kl}^R = 0$, then we automatically also require $F_{kl}^L + F_{kl}^R = 0$, which means that we are actually imposing the much stronger constraints $F_{kl}^L = F_{kl}^R = 0$. These constraints are obviously only satisfied by the vacuum state $|0\rangle$. Thus the f_{kl} constraints are not consistent with the diagonal simplicity constraints. However, we will see in the last section that if we drop the requirement of imposing strongly the diagonal simplicity constraints then these f constraints appear to be the right constraints to consider: they allow to impose all the (diagonal and crossed) simplicity constraints weakly.

10.3.4 Using $F^L - (F^R)^\dagger$ Constraints

We now consider “holomorphic” constraints defined in terms of the F_{ij} and F_{ij}^\dagger operators by:

$$\mathcal{F}_{ij} \equiv F_{ij}^L - F_{ij}^{R\dagger}, \quad \mathcal{F}_{ij} = -\mathcal{F}_{ji}. \quad (10.105)$$

These new operators commute with each other:

$$[\mathcal{F}_{ij}, \mathcal{F}_{kl}] = 0 \quad (10.106)$$

and the commutator of these new constraints with the $u(N)$ generators \mathcal{C}_{ij} is now given by:

$$\begin{aligned} [\mathcal{C}_{ij}, \mathcal{F}_{kl}] &= [E_{ij}^L - E_{ji}^R, F_{kl}^L - F_{kl}^{R\dagger}] \\ &= \delta_{il}\mathcal{F}_{jk} - \delta_{ik}\mathcal{F}_{jl}. \end{aligned} \quad (10.107)$$

This shows two things. First, if we take $i = j$, the $u(N)$ generators are the diagonal simplicity constraints. This means that the holomorphic constraints are compatible with the diagonal simplicity constraints and together they form a closed Lie algebra: we can impose $\mathcal{C}_i = 0$ on the space of solutions to $\mathcal{F} = 0$ without obvious obstacle. Second, let us call $\mathcal{H}_{\mathcal{F}}$ the Hilbert space of states ψ satisfying $\mathcal{F}_{ij}|\psi\rangle = 0$ for all indices i, j . Then the previous commutator also means that there is a natural $U(N)$ action on this solution space $\mathcal{H}_{\mathcal{F}}$ generated by the operators \mathcal{C}_{ij} . In particular, once we identify a single solution to the holomorphic constraints \mathcal{F} then this induces a whole family of solutions obtained by acting with $U(N)$ transformations on that initial solution.

We introduce the Hilbert space $\mathcal{H}_{\mathcal{F}}^0$ of states satisfying the holomorphic constraints and the diagonal simplicity constraints \mathcal{C}_i . Then, for all solution states $\psi, \phi \in \mathcal{H}_{\mathcal{F}}^0$, the expectation values of the left and right scalar product operators are equal up to a correction of order $\mathcal{O}(j)$:

$$\begin{aligned} \langle \phi | \vec{J}_i^L \cdot \vec{J}_j^L | \psi \rangle &= \langle \phi | -\frac{1}{2}F_{ij}^{L\dagger}F_{ij}^L + \frac{1}{4}E_i^L E_j^L | \psi \rangle \\ &= \langle \phi | -\frac{1}{2}F_{ij}^R F_{ij}^{R\dagger} + \frac{1}{4}E_i^R E_j^R | \psi \rangle \\ &= \langle \phi | \vec{J}_i^R \cdot \vec{J}_j^R | \psi \rangle - \langle \phi | 1 + \frac{1}{2}(E_i + E_j) | \psi \rangle. \end{aligned} \quad (10.108)$$

To identify solution states in $\mathcal{H}_{\mathcal{F}}^0$, we start by the simplest case, which is to construct $U(N)$ -invariant states solution of this new set of constraints. We recall that while the E_{ij} -operators leave invariant the total sum of spins $E^{L,R}$, the $F_{ij}^{L,R}$ operators decrease by -1 respectively the left and right total areas $E^{L,R}$ and the $F_{ij}^{L,R\dagger}$ operators increase them by $+1$. That is why we consider a linear combination of $U(N)$ -invariant states for different areas J ; we use the $U(N)$ -invariant basis $|J\rangle$. It is straightforward to compute that ³:

$$F_{ij}^L |J\rangle = 2J(J+1)F_{ij}^{R\dagger} |J-1\rangle. \quad (10.109)$$

³The computation is similar to the computation of the multiplication action of F on the $U(N)$ coherent states, done from (10.73) to (10.75), replacing Z_{kl} by $2F_{kl}^{R\dagger}$: $F_{kl}^{R\dagger}$ is also antisymmetric in $k \leftrightarrow l$ and satisfies the Plücker relation $(F_{ik}^{R\dagger} F_{jl}^{R\dagger} - F_{il}^{R\dagger} F_{jk}^{R\dagger} =$

Then if we define the states:

$$|\alpha\rangle = \sum_J \frac{\alpha^J}{2^J J!(J+1)!} |J\rangle = \sum_J \frac{\alpha^J}{2^J J!(J+1)!} (f^\dagger)^J |0\rangle \quad \text{with } \alpha \in \mathbb{C} \quad (10.110)$$

they satisfy:

$$F_{ij}^L |\alpha\rangle = \alpha F_{ij}^{R\dagger} |\alpha\rangle \quad \forall i, j \quad \text{i.e. } \mathcal{F}_{ij} |\alpha\rangle = 0 \quad \forall i, j. \quad (10.111)$$

Thus for $\alpha = 1$, they are solution of the \mathcal{F} -constraints: $F_{ij}^L |\alpha = 1\rangle = F_{ij}^{R\dagger} |\alpha = 1\rangle$. Let us notice that these new states $|\alpha\rangle$ for the coupled L/R system are very similar to the coherent states $|\beta, \{z_k\}\rangle$ diagonalizing the F_{ij} operators acting on a single (left or right) sector. It's actually the exact same expression if we replace the spinor parameters Z_{ij} by the creation operators F_{ij}^\dagger of the other sector: instead of imposing by hand the values of the expectation values using the spinor labels, the behavior of the left sector is entirely dictated by the right sector, and vice-versa. As underlined in [136] in the context of loop quantum gravity on the 2-vertex graph, these states $|J\rangle$ and $|\alpha\rangle$ maximally entangle the left and right sectors.

Therefore, we have determined the unique $U(N)$ -invariant state solution to the \mathcal{F} constraints. The natural question is whether there exist other solutions to these \mathcal{F} -constraints, which would necessarily be non- $U(N)$ -invariant. At this point, we have not been able to identify such solutions and we would like to conjecture that they do not exist. We however postpone the precise analysis of such conjecture to future investigation. Nevertheless, we would like to point out that a promising line of tackling this issue would be to work in the coherent intertwiner basis and use the expression of the operators E, F, F^\dagger as differential operators on the spinor labels.

10.3.5 Including the Immirzi Parameter?

The next step is to extend our construction to the Euclidean case with a finite Immirzi parameter γ ($\gamma > 0, \gamma \neq 1$). At the discrete level, there is no equality between the left and the right parts of the scalar products anymore imposed by the simplicity constraints but the relation between the left and the right parts becomes a proportionality relation given by (10.2) and (10.3). We recall that the proportionality coefficient ρ is simply related to the Immirzi parameter γ by: $\rho \equiv \frac{\gamma+1}{|\gamma-1|}$ [96, 98]. Once again, we would like to use the $U(N)$ formalism to solve these constraints. We therefore focus on a $\text{Spin}(4)$ intertwiner with N legs labelled by $i \in \{1, \dots, N\}$. The issue remains that the crossed simplicity constraints $\vec{J}_i^L \cdot \vec{J}_j^L - \rho^2 \vec{J}_i^R \cdot \vec{J}_j^R = 0$ for all couples of legs $i \neq j$ do not form a closed algebra. Following the same idea as previously we would like to replace the simplicity constraints by simpler constraints expressed in term of the operators $E_{ij}^{L,R}$ or $F_{ij}^{L,R}$ and $(F_{ij}^{L,R})^\dagger$ which form a closed algebra. We tried all possible combinations of E and F constraints and the only way to get a closed algebra including all the simplicity constraints is to consider constraints of the form:

$$\begin{aligned} \mathcal{C}_i &= E_i^L - E_i^R = 0, \quad \forall i, \quad \text{for the diagonal simplicity constraints.} \\ \mathcal{F}_{ij}^\rho &\equiv F_{ij}^L - \rho (F_{ij}^R)^\dagger = 0 \quad \forall i, j \quad \text{for the cross simplicity constraints} \end{aligned} \quad (10.112)$$

Then,

$$[\mathcal{F}_{ij}^\rho, \mathcal{F}_{kl}^\rho] = 0 \quad \text{and} \quad [\mathcal{C}_i, \mathcal{F}_{kl}^\rho] = \delta_{il} \mathcal{F}_{ik}^\rho - \delta_{ik} \mathcal{F}_{il}^\rho. \quad (10.113)$$

We can again define a Hilbert space \mathcal{H}^ρ of states satisfying these constraints: $\mathcal{C}_i |\psi\rangle = 0 \quad \forall i, \mathcal{F}_{ij}^\rho |\psi\rangle = 0 \quad \forall i \neq j$. We already have one solution given by $|\alpha = \rho\rangle$ as defined in the previous subsection by (10.110). However,

$F_{ij}^{R\dagger} F_{kl}^{R\dagger}$). Therefore, we just recall the main steps:

$$[F_{ij}^L, f^\dagger] = 2 \underbrace{\sum_k F_{ik}^{R\dagger} E_{kj} - F_{jk}^{R\dagger} E_{ki}}_{= \mathcal{E}_{ij}^{L, F^{R\dagger}}} + 4 F_{ij}^{R\dagger}, \quad [\mathcal{E}_{ij}^{L, F^{R\dagger}}, f^\dagger] = 4 F_{ij}^{R\dagger} f^\dagger,$$

therefore we get:

$$F_{ij}^L |J\rangle = 2J(J+1) F_{ij}^{R\dagger} |J-1\rangle.$$

we still have the usual un-rescaled diagonal simplicity constraint which do not involve the Immirzi parameter. Then, as for the crossed simplicity constraints, the result is also disappointing and we have that $\forall |\psi\rangle, |\phi\rangle \in \mathcal{H}^\rho$:

$$\begin{aligned} \langle \psi | \vec{J}_i^L \cdot \vec{J}_j^L - \frac{1}{4} E_i^L E_j^R | \phi \rangle &= \langle \psi | -\frac{1}{2} F_{ij}^{L\dagger} F_{ij}^L | \phi \rangle \\ &= \rho^2 \langle \psi | -\frac{1}{2} F_{ij}^R F_{ij}^{R\dagger} | \phi \rangle \\ &= \rho^2 \langle \psi | \vec{J}_i^R \cdot \vec{J}_j^R - \frac{1}{4} (E_i^R + 2)(E_j^R + 2) | \phi \rangle. \end{aligned} \quad (10.114)$$

Thus, since $E_i^L = E_i^R$, we get at the leading order in j that the "right" observables $(\vec{J}_i^R \cdot \vec{J}_j^R - E_i E_j) \sim |J_i| |J_j| (\cos \theta_{ij}^R - 1)$ are rescaled by the proportionality coefficient ρ^2 with respect to the "left" observables $\vec{J}_i^L \cdot \vec{J}_j^L - E_i E_j \sim |J_i| |J_j| (\cos \theta_{ij}^L - 1)$ where θ_{ij} is the angle between the two vectors \vec{J}_i and \vec{J}_j . However, these observables which are corrected observables compared to the scalar product observables, do not have any real interesting geometrical interpretations and it does not seem possible to extract the expected relation: $\langle \vec{J}_i^L \cdot \vec{J}_j^L \rangle = \rho^2 \langle \vec{J}_i^R \cdot \vec{J}_j^R \rangle$.

Here again, it seems that the main obstacle is imposing strongly the diagonal simplicity constraints. In the following section, we will show how to relax the diagonal simplicity constraints and solve weakly all the simplicity constraints using coherent states for an arbitrary value of the Immirzi parameter.

10.4 Weakening the constraints and using the $U(N)$ coherent states

Until now we tried to solve the crossed simplicity constraints weakly whereas the diagonal simplicity constraints were imposed strongly. Indeed, in the previous section, we focused on the issue of the cross-diagonal simplicity constraints $\vec{J}_i^L \cdot \vec{J}_j^L - \vec{J}_i^R \cdot \vec{J}_j^R = 0$ which have to be imposed weakly since they do not form a closed algebra. We defined some new sets of constraints $\{C_{ij}, i < j\}$ or $\{\mathcal{F}_{ij}\}$ which allow to solve the cross simplicity constraints weakly and which are compatible with the diagonal simplicity constraints in such a way that the sets of all constraints form a closed algebra and therefore can all be imposed strongly in a consistent way. Here, we propose to relax all simplicity constraints because there are in fact physically on an equal footing and there is no physical reason to deal with the diagonal simplicity constraints in a different way from the cross simplicity ones. The idea is to use coherent states to solve weakly all simplicity constraints in the semi-classical regime. We first go back to the usual $SU(2)$ coherent states, then we will propose the $U(N)$ coherent states that solve weakly all simplicity conditions for arbitrary Immirzi parameter.

10.4.1 Back to $SU(2)$ coherent intertwiners

The $SU(2)$ coherent intertwiners $|j_i, \hat{n}_i\rangle_L \otimes |j_i, \hat{n}_i\rangle_R$ are currently used to solve the simplicity constraints. The usual analysis has been recalled in section 8.2. It is interesting to notice that these intertwiners are strong solutions to the diagonal simplicity constraints and that there does not seem to exist any other exact equation strongly solved by these states in order to weakly solve the cross diagonal simplicity constraints even in the semi-classical regime.

In fact, $|j_i, \hat{n}_i\rangle \otimes |j_i, \hat{n}_i\rangle = \int_{\text{Spin}4} dG G \triangleright \otimes_{i=1}^N |2j_i, \hat{n}_i\rangle$ span a Hilbert space of intertwiners which is the Hilbert space of intertwiners symmetric under the exchange of the left and right part. We denote it \mathcal{H}_{sym} . This symmetric Hilbert space \mathcal{H}_{sym} is generated by applying the operators $E_{ij}^L E_{ij}^R, F_{ij}^L F_{ij}^R, F_{ij}^{L\dagger} F_{ij}^{R\dagger}$ on the vacuum state $|0\rangle$. It is obvious that any state $\psi \in \mathcal{H}_{\text{sym}}$ satisfies all the non-diagonal simplicity constraints $\langle \vec{J}_i^L \cdot \vec{J}_j^L \rangle = \langle \vec{J}_i^R \cdot \vec{J}_j^R \rangle$ in expectation values. \mathcal{H}_{sym} is even the largest Hilbert space such that all the matrix elements of the constraints vanish:

$$\forall \psi, \phi \in \mathcal{H}_{\text{sym}}, \quad \langle \psi | \vec{J}_i^L \cdot \vec{J}_j^L - \vec{J}_i^R \cdot \vec{J}_j^R | \phi \rangle = 0. \quad (10.115)$$

However, this symmetry property of the states does not seem to be fundamental. Indeed, we have seen in Section 8.2.1 that there is a second sector solution to the cross simplicity constraints given by the states

$||j_i, -\hat{n}_i\rangle_L \otimes ||j_i, \hat{n}_i\rangle_R$. These states are not symmetric anymore in the exchange of the left and right part but they clearly satisfy the simplicity constraints in expectation value. Moreover, the previous analysis is not generalizable to the case of Euclidean gravity with a finite Immirzi parameter γ : the cross simplicity constraints become $\vec{J}_i^L \cdot \vec{J}_j^L = \rho^2 \vec{J}_i^R \cdot \vec{J}_j^R$ and thus, the symmetric intertwiners cannot be used to solve them weakly anymore. The resolution done in 8.2.1 is not generalizable when the Immirzi parameter is taken into account; usually the diagonal simplicity constraints are imposed strongly and the quadratic cross simplicity constraints are replaced by linear constraints $\vec{J}_i^L = \pm \rho \vec{J}_i^R$ which are then used to construct a so-called Master constraint in order to solve weakly the off-diagonal simplicity constraints [98].

We will now see that it is in fact possible to keep the standard quadratic simplicity constraints and to solve weakly all the simplicity constraints for any finite value of the Immirzi parameter.

10.4.2 The final proposal: using $U(N)$ coherent states

Following the coherent state approach to solving the simplicity constraints, we propose to use the $U(N)$ coherent states instead of the usual $SU(2)$ coherent intertwiners. As we have already reviewed earlier, a $U(N)$ coherent state $|J, \{z_k\}\rangle$ is labeled by the total area J and the N spinors z_k which define the semi-classical geometry underlying the intertwiner state. Now, considering $\text{Spin}(4)$ -intertwiners, we consider tensor products of $U(N)$ coherent states for both the left and right sectors, that is $|J_L, \{z_k^L\}\rangle \otimes |J_R, \{z_k^R\}\rangle$. We would like to relax all simplicity constraints. Since we also relax the diagonal simplicity constraints, we do not require the matching of the total areas of the left and right sectors and we work with a priori two different $U(N)$ representations, $J_L \neq J_R$. Then, the simplicity constraints impose that the classical geometry of the left and right intertwiners are the same up to an overall scale. This will translate into relations between the spinors of the left and right sectors, z_k^L and z_k^R .

Let us start by recalling the norm of the $U(N)$ coherent states and the expectation values (normalized by the norm) of the geometric observables on them:

$$\langle J, \{z_k\} | J, \{z_k\} \rangle = A(z)^{2J}, \quad A(z) = \frac{1}{2} \sum_k \langle z_k | z_k \rangle \quad (10.116)$$

$$\langle E_{ij} \rangle = J \frac{\langle z_i | z_j \rangle}{A(z)}, \quad \forall i, j$$

$$\langle \vec{J}_i \cdot \vec{J}_j \rangle = \frac{1}{4} \frac{J^2}{A(z)^2} \vec{V}(z_i) \cdot \vec{V}(z_j) + \frac{J}{8 A(z)^2} \left(\vec{V}(z_i) \cdot \vec{V}(z_j) - 3 |\vec{V}(z_i)| |\vec{V}(z_j)| \right), \quad \forall i \neq j,$$

where we have implicitly assumed that the spinors z_k satisfy the closure conditions. In case they do not close, the formulas above still hold up to replacing $A(z)$ by the determinant $\sqrt{\det X(z)}$ as explained in the previous sections.

From these expressions, two things are clear. First, the total area label J is simply a scale factor, it does not affect further the details of the classical geometry determined by the spinor labels. Thus, it appears that the ratio of the total area of the left and right sectors defines directly the Immirzi parameter $\rho = \frac{J_L}{J_R}$. Second, if we want to match up to an overall factor the expectation values of the scalar product $\langle \vec{J}_i \cdot \vec{J}_j \rangle$ of the left and right sectors, it is clear that we have to require that the 3-vectors $\vec{V}(z_k)$ are the same up to a sign for the left and right sectors. Thus we distinguish two classes of solutions, which correspond to the two regimes, standard (s) and dual (\star), of simplicity constraints:

1. We require $z_k^L = z_k^R$ and consider the tensor product $|J_L, \{z_k\}\rangle \otimes |J_R, \{z_k\}\rangle$. This means that $\vec{V}(z_k^L) = \vec{V}(z_k^R)$. This corresponds to the **standard simplicity regime (s)**. At leading order in the total area $J_{L,R}$, we have the equality of the expectation values of the scalar product observables:

$$\langle \vec{J}_i^L \cdot \vec{J}_j^L \rangle \sim \rho^2 \langle \vec{J}_i^R \cdot \vec{J}_j^R \rangle, \quad \rho = \frac{J_L}{J_R}. \quad (10.117)$$

Moreover, we also have the exact equality of the expectation values of the $\mathfrak{u}(N)$ generators:

$$\langle E_{ij}^L \rangle = \rho \langle E_{ij}^R \rangle. \quad (10.118)$$

There is still a $U(N)$ action on the set of coherent states $|J_L, \{z_k\}\rangle \otimes |J_R, \{z_k\}\rangle$. Indeed the diagonal action (u, u) acts simultaneously on the two sets of spinors, $(z_k, z_k) \rightarrow ((uz)_k, (uz)_k)$. Thus these are still coherent states *à la* Perelomov.

2. We require $z_k^L = \varsigma z_k^R$ and consider the tensor product $|J_L, \{z_k\}\rangle \otimes |J_R, \{\varsigma z_k\}\rangle$. This means that $\vec{V}(z_k^L) = -\vec{V}(z_k^R)$ and corresponds to the **dual simplicity regime** (\star) . At leading order in the total area $J_{L,R}$, we still have the equality of the expectation values of the scalar product observables:

$$\langle \vec{J}_i^L \cdot \vec{J}_j^L \rangle \sim \rho^2 \langle \vec{J}_i^R \cdot \vec{J}_j^R \rangle, \quad \rho = \frac{J_L}{J_R}. \quad (10.119)$$

However the equality of the expectation values of the $u(N)$ generators is slightly modified due to the fact that the ς map is anti-unitary. Indeed, taking into account that $\langle \varsigma z_i | \varsigma z_j \rangle = \langle z_j | z_i \rangle = \overline{\langle z_j | z_i \rangle}$, we now have:

$$\langle E_{ij}^L \rangle = \rho \langle E_{ij}^R \rangle = \overline{\rho \langle E_{ij}^R \rangle}. \quad (10.120)$$

The $U(N)$ action which is consistent with this set of coherent states $|J_L, \{z_k\}\rangle \otimes |J_R, \{\varsigma z_k\}\rangle$ is the diagonal action (u, \bar{u}) which is actually generated by our $u(N)$ simplicity condition \mathcal{C}_{ij} and which acts simultaneously on the two sets of spinors as $(u, \bar{u}) \triangleright (z_k, \varsigma z_k) = ((uz)_k, \varsigma(uz)_k)$. Thus these are also coherent states *à la* Perelomov.

Therefore, just like when using coherent intertwiners to solve weakly the simplicity constraints, we can clearly implement the two regimes of simplicity for the intertwiners. However, there are clear advantages of this new approach over the usual one. First, there are no big difference in the properties of the $U(N)$ coherent states corresponding to the two sectors. Second, the E_{ij} observables allow to easily distinguish the two sectors. Third, we have $U(N)$ actions in both cases which allow consistently deform these intertwiners, thus endowing them with a true structure of coherent states and not mere semi-classical states.

For the moment, we have managed to solve weakly both diagonal and cross simplicity constraints using the coherent states $|J_L, \{z_k^L\}\rangle \otimes |J_R, \{z_k^R\}\rangle$ with $z_k^L = z_k^R$ or $z_k^L = \varsigma z_k^R$. This provides solutions to the simplicity constraints for values of the Immirzi parameter corresponding to the ratio $\rho = J_L/J_R$. This parameter still takes discrete values. However, since we have decided to relax the diagonal simplicity constraints and thus *not* require an exact match between the individual spins $j_i^{L,R}$ of the left and right sectors, we can further relax our implicit assumption that the total area need to be fixed. Then we would only require a matching of the total areas of the left and right sectors in expectation value and the parameter $\rho = \langle J_L \rangle / \langle J_R \rangle$ will be allowed to take any (positive) real value.

To implement this, we come back to the F -constraints considered earlier in section 10.3.3 and in section 10.3.5 :

$$F_{ij}^L = \rho F_{ij}^R. \quad (10.121)$$

These constraints were not compatible with the diagonal simplicity constraints. However, since we have decided to relax these diagonal simplicity constraints, we can neglect them and impose the F -constraints strongly. We can easily solve these constraints since we know how to diagonalize the annihilation operators F_{ij} . Indeed, a generic solution will be given by the tensor product of β -states:

$$|\beta_L, \{z_k^L\}\rangle \otimes |\beta_R, \{z_k^R\}\rangle, \quad \text{with } \beta_L = \rho \beta_R \quad \text{and} \quad z_k^L = z_k^R. \quad (10.122)$$

We remind the definition of the β -states as superpositions of coherent states for different values of the total area:

$$|\beta, \{z_k\}\rangle = \sum_J \frac{\beta^{2J}}{\sqrt{J!(J+1)!}} |J, \{z_k\}\rangle, \quad (10.123)$$

which satisfy the eigenvalue equation:

$$F_{ij} |\beta, \{z_k\}\rangle = \beta^2 Z_{ij} |\beta, \{z_k\}\rangle, \quad \text{with } Z_{ij} = (z_i^0 z_j^1 - z_i^1 z_j^0).$$

Once again, we can easily compute the norm of these states, as well as the expectation values of the geometric observables :

$$\begin{aligned} \langle \beta, \{z_k\} | \beta, \{z_k\} \rangle &= \frac{I_1(2x)}{x}, \quad \text{with } x = |\beta|^2 A(z), \\ \langle E_{ij} \rangle &= \frac{x I_2(2x)}{I_1(2x)} \frac{\langle z_i | z_j \rangle}{A(z)}, \quad \forall i, j \\ \langle \vec{J}_i \cdot \vec{J}_j \rangle &= \frac{1}{4} \frac{\vec{V}(z_i) \cdot \vec{V}(z_j)}{A(z)^2} \frac{x \left(\frac{3}{2} I_2(2x) + x I_3(2x) \right)}{I_1(2x)} - \frac{3}{8} \frac{|\vec{V}(z_i)| |\vec{V}(z_j)|}{A(z)^2} \frac{x I_2(2x)}{I_1(2x)}, \quad \forall i \neq j, \end{aligned} \quad (10.124)$$

where the I_n 's are the modified Bessel functions of the first kind and the parameter $x = |\beta|^2 A(z)$ depends very simply on the label β . For large values of x , i.e for large area $A(z)$ or large value of β (this is more or less the same since the label β can be entirely absorbed as a overall rescaling of the spinors z_k in the definition of the β -states), these expressions simplify at leading order and we get :

$$\begin{aligned} \langle E_{ij} \rangle &\sim x \frac{\langle z_i | z_j \rangle}{A(z)}, \quad \forall i, j \\ \langle \vec{J}_i \cdot \vec{J}_j \rangle &\sim \frac{x^2}{4} \frac{\vec{V}(z_i) \cdot \vec{V}(z_j)}{A(z)^2}, \quad \forall i \neq j. \end{aligned} \quad (10.125)$$

Thus, considering tensor product states $|\rho\beta, \{z_k\}\rangle \otimes |\beta, \{z_k\}\rangle$ with $\beta_L = \rho\beta_R$ and $z_k^L = z_k^R$, we obtain exact solutions to the F -constraints $(F_{ij}^L - \rho F_{ij}^R) |\psi\rangle = 0$. And these solutions satisfy weakly the simplicity conditions at leading order in the semi-classical limit, $\langle \vec{J}_i^L \cdot \vec{J}_j^L \rangle \sim \rho^2 \langle \vec{J}_i^R \cdot \vec{J}_j^R \rangle$ and $\langle E_{ij}^L \rangle \sim \rho \langle E_{ij}^R \rangle$.

We proceed similarly with the other sectors and consider tensor product states $|\rho\beta, \{z_k\}\rangle \otimes |\beta, \{\varsigma z_k\}\rangle$, with $\beta_L = \rho\beta_R$ and $z_k^R = \varsigma z_k^L$. These solutions satisfy weakly the simplicity conditions at leading order in the semi-classical limit. Indeed, we have obviously $\langle \vec{J}_i^L \cdot \vec{J}_j^L \rangle \sim \rho^2 \langle \vec{J}_i^R \cdot \vec{J}_j^R \rangle$, but $\langle E_{ij}^L \rangle \sim \rho \overline{\langle E_{ij}^R \rangle}$. However, the main difference is that we have not been able to identify a set of constraints as the F -constraints which would characterize these tensor states. Indeed, looking at the action of the F_{ij} operators, we get:

$$\begin{aligned} F_{ij}^L |\rho\beta, \{z_k\}\rangle \otimes |\beta, \{\varsigma z_k\}\rangle &= \rho\beta Z_{ij} |\rho\beta, \{z_k\}\rangle \otimes |\beta, \{\varsigma z_k\}\rangle, \\ F_{ij}^R |\rho\beta, \{z_k\}\rangle \otimes |\beta, \{\varsigma z_k\}\rangle &= \beta \overline{Z_{ij}} |\rho\beta, \{z_k\}\rangle \otimes |\beta, \{\varsigma z_k\}\rangle, \end{aligned}$$

and we actually don't know any operator which would act anti-holomorphically on states $|\beta, \{z_k\}\rangle$ so as to produce the value $\overline{Z_{ij}}$. This is very similar to what happens when solving the simplicity constraints using the standard coherent intertwiners: the coherent intertwiner span a subspace in the standard regime (s) while they still span the whole Hilbert space of intertwiners in the dual regime (\star). However, our approach still has two very interesting advantages: the $U(N)$ action on our solution states and the straightforward inclusion of the Immirzi parameter in our framework as a simple scale factor.

We would like to finish this last section with a remark on the phase of the spinors. Indeed, the matching of the expectation values of the scalar product observables of the left and right sectors only requires a matching of the 3-vectors $\vec{V}(z_k^L) = \pm \vec{V}(z_k^R)$ with the sign depending on whether we are in the standard regime or the dual regime. In order to impose these equalities, we have required that $z_k^R = z_k^L$ or that $z_k^R = \varsigma z_k^L$. However, the 3-vector $\vec{V}(z)$ only determines the spinor z up to a global phase, $z \rightarrow e^{i\theta} z$. We can thus multiply any of the $2N$ spinors z_k^L and z_k^R by arbitrary phases without affecting the expectation values $\langle \vec{J}_i^L \cdot \vec{J}_j^L \rangle$ and $\langle \vec{J}_i^R \cdot \vec{J}_j^R \rangle$. Therefore, we can consider generally coherent states $|\rho J, \{e^{i\theta_k^L} z_k\}\rangle \otimes |J, \{e^{i\theta_k^R} z_k\}\rangle$ with arbitrary phases θ_k^L, θ_k^R . These tensor products will still solve weakly the quadratic simplicity constraints on the scalar product operators. The expectation values of the $u(N)$ generators $\langle E_{ij}^{L,R} \rangle$ are nevertheless sensitive to these phases and are equal only up a phase. Since the geometry of the 3-vectors $\vec{V}(z_k^{L,R})$, and thus the geometry of the intertwiner, do not depend on the phases of the spinors, it is natural to wonder about their physical/mathematical relevance.

The answer proposed in [9] is that these phases are relevant to the spin network construction when we glue intertwiners together. Indeed, following the interpretation of loop quantum gravity in term of discrete twisted

geometries [129], these phases (or more precisely the relative phase between two intertwiners glued along an edge) encode the extrinsic curvature at the discrete level. In our context, having these freedom in shifting these phase without affecting the intrinsic geometry of the intertwiner (defined in term of the 3-vectors) should allow to glue these $U(N)$ coherent intertwiners in a consistent way without interfering with the simplicity constraints.

Part III

Spinfoam models and the semi-classical limit

Spin foam models define transition amplitudes between quantum states of geometry through state-sum models which can be understood as discrete space-time geometries. They are supposed to describe the quantum space-time structure at the Planck scale. One of the main issues is then to extract some semi-classical information from the formalism and to show its relation to the more standard perturbative approach to the quantization of general relativity based on quantum field theory. In particular one would hope to understand why such perturbative approach fails. The quantum gravity semi-classical limit analysis amounts to proving that we can recover general relativity in a large scale (or low energy) regime of the spinfoam models and to showing how to compute the quantum corrections to the classical dynamics of the gravitational field. We will detail in Chapter 13, Chapter 14 and Chapter 15 three projects relevant to tackle this open problem but let us first introduce the framework.

In the spin foam context, a proposal for reconstructing the graviton propagator in this discrete setting from correlations between geometrical observables such as the areas of elementary surfaces [10, 11] has been developed. This proposal allows to extract semi-classical correlations at large scales, which we hope to compare with the perturbative calculations performed in quantum general relativity treated as a quantum field theory. The main ingredients of these “spin foam graviton propagator” calculations are

1. a suitable boundary state peaked on a classical 3-geometry,
2. the spin foam amplitudes for the bulk geometry,
3. the relevant observables probing the space-time geometry.

Since the original proposal, there have been a lot of works developing this line of research. They mainly focused on creating the new mathematical tools needed for these semi-classical calculations and on using these computations as a criteria to select spinfoam models with a correct semi-classical behavior and as a result to discriminate some of them (see e.g [138]). All these developments hint towards the fact that the graviton propagator in spin foam models lead back to Newton’s law for gravity at large scales while being regularized at the Planck scale. This behavior has been confirmed by numerical simulations in the simplest cases [139, 114].

However, up to now, the most explicit calculations have been done at the leading order (in the scale parameter) and for the simplest space-time triangulation (a single tetrahedron in 3d and a single 4-simplex in 4d). In order to make the link with the standard quantum field theory perturbative expansion, we need to do calculations with physical boundary states, i.e. states that solve the Hamiltonian constraint on the boundary. Moreover, we need to be able to push these calculations further and calculate the correlations both at higher order (“loop corrections”) and more refined triangulations (smoother boundary state). The three key elements to improve our understanding of the spinfoam graviton are therefore to

- (i) determine the exact correlations when considering *physical* boundary states;
- (ii) determine the higher order corrections to the correlations (the leading order of the correlations gives the classical propagator of the graviton) by studying the asymptotic behavior of the vertex amplitude;
- (iii) determine the behavior of the correlations by considering different (physical) boundary states.

We have focused on (i) in the context of 4d gravity. Up to now, most of the recent works have focused on building quantum coherent states with good semi-classical properties. One important issue is the requirement that the states are physical i.e. solve the Hamiltonian constraint on the 3d boundary. The requirement of working with a physical state should allow us to determine explicitly the width of the gaussian state defining the boundary state (see [14] for 3d gravity). This width is relevant in the context of the geometrical correlations because it enters the exact numerical factor in front of these correlations. Therefore, if we want to have the *exact* correlations and not only their scaling properties, we need a definite prediction of that width.

We have addressed the issue of (ii) in the context of 3d gravity. Considering a single tetrahedron, the solution of this issue requires understanding the corrections to the asymptotical behavior of the spin foam vertex amplitude associated to a single tetrahedron. We recall that this is the basic building block of of a 3d spin foam model, since a spin foam can then be constructed by gluing these spin foam vertices in order to describe the whole quantum space-time. In the Ponzano-Regge model (see Chapter 6.1), the spinfoam vertex

is given by the $\{6j\}$ -symbol from the recoupling theory of the representations of $SU(2)$. Therefore, a necessary step towards providing explicit formulae or procedures to compute all orders of the perturbative expansion (in term of the length scale) of the graviton correlations in the Ponzano-Regge model is to compute all orders of the asymptotic expansion of the $\{6j\}$ -symbol.

Let us now detail the plan of this last part. We will first give a quick review of the *spin foam graviton propagator* framework in the next chapter. In Chapter 12.1, we will define explicitly the 3d "spin foam graviton" for the simplest possible setting given by the 3d toy model introduced in [140, 141]. In Chapters 13 and 14, we will present two different methods to develop the asymptotic of the $\{6j\}$ -symbol: either from a brute-force calculation based on the explicit formula of the $\{6j\}$ -symbol in term of factorials [12], or from recursion relations for the $\{6j\}$ -symbol [13]. Finally, in Chapter 15, we will show that it is possible to define a physical boundary state for a spin foam model for 4d quantum gravity. These results were published in [15] in which the consequences of the physical state requirement for the Euclidean Barrett-Crane model for the simplest case of a space-time triangulation constructed from a single 4-simplex have been investigated.

Chapter 11

The graviton propagator

Let us describe the spin foam framework for deriving the graviton propagator from correlations between area observables. We recall that the kinematical Hilbert space of quantum geometry states for loop quantum gravity is spanned by spin network states $|\psi\rangle = |\gamma, j_l, i_n\rangle$ where γ is a graph, j_l is a “spin” labeling an irreducible representation of the gauge group G associated to the link l of the graph, and i_n is associated to the node n of γ and labels intertwiners.

The gauge group G will be specified when we consider a specific spin foam model. Note that we changed the notations: a spin network is now denoted by ψ whereas it was called s in the previous parts. In this part s will represent the specific spin network associated to the boundary graph of a 4-simplex.

We now consider a 4d space-time region \mathcal{M} with a 3d boundary Σ . The spin network state $|\psi\rangle$ defines the quantum state of geometry of the boundary Σ , the spin foam amplitude $K[\psi]$ (6.4) defines the dynamical probability amplitude of that state and is supposed to contain the whole dynamical content of quantum gravity.

We consider in this part the case where the boundary Σ is connected and the kernel K is then defined as a function of only one boundary spin network $\psi = (\gamma, j_l, i_n)$.

$$K[\psi] = \sum_{\mathcal{F}|\partial\mathcal{F}=\psi} \mathcal{A}_{\mathcal{F}}[\psi], \quad (11.1)$$

where we used the same compact notation as in (6.5). We recall that the sum is over spin foams $\mathcal{F} = (C, c)$ such that their two-complexes are compatible with the graph γ and their colorings c are compatible with the representations and intertwiners (j_l, i_n) . We start by considering a semi-classical spin network functional $\Psi_q[\psi]$ peaked on a classical 3d metric q for the boundary Σ . We further require that this boundary state $\Psi_q[\psi]$ induces a space-time structure in the bulk peaked around the flat Minkowski metric. In particular, this normally fixes the classical boundary q to be the 3-metric induced on Σ by the Minkowski metric on \mathcal{M} . Then we construct correlations W between the metric fluctuations for the chosen boundary state Ψ_q .

$$W^{abcd}(x, y; q) = \sum_{\psi} K[\psi] \langle \psi | h^{ab}(x) h^{cd}(y) | \psi \rangle \Psi_q[\psi] = \text{Tr} [K h^{ab}(x) h^{cd}(y) \Psi_q], \quad (11.2)$$

where the trace is taken over the Hilbert of spin networks. Here x and y are two points localized on the boundary Σ . In our discrete spin network setting, they are usually determined as nodes of the graph γ underlying the spin network state Ψ_q . The metric fluctuations $h^{ab}(x) h^{cd}(y)$ are usually constructed as geometrical quantities. There are two basic types of such geometric observables in the discretized geometry setting of spinfoams: the diagonal component of the metric tensor can be interpreted as areas and the off-diagonal components as dihedral angles between simplices. More details on the 3d case are given in the next chapter 12.1.

Finally, this formula defines the 2-point function for the gravitational field in the spinfoam framework. It can be considered as the equivalent of the standard 2-point function of the conventional quantum field theory framework, which defines the graviton propagator¹ [10].

$$W_{\mu\nu\rho\sigma}(x, y) = \langle 0 | T \{ h_{\mu\nu}(x) h_{\rho\sigma}(y) \} | 0 \rangle. \quad (11.3)$$

¹In the following formula, T stands for the standard time-ordering prescription.

Physical observables of the theory. The goal of the proposal for computing a "spin foam graviton propagator" is to probe the geometry induced by the spin foam amplitudes through calculating correlations between geometric observables. Thus, we first need to identify appropriate observables. As we already mentioned it, geometrical observables such as areas or dihedral angles appear in the metric fluctuations $h^{ab}(x)h^{cd}(y)$ which enter into the 2-points function definition (11.2). That is to consider correlations between different components of the metric amounts to defining the correlations between areas and volumes (which can be defined from area and dihedral angles variables [142]) at different points on the boundary Σ defined by the labels (j_l, i_n) . Indeed, the data (j_l, i_n) living on the boundary graph γ encodes the geometrical information of the boundary Σ : the representation j_l gives the area of the triangle $\Delta \in \Delta_\partial$ dual to the link $l \in \Delta_\partial^*$ and the intertwiner i_n describes the shape and the volume of the tetrahedron of the triangulation Δ_∂ dual to the node $n \in \Delta_\partial^*$. These boundary representations and intertwiners are thus the typical geometrical observables that we consider for the "spin foam graviton propagator".

The boundary state. In the spin foam setting, $\Psi_q[\psi]$ is a semi-classical state peaked on both intrinsic and extrinsic geometry [10]. It is the extrinsic data that determines the 4-metric induced in the bulk. Considering boundary states, while most of the recent work has focused on building quantum coherent states with good semi-classical properties, one important issue is the requirement that the states are physical i.e solve the Hamiltonian constraint on the 3d boundary. This "physical state" criteria can be entirely formulated in term of a compatibility equation between the boundary state and the spinfoam bulk amplitude by the two following conditions:

$$\begin{cases} \sum_\psi |\Psi_q[\psi]|^2 = 1 \\ \sum_\psi K[\psi] \Psi_q[\psi] = 1 \end{cases} \quad (11.4)$$

The first condition is the normalization of the boundary state, while the second condition translates truthfully the requirement to work with a physical state and can be considered as the "Wheeler-deWitt" condition.

The consequences of this last condition were investigated in the framework of the Ponzano-Regge spinfoam model for 3d quantum gravity, more particularly in a toy model where the 3d space-time is triangulated by a single tetrahedron [140, 141]. This 3d toy model is introduced in Chapter 12.1.

We studied the consequences of both conditions (11.4) on Ψ_q in the context of the Barrett-Crane model [15]. These results are presented in Chapter 15.

The kernel. The main spinfoam models used to define the bulk amplitudes are the Barrett-Crane model (see Chapter 7), which exists in both its Euclidean version [103, 143] and its Lorentzian counterpart [104, 115], and the more recent EPRL-FK models (see Chapter 8 and [95, 98, 96, 97, 106]) and their generalizations [118, 144] for 4d gravity. Details concerning the Barrett-Crane kernel are given in the Chapter 15.

Chapter 12

The asymptotic expansion in 3d

Most of the explicit calculations in the "spin foam graviton" framework have been done at the leading order (in the scale parameter) and for the simplest space-time triangulation (i.e. a single tetrahedron in 3d and a single 4-simplex in 4d). The graviton propagator in spin foam models seems to lead back to Newton's law for gravity at large scales while being regularized at the Planck scale. This behavior has been confirmed by numerical simulations in the simplest cases [139, 114]. In order to make the link with the standard quantum field theory perturbative expansion, we now need to be able to push these calculations further and calculate the correlations both at higher order ("loop corrections") and for more refined triangulations (smoother boundary state). In both works [12, 13] presented respectively in Chapter 13 and Chapter 14, we focus on the first aspect: the leading order of the correlations gives the classical propagator of the graviton and we would like to compute the higher order (quantum) corrections. Following the lines of [141, 145, 146], this requires understanding the corrections to the asymptotical behavior of the spinfoam vertex amplitude, which is the amplitude associated to a single tetrahedron in 3d quantum gravity or to a single 4-simplex in 4d models.

In this chapter, we focus on 3d quantum gravity although 3d general relativity has no local degrees of freedom. Indeed, the 2-point function of the linearised quantum theory (11.3) is a well defined quantity that can be evaluated once a gauge-fixing is chosen. However, this quantity is a pure gauge and the quantum theory does not properly have a propagating graviton [147]. It provides nevertheless a nice laboratory to test the ideas which have been proposed in the 4d case since the 3d quantum gravity model is much simpler than the 4d one.

The canonical framework to compute 3d correlation in quantum gravity is reviewed in the next section ; we will see that the structure of this "spin foam graviton" framework is particularly clear in 3d. Then the study of the $\{6j\}$ -symbol is presented in Section 12.2, as well as Chapters 13 and 14.

12.1 The canonical framework for 3d correlation in gravity/ The boundary states and the kernel for 3d correlation in gravity

We present in this Section the simplest setting – given by a 3d toy model introduced in [140, 141] – to illustrate the "spin foam graviton propagator" framework and to point out the importance to study the asymptotic behavior of the $\{6j\}$ -symbol. In spite of the simplicity of the model, we will see that the framework developed here, has rather generic features for computing graviton propagator/correlations in non-perturbative quantum gravity from spin foam amplitudes.

We consider a triangulation consisting of a single tetrahedron embedded in flat 3d Euclidean space-time: we are interested in the correlations of length fluctuations of the bottom edge and of the top edge of the tetrahedron (see Fig. 12.1). In order to define transition amplitudes in a background independent context for a certain region of space-time, we perform a perturbative expansion with respect to the geometry of the boundary. It is the classical geometry which will act as a background for the perturbative expansion. This classical geometry in the case of a single tetrahedron is defined by its edge lengths and its dihedral angles since these quantities specify respectively the intrinsic and extrinsic curvatures of the boundary.

More precisely, given a background that we will precise in the following, to compute the correlations between

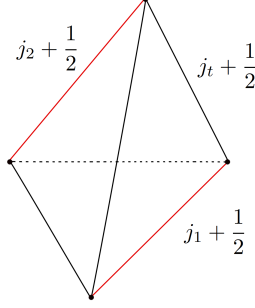


Figure 12.1: The dynamical tetrahedron as evolution between two hyperplanes containing e_1 and e_2 . The labels give the physical lengths: $l_1 = j_1 + 1/2$, $l_2 = j_2 + 1/2$ and we assume to have measured the time $T = (j_t + 1/2)/\sqrt{2}$. ($j_1, j_2, j_t \in \mathbb{N}/2$)

fluctuations around the background of the length of the bottom edge $l_1 \equiv j_1 + 1/2$ and the top edge $l_2 \equiv j_2 + 1/2$ of the tetrahedron represented in Fig. 12.1, we consider the situation where the edge lengths of the four other edges are fixed to the unique value $j_t + 1/2$. In this setting, which is referred to as the time-gauge setting, the four imposed bulk edge length can be interpreted as representing the time measured between two planes containing l_1 and l_2 given by $T = (j_t + 1/2)/\sqrt{2}$. The background around which we study the fluctuations is introduced by the state $|\psi\rangle$ which will peak j_1 and j_2 around a given value j_0 . Then to study the perturbative expansion of the 2-point function, we choose a Coulomb-like gauge and for simplicity we also take $j_t = j_0$ and our starting point becomes

$$W^{1122} = \frac{1}{\mathcal{N}} \sum_{j_1, j_2} \mathcal{O}_{j_1}(j_0) \Psi_{e_1}(j_1) \mathcal{O}_{j_2}(j_0) \Psi_{e_2}(j_2) \left\{ \begin{matrix} j_1 & j_0 & j_0 \\ j_2 & j_0 & j_0 \end{matrix} \right\} \quad (12.1)$$

with $\mathcal{O}_j(j_0) \equiv \frac{1}{d_{j_0}^2} (d_j^2 - d_{j_0}^2)$ and $\Psi_e(j) \equiv \exp\left(-\frac{\alpha}{2}(\delta_{d_j})^2 + i\theta \frac{d_j}{2}\right)$

where \mathcal{N} is the normalization factor given by the same sum without the observable insertions $\mathcal{O}_{j_e}(j_0)$. Moreover, $d_j \equiv 2j + 1 = l/2$ and $\delta_{d_j} = d_j - d_{j_0}$ and we recall that the $\{6j\}$ symbol is the Ponzano-Regge kernel (see Chapter 6.1). To define the boundary state Ψ , we used the Gaussian ansatz. Ψ peaks the geometry around the equilateral tetrahedra which all edges are equal to $l_0 = j_0 + 1/2 = d_{j_0}/2$ and all dihedral angles (defined as the angles between the external normal to the triangles) have the same value $\theta = \arccos(-1/3)$. W_{1122} then measures the correlations between length fluctuations for the edges e_1 and e_2 for the tetrahedron, and it can be interpreted as the 2-point function for gravity, contracted along the directions of e_1 and e_2 [140].

Thus, the perturbative expansion of this propagator needs the knowledge of the expansion of the $\{6j\}$ -symbol. The well-known asymptotics of the $\{6j\}$ symbol is given by [21, 148, 117, 111]

$$\left\{ \begin{matrix} j_1 & j_0 & j_0 \\ j_2 & j_0 & j_0 \end{matrix} \right\} \sim \frac{\cos(S_R[j_e] + \pi/4)}{\sqrt{12\pi V(j_1, j_2, j_0)}}, \quad (12.2)$$

where $V(j_1, j_2, j_0) = \frac{1}{12} \sqrt{4l_0^2 l_1^2 l_2^2 - l_1^2 l_2^4 - l_1^4 l_2^2}$ is the volume of the tetrahedron and $S_R[j_e]$ is the Regge action

$$S_R[j_e] = \sum_e (j_e + \frac{1}{2}) \theta_e(j_e), \quad (12.3)$$

where θ_e are dihedral angles. The Regge action is a discretized version of general relativity, which captures the non-linearity of the theory [112]. In the perturbative expansion of the propagator (12.1), there are therefore two sources of correction: contributions coming from higher orders in the expansion of the Regge action and

contributions coming from higher orders in the expansion of the $\{6j\}$ symbol. We focus now on the second aspect and we propose in the next section different methods to study the asymptotic expansion of the $\{6j\}$ symbol.

12.2 How to study the $\{6j\}$ -symbol?

There are three basic ways to compute the leading order asymptotics of the $\{6j\}$ -symbol and to show its relation to the Regge action for 3d gravity.

- *Recursion relations* [149, 150]. Using the invariance of the $\{6j\}$ -symbol under Pachner moves (Biedenharn-Elliott identity) or directly its definition as a recoupling coefficient, one can derive a recursion relation for the $\{6j\}$ -symbol. This recursion formula is actually very useful for numerical computations, but it can also be approximated at large spins by a (second order) differential equation. One then derives the asymptotics from a WKB approximation.
- *Integral formula* [151, 117]. One can write the square of the $\{6j\}$ -symbol as an integral over four copies of $SU(2)$. In the large spin regime, we can use saddle point techniques and one derives the right asymptotics after a careful analysis of non-degenerate and degenerate configurations for the saddle points. This is the technique used to derive the asymptotics of the Barrett-Crane and EPR-FK vertex amplitudes.
- *Brute-force approximation* [152]. One can start from the explicit algebraic formula of the $\{6j\}$ -symbol as a sum over some products of factorials. Using the Stirling formula and after lengthy calculations, we approximate the sum by an integral and use saddle point techniques again which lead to the same asymptotics.

We would like to mention also the more sophisticated and rigorous proof of the asymptotics by Roberts [148] based on geometric quantization, but he also uses an integral formula and the saddle point method.

Chapter 13

Group integral techniques and the asymptotic expansion of the $\{6j\}$

The method is based on the explicit algebraic formula of the $\{6j\}$ -symbol as a sum over some products of factorials. Using the Stirling formula, we approximate the sum by an integral and use saddle point techniques. These results were published in [12]

13.1 The $\{6j\}$ -symbol and the Racah's single sum formula

The $\{6j\}$ -symbol is the basic building block of the Ponzano-Regge model which is a state sum model for 3d Euclidean gravity formulated as a $SU(2)$ gauge theory. The Ponzano-Regge model is defined over a triangulation of space-time: we build the 3d space-time manifold from tetrahedra glued together along their respective triangles and edges. We assign an irreducible representation (irreps) of $SU(2)$ to each edge e of the triangulation. These irreps are labeled by a half-integer $j_e \in \mathbb{N}/2$, the spin, and the dimension of the corresponding representation space is given by $d_{j_e} = 2j_e + 1$. Each tetrahedron of the triangulation has six edges labeled by six spins j_{e_1}, \dots, j_{e_6} and we associate it with the corresponding $\{6j\}$ -symbol, which is the unique (non-trivial) $SU(2)$ invariant built from these six representations. It is giving by combining four normalized Clebsch-Gordan coefficients corresponding to the four triangles of the tetrahedron. Finally, the Ponzano-Regge amplitude for a given colored triangulation is simply given by the product of the $\{6j\}$ -symbols associated to all its tetrahedra.

Looking more closely at a single tetrahedron, we label its four triangles by $I = 0, \dots, 3$. Then each of its six edges is labeled by the couple of triangles to which it belongs, (IJ) with $0 \leq I < J \leq 3$. To each edge is attached a $SU(2)$ irrep of spin j_{IJ} , which defines the length of that edge $j_{IJ} + \frac{1}{2} = \frac{d_{j_{IJ}}}{2}$ (see Fig. 13.1). There

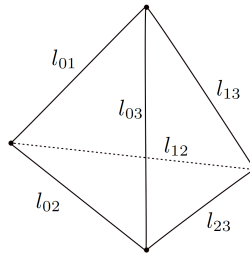


Figure 13.1: A single tetrahedron: the edge lengths are given by $l_{IJ} = \frac{d_{j_{IJ}}}{2}$.

are several ways of expressing the $\{6j\}$ -symbol. The basic formula is the Racah's single sum formula which expresses the $\{6j\}$ -symbol as a sum over some products of factorials (see Appendix E). This is our starting

point as in [152] :

$$\left\{ \begin{array}{ccc} j_{01} & j_{02} & j_{03} \\ j_{23} & j_{13} & j_{12} \end{array} \right\} = \sqrt{\Delta(j_{01}, j_{02}, j_{03})\Delta(j_{23}, j_{02}, j_{12})\Delta(j_{23}, j_{13}, j_{03})\Delta(j_{01}, j_{13}, j_{12})} \sum_{\max v_I}^{\min p_J} \frac{(-1)^t (t+1)!}{\prod_I (t - v_I)! \prod_J (p_J - t)!} \quad (13.1)$$

where the v_I and p_i are given by the following sums:

$$\forall K = 0..3, \quad v_K = \sum_{I \neq K} j_{IK}, \quad \forall k = 1..3, \quad p_k = \sum_{i \neq 0, k} (j_{0i} + j_{ki}).$$

The factors $\Delta(j_{01}, j_{02}, j_{03})$ are weights associated to each triangle and are defined by:

$$\Delta(j_{01}, j_{02}, j_{03}) = \frac{(j_{01} + j_{02} - j_{03})!(j_{01} - j_{02} + j_{03})!(-j_{01} + j_{02} + j_{03})!}{(j_{01} + j_{02} + j_{03} + 1)!}.$$

From this point, in all sums and products throughout this paper, capital indices K will run from 0 to 3 and lower-cases indices k will run from 1 to 3.

We are interested in the large spin expansion of the $\{6j\}$ -symbol when scaling all the spins homogeneously. Actually we will scale the lengths $d_{j_{IJ}}/2$ instead of the spins j_{IJ} because the structure of the expansion will be simpler (we expect an alternation of cosines and sines without any mixing up at all orders as in [145]) and the geometrical interpretation (when possible) is expected to be simpler. Then we rescale all $d_{j_{IJ}}$ by $\lambda d_{j_{IJ}}$ in (13.1), which is equivalent to changing $j_{IJ} = \frac{d_{j_{IJ}}}{2} - \frac{1}{2}$ to $\lambda \frac{d_{j_{IJ}}}{2} - \frac{1}{2}$. This gives:

$$\left\{ \begin{array}{ccc} \lambda d_{j_{01}}/2 - 1/2 & \lambda d_{j_{02}}/2 - 1/2 & \lambda d_{j_{03}}/2 - 1/2 \\ \lambda d_{j_{23}}/2 - 1/2 & \lambda d_{j_{13}}/2 - 1/2 & \lambda d_{j_{12}}/2 - 1/2 \end{array} \right\} = \sqrt{\Delta(\lambda d_{j_{01}}, \lambda d_{j_{02}}, \lambda d_{j_{03}})\Delta(\lambda d_{j_{23}}, \lambda d_{j_{02}}, \lambda d_{j_{12}})\Delta(\lambda d_{j_{23}}, \lambda d_{j_{13}}, \lambda d_{j_{03}})\Delta(\lambda d_{j_{01}}, \lambda d_{j_{13}}, \lambda d_{j_{12}})} \quad (13.2)$$

$$\sum_{\lambda \min \tilde{v}_J - 2}^{\lambda \min \tilde{p}_J - 2} (-1)^t \frac{(t+1)!}{\prod_i (t - \lambda \tilde{v}_I + \frac{3}{2})! \prod_j (\lambda \tilde{p}_j - t - 2)!}$$

with the new conventions:

$$\tilde{v}_K = \sum_{I \neq K} \frac{d_{j_{IK}}}{2}, \quad \tilde{p}_k = \sum_{i \neq 0, k} \frac{(d_{j_{0i}} + d_{j_{ki}})}{2},$$

$$\Delta(\lambda d_{j_{01}}, \lambda d_{j_{02}}, \lambda d_{j_{03}}) = \frac{(\frac{\lambda}{2}(d_{j_{01}} + d_{j_{02}} - d_{j_{03}}) - \frac{1}{2})! (\frac{\lambda}{2}(d_{j_{01}} - d_{j_{02}} + d_{j_{03}}) - \frac{1}{2})! (\frac{\lambda}{2}(-d_{j_{01}} + d_{j_{02}} + d_{j_{03}}) - \frac{1}{2})!}{(\frac{\lambda}{2}(d_{j_{01}} + d_{j_{02}} + d_{j_{03}}) - \frac{1}{2})!}.$$

The quantity \tilde{v}_K gives the perimeter of the triangle K while the \tilde{p}_k 's are the perimeters of (non-planar) quadrilaterals.

13.2 Perturbative expansion of the $6j$ -symbol

In this section, we will give a procedure to obtain the full perturbative expansion of the $\{6j\}$ -symbol in term of the length scale λ and we compute explicitly the leading order (Ponzano-Regge formulae) then the next-to-leading order analytically.

13.2.1 General procedure

We give all the necessary formulae to obtain the Ponzano-Regge corrections at any order. But calculations are only performed explicitly at the next-to-leading order for a generic $\{6j\}$ -symbol. We start from equation (13.2).

First approximation: factorials. The factorial can be expanded in a series:

$$n! = \sqrt{2\pi n} \left(\frac{n}{e}\right)^n \left(1 + \frac{1}{12n} + \frac{1}{288n^2} - \frac{139}{51840n^3} - \frac{571}{2488320n^4} + \dots\right) \quad (13.3)$$

In equation (13.2), there are factorials of the form: $n!$, $(n+1/2)!$ and $(n-1/2)!$, which are rigourously defined through Euler's Γ function. From (13.3) we deduce asymptotic expansions for $(n+1/2)!$ and $(n-1/2)!$ (see the details in appendix F). In order to get the next-to-leading order (NLO) in the $1/\lambda$ expansion of the $\{6j\}$ -symbol, we replace the factorials in equation (13.2) by their respective asymptotic expansion:

$$\begin{aligned} n! &\sim \sqrt{2\pi} e^{(n+\frac{1}{2})\ln(n)-n} \left(1 + \frac{1}{12n}\right) \\ (n + \tfrac{1}{2})! &\sim \sqrt{2\pi} e^{(n+1)\ln(n)-n} \left(1 + \frac{11}{24n}\right) \\ (n - \tfrac{1}{2})! &\sim \sqrt{2\pi} e^{n\ln(n)-n} \left(1 - \frac{1}{24n}\right). \end{aligned} \quad (13.4)$$

Then, equation (13.2) reads at first order as:

$$\left\{ \begin{array}{ccc} \lambda d_{j_{01}}/2 - 1/2 & \lambda d_{j_{02}}/2 - 1/2 & \lambda d_{j_{03}}/2 - 1/2 \\ \lambda d_{j_{23}}/2 - 1/2 & \lambda d_{j_{13}}/2 - 1/2 & \lambda d_{j_{12}}/2 - 1/2 \end{array} \right\} = \frac{1}{2\pi} e^{\frac{\lambda}{2} h(d_{j_{IJ}})} \left(1 - \frac{1}{24\lambda} H(d_{j_{IJ}}) + O\left(\frac{1}{\lambda^2}\right)\right) \Sigma. \quad (13.5)$$

The first factor is given by:

$$\begin{aligned} h(d_{j_{IJ}}) &= \sum_{I < J} d_{j_{IJ}} h_{d_{j_{IJ}}} \\ \text{with } h_{d_{j_{IJ}}} &= \frac{1}{2} \ln \left(\frac{(d_{j_{IJ}} - d_{j_{IK}} + d_{j_{IL}})(d_{j_{IJ}} + d_{j_{IK}} - d_{j_{IL}})(d_{j_{IJ}} - d_{j_{JK}} + d_{j_{JL}})(d_{j_{IJ}} + d_{j_{JK}} - d_{j_{JL}})}{(d_{j_{IJ}} + d_{j_{IK}} + d_{j_{IL}})(-d_{j_{IJ}} + d_{j_{IK}} + d_{j_{IL}})(d_{j_{IJ}} + d_{j_{JK}} + d_{j_{JL}})(-d_{j_{IJ}} + d_{j_{JK}} + d_{j_{JL}})} \right), \end{aligned} \quad (13.6)$$

where (KL) is the opposite side to (IJ) , that is $K \neq L$ and $K, L \neq I, J$. The second factor is due to the NLO of the factorials:

$$H(d_{j_{IJ}}) = 2 \sum_{j,K} \frac{1}{\tilde{p}_j - \tilde{v}_K} - 2 \sum_K \frac{1}{\tilde{v}_K} = \sum_I \left[\frac{-r^I + \sum_{K \neq I} r_K^I}{2A_I} \right], \quad (13.7)$$

where A_I is the area of triangle I , r^I is the radius of the incircle of triangle I and r_K^I is the radius of the excircle to the triangle I tangent to the side $d_{j_{IK}}$ of the triangle I . Finally, Σ is a Riemann sum:

$$\Sigma = \frac{1}{\lambda^2} \sum_{x=\max \tilde{v}_I/2}^{\min \tilde{p}_j/2} e^{F(x)} \left(1 - \frac{1}{12\lambda} G(x) + O\left(\frac{1}{\lambda^2}\right)\right) e^{\lambda f(x)} \quad (13.8)$$

with the pre-factor and the action given by:

$$\begin{aligned} f(x) &= i\pi x + x \ln(x) - \sum_K (x - \tilde{v}_K) \ln(x - \tilde{v}_K) - \sum_j (\tilde{p}_j - x) \ln(\tilde{p}_j - x), \\ F(x) &= \frac{1}{2} \ln \left(\frac{x^3 \prod_j (\tilde{p}_j - x)^3}{\prod_K (x - \tilde{v}_K)^4} \right), \\ G(x) &= -\frac{13}{x} + \frac{47}{2} \sum_K \frac{1}{x - \tilde{v}_K} + 13 \sum_j \frac{1}{\tilde{p}_j - x}. \end{aligned} \quad (13.9)$$

The details of the computation are given in Appendix G.

Second approximation: Riemann sum. The second approximation consists in replacing the Riemann sum Σ of (13.5) by an integral. One k^{-1} factor of Σ plays the role of dx . We can then rewrite equation (13.5) as:

$$\{6j\} \sim \frac{1}{2\pi} \left(1 - \frac{1}{24\lambda} H(d_{jIJ}) + O\left(\frac{1}{\lambda}\right)\right) e^{\frac{\lambda}{2} h(d_{jIJ})} \frac{1}{\lambda} \int_{\max \frac{\tilde{v}_I}{2}}^{\min \frac{\tilde{v}_J}{2}} dx e^{F(x)} \left(1 - \frac{1}{12\lambda} G(x) + O\left(\frac{1}{\lambda^2}\right)\right) e^{\lambda f(x)}. \quad (13.10)$$

This approximation does not generate any corrections at leading order and at first order. It will nevertheless enter at second order in terms in $1/\lambda^2$.

Third approximation: saddle point approximation. We have to study an integral of the form $I = \int_a^b dx g(x) e^{\lambda f(x)}$ where λ is a large parameter. The asymptotic expansion of such an integral is given by contributions around the stationary points of the action f which are points, denoted x_0 , of the complex plane such that $f'(x_0) = 0$. We expand the action $f(x)$ and the function $g(x)$ around the stationary points x_0 in term of $\delta x = x - x_0$:

$$f(x) = \sum_{j=0}^{\infty} \frac{f(x_0)^{(j)}}{j!} (\delta x)^j = f(x_0) + \frac{f''(x_0)}{2} (\delta x)^2 + f_{x_0}^{>2}(\delta x) \quad \text{and} \quad g(x) = \sum_{j=0}^{\infty} \frac{g(x_0)^{(j)}}{j!} (\delta x)^j = g(\delta x).$$

We then expand $K(\delta x) = g(\delta x) e^{kf_{x_0}^{>2}(\delta x)}$ in power of δx . Following the standard stationary phase approximation, we extend the integration domain to the whole \mathbb{R} . The integrals are then “generalized Gaussians” which can easily be computed. We group the resulting terms according to their dependence on $1/\lambda$, being careful because of the function $g(x)$ which depends on $1/\lambda$. We recall that $g(x)$ was obtained by replacing the factorials in (13.2) by their series expansion and we write $g(x)$ under the general form:

$$g(x) = \sum_{i=1}^{\infty} \frac{g_i(x)}{i! \lambda^i}.$$

Then the complete perturbative expansion of I can be written as:

$$I = \sum_{x_0} e^{\lambda f(x_0)} \sqrt{\frac{2\pi}{-f''(x_0)\lambda}} \left(1 + \sum_{n=1}^{\infty} \frac{1}{\lambda^n} \left[\sum_{p=0}^{n-1} \tilde{N}_p \frac{(2p-1)!!}{(-f''(x_0))^p} + \sum_{p=0}^{2n} N_p \frac{(2n+2p-1)!!}{(-f''(x_0))^{n+p}} \right] \right) \quad (13.11)$$

where

$$\begin{aligned} \tilde{N}_p &= \sum_{i=1}^{E[\frac{2p}{3}]} \frac{1}{i!(n-p+i)!} \sum_{l_1 \dots l_i=3}^{E[\frac{2p}{i}]} \frac{g_{n-p+i}^{(2p-\sum_{j=1}^i l_j)}(x_0)}{(2p-\sum_{j=1}^i l_j)!} \prod_{j=1}^i \frac{f^{l_j}(x_0)}{(l_j)!} \\ N_0 &= \frac{g_0^{(2n)}(x_0)}{(2n)!} + \sum_{i=1}^{E[\frac{2n}{3}]} \frac{1}{(i!)^2} \sum_{l_1 \dots l_i=3}^{E[\frac{2n}{i}]} \frac{g_i^{(2n-\sum_{j=1}^i l_j)}(x_0)}{(2p-\sum_{j=1}^i l_j)!} \prod_{j=1}^i \frac{f^{l_j}(x_0)}{(l_j)!} \\ N_p &= \sum_{i=p}^{E[\frac{2(p+n)}{3}]} \frac{1}{i!(i-p)!} \sum_{l_1 \dots l_i=3}^{E[\frac{2(n+p)}{i}]} \frac{g_{i-p}^{(2(n+p)-\sum_{j=1}^i l_j)}(x_0)}{(2(n+p)-\sum_{j=1}^i l_j)!} \prod_{j=1}^i \frac{f^{l_j}(x_0)}{(l_j)!} \quad \text{for } p \geq 1 \end{aligned} \quad (13.12)$$

The details of the computation are given in Appendix H. From this expansion and adjusting the first approximation to get the proper dependence on λ for g and the pre-factors, it is possible to compute analytically the whole asymptotic expansion of the $\{6j\}$ -symbol.

Here to get explicitly the next-to-leading order of the $\{6j\}$ -symbol asymptotic expansion, we only need the next-to-leading order of the $1/\lambda$ expansion of I , so we cut the previous formulae at $n = 1$, then

$$I \sim \sum_{x_0} e^{\lambda f(x_0)} \sqrt{\frac{2\pi}{-f''(x_0)\lambda}} \left(1 + \frac{1}{\lambda} \left(\tilde{N}_0 + \frac{N_0}{-f''(x_0)} + \frac{3N_1}{(-f''(x_0))^2} + \frac{15N_2}{(-f''(x_0))^3} \right) \right)$$

with the expansion coefficients given by

$$\tilde{N}_0 = g_1(x_0), \quad N_0 = \frac{g_0''(x_0)}{2}, \quad N_1 = \frac{f^{(3)}(x_0)g_0'(x_0)}{3!} + \frac{f^{(4)}(x_0)g_0(x_0)}{4!}, \quad N_2 = \frac{g_0(x_0)}{2} \left(\frac{f^{(3)}(x_0)}{3!} \right)^2.$$

We recall that $g(x) = e^{F(x)} \left(1 - \frac{G(x)}{12\lambda} \right)$; that is: $g_0(x) = e^{F(x)}$ and $g_1(x) = -\frac{G(x)}{12} e^{F(x)}$. Finally, we obtain the approximation:

$$I \sim \sum_{x_0} \sqrt{\frac{2\pi}{-f''(x_0)\lambda}} e^{F(x_0) + \lambda f(x_0)} \left[1 + \frac{1}{\lambda} \left(-\frac{G(x_0)}{12} - \frac{F''(x_0) + (F'(x_0))^2}{2f''(x_0)} + \frac{f^{(4)}(x_0) + 4f^{(3)}(x_0)F'(x_0)}{8(f''(x_0))^2} - \frac{5(f^{(3)}(x_0))^2}{24(f''(x_0))^3} \right) + O\left(\frac{1}{\lambda^2}\right) \right] \quad (13.13)$$

This gives us the following expression for the asymptotic expansion of the $\{6j\}$ -symbol at second order:

$$\begin{aligned} & \begin{Bmatrix} \lambda d_{j_{01}}/2 - 1/2 & \lambda d_{j_{02}}/2 - 1/2 & \lambda d_{j_{03}}/2 - 1/2 \\ \lambda d_{j_{23}}/2 - 1/2 & \lambda d_{j_{13}}/2 - 1/2 & \lambda d_{j_{12}}/2 - 1/2 \end{Bmatrix} \\ & \sim \sum_{x_0} \sqrt{\frac{1}{-f''(x_0)2\pi\lambda^3}} \exp(F(x_0) + \lambda f(x_0)) \exp\left(\sum_{I < J} \frac{\lambda d_{j_{IJ}}}{2} h_{d_{j_{IJ}}}\right) \\ & \left[1 + \frac{1}{\lambda} \left(-\frac{H(j_{IJ})}{24} - \frac{G(x_0)}{12} - \frac{F''(x_0) + (F'(x_0))^2}{2f''(x_0)} + \frac{f^{(4)}(x_0) + 4f^{(3)}(x_0)F'(x_0)}{8(f''(x_0))^2} - \frac{5(f^{(3)}(x_0))^2}{24(f''(x_0))^3} \right) + O\left(\frac{1}{\lambda^2}\right) \right] \end{aligned} \quad (13.14)$$

where x_0 are the stationary points of the phase, i.e. $f'(x_0) = 0$. The next step is to identify these stationary points.

13.2.2 Contributions of the stationary points

The phase $f(x)$ is an analytical function given by:

$$f(x) = i\pi x + x \ln(x) - \sum_K \left(x - \frac{\tilde{v}_K}{2} \right) \ln \left(x - \frac{\tilde{v}_K}{2} \right) - \sum_j \left(\frac{\tilde{p}_j}{2} - x \right) \ln \left(\frac{\tilde{p}_j}{2} - x \right) \quad (13.15)$$

therefore the stationary points x_0 satisfy the following equation as shown in [152]:

$$f'(x) = i\pi + \ln(x) - \sum \ln(x - \tilde{v}_K/2) + \sum \ln(\tilde{p}_j/2 - x) = 0 \quad (13.16)$$

which is equivalent to

$$x \prod_j (p_j - x) = - \prod_K (x - v_K) \quad (13.17)$$

The previous equation reduces to a quadratic equation $Ax^2 - Bx + C = 0$ with

$$\begin{aligned} A &= - \sum_{j < l} \tilde{p}_j \tilde{p}_l + \sum_{K < L} \tilde{v}_K \tilde{v}_L = \frac{1}{2} \left(\sum_{\substack{I < J, K < L, \\ (I, J) \neq (K, L)}} d_{j_{IJ}} d_{j_{KL}} \right) \\ B &= -\tilde{p}_1 \tilde{p}_2 \tilde{p}_3 + \sum_{I < J < K} \tilde{v}_I \tilde{v}_J \tilde{v}_K = \frac{1}{4} \left[\left(\sum_{\substack{I < J, K < L, \\ (I, J) \neq (K, L)}} d_{j_{IJ}} d_{j_{KL}} \right) \left(\sum_{I < J} d_{j_{IJ}} \right) + \sum_J \left(\prod_{K \neq J} d_{j_{JK}} \right) \right] \\ C &= \prod_K v_K \end{aligned} \quad (13.18)$$

As shown in [152], the discriminant $\Delta = -(B^2 - 4AC)$ is given in terms of the d_{jIJ} by:

$$\Delta = \frac{1}{16} \left[\sum_{\substack{I < J, \\ K < L, \\ (I, J) \neq (K, L)}} d_{jIJ} d_{jKL} \left(\sum_{\substack{M < N, \\ (M, N) \neq (I, J), \\ (M, N) \neq (K, L)}} d_{jMN}^2 - d_{jIJ}^2 - d_{jKL}^2 \right) - \sum_K \prod_{L \neq K} d_{jKL}^2 \right] \quad (13.19)$$

$$= 2 \begin{vmatrix} 0 & \left(\frac{d_{j23}}{2}\right)^2 & \left(\frac{d_{j13}}{2}\right)^2 & \left(\frac{d_{j12}}{2}\right)^2 & 1 \\ \left(\frac{d_{j23}}{2}\right)^2 & 0 & \left(\frac{d_{j03}}{2}\right)^2 & \left(\frac{d_{j02}}{2}\right)^2 & 1 \\ \left(\frac{d_{j13}}{2}\right)^2 & \left(\frac{d_{j03}}{2}\right)^2 & 0 & \left(\frac{d_{j01}}{2}\right)^2 & 1 \\ \left(\frac{d_{j12}}{2}\right)^2 & \left(\frac{d_{j02}}{2}\right)^2 & \left(\frac{d_{j01}}{2}\right)^2 & 0 & 1 \\ 1 & 1 & 1 & 1 & 0 \end{vmatrix} = 2^4 (3!)^2 V^2$$

where V is the volume of the tetrahedron of edge length $d_{jIJ}/2$. In the following we will focus on the case where $\Delta > 0$, i.e. $V^2 > 0$, which corresponds to tetrahedra in flat Euclidean space. The other case $\Delta < 0$ corresponds to tetrahedra admitting an embedding in the 2+1d Minkowski space-time. And so, we get two stationary points:

$$x_{\pm} = \frac{B \pm i\sqrt{\Delta}}{2A} \quad (13.20)$$

The geometrical interpretation of the stationary points is not clear yet. We have shown that Δ is related to the volume of the tetrahedron. B and A are also related to invariant of the tetrahedron:

$$B = \sum_I \frac{v_I}{2} A + 24V \cot \theta$$

where we recall that v_I is the perimeter of the triangle I of the tetrahedron. The angle θ is the Brocard angle of the tetrahedron. Indeed, $\frac{d_{j01}}{2} \frac{d_{j02}}{2} \frac{d_{j03}}{2} :: \frac{d_{j03}}{2} \frac{d_{j23}}{2} \frac{d_{j13}}{2} :: \frac{d_{j12}}{2} \frac{d_{j02}}{2} \frac{d_{j23}}{2} :: \frac{d_{j01}}{2} \frac{d_{j12}}{2} \frac{d_{j13}}{2}$ are the barycentric coordinates of the second Lemoine point of the tetrahedron denoted L . This point is such that the distance from L to the face I of the tetrahedron is equal to $R_I \tan \theta$ where R_I is the radius of the circumscribed circle

of the triangle I and θ is then defined by $\sum_J \left(\prod_{K \neq J} \frac{d_{jJK}}{2} \right) = 12V \cot \theta$.

The geometrical significance of the stationary points still has to be understood. However, we can now give the explicit form of the leading order and of the next to leading order of the $\{6j\}$ -symbol.

Leading order. We first focus on the leading order and on the x_+ contribution. This analysis has already been done in [152] and we just recall the main steps and give the notations:

$$f(x_+) = \sum_{I < J} \frac{d_{jIJ}}{2} f_{d_{jIJ}} \text{ where}$$

$$f_{d_{j0i}} = \ln \left[\frac{(x_+ - \tilde{v}_0)(x_+ - \tilde{v}_i)}{\prod_{j \neq i} (\tilde{p}_j - x_+)} \right] \text{ for } i, j \in \{1, \dots, 3\}$$

$$f_{d_{j_{ik}}} = \ln \left[\frac{(x_+ - \tilde{v}_k)(x_+ - \tilde{v}_i)}{(\tilde{p}_k - x_+)(\tilde{p}_i - x_+)} \right] \text{ for } i, k \in \{1, \dots, 3\}$$
(13.21)

The second derivative of f is given by:

$$\begin{aligned} -f''(x_+) &= \sum_K \frac{1}{x_+ - \tilde{v}_K} + \sum_j \frac{1}{\tilde{p}_j - x_+} - \frac{1}{x_+} \\ &= -i\sqrt{\Delta} \exp(-\ln(x_+ \prod_j (\tilde{p}_j - x_+))) \end{aligned}$$

where we have used the equation (13.17) which gives $x_+ \prod_j (\tilde{p}_j - x_+) = -\prod_K (x_+ - \tilde{v}_K)$. In the same way, we can simplify $F(x_+) = -\frac{1}{2} \ln \left(x_+ \prod_j (\tilde{p}_j - x_+) \right)$. The exponential piece of $f''(x_+)$ and $e^{F(x_+)}$ compensate and we get:

$$\frac{1}{\sqrt{-f''(x_+)}} e^{F(x_+)} = \frac{1}{\sqrt{-i\sqrt{\Delta}}}$$

Collecting these different results yields the following contribution of the x_+ stationary point:

$$\begin{aligned} & \sqrt{\frac{1}{-f''(x_+)2\pi\lambda^3}} \exp(F(x_+) + \lambda f(x_+)) \exp\left(\sum_{I<J} \frac{\lambda d_{j_{IJ}}}{2} h_{d_{j_{IJ}}}\right) = \\ & \frac{1}{\sqrt{2\pi\lambda^3\sqrt{\Delta}}} \exp\left[i\frac{\pi}{4} + \sum_{IJ} (\lambda d_{j_{IJ}}/2)(h_{d_{j_{IJ}}} + f_{d_{j_{IJ}}})\right] \end{aligned} \quad (13.22)$$

The same analysis for the x_- contribution yields the same contribution as the previous one with an opposite phase:

$$\begin{aligned} & \sqrt{\frac{1}{-f''(x_-)2\pi\lambda^3}} \exp(F(x_-) + \lambda f(x_-)) \exp\left(\sum_{I<J} \frac{\lambda d_{j_{IJ}}}{2} h_{d_{j_{IJ}}}\right) = \\ & \frac{1}{\sqrt{2\pi\lambda^3\sqrt{\Delta}}} \exp\left[-i\frac{\pi}{4} + \sum_{IJ} (\lambda d_{j_{IJ}}/2)(h_{d_{j_{IJ}}} + \overline{f_{d_{j_{IJ}}}})\right] \end{aligned} \quad (13.23)$$

We must now compute $f_{d_{j_{IJ}}}$ which is a complex logarithm. We recall that the principal value of the logarithm is defined by $\text{Log} z := \ln|z| + i\text{Arg} z$. Therefore, we have to compute $\Im(f_{d_{j_{IJ}}}) = \theta_{IJ}$. From (13.21), we can write that:

$$\begin{aligned} \theta_{0i} &= \text{Arg}(x_+ - \tilde{v}_0) + \text{Arg}(x_+ - \tilde{v}_i) - \sum_{j \neq i} \text{Arg}(\tilde{p}_j - x_+) \\ \theta_{ik} &= \text{Arg}(x_+ - \tilde{v}_k) + \text{Arg}(x_+ - \tilde{v}_i) - \text{Arg}(\tilde{p}_k - x_+) - \text{Arg}(\tilde{p}_i - x_+) \end{aligned} \quad (13.24)$$

The analysis done in [152] shows that θ_{IJ} can be identified as the (exterior) dihedral angles of the tetrahedron. Moreover,

$$\begin{aligned} \Re(f_{d_{j_{0i}}}) &= \ln \left| \frac{(x_+ - \tilde{v}_0)(x_+ - \tilde{v}_i)}{\prod_{j \neq i} (\tilde{p}_j - x_+)} \right| \\ \Re(f_{d_{j_{ik}}}) &= \ln \left| \frac{(x_+ - \tilde{v}_k)(x_+ - \tilde{v}_i)}{(\tilde{p}_i - x_+)(\tilde{p}_k - x_+)} \right| \end{aligned} \quad (13.25)$$

A tedious (but interesting) computation shows that:

$$\Re(f_{d_{j_{IJ}}}) + h_{d_{j_{IJ}}} = 0 \quad (13.26)$$

Then, summing the contributions of x_+ and x_- we get the leading order of the 6j-symbol:

$$\left\{ \begin{array}{ccc} \lambda d_{j_{01}}/2 - 1/2 & \lambda d_{j_{02}}/2 - 1/2 & \lambda d_{j_{03}}/2 - 1/2 \\ \lambda d_{j_{23}}/2 - 1/2 & \lambda d_{j_{13}}/2 - 1/2 & \lambda d_{j_{12}}/2 - 1/2 \end{array} \right\}^{\text{L.O.}} \sim \sqrt{\frac{1}{12\pi\lambda^3 V}} \cos\left[\frac{\pi}{4} + S_R\right] \quad (13.27)$$

where $S_R = \sum_{I<J} \frac{\lambda d_{j_{IJ}}}{2} \theta_{IJ}$ is the Regge action. This is the well-known limit given by Ponzano and Regge [21] and which has justified their state sum model for 3d Euclidean gravity where the $\{6j\}$ -symbol is the spinfoam amplitude for a single tetrahedron.

Next to leading order. The next-to-leading order is then given by the term in $\frac{1}{\lambda^{5/2}}$ in equation (13.14). Using equations (13.7-13.6-13.8), we rewrite the leading order in terms of $x_{\pm}, \tilde{v}_I, \tilde{p}_j$ and Δ :

$$\frac{1}{\sqrt{48\pi\lambda^5 V}} \left\{ A(x_+, \tilde{v}_I, \tilde{p}_j, \Delta) e^{i(S_R + \frac{\pi}{4})} + A(x_-, \tilde{v}_I, \tilde{p}_j, \Delta) e^{-i(S_R + \frac{\pi}{4})} \right\} \quad (13.28)$$

where

$$\begin{aligned}
A(x_+, \tilde{v}_I, \tilde{p}_j, \Delta) = & -\frac{H(d_{j_{IJ}})}{24} + \frac{1}{24i\sqrt{\Delta}\Delta\prod_I(x_+-\tilde{v}_I)}[-\Delta^2 - 3i(\sum_K \prod_{L \neq K} (x_+ - \tilde{v}_L))\Delta\sqrt{\Delta} \\
& + (9\sum_K \prod_{L \neq K} (x_+ - \tilde{v}_L)^2 + 6\prod_I (x_+ - \tilde{v}_I) \sum_{K < L} (x_+ - \tilde{v}_K)(x_+ - \tilde{v}_L))\Delta \\
& - 6i(-\prod_j (\tilde{p}_j - x_+)^3 - \sum_K \prod_{L \neq K} (x_+ - \tilde{v}_L)^3 + \sum_j x_+^3 \prod_{l \neq j} (\tilde{p}_l - x_+)^3 \\
& - (\sum_K \prod_{L \neq K} (x_+ - \tilde{v}_L))(-\prod_j (\tilde{p}_j - x_+)^2 + \sum_K \prod_{L \neq K} (x_+ - \tilde{v}_L)^2 - \sum_j x_+^2 \prod_{l \neq j} (\tilde{p}_l - x_+)^2))\sqrt{\Delta} \\
& - 5(-\prod_j (\tilde{p}_j - x_+)^2 + \sum_K \prod_{L \neq K} (x_+ - \tilde{v}_L)^2 - \sum_j x_+^2 \prod_{l \neq j} (\tilde{p}_l - x_+)^2)]
\end{aligned} \tag{13.29}$$

Since x_{\pm} are conjugated to each other, we obviously have $A(x_+) = \overline{A(x_-)}$. Moreover, numerical computations shows that $\Re(A(x_{\pm}, \tilde{v}_I, \tilde{p}_j, \Delta)) = 0$, and in particular $A(x_+) = -A(x_-)$. This is a priori a non-trivial result to obtain from the previous formulas. Nevertheless, we tested it numerically for various choices of spin and it always turned out true. Thus we believe that there should be a way to show it analytically. We can then give an explicit formula of the NLO of the $\{6j\}$ -symbol:

$$\{6j\}_{\lambda \rightarrow \infty} \sim \{6j\}_{NLO} = \frac{1}{\sqrt{12\pi\lambda^3 V}} \cos\left[\frac{\pi}{4} + S_R\right] - \frac{1}{\sqrt{12\pi\lambda^5 V}} \Im(A(x_+, \tilde{v}_I, \tilde{p}_j, \Delta)) \sin(S_R + \pi/4). \tag{13.30}$$

This result is confirmed by numerical simulations. The plots in Fig. 13.2 represent numerical simulations of the $\{6j\}$ -symbol minus its approximation given above (13.30). Moreover, to enhance the comparison, we have multiplied by $\lambda^{5/2}$ to see how the coefficient of the next to leading order is approached and we have divided by $\cos(S_R + \pi/4)$ (oscillations of the next-to-next-to-leading order) to suppress the oscillations; that is we have plotted:

$$\delta_{NLO} \equiv \lambda^{5/2} \frac{\{6j\} - \{6j\}_{NLO}}{\cos(S_R + \pi/4)}. \tag{13.31}$$

As expected, the numerical simulations show that this rescaled difference δ_{NLO} goes to 0 as $1/\lambda$ when λ goes to ∞ . Moreover, the data for δ_{NLO} without any oscillation suggest that we correctly divided by $\cos(S_R + \pi/4)$ and thus the NNLO of the $\{6j\}$ -symbol should oscillate in $\cos(S_R + \pi/4)$. Therefore, this strongly suggest that the asymptotic expansion of the $\{6j\}$ -symbol in term of the length scale λ is given by an alternative of cosines and sinus at each order. We strongly underline that this is true because we have rescaled the edge lengths $d_{j_{IJ}}$. If we had instead rescaled the spins j_{IJ} as usually done, we would have found an oscillatory behavior controlled by a mixing of cos and sin at each order (as shown explicitly for the case of the isosceles tetrahedron in [145]). This suggests that the $d_{j_{IJ}}$ are indeed the right parameter to consider when studying the semi-classical behavior of the $\{6j\}$ -symbol.

The only thing left to do in the present analysis is to provide the NLO coefficient $\Im(A(x_+))$ with a geometrical interpretation and to show rigourously that $\Re(A(x_+))$ vanishes.

Finally, we rewrite the approximation up to NLO of the $\{6j\}$ -symbol in a slightly different manner:

$$\{6j\} \sim \frac{1}{\sqrt{12\pi\lambda^3 V}} \cos\left[\frac{\pi}{4} + S_R + \frac{1}{\lambda} \Im(A(x_+)) + O\left(\frac{1}{\lambda^2}\right)\right]. \tag{13.32}$$

This shows that the next-to-leading corrections to the $\{6j\}$ -symbol can be directly considered as corrections to the Regge action for (3d) gravity:

$$S_R^{corrected} \equiv S_R + \frac{1}{\lambda} \Im(A(x_+)).$$

We point out that an expansion in $1/\lambda$ with alternating cos and sin could be similarly re-absorbed as corrections to the Regge action. This would define in the spinfoam framework the quantum gravity corrections to classical 3d gravity due to the fundamental discreteness of the theory. Such correction would enter the gravitational correlations (of the “graviton propagator” type) at second order as suggested in [153].

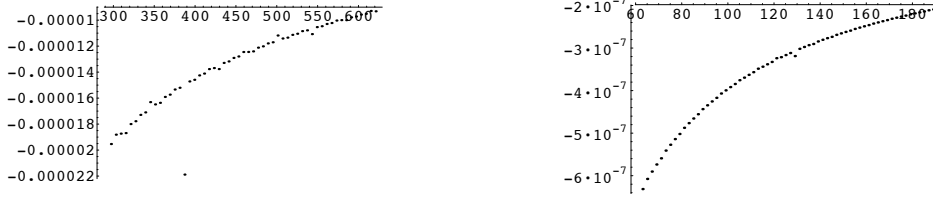


Figure 13.2: Plots of the difference δ_{NLO} between the $\{6j\}$ -symbol and its analytical approximation up to NLO. On the left, we look at the $\{6j\}$ -symbol for $d_1 = 5\lambda, d_2 = 7\lambda, d_3 = 9\lambda, d_4 = 7\lambda, d_5 = 9\lambda, d_6 = 9\lambda$ with the x-coordinate standing for 3λ . On the right, we've plotted the case $d_1 = 15\lambda, d_2 = 17\lambda, d_3 = 19\lambda, d_4 = 19\lambda, d_5 = 21\lambda, d_6 = 17\lambda$ with λ running from 60 to 200.

13.3 Some particular cases

13.3.1 The equilateral tetrahedron

For the equilateral tetrahedron, all the edges have the same length: that is $\forall I, J, d_{IJ} = d$. The tetrahedron with edge length $d/2$ has a volume $V = (d/2)^3 \sqrt{2}/12$ and has all equal dihedral angles $\theta = \arccos(-1/3)$. In this case, the expressions greatly simplify. For instance, the stationary points are $x_{\pm} = \frac{11 \pm i\sqrt{\frac{1}{2}}}{6}d$. Equations (14.4) and (13.28) reduce to:

$$\{6j\}_{\text{equi}}^{\text{NLO}} = \frac{2^{5/4}}{\sqrt{\pi d^3}} \cos\left(S_R + \frac{\pi}{4}\right) - \frac{31}{72\sqrt{\sqrt{2}\pi d^5}} \sin\left(S_R + \frac{\pi}{4}\right) \quad (13.33)$$

where the Regge action is $S_R = 3d\theta$. The result was already obtained in [145]. We confirm it by numerical simulations. The plot in fig.13.3 gives the equilateral $\{6j\}$ -symbol minus its NLO approximation (13.33). Like for the previous plots, we have multiplied by $\lambda^{5/2}$ to see how the coefficient of the next to leading order is approached and we have divided by $\cos(S_R + \pi/4)$ (oscillations of the next to next to leading order) to suppress the oscillations.

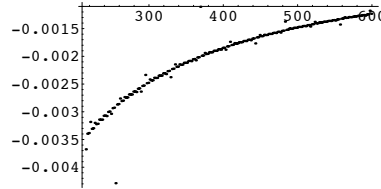


Figure 13.3: Difference between the equilateral $\{6j\}$ -symbol and the analytical result (13.33). The x-axis stands for d and d goes from 200 to 600.

13.3.2 The isosceles tetrahedron

We now consider an isosceles tetrahedron that is a tetrahedron which has two opposite edges of length equal to $\frac{d_1}{2}$ and $\frac{d_2}{2}$ and the remaining four edges of the same length equal to $\frac{d}{2}$ (see Fig. 13.4). The volume of the tetrahedron is:

$$V^2 = \frac{1}{2^8(3!)^2} d_1^2 d_2^2 (4d^2 - d_1^2 - d_2^2),$$

and the dihedral angles are:

$$\theta = \arccos \left(\frac{-d_1 d_2}{\sqrt{4d^2 - d_1^2} \sqrt{4d^2 - d_2^2}} \right), \quad \theta_{1,2} = 2 \arccos \left(\frac{d_{2,1}}{\sqrt{4d^2 - d_{1,2}^2}} \right).$$

Once again, equations (14.4) and (13.28) simplify and we get :

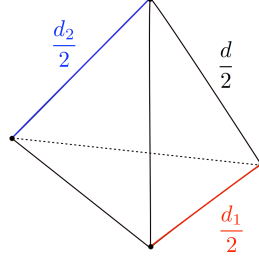


Figure 13.4: The isosceles tetrahedron

$$\{6j\}_{\text{NLO}}^{(\text{iso})} = \frac{1}{\sqrt{12\pi V \lambda^3}} \cos \left(S_R + \frac{\pi}{4} \right) - \frac{F(d, d_1, d_2)}{24V \lambda \sqrt{12\pi V \lambda^3}} \sin \left(S_R + \frac{\pi}{4} \right) \quad (13.34)$$

where $F(d, d_1, d_2) = \frac{768d^6(d^2 - d_1^2 - d_2^2) + 736d^4 d_1^2 d_2^2 + 240d^4(d_1^4 + d_2^4) - 176d^2 d_1^2 d_2^2(d_1^2 + d_2^2) - 24d^2(d_1^6 + d_2^6) + 10d_1^2 d_2^2(d_1^4 + d_2^4) + 25d_1^4 d_2^4}{96(4d^2 - d_1^2)(4d^2 - d_2^2)(4d^2 - d_1^2 - d_2^2)}$,

and the Regge action $S_R = 2d\theta + \frac{d_1}{2}\theta_1 + \frac{d_2}{2}\theta_2$. Let us point out that the volume increases as λ^3 while F goes as λ^2 , so that the NLO scales properly as $\lambda^{-5/2}$.

This reproduces the result previously obtained in [145]. We can easily check that this reduces to the previous equilateral case when $d_1 = d_2 = d$ and we further confirm it by numerical simulations. The plots in Fig. 13.5 represents numerical simulations of an isosceles $\{6j\}$ -symbol minus the analytical formula (13.34). Like for the previous plot, we have multiplied the data by $\lambda^{5/2}$ to see how the coefficient of the NNLO order is approached and we have divided by $\cos(S_R + \pi/4)$ (NNLO oscillations) to suppress the oscillations. Finally, the geometrical

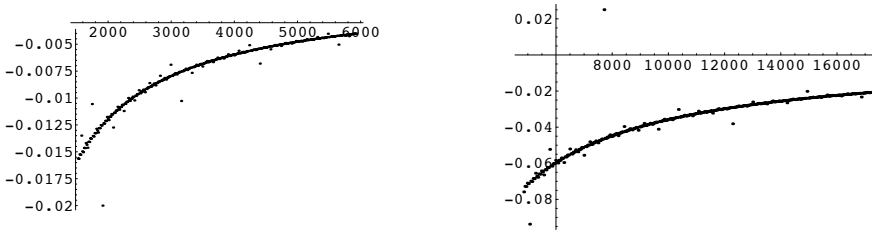


Figure 13.5: Differences between isosceles $\{6j\}$ -symbols and their analytical approximation (13.34). The x-axis stands for d with λ goes from 200 to 600. On the left hand side, we consider isosceles tetrahedra with $d_1 = 3\lambda, d_2 = 3\lambda, d = 7\lambda$. On the right hand side, we've plotted the case $d_1 = 9\lambda, d_2 = 3\lambda, d = 21\lambda$.

interpretation of the term $F(d, d_1, d_2)$ remains to be understood. If we can't provide it with a geometrical meaning, there is little hope to interpret the NLO coefficient $\Im(A(x_+))$ in the generic case. Nevertheless, we give a more compact expression for the denominator of F :

$$96(4d^2 - d_1^2)(4d^2 - d_2^2)(4d^2 - d_1^2 - d_2^2) = 96^3 \frac{V^2}{\cos^2 \theta}. \quad (13.35)$$

We still need to express the numerator of F in term of geometrical objects. For instance, we could express it in term of d^2 , $(4d^2 - d_1^2)(4d^2 - d_2^2)$ and $(4d^2 - d_1^2 - d_2^2)$, which would provide a formula in term of the volume and the dihedral angles. Nevertheless, we haven't been able to find such a useful rewriting of this NLO coefficient.

Chapter 14

Recursion relations and the asymptotic expansion of the $\{6j\}$

An alternative way to proceed in order to probe the asymptotic behavior and the induced corrections of the correlations is to use the exact recursion relations satisfied by the $\{6j\}$ -symbol. It is this method we present in this Chapter. Let us point out that recursion relations satisfied by other spin foam amplitudes have been investigated in [154]. The following results have been published in [13].

14.1 Exact and Approximate Recursion Relation for the Isosceles Tetrahedron

We will focus on the isosceles tetrahedron, which is relevant for the computations of geometrical correlations in the simplest non-trivial toy model in 3d quantum gravity [140]. Such tetrahedron has four of its edges of equal length with the two remaining opposite edges of arbitrary length. The corresponding isosceles $\{6j\}$ -symbol is:

$$\{a, b\}_J \equiv \left\{ \begin{array}{ccc} a & J & J \\ b & J & J \end{array} \right\},$$

where $J \in \mathbb{N}/2$ and a, b are integers smaller than $2J$ (to satisfy the triangular inequality). The associated tetrahedron has edge lengths $l_j = d_j/2$ for $j = a, b, J$, where $d_j = 2j + 1$ is the dimension of the $SU(2)$ representation of spin j . The volume V of the tetrahedron is given by the simple formula:

$$V_J(a, b) = \frac{1}{12} l_a l_b \sqrt{4l_J^2 - (l_a^2 + l_b^2)}, \quad (14.1)$$

while the (exterior) dihedral angles θ_j can also be written in term of the edge lengths (see e.g. [145] for more details):

$$\cos \theta_a = -\frac{4l_J^2 - l_a^2 - 2l_b^2}{4l_J^2 - l_a^2}, \quad \cos \theta_b = -\frac{4l_J^2 - l_b^2 - 2l_a^2}{4l_J^2 - l_b^2}, \quad \cos \theta_J = \frac{-l_a l_b}{\sqrt{4l_J^2 - l_a^2} \sqrt{4l_J^2 - l_b^2}}. \quad (14.2)$$

The general recursion relation for the $\{6j\}$ -symbol given by Schulten and Gordon in [149, 150] simplifies in this specific isosceles case:

$$(l_a + \frac{1}{2}) \left[4l_J^2 - (l_a + \frac{1}{2})^2 \right] \{a+1, b\}_J - 2l_a \left[(4l_J^2 - l_a^2) \cos(\theta_a) + \frac{1}{4} \right] \{a, b\}_J + (l_a - \frac{1}{2}) \left[4l_J^2 - (l_a - \frac{1}{2})^2 \right] \{a-1, b\}_J = 0 \quad (14.3)$$

In the asymptotic regime, we know (analytically and numerically) the behavior of the $\{6j\}$ -symbol at the leading order:

$$\{a, b\}_J \sim \{a, b\}_J^{LO} \equiv \frac{1}{\sqrt{12\pi V}} \cos \left(l_a \theta_a + l_b \theta_b + 4l_J \theta_J + \frac{\pi}{4} \right), \quad (14.4)$$

which is actually valid under the assumption that the tetrahedron with edge lengths l_a, l_b, l_J exists (else the generic asymptotics can be expressed in term of Airy functions). The oscillatory phase is given by the Regge action $S_R = l_a \theta_a + l_b \theta_b + 4l_J \theta_J$. Using the obvious trigonometric identity $\cos((n+1)\phi) + \cos((n-1)\phi) = 2\cos\phi \cos n\phi$, we can write an exact recursion relation for the leading order of the $\{6j\}$ -symbol:

$$\sqrt{V_J(a+1, b)} \{a+1, b\}_J^{LO} - 2\cos\theta_a \sqrt{V_J(a, b)} \{a, b\}_J^{LO} + \sqrt{V_J(a-1, b)} \{a-1, b\}_J^{LO} = 0. \quad (14.5)$$

A similar recursion relation holds for b -shifts and also J -shifts.

The most natural idea is to compare this recursion relation for the leading order to the previous equation on the exact $\{6j\}$ -symbol to see how to use them to extract the next-to-leading correction to the asymptotic behavior. We can first find the link between the leading order of equation (14.3) and the leading order of equation (14.5). Both equations can be written under the same form at the leading order:

$$\{a+1, b\}_J - 2\cos\theta_a \{a, b\}_J + \{a-1, b\}_J \approx 0, \quad (14.6)$$

which turns into a simple second order differential equation in the large spin limit. Then the next-to-leading order of the equation (14.3):

$$\begin{aligned} \sqrt{V_J(a, b)} \left(1 + \frac{1}{2l_a} \left(1 - \frac{2l_a^2}{4l_J^2 - l_a^2}\right)\right) \{a+1, b\}_J - 2\cos\theta_a \sqrt{V_J(a, b)} \{a, b\}_J \\ + \sqrt{V_J(a, b)} \left(1 - \frac{1}{2l_a} \left(1 - \frac{2l_a^2}{4l_J^2 - l_a^2}\right)\right) \{a-1, b\}_J \approx 0 \end{aligned} \quad (14.7)$$

will have to be compared to an recursion relation for the next-to-leading order of the $\{6j\}$ -symbol.

14.2 Pushing to the Next-to-Leading Order

We are interested in the asymptotic expansion of the $\{6j\}$ -symbol. It was shown in previous works [145, 12] that l_j seems to be the right parameter to consider when studying the semi-classical behavior of the $\{6j\}$ -symbol. So from now we write:

$$\left\{ \begin{array}{ccc} a & J & J \\ b & J & J \end{array} \right\} \equiv \{l_a, l_b\}_{l_J}.$$

Notice that shifting a by ± 1 is equivalent to shifting the edge length $l_a = a + 1/2$ by ± 1 . We rescale now l_j by λl_j and we replace the exact $\{6j\}$ -symbol by a series in $1/\lambda$ alternating cosines and sinus of the Regge action (shifted by $\pi/4$) in the previous equation (14.3). The fact that there is no mixing up of cosines and sinus at all order was show in [145]. More precisely, we write the $\{6j\}$ -symbol asymptotic expansion under the form:

$$\begin{aligned} \{\lambda l_a, \lambda l_b\}_{\lambda l_J} = \frac{1}{\lambda^{3/2} D(l_a, l_b, l_J)} [\cos(\lambda S_R + \pi/4) + \frac{F^{(1)}(l_a, l_b, l_J)}{\lambda} \sin(\lambda S_R + \pi/4) + \frac{G^{(1)}(l_a, l_b, l_J)}{\lambda} \cos(\lambda S_R + \pi/4)) \\ + \frac{F^{(2)}(l_a, l_b, l_J)}{\lambda^2} \cos(\lambda S_R + \pi/4) + \frac{G^{(2)}(l_a, l_b, l_J)}{\lambda^2} \sin(\lambda S_R + \pi/4)) \\ + \frac{F^{(3)}(l_a, l_b, l_J)}{\lambda^3} \sin(\lambda S_R + \pi/4) + \frac{G^{(3)}(l_a, l_b, l_J)}{\lambda^3} \cos(\lambda S_R + \pi/4) \\ + \frac{F^{(4)}(l_a, l_b, l_J)}{\lambda^4} \cos(\lambda S_R + \pi/4) + \frac{G^{(4)}(l_a, l_b, l_J)}{\lambda^4} \sin(\lambda S_R + \pi/4) + O(\lambda^{-5})], \end{aligned} \quad (14.8)$$

where the pre-factor denominator $D(l_a, l_b, l_J)$ is given by the square-root of the tetrahedron volume as in equation (14.4). To study the asymptotics, it is convenient to factorize the whole equation (14.3) by $\lambda^{3/2}$. We then write $\{l_a \pm 1/\lambda, l_b\}_{l_J}$ for $\{\lambda l_a \pm 1, \lambda l_b\}_{\lambda l_J}$. We also factorize the coefficients of the recursion relation. We start by defining $C(l_j) = l_a(4l_J^2 - l_a^2) = \frac{16(A(l_a, l_J, l_J))^2}{l_a}$ where $A(a, b, c) = \frac{1}{4}\sqrt{(a+b+c)(a+b-c)(a-b+c)(-a+b+c)}$ is the area of the triangle of edge lengths given by a, b and c . The coefficient which appears in front of $\{l_a \pm 1/\lambda, l_b\}_{l_J}$ becomes $C(l_a \pm 1/(2\lambda), l_b, l_J) = (l_a \pm 1/(2\lambda))(4l_J^2 - (l_a \pm 1/(2\lambda)))$, where we underline that the shift is $\pm 1/(2\lambda)$ and not simply $\pm 1/\lambda$. We expand $C(l_a \pm 1/(2\lambda), l_b, l_J)$ in term of derivatives:

$$C(l_a \pm 1/(2\lambda), l_b, l_J) = \sum_n \frac{1}{n!} \frac{1}{(2\lambda)^n} \frac{\partial^n C}{\partial l_a^n}$$

with

$$\begin{cases} C = l_a(4l_J^2 - l_a^2) \\ \frac{\partial C}{\partial l_a} = 4l_J^2 - 3l_a^2 \\ \frac{\partial^2 C}{\partial l_a^2} = -6l_a^2 \\ \frac{\partial^3 C}{\partial l_a^3} = -6 \\ \frac{\partial^n C}{\partial l_a^n} = 0 \text{ for } n \geq 4 \end{cases} \quad (14.9)$$

Then to express $\{l_a \pm 1/\lambda, l_b\}_{l_J}$ we need to expand $D(l_a \pm 1/\lambda)$, $F^{(i)}(l_a \pm 1/\lambda)$, and $G^{(i)}(l_a \pm 1/\lambda)$: ($i \in \{1 \dots 4\}$)

$$\begin{cases} D(l_a \pm 1/\lambda) = D \pm \frac{1}{\lambda} \frac{\partial D}{\partial l_a} + \frac{1}{2\lambda^2} \frac{\partial^2 D}{\partial l_a^2} \pm \frac{1}{3!\lambda^3} \frac{\partial^3 D}{\partial l_a^3} + \frac{1}{4!\lambda^4} \frac{\partial^4 D}{\partial l_a^4} \\ F^{(i)}(l_a \pm 1/\lambda) = \sum_{k=0}^{4-i} (-1)^k \frac{1}{k!\lambda^k} \frac{\partial^k F^{(i)}}{\partial l_a^k} \\ G^{(i)}(l_a \pm 1/\lambda) = \sum_{k=0}^{4-i} (-1)^k \frac{1}{k!\lambda^k} \frac{\partial^k G^{(i)}}{\partial l_a^k} \end{cases} \quad (14.10)$$

$F^{(1)}(l_J)$ was computed in a previous paper [145, 12]. It was also suggested that the asymptotic expansion of the $\{6j\}$ -symbol in term of the length scale λ is given by an alternative of cosines and sinus at each order, so we expect that $G^{(i)}(l_J) = 0$ for $\forall i \geq 1$. Finally, we also need to expand the Regge action $\lambda S_R(l_a \pm \frac{1}{\lambda})$, remembering that $\theta_j = \theta_j(l_a)$:

$$\lambda S_R(l_a \pm \frac{1}{\lambda}) = \lambda S_R + \sum_{k=0}^4 \frac{(-1)^{k+1}}{(k+1)!\lambda^k} \frac{\partial^k \theta_a}{\partial l_a^k} \quad (14.11)$$

with

$$\begin{cases} \frac{\partial \theta_a}{\partial l_a} = \frac{-2l_a l_b}{(4l_J^2 - l_a^2)\sqrt{4l_J^2 - l_a^2 - l_b^2}} \\ \frac{\partial^2 \theta_a}{\partial l_a^2} = -\frac{2l_b(4l_J^2 l_a^2 - 2l_a^4 - l_a^2 l_b^2 + 16l_J^4 - 4l_b^2 l_J^2)}{(4l_J^2 - l_a^2)^2 [4l_J^2 - l_a^2 - l_b^2]^{3/2}} \\ \frac{\partial^3 \theta_a}{\partial l_a^3} = -\frac{2l_a l_b (24l_b^4 l_J^2 + 40l_J^2 l_a^2 l_b^2 - 12l_J^2 l_a^4 + 5l_a^4 l_b^2 - 192l_J^4 l_a^2 - 240l_J^4 l_b^2 + 2l_a^2 l_b^4 + 6l_a^6 + 576l_J^6)}{(4l_J^2 - l_a^2)^3 [4l_J^2 - l_a^2 - l_b^2]^{5/2}} \\ \frac{\partial^4 \theta_a}{\partial l_a^4} = \frac{1}{(4l_J^2 - l_a^2)^4 (4l_J^2 - l_a^2 - l_b^2)^{7/2}} (6(8l_a^{10} + 8l_a^8 l_b^2 + 152l_J^2 l_a^6 l_b^2 - 720l_J^4 l_a^6 + 7l_a^6 l_b^4 + 3520l_J^6 l_a^4 - 1472l_J^4 l_a^4 l_b^2 + 2l_a^4 l_b^6 \\ + 140l_a^4 l_b^4 l_J^2 - 560l_a^2 l_b^4 l_J^4 - 3840l_J^8 l_a^2 + 2432l_J^6 l_a^2 l_b^2 + 48l_a^2 l_J^2 l_b^6 + 2048l_J^8 l_b^2 - 448l_J^6 l_b^4 - 3072l_J^{10} + 32l_b^6 l_J^4) l_b) \end{cases}$$

We can now write an asymptotic recursion equation from equations (14.3), (14.9), (14.8), (14.10) and (14.11) in terms of λ neglecting terms of order $O(\lambda^{-4})$ and smaller, assuming that λ is large. This leads to a couple of equations at each order, one for the cos-oscillations and one for the term in sin:

- The first equation is given by the terms of order λ^0 and it is trivially satisfied ($0 = 0$) since we have already written the leading order of the $\{6j\}$ -symbol proportional to $\cos(S_R + \frac{\pi}{4})$ (the Ponzano-Regge asymptotic formulae).
- The second equation is given by the terms of order λ^{-1} :

$$\left(\frac{1}{2C} \frac{\partial C}{\partial l_a} - \frac{1}{D} \frac{\partial D}{\partial l_a} \right) \sin(\theta_a) + \frac{1}{2} \frac{\partial \theta_a}{\partial l_a} \cos(\theta_a) = 0 \quad (14.12)$$

which can be rewritten as a differential equation for D :

$$\frac{\partial \ln D}{\partial l_a} = \frac{1}{2} \left[\frac{\partial \theta_a}{\partial l_a} \frac{\cos \theta_a}{\sin \theta_a} + \frac{\partial \ln C}{\partial l_a} \right]. \quad (14.13)$$

This allows to determine D : $\ln D = \frac{1}{2} \ln(C \sin(\theta_a)) + K$, which simplifies into $D = K \sqrt{l_a l_b \sqrt{4l_J^2 - l_a^2 - l_b^2}}$ where K is a constant factor. Thus this second equation shows that D is correctly proportional

to the square-root of the volume V of the isosceles tetrahedron. To determine the normalization constant K (as well as $G^{(1)}$), the orthonormality property of $\{6j\}$ -coefficients can be employed: $\sum_a 4l_a \sqrt{l_b l_{b'}} \{a, b\}_J \{a, b'\}_J = \delta_{bb'}$ and we get the $K = \sqrt{12\pi}$. The details are given in the next section.

- The third equation is given by the terms of order λ^{-2} and which are proportional to $\cos(S_R + \frac{\pi}{4})$

$$\frac{\partial F^{(1)}}{\partial l_a} = \frac{l_a}{4C \sin \theta_a} + \left(\frac{1}{2C} \frac{\partial C}{\partial l_a} - \frac{1}{D} \frac{\partial D}{\partial l_a} \right) \frac{1}{2} \frac{\partial \theta_a}{\partial l_a} + \frac{1}{6} \frac{\partial^2 \theta_a}{\partial l_a^2} + \frac{\cos \theta_a}{\sin \theta_a} \left(\frac{1}{2D} \frac{\partial^2 D}{\partial l_a^2} - \frac{1}{8C} \frac{\partial^2 C}{\partial l_a^2} + \frac{1}{D} \frac{\partial D}{\partial l_a} \left(\frac{1}{2C} \frac{\partial C}{\partial l_a} - \frac{1}{D} \frac{\partial D}{\partial l_a} + \left(\frac{1}{2} \frac{\partial \theta_a}{\partial l_a} \right)^2 \right) \right) \quad (14.14)$$

where we used the fact that $\left(\frac{1}{2C} \frac{\partial C}{\partial l_a} - \frac{1}{D} \frac{\partial D}{\partial l_a} \right) \sin(\theta_a) + \frac{1}{2} \frac{\partial \theta_a}{\partial l_a} \cos(\theta_a) = 0$ (eqn. (15.24)) to remove all the terms proportional to $F^{(1)}$ itself. The first term of the right-hand side of the equation (14.14) comes from the variation of the coefficient in front of $\{a, b\}_J$ in the recursion equation (14.3). The terms with a derivative of C with respect to l_a come from the coefficients in front of $\{a \pm 1, b\}_J$ and $\{a, b\}_J$. The variation of C with respect to l_a is given by the variation of the areas of the triangles of the tetrahedron. From eqn.(15.24), we relate it to the variations of D (the volume) and to the variations of the dihedral angle θ_a : $\frac{1}{C} \frac{\partial C}{\partial l_a} = \frac{2}{D} \frac{\partial D}{\partial l_a} - \frac{\cos \theta_a}{\sin \theta_a} \frac{\partial \theta_a}{\partial l_a}$. The terms with a derivative of D with respect to l_a come from the variation of the leading order of the asymptotic of the $\{6j\}$ -symbol and the terms with a derivative of the dihedral angle θ_a come from the variations of the Regge action S_R . We can now compute the derivative of $F^{(1)}$ with respect of l_a (equation (14.14)) in terms of l_a , l_b and l_J the edge lengths of the tetrahedron:

$$\frac{\partial F^{(1)}}{\partial l_a} = - \frac{1}{48(l_a^2 - 4l_J^2 + l_a^2)^2(4l_J^2 - l_a^2 - l_b^2)^{(5/2)l_b}} (-32l_b^6 l_J^2 l_a^2 + 10l_b^6 l_a^4 + 96l_b^6 l_J^4 - 960l_J^6 l_b^4 + 15l_a^6 l_b^4 + 400l_J^4 l_b^4 l_a^2 - 100l_J^2 l_b^4 l_a^4 - 168l_J^2 l_b^6 l_a^2 - 1664l_J^6 l_b^2 l_a^2 + 20l_a^8 l_b^2 + 576l_J^4 l_b^2 l_a^4 + 3072l_J^8 l_b^2 - 3072l_J^{10} + 48l_J^4 l_a^6 + 2304l_J^8 l_a^2 - 576l_J^6 l_a^4) \quad (14.15)$$

and then easily integrate this equation over l_a :

$$F^{(1)}(l_J) = - \frac{768l_J^6(l_J^2 - l_a^2 - l_b^2) + 736l_J^4 l_a^2 l_b^2 + 240l_J^4(l_a^4 + l_b^4) - 176l_J^2 l_a^2 l_b^2(l_a^2 + l_b^2) - 24l_J^2(l_a^6 + l_b^6) + 10l_a^2 l_b^2(l_a^4 + l_b^4) + 25l_a^4 l_b^4}{24(4l_J^2 - l_b^2)(2l_J^2 - l_a^2)(4l_J^2 - l_b^2 - l_a^2)^{3/2} l_a l_b} + Z(l_b, l_J) \quad (14.16)$$

The integration constant $Z(l_b, l_J)$ can be determined using the symmetry properties of the $\{6j\}$ -symbol: symmetry of the isosceles $\{6j\}$ -symbol with respect to l_a and l_b , coupling of l_a , l_b and l_J by this isosceles $\{6j\}$ -symbol and homogeneity of $F^{(1)}$ ($[F^{(1)}] = l_J^{-1}$) imply that $Z(l_b, l_J) = 0$. Then this gives us the same result as in the previous paper [12]. Moreover, using the definitions of the tetrahedron volume (14.1) and of the dihedral angles (14.2), we can express $F^{(1)}$ in terms of some geometrical characteristics of the tetrahedron:

$$F^{(1)} = - \frac{\cos \theta_J (3(12V)^8 - (12V)^4 l_a^4 l_b^4 (3(l_a^2 - l_b^2)^2 + 2l_a^2 l_b^2) - l_a^{12} l_b^{12}) + 6l_a^{12} l_b^{12}}{48(12V)^3 l_a^8 l_b^8} \quad (14.17)$$

- The fourth equation is given by the terms of order λ^{-2} and which are proportional to $\sin(S_R + \frac{\pi}{4})$. It is the same equation as the previous one for $G^{(1)}$ but the right-hand side is now equal to zero (homogenous equation). That is we simply get that

$$\frac{\partial G^{(1)}}{\partial l_a} = 0 \quad (14.18)$$

so $G^{(1)} = Z(l_b, l_J)$ is just a constant of integration. Once again the symmetry properties of the $\{6j\}$ -symbol implies that $G^{(1)} = 0$.

- The next equation is given by the terms of order λ^{-3} and which are proportional to $\sin(S_R + \frac{\pi}{4})$. We get

an equation for the first derivative of $F^{(2)}$ with respect to l_a

$$\begin{aligned} \frac{\partial F^{(2)}(l_j)}{\partial l_a} &= \frac{\cos \theta_a}{2 \sin \theta_a} \frac{\partial^2 F^{(1)}}{\partial l_a^2} - \left(\frac{1}{\sin^2 \theta_a} \frac{\partial \theta_a}{\partial l_a} + F^{(1)} \right) \frac{\partial F^{(1)}}{\partial l_a} \\ &+ \frac{\cos \theta_a}{\sin \theta_a} \left[-\frac{1}{4!} \frac{\partial^3 \theta_a}{\partial l_a^3} + \left(\frac{1}{D} \frac{\partial D}{\partial l_a} \frac{1}{2C} \frac{\partial C}{\partial l_a} + \frac{1}{2D} \frac{\partial^2 D}{\partial l_a^2} - \left(\frac{1}{D} \frac{\partial D}{\partial l_a} \right)^2 - \frac{1}{8C} \frac{\partial^2 C}{\partial l_a^2} + \frac{1}{3!} \left(\frac{1}{2} \frac{\partial \theta_a}{\partial l_a} \right)^2 \right) \frac{1}{2} \frac{\partial \theta_a}{\partial l_a} + \left(\frac{1}{D} \frac{\partial D}{\partial l_a} - \frac{1}{2C} \frac{\partial C}{\partial l_a} \right) \frac{1}{3!} \frac{\partial^2 \theta_a}{\partial l_a^2} \right] \\ &+ \frac{1}{2C} \frac{\partial C}{\partial l_a} \frac{1}{2D} \frac{\partial^2 D}{\partial l_a^2} + \frac{1}{8C} \frac{\partial^2 C}{\partial l_a^2} \frac{1}{D} \frac{\partial D}{\partial l_a} + \left(\frac{1}{2C} \frac{\partial C}{\partial l_a} - \frac{1}{D} \frac{\partial D}{\partial l_a} \right) \frac{1}{2} \left(\frac{1}{2} \frac{\partial \theta_a}{\partial l_a} \right)^2 + \frac{1}{3!} \frac{\partial^2 \theta_a}{\partial l_a^2} \frac{1}{2} \frac{\partial \theta_a}{\partial l_a} + \left(\frac{1}{D} \frac{\partial D}{\partial l_a} \right)^3 - \frac{1}{D} \frac{\partial D}{\partial l_a} \frac{1}{D} \frac{\partial^2 D}{\partial l_a^2} + \frac{1}{3!D} \frac{\partial^3 D}{\partial l_a^3} \\ &- \frac{1}{8 \cdot 3!C} \frac{\partial^3 C}{\partial l_a^3} - \frac{1}{2C} \frac{\partial C}{\partial l_a} \left(\frac{1}{D} \frac{\partial D}{\partial l_a} \right)^2 \end{aligned} \quad (14.19)$$

We recall that D is proportional to the square root of the tetrahedron volume, C can be expressed in terms of the volume V and the sinus of the dihedral angle θ_a (see equation (15.24)). To integrate this equation, we first express explicitly¹ it in terms of l_a , l_b and l_j , and then deduce $F^{(2)}$:

$$\begin{aligned} F^{(2)}(l_j) &= \frac{-1}{4608((4l_j^2 - l_a^2)^2(4l_j^2 - l_b^2)^2(4l_j^2 - l_a^2 - l_b^2)^3 l_a^2 l_b^2)} (-2359296 l_a^2 l_j^{10} l_b^4 - 224512 l_a^6 l_j^6 l_b^4 + 100 l_a^{12} l_j^4 + 576 l_a^4 l_j^{12} + 112896 l_j^8 l_b^8 \\ &+ 2727936 l_a^4 l_j^{12} + 5308416 l_j^{16} + 212 l_b^{10} l_a^6 - 5898240 l_a^2 l_j^{14} - 11520 l_a^{10} l_j^6 + 941056 l_a^4 l_j^8 l_b^4 + 31584 l_a^8 l_j^4 l_b^4 \\ &- 2416 l_a^4 l_b^{10} l_j^2 - 79872 l_a^8 l_b^6 l_j^2 - 480 l_b^{12} l_j^2 l_a^2 - 7040 l_a^8 l_b^6 l_j^2 - 2416 l_a^{10} l_j^4 l_b^4 + 100 l_a^4 l_b^{12} + 212 l_a^{10} l_b^6 \\ &+ 2727936 l_j^{12} l_b^4 - 700416 l_j^{10} l_b^6 - 5898240 l_j^{14} l_b^2 - 11520 l_j^6 l_b^{10} - 700416 l_a^6 l_j^{10} + 609 l_a^8 l_b^8 + 112896 l_a^8 l_j^8 \\ &+ 576 l_a^{12} l_j^4 - 2359296 l_a^4 l_j^{10} l_b^2 + 528384 l_a^6 l_j^8 l_b^2 + 5849088 l_a^2 l_j^{12} l_b^2 - 79872 l_a^2 l_b^8 l_j^6 + 31584 l_a^4 l_b^8 l_j^4 - 7040 l_a^6 l_b^8 l_j^2 \\ &- 224512 l_a^4 l_b^6 l_j^4 + 58816 l_a^6 l_b^6 l_j^4 + 8640 l_a^{10} l_j^4 l_b^2 + 8640 l_b^{10} l_j^4 l_a^2 - 480 l_a^{12} l_j^2 l_b^2 + 528384 l_a^2 l_j^8 l_b^6) \end{aligned} \quad (14.20)$$

which is the only result with the required symmetries². The geometrical meaning of this function does not seem obvious. Nevertheless, we can give a more compact expression for the denominator of $F^{(2)}$:

$$(4l_j^2 - l_a^2)^2(4l_j^2 - l_b^2)^2(4l_j^2 - l_a^2 - l_b^2)^3 l_a^2 l_b^2 = \frac{(12V)^6}{\cos^4 \theta_j}. \quad (14.21)$$

- The next equation comes from the terms of order λ^{-3} which are proportional to $\cos(S_R + \frac{\pi}{4})$:

$$\frac{\partial G^{(2)}}{\partial l_a}(l_j) = 0 \quad (14.22)$$

which implies once again that $G^{(2)} = Z(l_b, l_j)$ is a constant of integration. Then the symmetry properties of the $\{6j\}$ -symbol implies $G^{(2)}(l_j) = 0$.

We can now give the asymptotic expansion of an isosceles $\{6j\}$ -symbol until the next to next to leading order (NNLO):

$$\{l_a, l_b\}_{l_j}^{\text{NNLO}} = \frac{1}{\sqrt{12\pi V_{l_j}(l_a, l_a)}} \left[\cos(S_R + \frac{\pi}{4}) + F^{(1)}(l_j) \sin(S_R + \frac{\pi}{4}) + F^{(2)}(l_j) \cos(S_R + \frac{\pi}{4}) \right] \quad (14.23)$$

where the expression for $F^{(1)}$ and $F^{(2)}$ are given by equations (14.17) and (14.20). This result seems to confirm that the expansion of the $\{6j\}$ -symbol is a series alternating cosines and sinus of the Regge action (shift by

$$\begin{aligned} \frac{1}{\partial l_a} F^{(2)}(l_j) &= -\frac{1}{2304((4l_j^2 - l_b^2)l_a^3(4l_j^2 - l_a^2)^3(4l_j^2 - l_a^2 + l_b^2)^4 l_b^2)} (-1604 l_a^8 l_b^8 l_j^2 + 1250816 l_a^4 l_b^8 l_j^6 - 207104 l_a^6 l_b^6 l_j^6 + 31904 l_a^{10} l_j^4 l_b^4 - \\ &169344 l_a^8 l_b^6 l_j^6 - 3920 l_a^6 l_b^{10} l_j^2 + 24992 l_a^6 l_b^8 l_j^4 - 46848 l_a^{10} l_b^6 l_j^2 - 7129088 l_a^4 l_b^{10} l_j^4 + 1770496 l_a^6 l_b^8 l_j^4 + 16832 l_a^4 l_b^{10} l_j^4 + 34368 l_a^8 l_b^4 l_j^6 - 6816 l_a^{12} l_j^4 l_b^2 - \\ &278912 l_a^8 l_b^6 l_j^4 + 14524416 l_a^2 l_j^{12} l_b^4 + 486144 l_a^2 l_j^8 l_b^8 - 560 l_b^{12} l_a^4 l_j^2 - 43776 l_a^2 l_b^{10} l_j^6 - 3317760 l_a^2 l_j^{10} l_b^6 + 22241280 l_a^4 l_j^{12} l_b^2 + 794 l_a^{12} l_b^6 - \\ &6955008 l_a^6 l_b^{10} l_j^2 + 2801664 l_j^{12} l_b^6 + 672 l_a^{14} l_j^2 l_b^2 - 26542080 l_a^4 l_j^{14} - 451584 l_j^{10} l_b^8 + 46080 l_j^8 l_b^{10} - 2304 l_j^{12} l_b^6 - 21233664 l_j^{18} + 37158912 l_j^{12} l_b^{16} + \\ &1072128 l_a^8 l_b^6 l_j^2 - 1528 l_a^{12} l_b^4 l_j^4 - 10911744 l_j^{14} l_b^4 - 35979264 l_a^2 l_j^{14} l_b^2 + 1728 l_b^{12} l_j^4 l_a^2 + 9953280 l_a^6 l_j^{12} + 228096 l_a^{10} l_j^8 - 10368 l_a^{12} l_j^6 - \\ &2073600 l_a^8 l_j^{10} + 27 l_a^{10} l_b^8 + 23592960 l_j^{16} l_b^2 + 400 l_a^8 l_b^{10} - 88 l_a^{14} l_b^4 - 8144 l_a^{10} l_b^6 l_j^2 + 100 l_b^{12} l_a^6) \end{aligned}$$

²If the result is not symmetric after integration, a non-null integration constant has to be added and its determination can be done using the symmetry properties of the $\{6j\}$ -symbol. Indeed, we have $\frac{\partial F^{(2)}}{\partial l_a} = H(l_a, l_b, l_j)$ so by integration over l_a , $F^{(2)}(l_j) = h(l_a, l_b, l_j) + Z(l_b, l_j)$. Moreover by symmetry, we must have $\frac{\partial F^{(2)}}{\partial l_b} = H(l_a = l_b, l_b = l_a, l_j)$ and then integrating over l_b , we obtain a second expression for $F^{(2)}$: $F^{(2)}(l_j) = h(l_a = l_b, l_b = l_a, l_j) + Z(l_a, l_j)$ which implies that the constant of integration satisfies $Z(l_b, l_j) - Z(l_a, l_j) = h(l_a = l_b, l_b = l_a, l_j) - h(l_a, l_b, l_j)$. This equation allows to determine Z and to get (14.20).

$\frac{\pi}{4}$). In the case of an equilateral tetrahedron, all the edges have the same length, that is $l_a = l_b = l_J = l$ and $V = \frac{\sqrt{2}}{12}l^3$. Then equation (14.23) reduces to:

$$\{6j\}_{\text{equi}}^{\text{NNLO}} = \frac{1}{\sqrt{\pi l^3 \sqrt{2}}} \cos(S_R + \frac{\pi}{4}) - \frac{31}{72 \cdot 2^{1/4} \cdot 2^{5/2} \sqrt{\pi l^5}} \sin(S_R + \frac{\pi}{4}) - \frac{45673}{20736} \frac{1}{2^{1/4} 2^4 \sqrt{\pi l^7}} \cos(S_R + \frac{\pi}{4}) \quad (14.24)$$

where the Regge action is given by $S_R = 6l\theta$ and $\theta = \theta_a = \theta_b = \theta_J = \arccos(-1/3)$. This result is confirmed by numerical simulations. The plot in Fig. 14.1 represents numerical simulations of the equilateral $\{6j\}$ -symbol minus its approximation (14.24). Moreover, to enhance the comparison, we have multiplied by $l^{7/2}$ to see how the coefficient of the NNLO is approached and we have divided by $\sin(S_R + \frac{\pi}{4})$ (oscillations of the next to next to next to leading order) to suppress the oscillations. This gives an error that decreases as expected as l^{-1} .

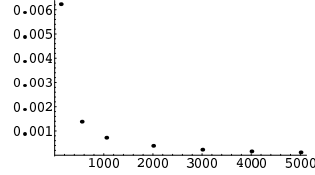


Figure 14.1: Difference between the equilateral $\{6j\}$ -symbol and the analytical result (14.24). The x-axis stands for $l = d/2$ and d goes from 100 to 5000. The error decreases as expected as l^{-1} confirming our asymptotic formula.

- The next two equations come from the terms of order λ^{-4} . The equation for $G^{(3)}$ is the same as the one for $G^{(1)}$ and $G^{(2)}$, that is: $\frac{\partial G^{(3)}}{\partial l_a} = 0$. Using the same arguments of symmetry we deduce that $G^{(3)} = 0$. This confirms our expectation of a series alternating cosines and sines in the asymptotic of the $\{6j\}$ -symbol:

$$\{\lambda_a, \lambda_b\}_{\lambda l_J} = \frac{1}{\lambda^{3/2} D(l_a, l_b, l_J)} \left[\cos(\lambda S_R + \frac{\pi}{4}) + \sum_{k=1}^{\infty} \frac{F^{(k)}(l_a, l_b, l_J)}{\lambda^k} \cos(\lambda S_R + \frac{\pi}{4} + \epsilon(k) \frac{\pi}{2}) \right], \quad (14.25)$$

where $\epsilon(k) = -1$ when k is odd and $\epsilon(k) = 0$ when k is even. We already have an expression for $F^{(1)}$ and $F^{(2)}$. The equation for $F^{(3)}$ is the second equation of order λ^{-4} and gives its first derivative with respect to l_a in terms of l_a , l_b and l_J . It is straightforward (though lengthy) to integrate it over l_a and get the expression³ of $F^{(3)}$ in terms of l_a , l_b and l_J . In the equilateral case ($l_a = l_b = l_J = l$), the formula reduces to:

$$F^{(3)} = \frac{28833535}{17915904} \frac{1}{2^{9/2} 2^{1/4} l^3} \quad (14.26)$$

Therefore, we have the expression of the asymptotic expansion of the equilateral $\{6j\}$ -symbol up to the next-to-next-to-next to leading order (NNNLO):

$$\{6j\}_{\text{equi}}^{\text{NNNLO}} = \frac{1}{2^{1/4} \sqrt{\pi l^3}} \left[\cos(S_R + \frac{\pi}{4}) - \frac{31}{72 \cdot 2^{5/2} l} \sin(S_R + \frac{\pi}{4}) \right]$$

$$\begin{aligned} {}^3F^{(3)}(l_j) &= -\frac{1}{3317760(l_a^2(l_a-2l_J)(l_a+2l_J)(4l_J^2-l_a^2)^3(4l_J^2-l_a^2-l_b^2)(9/2)l_b^3(4l_J^2-l_a^2)^2)} (-6965741568l_a^6l_J^{10}l_b^8 + 1069728l_a^6l_J^{16}l_b^2 + \\ &28270080l_a^{16}l_J^6l_b^2 - 743040l_a^4l_J^2l_b^{18} + 1750503260160l_J^{20}l_a^2l_b^2 + 379404800l_a^{12}l_J^6l_b^6 + 788705280l_a^{10}l_J^{10}l_b^4 - 33547200l_a^6l_J^{14}l_b^4 - \\ &98578608l_a^{12}l_J^8l_b^4 - 81032970240l_a^8l_J^{14}l_b^2 + 379404800l_a^6l_J^{12}l_b^6 - 389214720l_a^8l_J^{14}l_b^4 - 323813376000l_a^6l_J^{18}l_b^6 - 156036l_a^8l_J^{16}l_b^8 - 22176l_a^2l_J^{14}l_b^{18} - \\ &3824640l_a^{16}l_J^4l_b^4 - 28408l_a^{18}l_b^6 - 31104000l_a^{16}l_J^8l_b^8 - 1262270545920l_a^{18}l_J^2l_b^4 - 1262270545920l_a^{18}l_J^4l_b^2 + 461814497280l_J^{16}l_a^6l_b^6 + 1069728l_a^6l_J^6l_b^6 + \\ &74144841728l_a^{16}l_J^{12}l_b^6 + 824520278016l_J^{16}l_a^4l_b^4 + 461814497280l_J^{16}l_b^6 + 788705280l_J^{10}l_a^4l_b^{10} - 267541217280l_a^6l_J^{14}l_b^4 + 115174656l_a^6l_J^{14}l_b^{14} - \\ &999532800l_a^8l_J^{12}l_b^{12} + 68611276800l_a^8l_J^{16}l_b^6 - 3824640l_a^4l_J^{14}l_b^{16} - 1242078720l_J^{10}l_a^8l_b^6 + 28270080l_J^6l_a^6l_b^{16} + 38483472384l_J^{12}l_a^{12}l_b^8 + \\ &2157096960l_a^{12}l_J^{10}l_b^{12} - 1242078720l_a^6l_J^{10}l_b^{18} + 509607936000l_J^{24} - 33547200l_a^{14}l_J^4l_b^4 + 1222041600l_J^{12}l_a^{10}l_b^{10} + 11119152l_J^{12}l_a^{10}l_b^{12} - \\ &999532800l_a^{12}l_J^8l_b^4 + 783522201600l_J^{20}l_a^4 + 2157096960l_J^{10}l_a^2l_b^{12} - 28408l_a^6l_b^{18} - 389214720l_a^{14}l_J^8l_b^2 - 783601920l_a^8l_J^8l_b^8 - 98578608l_a^8l_J^4l_b^{12} - \\ &6965741568l_a^8l_J^{10}l_b^6 - 323813376000l_a^{18}l_J^6l_b^6 + 1222041600l_a^{10}l_J^{12}l_b^2 + 115174656l_a^{14}l_J^6l_b^4 - 743040l_a^{18}l_J^4l_b^2 - 22176l_a^{18}l_J^2l_b^4 - 81032970240l_J^{14}l_a^2l_b^8 + \\ &7201368l_a^{14}l_J^8l_b^2 - 114011616l_a^{10}l_J^{10}l_b^{14} - 985242009600l_J^{22}l_b^2 + 568565760l_a^{10}l_J^{18}l_b^6 - 1401753600l_J^{12}l_a^{12}l_b^2 - 267541217280l_J^{14}l_a^4l_b^{16} + \\ &568565760l_a^8l_J^{10}l_b^{10} + 11119152l_a^{10}l_J^{12}l_b^2 + 783522201600l_J^{20}l_a^4 - 342523l_a^{12}l_b^{12} + 38483472384l_a^8l_J^{12}l_b^4 - 3981312000l_a^{10}l_J^{14}l_b^8 - 156036l_a^6l_b^{16} - \\ &511602l_a^{10}l_J^{14}l_b^{10} + 344217600l_a^{14}l_J^{10}l_b^{10} - 1401753600l_J^{12}l_a^{12}l_b^2 + 1036800l_a^{18}l_J^6l_b^6 + 344217600l_a^{14}l_J^{10}l_b^{10} + 68611276800l_J^{16}l_b^8 - 3981312000l_J^{14}l_b^{10} - \\ &511602l_a^{14}l_b^{10} - 31104000l_a^6l_J^8l_b^8 - 985242009600l_J^{22}l_a^2 + 1036800l_a^{18}l_J^6l_b^6 + 7201368l_a^8l_b^{14}l_J^2) \end{aligned}$$

$$- \frac{45673}{20736 \cdot 2^4 l^2} \cos(S_R + \frac{\pi}{4}) + \frac{28833535}{17915904 \cdot 2^{9/2} l^3} \sin(S_R + \frac{\pi}{4}) \Big]. \quad (14.27)$$

We check this result numerically by computing it using Mathematica for two values of spins $j = 50$ and $j = 100$. More precisely, we computed the renormalized error $\frac{(\{6j\}_{\text{equi}} - \{6j\}_{\text{equi}}^{\text{NNNLO}}) l^{9/2}}{\cos(S_R + \frac{\pi}{4})}$ and we got the expected $1/\lambda$ -behavior. However for $l > 100$, Mathematica is not accurate enough and the numerical errors are too important to get exploitable results. In the general isosceles case, the expression of $F^{(3)}$ is quite complicated and its geometrical interpretation remains to be understood. Nevertheless, we can again give as before a more compact formula for the denominator of $F^{(3)}$:

$$\text{denominator}_{F^{(3)}} = 3317760(4l_J^2 - l_a^2 - l_b^2)^{9/2} l_a^3 l_b^3 (4l_J^2 - l_a^2)^3 (4l_J^2 - l_b^2)^3 = 30(48)^3 \frac{(12V_J(a, b))^9}{\cos^6 \theta_J} \quad (14.28)$$

From this equation, the equation giving the denominator of $F^{(2)}$ and remembering that the denominator of $F^{(1)}$ can be written under a similar form: $\text{denominator}_{F^{(1)}} = 48 \frac{(12V)^3}{\cos^2 \theta_J}$, we can conjecture that:

$$\text{denominator}_{F^{(k)}} \propto \frac{(12V_J(a, b))^{3k}}{(\cos \theta_J)^{2k}} \quad (14.29)$$

where $F^{(k)}$ are the terms appearing in the asymptotic expansion of the $\{6j\}$ -symbol (14.25). And consequently, the numerator of $F^{(k)}$ is a polynomial in l_j of degree $8k$.

So, using the recursion relation for the isosceles $\{6j\}$ -symbol as well as its symmetry properties, we have computed explicitly the asymptotic expansion of the isosceles $\{6j\}$ -symbol to the fourth order up to an overall factor K (this integration constant K comes from the integration of the first equation (15.24)). The well-known value $K = \sqrt{12\pi}$ which already appears in the Ponzano-Regge formula can be obtained easily using the unitary property of the $\{6j\}$ -symbol, as we show in the next section. The equilateral case has been checked against numerical calculations. This method using the recursion relation is fairly easy to implement. It requires integrating a rational fraction at each level and does not involve neither Riemann sum nor saddle point analysis. Moreover, since the coefficient C of the recursion relation (14.3) is a polynomial of degree 3; $\frac{\partial^n C}{\partial l_a^n} = 0$ for $n \geq 4$. Therefore, we expect to get a stable relation for the first derivative of $F^{(k)}$ and $G^{(k)}$ with respect to l_a for $k \geq 3$. On one hand, this allows to prove that $G^{(k)}$ always vanishes; and on the other hand, it should provide a systematic method to extract $F^{(k)}$ for arbitrary order k .

We conclude this section with a general remark on the asymptotic expansion of the $\{6j\}$ -symbol. In the context of 3d quantum gravity, it is often argued that the leading order of the $\{6j\}$ -symbol is a $\cos(S)$ instead of a complex phase $\exp(+iS)$, thus reflecting that the path integral is invariant under a change of (local) orientation (see e.g.[155]). This obviously neglects the $+\pi/4$ shifts, which can be considered as a quantum effect (like an ordering ambiguity). However, in the light of the present expansion, it is clear that we have terms of the type $\sin(S)$ beyond the leading order and such terms are not invariant under the change $S \rightarrow -S$. This means that the role of this symmetry in the spinfoam path integral should be more subtle than originally thought.

14.3 Consequences of the unitary property of the $\{6j\}$ -symbol

The orthogonality property of the $\{6j\}$ -symbols states that:

$$\sum_{l_a} 4l_a \sqrt{l_b l_{b'}} \{l_a, l_b\}_{l_J} \{l_a, l_{b'}\}_{l_J} = \delta_{l_b l_{b'}} \quad (14.30)$$

This relation corresponds to the unitarity of the evolution in the Ponzano-Regge 3d quantum gravity. We want to use this property to determine the constant of the leading order of the $\{6j\}$ -symbol. From the recursion relation we have shown that $\{l_a, l_b\}_{l_J}^{\text{LO}} = \frac{K}{\sqrt{V_J(a, b)}} \cos(S_R + \frac{\pi}{4})$; but K is still undetermined. For large spin and

for $l_b \approx l_{b'}$, we can approximate the unitary property at the leading order in $(l_b - l_{b'})$ by:

$$\int_0^\infty dl_a 4l_a l_b \frac{K^2}{V_J(a, b)} \cos(S_R(l_a, l_b) + \frac{\pi}{4}) \cos(S_R(l_a, l_{b'}) + \frac{\pi}{4}) \approx \delta(l_b - l_{b'}). \quad (14.31)$$

The product of the cosines can be simplified at leading order:

$$\begin{aligned} \cos(S_R(l_a, l_b) + \frac{\pi}{4}) \cos(S_R(l_a, l_{b'}) + \frac{\pi}{4}) &= \frac{1}{2} \left[\cos(S_R(l_a, l_b) + S_R(l_a, l_{b'}) + \frac{\pi}{2}) + \cos(S_R(l_a, l_b) - S_R(l_a, l_{b'})) \right] \\ &\sim \frac{1}{2} \left[\cos(2S_R(l_a, l_b) + \frac{\pi}{2}) + \cos((l_b - l_{b'})\theta_b) \right], \end{aligned}$$

where the dihedral angle $\theta_b = \arccos\left(-\frac{4l_J^2 - l_b^2 - 2l_a^2}{4l_J^2 - l_b^2}\right)$ is considered as a function of the length l_a . We do a saddle point approximation. The first term oscillates and its integral is exponentially suppressed. And we are left with the second term, which should satisfy the following equation:

$$\int_{-\infty}^\infty dl_a l_a l_b \frac{K^2}{V_J(a, b)} \cos((l_b - l_{b'})\theta_b) \approx \delta(l_b - l_{b'}) \quad (14.32)$$

We recall that:

$$\frac{1}{2\pi} \int_{-\infty}^\infty dl_a \cos(l_a(l_b - l_{b'})) = \delta(l_b - l_{b'})$$

therefore we can conclude that

$$l_a l_b \frac{K^2}{V} = \frac{1}{2\pi} \left| \frac{\partial \theta_b}{\partial l_a} \right|. \quad (14.33)$$

θ_b and l_b are so conjugate variables and K comes from the Jacobian of the change of variables between l_a and θ_b . Computing the derivative of the dihedral angle gives:

$$\frac{\partial \theta_b}{\partial l_a} = \frac{-2}{\sqrt{4l_J^2 - l_a^2 - l_b^2}} = \frac{-l_a l_b}{6V_J(a, b)} \Rightarrow K = \frac{1}{\sqrt{12\pi}}. \quad (14.34)$$

Moreover, pushing the approximation of the unitary property to the next to leading order in $(l_b - l_{b'})$ and using the next to leading order of the $\{6j\}$ -symbol shows that $G^{(1)} = 0$. This was already shown in the previous part using the recursion relation and the symmetry properties of the $\{6j\}$ -symbol and comes as a confirmation.

14.4 “Ward-Takahashi identities” for the spinfoam graviton propagator

We are interested in the two-point function in 3d quantum gravity for the simplest triangulation given by a single tetrahedron. This provides the first order of the “spinfoam graviton propagator” in 3d quantum gravity.

Considering the isosceles tetrahedron, we focus on the correlations between the two representations a and b :

$$\langle \mathcal{O}(a) \tilde{\mathcal{O}}(b) \rangle_{\psi_J} = \frac{1}{Z} \sum_{a, b} \psi_J(a) \psi_J(b) \mathcal{O}(a) \tilde{\mathcal{O}}(b) \{a, b\}_J, \quad Z \equiv \sum_{a, b} \psi_J(a) \psi_J(b) \{a, b\}_J, \quad (14.35)$$

where $\psi_J(j)$ is the boundary state, which depends also on the bulk length scale J , and $\mathcal{O}, \tilde{\mathcal{O}}$ are the observables whose correlation we are studying.

Now, inserting a recursion relation with shifts on a , b or J in the sum over the representation labels $\sum_{a, b}$ leads to equations relating the expectation values of different observables. We distinguish two cases: when the state ψ_J does not change or when the length scale J also varies.

14.4.1 Relating Observables

Inserting the recursion relation on a -shifts in the definition of the correlation function, we obtain the following exact identity:

$$\begin{aligned} \langle \frac{\psi_J(a-1)}{\psi_J(a)} \mathcal{O}(a-1) \tilde{\mathcal{O}}(b) (l_a - \frac{1}{2}) (4l_J^2 - (l_a - \frac{1}{2})^2) \rangle_\psi & - \langle \mathcal{O}(a) \tilde{\mathcal{O}}(b) 2l_a (2 \cos \theta_a (4l_J^2 - l_a^2) + \frac{1}{4}) \rangle_\psi \\ & + \langle \frac{\psi_J(a+1)}{\psi_J(a)} \mathcal{O}(a+1) \tilde{\mathcal{O}}(b) (l_a + \frac{1}{2}) (4l_J^2 - (l_a + \frac{1}{2})^2) \rangle_\psi = 0. \end{aligned} \quad (14.36)$$

We call this a Ward identity for our spinfoam correlation. If the observable diverges at $a = 0$, more precisely if it contains terms in $1/a$ or in $1/(a+1)$, then we need to take into account extra boundary terms in this equation corresponding to contributions at $a = 0$. But all observables usually considered are regular in this sense.

Then one can choose different sets of observables \mathcal{O} and $\tilde{\mathcal{O}}$ and one gets different identities on the correlation functions of the spinfoam model. For example, taking $\mathcal{O}(a) = l_a$, we get:

$$\begin{aligned} \langle \frac{\psi_J(a-1)}{\psi_J(a)} \tilde{\mathcal{O}}(b) (l_a - 1) (l_a - 1/2) (4l_J^2 - (l_a - 1/2)^2) \rangle_\psi & - \langle \tilde{\mathcal{O}}(b) (2 \cos \theta_a l_a^2 (4l_J^2 - l_a^2) + l_a^2/2) \rangle_\psi \\ & + \langle \frac{\psi_J(a+1)}{\psi_J(a)} \tilde{\mathcal{O}}(b) (l_a + 1) (l_a + 1/2) (4l_J^2 - (l_a + 1/2)^2) \rangle_\psi = 0. \end{aligned}$$

We recall that the area of the triangle of edge lengths given by l_a, l_J, l_J is equal to $A(l_a, l_J) = \frac{1}{4} l_a \sqrt{4l_J^2 - l_a^2}$; then $(l_a \pm 1)(l_a \pm 1/2)(4l_J^2 - (l_a \pm 1/2)^2) = 16[A^2(l_a \pm 1/2, l_J) \pm \frac{A^2(l_a \pm 1/2, l_J)}{2(l_a \pm 1/2)}]$, therefore we can rewrite the previous equation as an equation between correlation functions of the observable $\tilde{\mathcal{O}}(b)$ and different observables proportional to the square of the triangle area $A(l_a, l_J)$:

$$\begin{aligned} \langle \frac{\psi_J(a-1)}{\psi_J(a)} [A^2(l_a - 1/2, l_J) - \frac{A^2(l_a - 1/2, l_J)}{2(l_a - 1/2)}] \tilde{\mathcal{O}}(b) \rangle_\psi & - \langle (2 \cos \theta_a A^2(l_a, l_J) + l_a^2/2) \tilde{\mathcal{O}}(b) \rangle_\psi \\ & + \langle \frac{\psi_J(a+1)}{\psi_J(a)} [A^2(l_a + 1/2, l_J) + \frac{A^2(l_a + 1/2, l_J)}{2(l_a + 1/2)}] \tilde{\mathcal{O}}(b) \rangle_\psi = 0. \end{aligned}$$

The standard choice of boundary is a phased Gaussian [10, 140, 14]:

$$\psi_J(j) \sim e^{i2l_j \vartheta} e^{-2\alpha \frac{(l_j - l_J)^2}{l_J}}, \quad (14.37)$$

where ϑ is a fixed angle defining a posteriori the external curvature of the boundary and α is an arbitrary real positive number (which can be fixed by the requirement of a physical state [14]). In this case, we can compute explicitly the ratios $\psi(a \pm 1)/\psi(a)$ entering the Ward identity:

$$\frac{\psi_J(a \pm 1)}{\psi_J(a)} = e^{\pm i2\vartheta} e^{\mp 4\alpha \frac{l_a - l_J}{l_J}} e^{-\frac{2\alpha}{l_J}}$$

Of course, this ratios does not depend on b ; therefore if the observable $\tilde{\mathcal{O}}(b) = 1$, then the dependence on b only appears in one correlation function through the cosine of the dihedral angle θ_a . As another example, we consider $\mathcal{O}(a) = l_a^{-1}$ and $\tilde{\mathcal{O}}(b) = \frac{4l_J^2 - l_b^2}{(2l_J)^4}$, then:

$$\begin{aligned} \langle \frac{\psi_J(a-1)}{\psi_J(a)} \frac{l_a - 1/2}{l_a - 1} \frac{4l_J^2 - (l_a - 1/2)^2}{4l_J^2} \frac{4l_J^2 - l_b^2}{4l_J^2} \rangle_\psi & - 2 \langle \cos \theta_a \frac{4l_J^2 - l_a^2}{4l_J^2} \frac{4l_J^2 - l_b^2}{4l_J^2} + \frac{1}{16l_J^2} \frac{4l_J^2 - l_b^2}{4l_J^2} \rangle_\psi \\ & + \langle \frac{\psi_J(a+1)}{\psi_J(a)} \frac{l_a + 1/2}{l_a + 1} \frac{(4l_J^2 - (l_a + 1/2)^2)}{4l_J^2} \frac{4l_J^2 - l_b^2}{4l_J^2} \rangle_\psi = 0 \end{aligned}$$

which can be approximated by:

$$\langle e^{-i2\vartheta} e^{4\alpha \frac{l_a - l_J}{l_J}} \Delta((l_a - 1/2)^2) \Delta(l_b^2) \rangle_\psi - 2e^{\frac{2\alpha}{l_J}} \langle \cos \theta_a \Delta(l_a^2) \Delta(l_b^2) + \frac{1}{16l_J^2} \Delta(l_b^2) \rangle_\psi + \langle e^{i2\vartheta} e^{-4\alpha \frac{l_a - l_J}{l_J}} \Delta((l_a + 1/2)^2) \Delta(l_b^2) \rangle_\psi \approx 0$$

where $\Delta(l_J^2) = \frac{l_J^2 - 4l_J^2}{4l_J^2}$.

14.4.2 Rescaling the Tetrahedron

We can now vary also the length scale l_J . First let's notice that in the same way we wrote an exact recursion relation for the leading order of the isosceles $\{6j\}$ -symbol shifting the representation a (equation (14.5)), we can write a similar exact recursion relation for the leading order of the $\{6j\}$ -symbol shifting the label J ; that is

$$\sqrt{V_{J+1}(a, b)}\{a, b\}_{J+1}^{\text{LO}} - 2\cos(4\theta_J)\sqrt{V_J(a, b)}\{a, b\}_J^{\text{LO}} + \sqrt{V_{J-1}(a, b)}\{a, b\}_{J-1}^{\text{LO}} = 0 \quad (14.38)$$

Inserting this recursion relation on J -shifts in the definition correlation function, we obtain the following identity:

$$\begin{aligned} \langle \sqrt{V_{J+1}(a, b)} \frac{\psi_J(a)\psi_J(b)}{\psi_{J+1}(a)\psi_{J+1}(b)} \mathcal{O}(a)\tilde{\mathcal{O}}(b) \rangle_\psi &+ \langle \sqrt{V_{J-1}(a, b)} \frac{\psi_J(a)\psi_J(b)}{\psi_{J-1}(a)\psi_{J-1}(b)} \mathcal{O}(a)\tilde{\mathcal{O}}(b) \rangle_\psi \\ &- 2\langle \cos(4\theta_J)\sqrt{V_J(a, b)} \mathcal{O}(a)\tilde{\mathcal{O}}(b) \rangle_\psi = 0 \end{aligned} \quad (14.39)$$

The correlation functions appearing in this equation are in fact approximation. We are allowed to use the leading order of the $\{6j\}$ -symbol because the boundary state used picks the function on large j_0 . And for the same reason, we can expand $\sqrt{V_{J\pm 1}(a, b)}$ and the ratios $\frac{\psi_J(a)\psi_J(b)}{\psi_{J\pm 1}(a)\psi_{J\pm 1}(b)}$:

$$\begin{aligned} \langle \sqrt{V_J(a, b)} \left(1 - \frac{2l_J}{4l_J^2 - l_a^2 - l_b^2}\right) e^{-4\alpha \frac{(2l_J - (l_a + l_b))}{l_J} [1 + \frac{3l_J - 2(l_a + l_b)}{2l_J(2l_J - l_a - l_b)]} } \mathcal{O}(a)\tilde{\mathcal{O}}(b) \rangle_\psi &- 2\langle \cos(4\theta_J)\sqrt{V_J(a, b)} \mathcal{O}(a)\tilde{\mathcal{O}}(b) \rangle_\psi \\ &+ \langle \sqrt{V_J(a, b)} \left(1 + \frac{2l_J}{4l_J^2 - l_a^2 - l_b^2}\right) e^{4\alpha \frac{(2l_J - (l_a + l_b))}{l_J} [1 - \frac{3l_J - 2(l_a + l_b)}{2l_J(2l_J - l_a - l_b)]} } \mathcal{O}(a)\tilde{\mathcal{O}}(b) \rangle_\psi \approx 0. \end{aligned} \quad (14.40)$$

We hope that such equation will turn out useful to study the asymptotic properties of the correlations function as the length scale J grows large, but we leave this for future investigation.

Chapter 15

Physical boundary state for the quantum 4-simplex

As we already mentioned it, Ψ_q in (11.2) needs to be a physical boundary state. In this Chapter, we work in the context of 4d gravity and we present results published in [15] where we investigate the consequences of the physical state requirement (11.4) for the Euclidean Barrett-Crane model (see Chapter 7) for the simplest case of a space-time triangulation constructed from a single 4-simplex. In this context, we show that this requirement fixes uniquely the width of the quantum boundary state (in term of the classical data) similarly to what happens in the 3d toy model.

We recall that the Barrett-Crane vertex amplitude is given by

$$A_v = \tilde{j} = \int_{\text{SU}(2)} [dg_a]^{\otimes 5} \prod_{a < b} \chi_{j_{ab}}(g_a g_b^{-1}), \quad (15.1)$$

where $a, b = 1, \dots, 5$ label the nodes of the dual graph – a pentahedral graph – of the 4-simplex. Therefore the propagator kernel

$$K[s] = \mathcal{A}[d_{j_{ab}}] = \prod_{a < b} (d_{j_{ab}})^2 \prod_{a < b} (A_e(d_{j_{ab}}))^{1/2} \tilde{j} \quad (15.2)$$

is independent of the intertwiners and we can rewrite the two conditions (11.4) as¹:

$$\sum_{j_{ab}} |\psi_q(d_{j_{ab}})|^2 = 1 \quad \text{for the normalized condition,} \quad (15.6)$$

$$\sum_{j_{ab}} K(d_{j_{ab}}) \psi(d_{j_{ab}}) = 1 \quad \text{for the "Wheeler-deWitt" condition,} \quad (15.7)$$

with the propagator kernel a function of the dimensions $d_{j_{ab}}$ only

$$K[j_{ab}] = \mu \left(\prod_{a < b} d_{j_{ab}} \right)^\sigma \tilde{j} \quad (15.8)$$

¹Choose factorizable ansatz, product state $\psi(j_1, \dots, j_{10}) = \prod_{i=1}^{10} \phi_i(j_i)$. Then equilateral ansatz, $\phi_i(j) = \phi(j)$ for all triangles $i = 1..10$. Then following [110], we introduce the Fourier transform of the state:

$$f(g) = \sum_j \phi(j) \chi_j(g). \quad (15.3)$$

Then the two conditions for a physical state simply translates to:

$$\int dg |f(g)|^2 = 1, \quad (15.4)$$

$$\int [dg_m]^5 \prod_{a < b} f(g_m g_n^{-1}) = \int [d\theta_{mn}]^{10} \delta(\det[\cos \theta_{mn}]) \prod_{m < n} f(\theta_{mn}) = 1. \quad (15.5)$$

with μ and σ undetermined coefficients. The edge amplitude A_e is taken into account in this factor $\mu \left(\prod_{a<b} d_{jab} \right)^\sigma$.

For more generic spinfoam models such as the EPRL-FK models (see Chapter 8), we need to take into account the intertwiners too in the definition of the spinfoam vertex and of the physical states.

In the following, we will work on the Barrett-Crane model in the large spin limit. Thus, in the propagator kernel formula (15.8), we consider the asymptotic formula of the \tilde{j} -symbol

$$\tilde{j} \sim P(d_{jab}) \cos \left(\frac{1}{l_P^2} S_R[d_{jab}] \right) + D(d_{jab}) \quad (15.9)$$

where we recall that $S_R[d_{jab}] = \sum_{a<b} d_{jab} \theta_{ab}$ and the function $P(d_{jab})$ is a slowly varying factor, that grows as $\zeta^{-9/2}$ when scaling all triangle areas d_{jab} by ζ . In the large d_{j_0} limit, we can thus write $P(d_{jab} = d_{j_0}) = \frac{P}{d_{j_0}^{9/2}}$, where P is a constant, that we can choose positive. $D(d_{jab})$ is a contribution coming from degenerate configurations of the 4-simplex. This is a non-oscillating term which has no geometrical meaning scaling like $1/\zeta^2$. However, this sick term is negligible in most computations we are interested in, such as in the computation of (11.2) (see [10, 11]) or as we will see in the computation of (11.4), because it will not match the boundary data induced by Ψ_q which peaks the asymptotic around the non-degenerate semi-classical configuration.

We now focus on the issue of the semi-classical boundary state. The function Ψ_q should describe the boundary value of the gravitational field on the boundary 4-simplex. We thus consider a state peaked on the geometry of a regular 4-simplex: $q = (d_{j_0}, \Theta)$. The simplest possibility is to choose a Gaussian peaked on theses values:

$$\Psi_{(d_{j_0}, \Theta)}(d_{jab}) = e^{-\sum_{a<b, c<d} \alpha_{cd}^{ab} (d_{jab} - d_{j_0})(d_{jcd} - d_{j_0}) + i \sum_{a<b} \Theta_{jab} d_{jab}} \quad (15.10)$$

The phase of this semi-classical state determines where the state is peaked in the conjugate variables: Θ is the variable conjugate to the spin j_0 and it codes the extrinsic geometry of the boundary. α_{cd}^{ab} is a given ten by ten matrix. It depends on d_{j_0} in such a way that the relative uncertainties of area and angle on this state become small in the large d_{j_0} limit, namely:

$$\frac{\langle \Psi_q | \Delta d_{jab} | \Psi_q \rangle}{\langle \Psi_q | d_{jab} | \Psi_q \rangle} \rightarrow 0, \quad \frac{\langle \Psi_q | \Delta \theta_{ab} | \Psi_q \rangle}{\langle \Psi_q | \theta_{ab} | \Psi_q \rangle} \rightarrow 0 \quad \forall a < b \quad (15.11)$$

Assuming that the matrix elements $\alpha_{cd}^{ab} \sim \alpha d_{j_0}^{-n}$ in the large spin limit with α which does not scale with d_{j_0} , the fluctuation determined by the gaussian state (15.10) are of the order:

$$\frac{\langle \Psi_q | \Delta d_{jab} | \Psi_q \rangle}{\langle \Psi_q | d_{jab} | \Psi_q \rangle} \sim \frac{d_{j_0}^{n/2-1}}{\sqrt{\alpha}}, \quad \frac{\langle \Psi_q | \Delta \theta_{ab} | \Psi_q \rangle}{\langle \Psi_q | \theta_{ab} | \Psi_q \rangle} \sim d_{j_0}^{-n/2} \sqrt{\alpha} \quad (15.12)$$

which restricts $n \in]0, 2[$.

In the following, we thus focus on a Gaussian state as boundary state such as the matrix elements of the ten by ten matrix α_{cd}^{ab} are given by

$$\alpha_{cd}^{ab} \sim \frac{\alpha}{d_{j_0}^n} = \frac{a + ib}{d_{j_0}^n} \quad \text{with } n \in]0, 2[\text{ and } a, b \in \mathbb{R} \quad (15.13)$$

in the large spin limit. We now study the consequences of the two conditions (15.6) and (15.7) on this boundary state. That is the aim is now to determine the consequences on α_{cd}^{ab} of the requirement that our boundary state is a physical state.

15.1 Semi-Classical States: the Decoupled Gaussian Ansatz

We first start by considering an additional ansatz for the boundary state. We take a factorized boundary state:

$$\Psi_q[j_{ab}] = \prod_{a<b} \phi(j_{ab}) \quad (15.14)$$

where each $\phi(j_{ab})$ is peaked around the background value $q = (d_{j_0}, \Theta)$ which corresponds to an equilateral 4-simplex. In this simplest case, the ten by ten matrix α_{cd}^{ab} reduces to a diagonal matrix $\alpha \mathbb{I}_{10 \times 10}$. Such a boundary state has been used in [?] since it is up to now the only setting in which numerical simulations can be performed. However, this assumption has not been tested yet. Could such a decoupled gaussian state capture a true physical state? Could it satisfy conditions (15.6) and (15.7)?

Two choices for a factorized boundary state have so far appeared in the literature:

- the Gaussian state [?, ?], where each factor is given by,

$$\phi(j) = e^{-\alpha(d_j - d_{j_0})^2} e^{i\Theta d_j} \quad (15.15)$$

where α is a complex number.

- The Bessel-based state [?, ?], where each factor is given by:

$$\phi_B(j) = \frac{I_{|d_j - d_{j_0}|}(\frac{d_{j_0}}{\alpha}) - I_{d_j + d_{j_0}}(\frac{d_{j_0}}{\alpha})}{\sqrt{I_0(\frac{2d_{j_0}}{\alpha}) - I_{2d_{j_0}+1}(\frac{2d_{j_0}}{\alpha})}} \cos(d_j \Theta) \quad (15.16)$$

In the large spin limit regime, we focus only on the Gaussian ansatz. Indeed, in the large spin limit the Bessel part of (15.16) reduces to the Gaussian in (15.15). Therefore, at the leading order, the only difference between (15.15) and (15.16) is in the phase: the phase in (15.15) is complex whereas the phase in (15.16) is real. A gaussian state with a real phase would lead to the same results as a gaussian state with a complex phase. The interested reader can find details concerning the case of a gaussian state with a real phase in appendix I and we now tackle the issue of defining a physical state coming from a decoupled gaussian state with a complex phase. Therefore, we consider a boundary state of the form,

$$\Psi_{(d_{j_0}, \Theta)}[j_{ab}] = \frac{1}{\mathcal{N}} \prod_{a < b} e^{-\alpha(d_{j_{ab}} - d_{j_0})^2} e^{-i\Theta d_{j_{ab}}} \quad (15.17)$$

with \mathcal{N} the normalization constant and $\alpha \in \mathbb{C}$. We now want to test this assumption using conditions (15.6) and (15.7). These conditions lead to the two following equations on \mathcal{N} and α :

$$1 = \sum_{j_{ab}} |\Psi_{(d_{j_0}, \Theta)}(j_{ab})|^2 = \frac{1}{(\mathcal{N}^2)^{10}} \sum_{\{j_{ab}\}} e^{-2\Re(\alpha) \sum_{a < b} (d_{j_{ab}} - d_{j_0})^2} \quad (15.18)$$

and,

$$1 = \sum_{j_{ab}} K[d_{j_{ab}}] \Psi_{(d_{j_0}, \Theta)}(j_{ab}) \simeq \frac{\mu}{\mathcal{N}^{10}} \sum_{\{j_{ab}\}} \left(\prod_{a < b} d_{j_{ab}} \right)^\sigma P(d_{j_{ab}}) \sum_{\epsilon = \pm 1} e^{-\Re(\alpha) \sum_{a < b} (d_{j_{ab}} - d_{j_0})^2 + i \sum_{a < b} [d_{j_{ab}} (\epsilon \theta_{ab} - \Theta) - \Im(\alpha) (d_{j_{ab}} - d_{j_0})^2]} \quad (15.19)$$

The first equation corresponds to the normalization condition (15.6) for $\Psi_{(d_{j_0}, \Theta)}[j_{ab}]$. The second equation is the "Wheeler-deWitt" condition for $\Psi_{(d_{j_0}, \Theta)}[j_{ab}]$ in the simple case $K[j_{ab}] = \mu \left(\prod_{a < b} d_{j_{ab}} \right)^\sigma \tilde{j}$. Solving them allow to determine uniquely \mathcal{N} and α in term of the coefficients μ and ρ . The analysis is done in the large spin limit regime. In equation (15.19), we have already used the asymptotic formulae of the \tilde{j} -symbol. Moreover, we also replace α in (15.18) and (15.19) by its asymptotic expression

$$\alpha \sim \frac{a + ib}{d_{j_0}^n} \quad (15.20)$$

with $a, b \in \mathbb{R}$ and n restricted to belonging to $]0, 2[$ in order that the asymptotic behavior of the relative uncertainties of the area and angle on this state is correct. Then solving the two obtained equations requires to distinguish three cases with respect to the value of the power $n \in]0, 2[$. The final result can be stated as:

Proposition 15.1.1. *The requirement on a factorized Gaussian state (15.17) to be a physical state fixes the width of the Gaussian α for certain values of the power n :*

1. $0 < n < 1$: the width of the Gaussian α is uniquely determined and the coefficient σ is restricted. More precisely,

$$\begin{cases} \alpha \in \mathbb{R}_+, \\ a = \frac{(\mu P)^{2/5} \pi}{2}, b = 0 \\ \sigma = \frac{1}{4} \left(\frac{2}{5} - n \right) \text{ and } \sigma > \frac{1}{5}, \end{cases} \quad (15.21)$$

2. $1 < n < 2$: there is no solution in this case.

3. $n = 1$: A solution exists for

$$\sigma = \frac{1}{5}$$

and then, the value of α can be determined graphically. For example,

$$a \simeq 0.1 \text{ and } b \simeq 1.9 \text{ for } P = \mu = 1.$$

Before proving this result, let us comment on the third case. This last case should be the most natural since the semi-classical state is then peaked on the same way on Θ encoding the extrinsic geometry of the boundary and on $d_{j_0} = A_0$ encoding the intrinsic geometry, and it is in fact not at all transparent. This leads to the conclusion that the choice of a decoupled gaussian state to define a physical state might be too simple and should be modified. A new proposition is given in the next subsection. Let us now give the proof of the results stated above.

Proof. In the large spin limit, the summation in equations (15.18) and (15.19) can then be approximated with an integral and we can write:

$$1 \simeq \frac{1}{2\mathcal{N}^2} \int d(d_j) e^{-2\Re(\alpha)(d_j - d_{j_0})^2} \quad (15.22)$$

and

$$1 \simeq \frac{\mu}{(2\mathcal{N})^{10}} \int \prod_{a < b} d[d_{j_{ab}}] \left(\prod_{a < b} d_{j_{ab}} \right)^\sigma P(d_{j_{ab}}) \sum_{\epsilon = \pm 1} e^{-\Re(\alpha) \sum_{a < b} (d_{j_{ab}} - d_{j_0})^2 + i \sum_{a < b} [d_{j_{ab}} (\epsilon \theta_{ab} - \Theta) - \Im(\alpha) (d_{j_{ab}} - d_{j_0})^2]} \quad (15.23)$$

The first integral (15.22) is just a Gaussian integral, which can be integrated directly:

$$\mathcal{N}^2 = \frac{1}{2} \sqrt{\frac{\pi}{2\Re(\alpha)}} \quad (15.24)$$

given a first relation at the leading order between \mathcal{N} and α .

To evaluate the second integral (15.23) in the large spin limit, we first notice that the Gaussian implies

$$\delta d_{j_{ab}} = d_{j_{ab}} - d_{j_0} \ll 1 \quad \forall a < b,$$

thus we can expand the Regge action around d_{j_0} :

$$S_R[d_{j_{ab}}] = \sum_{a < b} d_{j_{ab}} \theta_{ab}(d_j) \simeq \sum_{a < b} d_{j_0} \Theta + \sum_{a < b} \frac{\partial S_R}{\partial d_{j_{ab}}} \Big|_{d_j = d_{j_0}} \delta d_{j_{ab}} + \frac{1}{2} \sum_{a < b, c < d} \frac{\partial^2 S_R}{\partial d_{j_{ab}} \partial d_{j_{cd}}} \Big|_{d_j = d_{j_0}} \delta d_{j_{ab}} \delta d_{j_{cd}} \quad (15.25)$$

The Schafli identity implies that

$$\frac{\partial S_R}{\partial d_{j_{ab}}} \Big|_{d_j = d_{j_0}} = \theta_{ab}(d_j) \Big|_{d_j = d_{j_0}} = \Theta$$

since in the equilateral 4-simplex, all the dihedral angles are equal to Θ . And we introduce the Hessian,

$$N_{cd}^{ab} = \frac{\partial^2 S_R}{\partial d_{j_{ab}} \partial d_{j_{cd}}} \Big|_{d_j = d_{j_0}} = \frac{\partial \theta_{ab}}{\partial d_{j_{cd}}} \Big|_{d_j = d_{j_0}}, \quad (15.26)$$

then:

$$S_R[d_{j_{ab}}] \simeq 10d_{j_0}\Theta + \Theta \sum_{a<b} \delta d_{j_{ab}} + \frac{1}{2} \sum_{a<b, c<d} N_{cd}^{ab} \delta d_{j_{ab}} \delta d_{j_{cd}} = \Theta \sum_{a<b} d_{j_{ab}} + \frac{1}{2} \sum_{a<b, c<d} N_{cd}^{ab} \delta d_{j_{ab}} \delta d_{j_{cd}}. \quad (15.27)$$

We replace $S_R[d_{j_{ab}}]$ by this expansion in (15.23):

$$1 \simeq \frac{\mu}{(2N)^{10}} \int \prod_{a<b} d[d_{j_{ab}}] (\prod_{a<b} d_{j_{ab}})^\sigma P(d_{j_{ab}}) \left[e^{-2i\Theta \sum_{a<b} d_{j_{ab}} - \frac{i}{2} \sum_{a<b, c<d} N_{cd}^{ab} \delta d_{j_{ab}} \delta d_{j_{cd}} - \alpha \sum_{a<b} \delta d_{j_{ab}}^2} + e^{\frac{i}{2} \sum_{a<b, c<d} N_{cd}^{ab} \delta d_{j_{ab}} \delta d_{j_{cd}} - \alpha \sum_{a<b} \delta d_{j_{ab}}^2} \right] \quad (15.28)$$

The first exponential is a rapidly oscillating term in $d_{j_{ab}}$ which will vanish when we perform the integration over $d_{j_{ab}}$ so we only have to consider the second term. Moreover, at the leading order in $\delta d_{j_{ab}}$ we can replace $(\prod_{a<b} d_{j_{ab}})^\sigma P(d_{j_{ab}})$ by $d_{j_0}^{10\sigma} P(d_{j_0})$ in the integral (15.23). And we recall that $P(d_{j_{ab}})$ grows as $\zeta^{-9/2}$ when scaling all triangle areas $d_{j_{ab}}$ by ζ , so we can write $P(d_{j_{ab}} = d_{j_0}) = \frac{P}{d_{j_0}^{9/2}}$ in the large d_{j_0} limit, where P is a constant, that we can choose positive. Therefore, once again we have to integrate a Gaussian integral:

$$1 \simeq \frac{\mu(d_{j_0})^{(10\sigma-9/2)} P}{(2N)^{10}} \int \prod_{a<b} d[\delta d_{j_{ab}}] e^{-\delta d_{j_{ab}} M_{cd}^{ab} \delta d_{j_{cd}}} \quad (15.29)$$

where M is a ten by ten matrix defined by

$$M_{cd}^{ab} = \alpha \delta_{cd}^{ab} - i N_{cd}^{ab} \quad a < b, c < d, \quad (15.30)$$

with $\delta_{cd}^{ab} = 1$ if the two couples of indices are the same and it vanishes otherwise; $N_{cd}^{ab} = \frac{\partial \theta_{ab}}{\partial d_{j_{cd}}} |_{d_j=d_{j_0}}$ was explicitly computed in [?]²:

$$N_{cd}^{ab} = \frac{\tilde{N}_{cd}^{ab}}{d_{j_0}} \quad (15.31)$$

where \tilde{N} is a ten by ten real symmetric constant matrix with all coefficients independent of d_{j_0} . In particular, $\tilde{N}_{ab}^{ab} = -\sqrt{\frac{3}{5}} \forall a < b$. Therefore, M is a symmetric matrix with all its diagonal coefficients equal to $\alpha + i\sqrt{\frac{3}{5}} \frac{1}{d_{j_0}}$.

At this stage we have to distinguish the three cases mentioned above. Assuming that α is of the form $\alpha = \frac{a+ib}{d_{j_0}^n}$, with $a, b \in \mathbb{R}$, $n \in]0, 2[$. The three cases with respect to the power $n \in]0, 2[$ are:

1. $0 < n < 1$ corresponds to $\alpha \gg \frac{1}{d_{j_0}}$. In this case, we could negligible the terms of the order $\frac{1}{d_{j_0}}$ with respect to α .
2. $1 < n < 2$ corresponds to $\alpha \ll \frac{1}{d_{j_0}}$. In this case, α will be negligible with respect to the terms of the order $\frac{1}{d_{j_0}}$.
3. $n = 1$ corresponds to $\alpha \sim \frac{1}{d_{j_0}}$. This case should be the most natural case since it peaks in the same way the triangle areas of the 4-simplex around the background value $A_0 = d_{j_0}$ and the dihedral angles around the background value Θ .

$$N_{cd}^{ab} = \frac{\sqrt{3}}{4\sqrt{5}d_{j_0}} \begin{pmatrix} -4 & 7/2 & 7/2 & 7/2 & 7/2 & 7/2 & 7/2 & -9 & -9 & -9 \\ 7/2 & -4 & 7/2 & 7/2 & 7/2 & -9 & -9 & 7/2 & 7/2 & -9 \\ 7/2 & 7/2 & -4 & 7/2 & -9 & 7/2 & -9 & 7/2 & -9 & 7/2 \\ 7/2 & 7/2 & 7/2 & -4 & -9 & -9 & 7/2 & -9 & 7/2 & 7/2 \\ 7/2 & 7/2 & -9 & -9 & -4 & 7/2 & 7/2 & 7/2 & 7/2 & -9 \\ 7/2 & -9 & 7/2 & -9 & 7/2 & -4 & 7/2 & 7/2 & -9 & 7/2 \\ 7/2 & -9 & -9 & 7/2 & 7/2 & 7/2 & -4 & -9 & 7/2 & 7/2 \\ -9 & 7/2 & 7/2 & -9 & 7/2 & 7/2 & -9 & -4 & 7/2 & 7/2 \\ -9 & 7/2 & -9 & 7/2 & 7/2 & -9 & 7/2 & 7/2 & -4 & 7/2 \\ -9 & -9 & 7/2 & 7/2 & -9 & 7/2 & 7/2 & 7/2 & 7/2 & -4 \end{pmatrix}$$

Let us now separately study the three cases to solve equation (15.29).

1. **The first case** $0 < n < 1$ is the easiest one.

Indeed in this case, the matrix $M \sim \frac{a+ib}{d_{j_0}^n} + \frac{\tilde{N}}{d_{j_0}}$ can be approximated by a ten by ten diagonal matrix: $M \simeq \alpha \mathbb{I} = (a + ib)\mathbb{I}$ since $\alpha \sim \frac{a+ib}{d_{j_0}^n} \gg \frac{1}{d_{j_0}}$ and the ten integrals are then decoupled. Thus, we just have to compute a one-dimensional Gaussian integral:

$$\mathcal{N} = \frac{(\mu P)^{1/10}}{2} (d_{j_0})^{(\sigma-9/20)} \int d[\delta d_j] e^{-\alpha(\delta d_j)^2} = \frac{(\mu P)^{1/10}}{2} d_{j_0}^{(\sigma-9/20)} \sqrt{\frac{\pi}{\alpha}} \quad (15.32)$$

which gives a second equation for \mathcal{N} and α . Therefore using equation (15.24), we obtain the following equation on α :

$$\frac{1}{2} \sqrt{\frac{\pi}{2\Re(\alpha)}} = \frac{(\mu P)^{1/5}}{4} d_{j_0}^{(2\sigma-9/10)} \frac{\pi}{\alpha} \quad (15.33)$$

Finally, expressing α under the form $\frac{a+ib}{d_{j_0}^n}$, $0 < n < 1$, we get that:

$$\begin{cases} \alpha \in \mathbb{R}_+, \\ \sigma = \frac{1}{4} \left(\frac{9}{5} - n \right) \text{ and } \sigma > \frac{1}{5}, \\ a = \frac{(\mu P)^{2/5} \pi}{2}, \quad b = 0. \end{cases} \quad (15.34)$$

In this case, α is real and positive. Furthermore, we get a condition on the normalization factor of the spinfoam vertex $\sigma > 1/5$.

2. **The second case** $1 < n < 2$ implies that $\alpha \sim \frac{a+ib}{d_{j_0}^n} \ll \frac{1}{d_{j_0}}$.

In this case, the matrix M reduces to $M = -iN$. We have to integrate: $\int d[\delta d_{j_{ab}}] \exp(i \sum \delta d_{j_{ab}} N_{cd}^{ab} \delta d_{j_{cd}})$. Recall that for a $m \times m$ symmetric invertible matrix A with signature $\sigma(A)$ we have:

$$\int_{\mathbb{R}^m} [dX_i] \exp \left[i \left(\sum_{i,j} X_i A_{ij} X_j \right) \right] = e^{i\sigma(A) \frac{\pi}{4}} \sqrt{\frac{\pi^m}{|\det(A)|}} \quad (15.35)$$

In our case, N is real, symmetric and its signature, which is the difference between the number of positive eigenvalues and the number of negative eigenvalues, is equal to -2 . Therefore, $e^{i\sigma(N) \frac{\pi}{4}} = -i$ and our Gaussian integral is an imaginary number which is not compatible with the first equation on \mathcal{N} (15.24). So, we cannot have $\alpha = \frac{a}{d_{j_0}^n}$ with $1 < n < 2$.

3. **The third case** $n = 1$ corresponds to $\alpha = \frac{a+ib}{d_{j_0}}$.

Then the determinant of M is a complex number: its real part and its imaginary part are polynomials of degree 10 and of arguments a and b . We thus obtain a complex equation for \mathcal{N} and α :

$$1 \simeq \frac{\mu(d_{j_0})^{(10\sigma-9/2)} P}{(2\mathcal{N})^{10}} \int \prod_{a < b} d[\delta d_{j_{ab}}] e^{-\delta d_{j_{ab}} M_{cd}^{ab} \delta d_{j_{cd}}} = \frac{\mu(d_{j_0})^{(10\sigma-9/2)} P}{(2\mathcal{N})^{10}} \sqrt{\frac{\pi^{10}}{\det(M)}} \quad (15.36)$$

Combining this equation with the first equation (15.24) that we already have on \mathcal{N} and $\Re(\alpha) = a$ we get a complex equation on a and b :

$$2^5 \left(\frac{d_{j_0} \pi}{2a} \right)^{5/2} - \mu(d_{j_0})^{(10\sigma-9/2+5)} P \sqrt{\frac{\pi^{10}}{\det(\tilde{M}(a, b))}} = 0 \quad (15.37)$$

with $\tilde{M} = d_{j_0} M$. This equation implies a condition on the normalization factor of the spinfoam vertex:

$$\sigma = \frac{1}{5}.$$

We can then solve numerically the previous equation by plotting a 3d graph representing the square of the norm of the complex number given by the left-hand side of the previous equation (15.37) in terms of a and b using Maple. For example, for $P = \mu = 1$, the value on the surface is null for

$$a \simeq 0.1 \quad \text{and} \quad b \simeq 1.9.$$

Therefore, there exists a specific value α for which $\Psi_{(d_{j_0}, \Theta)}$ is a physical state. However, whereas this case for which $\Psi_{(d_{j_0}, \Theta)}$ is peaked in the same way around the intrinsic and extrinsic geometry (d_{j_0}, Θ) should be the most natural, it is quite complicated.

□

The alternative is then to work with a more complication semi-classical state. Indeed although a factorized gaussian wave-packet is up to now the only one which has allowed to perform numerical simulations, the previous analysis seems to show that it is too simple to catch all the features of a physical state. We show in the next section that a tensorial Gaussian state is more adapted to describe a physical state. Indeed we will see that such a state allows to compensate the imaginary part which comes from the second derivative of the Regge action and given by the matrix iN and consequently to simplify the resolution of this third case studied above.

15.2 The Coupled Gaussian Ansatz

Our new assumption is to consider a boundary state of the form:

$$\psi_q[d_{j_{ab}}] = \frac{1}{\mathcal{N}} e^{-\sum_{a<b, c<d} \alpha_{cd}^{ab} (d_{j_{ab}} - d_{j_0})(d_{j_{cd}} - d_{j_0})} e^{i\Theta \sum_{a<b} d_{j_{ab}}} \quad (15.38)$$

where α is now a ten by ten complex matrix. And we choose

$$\alpha_{cd}^{ab} = \beta(d_{j_0}) \delta_{cd}^{ab} + iN_{cd}^{ab} \quad (15.39)$$

where $\beta \in \mathbb{R}$ and the imaginary part of α is now the conjugate variables of the dihedral angles of the tetrahedron in the semi-classical regime introduced in (15.26):

$$N_{cd}^{ab} = \frac{\partial \theta_{ab}}{\partial d_{j_{cd}}} \Big|_{d_j = d_{j_0}}.$$

N_{cd}^{ab} is the Hessian of S_R and we will see that it is this choice which allows to simplify the construction of a physical semi-classical state peaked in the same way on the extrinsic and extrinsic geometry of the 3d boundary. We recall that N depends on d_{j_0} such that $N = \frac{\tilde{N}}{d_{j_0}}$ with \tilde{N} a matrix with constant coefficients.

Proposition 15.2.1. *For $0 < n \leq 1$, the width β (the real part of the matrix α ; see (15.39)) of the Gaussian state (15.38) is uniquely defined and the coefficient σ is restricted. More precisely,*

$$\begin{cases} \beta \in \mathbb{R}_+, \\ a = \frac{(\mu P)^{2/5} \pi}{2}, b = 0 \\ \sigma = \frac{1}{4} \left(\frac{2}{5} - n \right) \text{ and } \sigma \geq \frac{1}{5}, \end{cases} \quad (15.40)$$

Therefore, the case $n = 1$ appears now in the continuity of the case $0 < n < 1$. This can be considered as an improvement compared to the previous case of a factorized Gaussian semi-classical state. However, the case $1 < n < 2$, which admitted no solution in the factorized Gaussian state, has not been solved yet. The resolution of this case needs the knowledge of the next to leading order of the asymptotic expansion of the $\{10j\}$ -symbol.

Proof. Regarding the asymptotic behavior of β , the real part of the matrix α , we distinguish the three same cases as in the decoupled gaussian state case. The result of the first case is not modified. Indeed, in the first case,

1. $\beta \sim \frac{a}{d_{j_0}^n}$ with $0 < n < 1$, therefore, $\beta \gg \frac{1}{d_{j_0}}$ and the matrix M can be approximated by a ten by ten diagonal matrix $M \simeq \beta \mathbb{I}$ and the state is again factorized and we obtain the same result as in (15.21):

$$\begin{cases} \beta \in \mathbb{R}_+ \\ a = \frac{(\mu P)^{2/5} \pi}{\sigma} \\ \sigma = \frac{1}{4} \left(\frac{9}{5} - n \right) \text{ and } \sigma > \frac{1}{5} \end{cases} \quad (15.41)$$

2. The second case is when $]0, 2[$ in $\beta \sim \frac{a}{d_{j_0}^n}$ ($a \in \mathbb{R}$). Since $\beta \ll \frac{1}{d_{j_0}}$ in this case, the real part of α is negligible compare to its imaginary part. Consequently since this imaginary part compensates the second derivative of the Regge action in the exponential of the second condition (15.7), we should go to the next order in δd_j . To compute this expansion in δd_j we need to know the next to leading order of the asymptotic expansion of the \tilde{j} -symbol. We can thus say nothing now in this case for the moment.
3. The third case, $\beta \sim \frac{a}{d_{j_0}}$ ($a \in \mathbb{R}$), is greatly simplified compared to the equivalent case for the decoupled gaussian wave-packet. Indeed, applying condition (15.6) and condition (15.7) to this state, we obtain the two following equations for \mathcal{N} and a :

$$\begin{cases} 1 \simeq \frac{1}{2^{10}\mathcal{N}^2} \left(\int d[\delta d_j] e^{-2\frac{a}{d_{j_0}}(\delta d_j)^2} \right)^{10} = \frac{1}{2^{10}\mathcal{N}^2} \left(\frac{\pi d_{j_0}}{2a} \right)^5 \\ 1 \simeq \frac{d_{j_0}^{10\sigma-9/2} \mu P}{2^{10}\mathcal{N}} \left(\int d[\delta d_j] e^{-\frac{a}{d_{j_0}}(\delta d_j)^2} \right)^{10} = \frac{d_{j_0}^{10\sigma-9/2} \mu P}{2^{10}\mathcal{N}} \left(\frac{\pi d_{j_0}}{a} \right)^5 \end{cases} \quad (15.42)$$

where we use to compute the second equation the same analysis as in the factorized gaussian state case. The key element which simplifies everything is that the second derivative of the Regge action added to the imaginary part of α is null since α imaginary part is the Hessian. This system of equations can then be simplified in a single equation for a :

$$\frac{1}{2^{10}} \left(\frac{\pi d_{j_0}}{2a} \right)^5 = \frac{d_{j_0}^{(20\sigma-9)} (\mu P)^2}{2^{20}} \left(\frac{\pi d_{j_0}}{a} \right)^{10} \quad (15.43)$$

which implies a condition on the normalization factor of the \tilde{j} -symbol in the spinfoam vertex:

$$\sigma = \frac{1}{5} \quad (15.44)$$

and the unique solution for a :

$$a = \frac{\pi(\mu P)^{2/5}}{2}. \quad (15.45)$$

Therefore, we now get the same value of a in this case as in the first case. Moreover, σ is now uniquely determined since $n = 1$.

□

This analysis on the consequences of conditions (15.6) and (15.7) on a coupled gaussian wave-packet (15.38) is therefore more convicting on the ability of such a state to capture a true physical rather than a too simple state defined as a factorized gaussian state. Indeed, the width α of the coupled gaussian state is now uniquely determined by the requirement of a normalized physical state.

Let us recall that in all our calculations presented in this Chapter, we used $K_1[s]$ the lowest order term in the expansion of the propagator kernel $K[s]$ in the group field theory coupling constant³ $\lambda - s$ symbolizes the 4-simplex boundary graph. The total propagator kernel $K[s]$ is given by $K[s] = \sum_{V=1}^{\infty} \lambda^V K_V[s]$. This operator

³The lowest order term in the expansion of the propagator kernel $K[s]$ in the group field coupling constant λ is in fact K_0 but we are expecting no contribution of zero order to the sum coming from K_0 [11].

should describe a unitary "evolution". In the spin foam framework the notion of evolution is not well-defined, however we can require the following normalization condition on $K[s]$

$$K[s]\bar{K}[s] = (K[s])^2 = 1 \quad (15.46)$$

that describes the process of creation of a 4-simplex starting from a null 4-volume following by the annihilation of this 4-simplex into a null 4-volume again. This condition also says that K is by definition a physical state. Using the λ expansion of $K[s] = \sum_{V=1}^{\infty} \lambda^V K_V[s]$, we can expand this normalization condition in power of λ

$$\sum_{V=1}^{\infty} \lambda^V \sum_{V_1, V_2 / V_1 + V_2 = V+1} K_{V_1} K_{V_2} = 1 \quad (15.47)$$

which simplifies at the leading order in λ in

$$\lambda^2 K_1[s]^2 = 1 \quad (15.48)$$

meaning that approximatively $\lambda K_1[s]$ is a physical state and introducing a new constraint on $\lambda K_1[s] = \lambda \mu \prod_{a < b} d_{jab}^{\sigma} \tilde{j}$. It is this new constraint which allows to determine μ :

$$(\lambda \mu)^2 = \frac{1}{(\prod_{a < b} d_{jab})^{2\sigma} \tilde{j}^2} \quad (15.49)$$

where $\sigma \geq 1/5$ in order that μ is finite. This restriction on the domain of validity of σ is consistent with the results obtained previously.

Since up to now we have only considered the lowest order term in the expansion of $K[s]$ in λ , we have in fact fixed the simplest bulk triangulation and taken into account only a finite number of degrees of freedom. The next step would be, keeping the same boundary spin network s , to explicitly write the next terms: K_2, K_3, \dots of the λ -expansion of $K[s] = \sum_{V=1}^{\infty} \lambda^V K_V[s]$. This is not obvious. A priori, K_4 could be determined from K_1 by doing a 5-1 move. Otherwise, from an effective field theory point of view we can write $K[s] = K_1[s] + k[s]$ where k takes into account all the possible counter-terms and therefore all the possible bulk geometries for a given boundary spin network. This is equivalent to look at a coarse-grained lattice in which all vertices can be considered as shrunk to a single effective vertex. $k[s]$ is then the weight associated to this effective vertex. In this weight $k[s]$, we are expected to get a term proportional to the Barrett-Crane spin foam vertex amplitude, $\epsilon \tilde{j}$, which would come from the contribution of the flat 4-simplex. Moreover, an additional contribution of the form $\rho \int dG P(G) \Gamma_{10j}(G)$ should come from the non-flat 4-simplices where $P(G)$ is a factor term and Γ_{10j} such that $\Gamma_{10j}(\mathbb{I}) = \tilde{j}$ takes into account the curvature. Otherwise, other terms should certainly appear in a more precise analysis. The issue would be then to determine which terms of $k[s]$ contribute in the requirement of a physical state for ψ_q ; that is, we should understand how the condition $\sum_{jab} K[d_{jab}] \psi(d_{jab}) = 1$ is explicitly modified by the term $k[d_{jab}]$ of $K[d_{jab}]$. We would expect that the requirement for the boundary state to be a physical state selects the bulk triangulation. It is the choice of the phase which seems to be important. The choice of a different phase for Ψ_q should select another bulk triangulation Γ which could not be flat anymore.

To conclude this chapter, let us summarize. In the context of 4d gravity we have investigated the consequences of the physical state requirement (11.4) for the Euclidean Barrett-Crane model for the simplest case of a space-time triangulation constructed from a single 4-simplex. In this context, we have shown that this requirement fixes uniquely the width of the quantum boundary state (in term of the classical data) similarly to what happens in the 3d toy model. The results presented above are therefore relevant in order to perform numerical computations in the context of the spin foam graviton propagator framework. Moreover, an important conclusion of this analysis is that a too simple boundary state, such as a factorized Gaussian state, does not easily capture a true physical state and that a better ansatz is to consider a more complicated state, such as a coupled gaussian state.

Chapter 16

Conclusion

In this last Chapter, we will recall some of the key-issues of the loop quantum gravity/spinfoam approaches and we will review the new results we have obtained while addressing these issues. We will also point out some problems which have been left open and some new questions that have arisen.

Our research has focused on the loop quantum gravity and spin foam frameworks [2, 3]. Loop quantum gravity has been established as a background independent and non perturbative quantization of general relativity, through the canonical quantization scheme. The loop quantum gravity kinematical aspects are well under control and its building blocks are the so-called *spin network states*. These provide a basis for the kinematical Hilbert space and diagonalize some geometric operators, such as the area operator. On the other side, the loop quantum gravity dynamical aspects are encoded in the Hamiltonian constraint and the physical states solving this constraint, i.e. the kernel of the constraint. They are still to be completely understood. As a tentative answer to this issue, the spin foam framework was introduced in order to provide a history formalism for loop quantum gravity, thus defining dynamics and transition amplitudes between spin network states. Spin foam models can also be naturally interpreted as a form of path integral approach to quantum gravity, the covariant approach, as opposed to the canonical approach which relies in splitting space-time into “space” and “time”. The spin foam framework has been the starting point of all our work.

Let us recall the main issues we discussed.

- (1.) This spin foam framework in 4d is based on the following observation: 4d general relativity can be seen as a topological theory (i.e. with non-local degrees of freedom) plus constraints (which reintroduce local degrees of freedom). The constraints are directly imposed at the quantum level and the key-issue is to understand how to implement these constraints to obtain a consistent quantum gravity model.
- (2.) The precise link between spin foam models and loop quantum gravity is still missing in 4d (for the 3d case, see [156]). Spin foam models and loop quantum gravity are different approaches which use different methods and lead to different results. For example, a discrepancy comes from the fact that most of the spin foam models for 4d gravity have been constructed as discretized path integral for constrained BF field theories with the Lorentz group $SL(2, \mathbb{C})$ as gauge group. Consequently, their boundary are resulting $SL(2, \mathbb{C})$ -invariant spin network states while the kinematical Hilbert space of loop quantum gravity is spanned by $SU(2)$ spin networks.
- (3.) The semi-classical limit is another important open issue in the loop quantum gravity/spin foam approaches. It is very important to understand the semi-classical features of the quantum gravity firstly to check that we can really recover gravity in the classical regime and secondly to calculate the corrections due to quantum gravitational effects in the semi-classical regime.

In Chapter 10, we addressed the issue (1.) in the context of Euclidean 4d gravity from an original perspective [6] which uses the recently developed $U(N)$ framework. We recall that in the spin foam quantization procedure, the simplicity constraints which turn the $SO(4)$ BF theory into 4d Euclidean gravity theory, are discretized and

have to be imposed on the Spin(4)-intertwiners from which are built the quantum states of geometry and the spinfoam transition amplitudes. The issue to implement the simplicity constraints without freezing too many local degrees of freedom comes from the fact that they do not form a closed algebra at the discrete level and cannot be imposed strongly.

We revisited the implementation of the discrete simplicity constraints [6] using the $U(N)$ framework initially developed for $SU(2)$ -intertwiners in [7, 8, 9]. Based on the Schwinger representation of the $\mathfrak{su}(2)$ Lie algebra in term of a couple of harmonic oscillators, this framework introduces a new set of $SU(2)$ -invariant operators acting on the space of $SU(2)$ -intertwiners. These operators act on pairs of legs (i, j) of the intertwiners: E_{ij} generates $U(N)$ transformations that deform the shape of the intertwiner, while F_{ij} and F_{ij}^\dagger act as annihilation and creation operators consistent with the $U(N)$ -action. The key result of this approach is that these $SU(2)$ -invariant observables form a closed algebra.

In the spinfoam context, we deal with the Spin(4)-intertwiners. Using the decomposition of $\text{Spin}(4) = SU(2)_L \times SU(2)_R$ in left and right sectors, we now have invariant operators acting on both sectors $E_{ij}^{L,R}, F_{ij}^{L,R}, F_{ij}^{L,R\dagger}$ which can be used to investigate how to impose the simplicity constraints. More precisely, the idea we developed has been to recast the discrete simplicity constraints in term of observables – defined in term of the $U(N)$ operators – that form a closed algebra. At the end of the day, it allowed us to propose a set of $U(N)$ coherent states that solve the simplicity constraints weakly at large scale for arbitrary values of the Immirzi parameter.

More precisely, we have reviewed the $U(N)$ coherent states introduced in [9]. For a N -valent $SU(2)$ -intertwiner, they are labeled by the total area $J = \sum_i j_i$ and a set of N spinors z_k . These coherent states $|J, \{z_k\}\rangle$ form an over-complete basis for the space of $SU(2)$ -intertwiners at fixed area J and are simply related to the Livine-Speziale coherent intertwiners [106]. Moreover, we gave explicitly the action of the $SU(2)$ invariant operators on these $U(N)$ coherent states as differential operators. As such, we have firstly completed the analysis of the $U(N)$ framework for $SU(2)$ -intertwiners initiated in [7, 8, 9].

Secondly, we have applied these new $U(N)$ tools to the analysis of the simplicity constraints for Spin(4)-intertwiners. The simplicity constraints couple the left and right sectors of the intertwiners. We have focused in re-expressing them in term of the E, F, F^\dagger operators of the $U(N)$ formalism. Following the usual approach, we have always distinguished the diagonal simplicity constraints from the cross simplicity constraints. The diagonal constraints act on single legs of the intertwiner and require that the Spin(4)-representation living on a leg i be simple i.e. that the left and right spins are equal $j_i^L = j_i^R$ (or $j_i^L = \rho j_i^R$ for a non-trivial Immirzi parameter). These diagonal constraints are always imposed strongly on the intertwiner states. On the other hand, the cross simplicity constraints deal with pairs of legs and are standardly solved weakly in the most recent spinfoam models i.e. only in expectation value (with minimal uncertainty). We started by showing that the discrete simplicity constraints which do not form a closed algebra can be replaced by a new set of constraints $\{C_{ij}\}$ which forms a $\mathfrak{u}(N)$ -algebra. These new $\mathfrak{u}(N)$ simplicity constraints are very simply constructed in terms of the E -operators. We also explored other possibilities of constraint operators based on the operators F and F^\dagger . In the end, it appeared that distinguishing the diagonal constraints from the cross constraints and imposing the first strongly while solving the later only weakly always lead to difficulties. Thus, in the last part of our work, we proposed to put all (diagonal and cross) simplicity constraints on the same footing and to solve all of them at once in a weak way. This led us to introduce constraints $F_{ij}^L - F_{ij}^R = 0$ involving only annihilation operators. These constraints can be considered as the holomorphic constraints of the Gupta-Bleuler quantization procedure. Solving them in term of $U(N)$ coherent states provided us with weak solutions to all simplicity constraints, for arbitrary values of the Immirzi parameter.

The next important question to explore is how to generalize this framework to the Lorentzian case in order to check whether it is also possible to construct coherent states which could solve all simplicity constraints with an arbitrary Immirzi parameter. Another issue is to understand how to glue these $U(N)$ coherent intertwiners consistently into spin network states in order to generalize our analysis to triangulations formed of an arbitrary number of polyhedra glued together. Finally, we hope that the introduction of these $U(N)$ coherent states as a basis of the boundary physical Hilbert space of spinfoam model could help to understand the symmetries of the spinfoam amplitudes and their behavior under (discrete) deformations or diffeomorphisms.

In Chapter 9, we have addressed the issue (2.) in the context of the Lorentz 4d quantum gravity investigating

the correspondence between the $SU(2)$ spin network states of the canonical loop quantum gravity framework and the projected spin networks arising in spin foam models [5]. We first introduced the projection map from projected cylindrical functions down to $SU(2)$ cylindrical functions. Reversely, we have studied the lifting maps allowing to inverse this projection map and raise $SU(2)$ spin network to projected spin networks on $SL(2, \mathbb{C})$. We have obtained a whole family of such lifting maps, parameterized by the Immirzi parameter. In this way, we established an isomorphism between the space of $SU(2)$ spin networks and the space of proper projected cylindrical functions at fixed Immirzi parameter. We have also shown that allowing the Immirzi parameter to run through all possible real values, we sweep the whole space of proper projected cylindrical functions. Finally, we have analyzed the differences between the two scalar products respectively for $SU(2)$ functionals and $SL(2, \mathbb{C})$ functionals, and we have explained how to modify the lifting maps so as to ensure that these two scalar products match exactly.

This work hints towards considering that the most useful perspective would be to compare $SU(2)$ spin networks to projected spin networks and not directly to $SL(2, \mathbb{C})$ spin networks as was done in recent work on bridging between the EPRL-FK spinfoam models and the canonical approach [118].

Physically, $SL(2, \mathbb{C})$ spin networks erase all data about the time-normal field, which is actually instrumental in properly implementing the simplicity constraints. Mathematically, both $SU(2)$ spin networks and projected spin networks involve $SU(2)$ intertwiners, which allows for a direct map between the two Hilbert spaces. Therefore, we propose to use consistently projected spin networks as boundary states for the EPRL-FK spinfoam models and we hope that the present work will be useful in order to consistently translate loop quantum gravity's dynamics into spinfoam amplitudes.

We would like to also point out that our projected cylindrical functions obtained through a lift of $SU(2)$ spin networks look similar to the recently introduced “holomorphic” spin network functionals introduced to study the semi-classical behavior of the EPRL-FK spin amplitudes [157, 158]. We think that this is an issue worth studying in more details.

Finally, we hope that the relation between $SU(2)$ spin networks and projected functionals which we uncovered will trigger more interest in studying the structure of the space of projected spin networks. More particularly, we would like to put emphasis on two issues. First, it would be interesting to understand the geometrical interpretation of un-proper projected spin networks i.e. states carrying two different spins per edge $j_e^s \neq j_e^t$ (when the spin along an edge is different at its source vertex and at its target vertex). Then, it would be interesting to investigate the coarse-graining of projected cylindrical functions and see if we can construct a projective limit à la Ashtekar-Lewandowski as was done in loop quantum gravity [58]. Such techniques have failed up to now when applied to spin network states for non-compact gauge groups such as the Lorentz group $SL(2, \mathbb{C})$. Nevertheless, we believe that this could be different when dealing with projected spin networks due to their effective $SU(2)$ gauge invariance and their mapping into $SU(2)$ spin networks.

In both Chapters 13 and 14, we have focused on the issue (3.) in the context of 3d gravity. In order to better understand the low-energy regime interpretation of the spin foam model, we investigated in Chapter 13 the asymptotical behavior of the $\{6j\}$ -symbol which is relevant in the construction of spin foam amplitudes. Starting from its expression as a (finite) sum over (half-)integers of algebraic combinations of factorials, we followed the footsteps of [152] and showed that one can derive systematically the corrections to the leading order formula at any order [12]. The method relied on three steps. First, we used the Stirling formula (with the appropriate corrections) to approximate the factorials. Second, we considered the sum as a Riemann sum and approximate it by an integral (over the real line). Finally, we performed a saddle point approximation to compute the behavior of the $\{6j\}$ -symbol for (homogeneously) large spins.

Using this framework, we showed that we recover an oscillating leading order (LO) with frequency given by the Regge action as is well-known and was already proved in [152]. Then we computed analytically the next-to-leading (NLO) corrections. The formula that we obtained is explicit, although not compact, and we could not interpret it geometrically in a clear way. Nevertheless, we performed two simple checks. First, we checked that our complicated formula reduced to the known expression for the NLO for isosceles tetrahedra [145]. Second, we checked it numerically in various cases and found a perfect fit. These numerical simulations also confirmed that the NLO is a $\frac{\pi}{2}$ -phase shift with respect to the LO (the NLO is given by a sin instead of a cos) and that the NNLO is back in phase with the LO (again a cos), which confirmed our expectation of an

alternating asymptotical series in $\cos + \frac{1}{j} \sin + \frac{1}{j^2} \cos + \frac{1}{j^3} \sin + \dots$.

We point out that we computed in details the corrections due to the Stirling formula and to the saddle point approximation. However we did not study the Riemann sum approximation. It does not contribute to the LO and NLO. It will only enter at the level of the NNLO.

This work, mainly technical, can be applied to the computation of gravitational correlations for 3d quantum gravity following [10, 141, 145, 146]. It will enter the quantum corrections to the propagator/correlations at second order, as was shown in [141]. Indeed, the first order corrections are derived from the path integral of the Regge action, while the deviations from the Regge action as computed here enter at second order (as two-loop corrections). From this perspective, this NLO of the $\{6j\}$ -symbol describes the leading order deviation of quantum gravity with respect to the classical gravity.

Beyond the technicality of these results, our purpose was to show that computing such corrections is indeed possible (although it does lead to complicated expressions) and that similar methods could be used for 4d spinfoam gravity. Although these methods allow straightforward (but lengthy) analytical calculations, which might be handled by a computer program, their drawback is the loss of the geometrical meaning of the expressions obtained. An alternative way to proceed is to use the exact recursion relations satisfied by the $\{6j\}$ -symbol (see [149, 150]) and other spinfoam amplitudes (see [154]) to probe the asymptotic behavior and the induced corrections of the correlations.

In Chapter 14, we have actually studied this alternative method in the context of 3d gravity [13]. We have used the recursion relation satisfied by the $\{6j\}$ -symbol to study the structure of its asymptotical expansion for large spins. The exact recursion relation allowed us to compute explicitly the asymptotical approximation of the isosceles $\{6j\}$ -symbol up to fourth order. This confirmed previous results [145, 12] and introduced techniques allowing further systematic analytical calculations of the corrections to the behavior of the $\{6j\}$ -symbol at large spins. However a clear and simple geometrical interpretation of the polynomials appearing in this expansion is still missing.

This work using recursion relation is useful in particular for the study of large scale correlations in the spinfoam model for 3d quantum gravity. In this context, the recursion relation allowed us to write equations satisfied by the spinfoam correlations similar to the Ward identities of standard quantum field theory. Such recursion techniques have been shown to be further applied to the study of 4d spinfoam amplitudes and the resulting spinfoam graviton propagator [154].

A framework to address issue (3.) is the spin foam graviton proposal [10]. The graviton propagator is based on the extraction of some semi-classical correlations at large scale thanks to a suitable boundary state peaked on a given classical 3-geometry. One issue which has not been explored up to now in the context of 4d gravity is that this boundary state should be physical, i.e. solve the Hamiltonian constraint on the 3d boundary. We addressed this issue in Chapter 15 and showed that it is possible to determine a physical semi-classical state for the Barrett-Crane model in the case of the simplest triangulation given by a 4-simplex [15]. The requirement of a normalized physical state determines uniquely the Gaussian width. This analysis showed also that we cannot take a too simple semi-classical state. Indeed, we have seen that a decoupled gaussian state which is peaked on the geometry of an equilateral 4-simplex does not seem to be able to capture a true physical state. Instead, a coupled gaussian state appears as defining more naturally a physical semi-classical state.

Our analysis seemed to indicate that the requirement for the boundary state to be a physical state selects the bulk triangulation. However, a detailed investigation dealing with more refined boundary states is required to confirm this intuition and to really understand the dominant terms in the computation of the two-point function of the gravitational field.

Another step would be to deal with the EPRL-FK models instead of the Barrett-Crane model. Since the EPRL-FK vertex has also for asymptotic the exponential of the Regge action, we expect to get similar results in the restricted case of a single 4-simplex. However, the behavior under renormalization should be quite different since the space of intertwiners in the EPRL-FK model introduces new degrees of freedom in the 3d space geometry compared to the Barrett-Crane geometry which is describe by a unique intertwiner and seems to have too many degrees of freedom frozen. These degrees of freedom will have to be taken into account when gluing 4-simplices together.

Some key-issues of the spin foam framework for quantum gravity have been tackled here and some relevant results proposed. There have been many techniques developed to build and to study the spin foam amplitudes but there are still a lot of issues to clear up and understand, much more than what has already be done! For example, one issue not really taken into account yet concerns the issue of the renormalization in the spin foam models. Indeed, an important aspect to keep in mind is that it is fundamental to develop a framework with the appropriate tools to study the coarse-graining of spin foam amplitudes in order to truly define the continuum limit of spinfoam models and their semi-classical limit. And beyond this, we need to identify a family of models parametrized by a finite number of parameters. That is, we need to understand what are the physical relevant coupling constants such as it has been done in standard quantum field theory and to identify a family of spin foam models stable under coarse-graining.

To be continued....

Appendix A

Quick Overview of $\text{SL}(2, \mathbb{C})$ Representations

The Plancherel decomposition formula for $\text{SL}(2, \mathbb{C})$ states that L^2 functions with respect to the Haar measure on $\text{SL}(2, \mathbb{C})$ uniquely decompose in term of the matrix elements of the group element in the unitary irreducible representations of $\text{SL}(2, \mathbb{C})$ of the principal series. Such irreducible representation (irreps) are labeled by a couple of numbers (n, ρ) , where $n \in \mathbb{N}/2$ is a half-integer and $\rho \in \mathbb{R}$ a real number. There also exists a supplementary series of unitary irreps, labeled by a single real number bounded by 1 in modulus, but they do not enter the Plancherel decomposition. Then the Plancherel formula for a function $f \in L^2(\text{SL}(2, \mathbb{C}))$ reads:

$$f(G) = \frac{1}{8\pi^4} \sum_n \int \mu(n, \rho) d\rho \text{tr} \left[F(n, \rho) D^{(n, \rho)}(G) \right], \quad (\text{A.1})$$

where the Fourier components $F(n, \rho)$ are matrices in the Hilbert space of the representation (n, ρ) and are obtained by the reverse formula:

$$F(n, \rho) = \int dG f(G) D^{(n, \rho)}(G^{-1}). \quad (\text{A.2})$$

The measure of integration over the representation labels $\mu(n, \rho) d\rho \equiv (n^2 + \rho^2) d\rho$ is called by the Plancherel measure. This Plancherel decomposition relies on the fact that the matrix elements $D^{(n, \rho)}(G)$ form an orthogonal basis for the Hilbert space $L^2(\text{SL}(2, \mathbb{C}))$.

It will be useful for later to have the explicit action of the Lorentz generators in each (n, ρ) representation. The relevant basis for us is the $\text{SU}(2)$ basis obtained by decomposing the $\text{SL}(2, \mathbb{C})$ representation into $\text{SU}(2)$ irreducible representations. Indeed, one can show that the (n, ρ) representation decomposes onto all $\text{SU}(2)$ irreps with spin j bounded below by the half-integer n , thus implying that the Hilbert space of the (n, ρ) representation is the direct sum of the Hilbert spaces corresponding to these $\text{SU}(2)$ irreps:

$$R^{(n, \rho)} = \bigoplus_{j \in n + \mathbb{N}} V^j. \quad (\text{A.3})$$

Let us point out that we have chosen the canonical $\text{SU}(2)$ subgroup, which stabilizes the 4-vector ω or equivalently the identity matrix $\Omega = \mathbb{I}$ (as explained previously). Then we give the action of the $\mathfrak{su}(2)$ -rotation generators \vec{J} and boost generators \vec{K} in the standard basis for $\text{SU}(2)$ -representations in term of the spin j and the magnetic momentum m , diagonalizing the rotation operator J^3 :

$$J^3 |j, m\rangle = m |j, m\rangle, \quad (\text{A.4})$$

$$\begin{aligned} J^+ |j, m\rangle &= \sqrt{(j-m)(j+m+1)} |j, m+1\rangle, \\ J^- |j, m\rangle &= \sqrt{(j+m)(j-m+1)} |j, m-1\rangle, \\ K^3 |j, m\rangle &= -\alpha_j \sqrt{j^2 - m^2} |j-1, m\rangle - \beta_j m |j, m\rangle + \alpha_{j+1} \sqrt{(j+1)^2 - m^2} |j+1, m\rangle, \end{aligned} \quad (\text{A.5})$$

$$\begin{aligned}
K^+ |j, m\rangle &= -\alpha_j \sqrt{(j-m)(j-m-1)} |j-1, m+1\rangle - \beta_j \sqrt{(j-m)(j+m+1)} |j, m+1\rangle \\
&\quad - \alpha_{j+1} \sqrt{(j+m+1)(j+m+2)} |j+1, m+1\rangle, \\
K^- |j, m\rangle &= \alpha_j \sqrt{(j+m)(j+m-1)} |j-1, m-1\rangle - \beta_j \sqrt{(j+m)(j-m+1)} |j, m-1\rangle \\
&\quad + \alpha_{j+1} \sqrt{(j-m+1)(j-m+2)} |j+1, m-1\rangle,
\end{aligned}$$

where the coefficients defining the action of the boost generators are given by:

$$\beta_j = \frac{n\rho}{j(j+1)}, \quad \alpha_j = \frac{i}{j} \sqrt{\frac{(j^2 - n^2)(j^2 + \rho^2)}{4j^2 - 1}}. \quad (\text{A.6})$$

It is straightforward to check that this postulated action satisfied as expected the $\text{SL}(2, \mathbb{C})$ commutation relations¹. Moreover, since the coefficient $\alpha_n = 0$ vanishes for $j = n$, it is also clear that the truncation to spins $j \geq n$ is self-consistent. On the other hand, it is obvious that the coefficients α_j for $j > n$ will never vanish, thus there is no upper bound on the spin j . This is consistent with the fact that a unitary representation of $\text{SL}(2, \mathbb{C})$ necessarily has an infinite dimension.

From this action, we can check that the $\text{SU}(2)$ Casimir operator has the usual value $\vec{J}^2 = j(j+1)$. We can also compute the values of the two Casimir operators of $\text{SL}(2, \mathbb{C})$:

$$C_1 = \vec{K}^2 - \vec{J}^2 = \rho^2 - n^2 + 1, \quad C_2 = \vec{J} \cdot \vec{K} = 2n\rho. \quad (\text{A.7})$$

Finally, we introduce the characters of the $\text{SL}(2, \mathbb{C})$ representations, $\Theta^{(n, \rho)}(G) \equiv \text{tr } D^{(n, \rho)}(G)$. It is easy to evaluate it on $\text{SU}(2)$ group elements since we know the decomposition of the $\text{SL}(2, \mathbb{C})$ representation into $\text{SU}(2)$ representations²:

$$\forall g \in \text{SU}(2), \Theta^{(n, \rho)}(g) = \sum_{j \in n + \mathbb{N}} \chi^j(g) = \sum_{j \in n + \mathbb{N}} \frac{\sin(2j+1)\theta}{\sin \theta} = \frac{\cos 2n\theta}{2 \sin^2 \theta}, \quad (\text{A.8})$$

where θ is the class angle of the group element g , i.e meaning that g is conjugate to the diagonal matrix with entries $[e^{i\theta}, e^{-i\theta}]$.

Now that we have quickly reviewed these basic facts on $\text{SL}(2, \mathbb{C})$ unitary representations and the Plancherel decomposition, we are ready to introduce the basis of projected spin networks for our Hilbert space \mathcal{H} of Lorentz invariant cylindrical functions.

¹The commutation relation of the $\text{SL}(2, \mathbb{C})$ Lie algebra are:

$$\begin{aligned}
[J^+, J^3] &= -J^+, \quad [J^-, J^3] = J^-, \quad [J^+, J^-] = 2J^3 \\
[J^+, K^+] &= [J^-, K^-] = [J^3, K^3] = 0, \quad [J^+, K^-] = -[J^-, K^+] = 2K^3, \\
[J^+, K^3] &= -K^+, \quad [J^-, K^3] = K^-, \quad [K^+, J^3] = -K^+, \quad [K^-, J^3] = K^-, \\
[K^+, K^3] &= J^+, \quad [K^-, K^3] = -J^-, \quad [K^+, K^-] = -2J^3.
\end{aligned}$$

²The character formula is straightforwardly generalizable to the whole $\text{SL}(2, \mathbb{C})$ group. Indeed, all group elements are conjugated to a diagonal matrix. Then we can evaluate the character on such matrices (see e.g. [159]):

$$\Theta_{(n, \rho)} \left(\begin{pmatrix} e^{\lambda+i\theta} & 0 \\ 0 & e^{-\lambda-i\theta} \end{pmatrix} \right) = \frac{e^{i\rho\lambda} e^{i2n\theta} + e^{-i\rho\lambda} e^{-i2n\theta}}{|e^{\lambda+i\theta} - e^{-\lambda-i\theta}|^2}.$$

Appendix B

Coherent States for the Harmonic Oscillator

Let us review the standard definition of coherent states for a single harmonic oscillator, defined by its creation and annihilation operators satisfying the commutation relation $[a, a^\dagger] = 1$. The standard basis is defined by the number of quanta:

$$a|n\rangle = \sqrt{n}|n-1\rangle, \quad a^\dagger|n\rangle = \sqrt{n+1}|n+1\rangle, \quad a^\dagger a|n\rangle = n|n\rangle. \quad (\text{B.1})$$

Coherent states are defined through a sum over the standard basis:

$$|z\rangle = \sum_n \frac{z^n}{\sqrt{n!}} |n\rangle = \sum_n \frac{z^n}{\sqrt{n!}} \frac{(a^\dagger)^n}{\sqrt{n!}} |0\rangle = e^{z a^\dagger} |0\rangle. \quad (\text{B.2})$$

This definition is not normalized, but we can easily compute its norm and define normalized states:

$$\langle z|z\rangle = e^{|z|^2}, \quad |z\rangle_N \equiv e^{-\frac{|z|^2}{2}} |z\rangle. \quad (\text{B.3})$$

The action of the a, a^\dagger operators can be derived directly from the definition of the coherent states as series. The coherent states diagonalize the annihilation operator a while the creation operator a^\dagger acts as a derivation:

$$a|z\rangle = z|z\rangle, \quad a^\dagger|z\rangle = \sum_{n \geq 1} n \frac{z^{n-1}}{\sqrt{n!}} |n\rangle = \partial_z |z\rangle. \quad (\text{B.4})$$

This action can be straightforwardly on the normalized coherent states. Then we get a anti-holomorphic shift in the a^\dagger action:

$$a|z\rangle_N = z|z\rangle_N, \quad a^\dagger|z\rangle_N = \partial_z e^{-\frac{|z|^2}{2}} |z\rangle = \left(\partial_z - \frac{\bar{z}}{2}\right) |z\rangle_N. \quad (\text{B.5})$$

The coherent states naturally provides an over-complete basis and a new decomposition of the identity:

$$\begin{aligned} \int \frac{d^2 z}{\pi} |z\rangle_N \langle z| &= \int \frac{d^2 z}{\pi} e^{-|z|^2} |z\rangle \langle z| = \sum_{m,n} \frac{|m\rangle \langle n|}{\sqrt{m!} \sqrt{n!}} \int \frac{d^2 z}{\pi} e^{-|z|^2} \bar{z}^n z^m \\ &= \sum_{m,n} \frac{|m\rangle \langle n|}{\sqrt{m!} \sqrt{n!}} \int_0^{+\infty} dr e^{-r^2} r^{m+n+1} \int_0^{2\pi} \frac{d\theta}{\pi} e^{i(m-n)\theta} \\ &= \sum_n \frac{2}{n!} |n\rangle \langle n| \int_0^{+\infty} dr e^{-r^2} r^{2n+1} = \mathbb{I}. \end{aligned} \quad (\text{B.6})$$

We can also check explicitly that the action of a^\dagger on coherent states is correctly given by the adjoint of the action of the annihilation operator a :

$$\int [d^2 z d^2 w] \overline{\phi(z)} \psi(w) \langle z|a^\dagger|w\rangle = - \int [d^2 z d^2 w] \overline{\phi(z)} \partial_w \psi(w) \langle z|w\rangle = \int [d^2 z d^2 w] \overline{\phi(z)} \psi(w) \partial_w (e^{\bar{z}w})$$

$$= \int [d^2 z d^2 w] \bar{z} \overline{\phi(z)} \psi(w) \langle z|w \rangle = \int [d^2 z d^2 w] \overline{\phi(z)} \psi(w) \langle az|w \rangle. \quad (\text{B.7})$$

Finally, these coherent states transform consistently under the $U(1)$ -action generated by the number of quanta operator $a^\dagger a$:

$$e^{i\tau a^\dagger a} |z\rangle = \sum_n \frac{z^n}{\sqrt{n!}} e^{i\tau n} |n\rangle = |e^{i\tau} z\rangle. \quad (\text{B.8})$$

Appendix C

Commutation Relations Of the E, F, F^\dagger Action on Coherent States

The commutation relations between these F, F^\dagger and E operators acting on the $U(N)$ coherent states are straightforward to check:

$$\begin{aligned} [E_{ij}, E_{kl}] |J, \{z_q\}\rangle &= \delta_{kl}^z (\delta_{ij}^z (|J, \{z_k\}\rangle)) - \delta_{ij}^z (\delta_{kl}^z (|J, \{z_k\}\rangle)) \\ &= (\delta_{kj} \delta_{il}^z - \delta_{il} \delta_{kj}^z) |J, \{z_q\}\rangle = (\delta_{jk} E_{il} - \delta_{il} E_{kj}) |J, \{z_q\}\rangle, \end{aligned} \quad (C.1)$$

$$\begin{aligned} [E_{ij}, F_{kl}] |J, \{z_q\}\rangle &= \sqrt{J(J+1)} (Z_{kl} \delta_{ij}^z (|J-1, \{z_q\}\rangle) - \delta_{ij}^z (Z_{kl} |J-1, \{z_q\}\rangle)) \\ &= \sqrt{J(J+1)} (\delta_{il} Z_{jk} - \delta_{ik} Z_{jl}) |J-1, \{z_q\}\rangle \\ &= (\delta_{il} F_{jk} - \delta_{ik} F_{jl}) |J, \{z_q\}\rangle, \end{aligned} \quad (C.2)$$

$$\begin{aligned} [E_{ij}, F_{kl}^\dagger] |J, \{z_q\}\rangle &= \frac{1}{\sqrt{(J+1)(J+2)}} (\Delta_{kl}^z (\delta_{ij}^z (|J+1, \{z_q\}\rangle)) - \delta_{ij}^z (\Delta_{kl}^z (|J+1, \{z_q\}\rangle))) \\ &= \frac{1}{\sqrt{(J+1)(J+2)}} (\delta_{kj} \Delta_{il}^z - \delta_{lj} \Delta_{ik}^z) |J+1, \{z_q\}\rangle \\ &= (\delta_{kj} F_{il}^\dagger - \delta_{lj} F_{ik}^\dagger) |J, \{z_q\}\rangle, \end{aligned} \quad (C.3)$$

$$\begin{aligned} [F_{ij}, F_{kl}^\dagger] |J, \{z_q\}\rangle &= \Delta_{kl}^z (Z_{ij} |J, \{z_q\}\rangle) - Z_{ij} \Delta_{kl}^z (|J, \{z_q\}\rangle) \\ &= (\delta_{ki} \delta_{lj}^z - \delta_{kj} \delta_{li}^z - \delta_{li} \delta_{kj}^z + \delta_{lj} \delta_{ki}^z + \Delta_{kl}^z (Z_{ij})) |J, \{z_q\}\rangle \\ &= (\delta_{ki} E_{lj} - \delta_{kj} E_{li} - \delta_{li} E_{kj} + \delta_{lj} E_{ki} + 2(\delta_{ki} \delta_{lj} - \delta_{li} \delta_{kj})) |J, \{z_q\}\rangle. \end{aligned} \quad (C.4)$$

Appendix D

Norm of the $U(N)$ -invariant state: $|J\rangle$

Following the previous work done in [136], we compute the norm of the $U(N)$ -invariant state $|J\rangle = (f^\dagger)^J|0\rangle$ where we have introduced the operator:

$$f^\dagger = \sum_{kl} F_{kl}^{L\dagger} F_{kl}^{R\dagger}. \quad (\text{D.1})$$

The norm of $|J\rangle$ is then given by:

$$\langle 0|f^J(f^\dagger)^J|0\rangle \quad (\text{D.2})$$

with $f = \sum_{kl} F_{kl}^L F_{kl}^R$. We need to determine the action of f on $|J\rangle$: $f|J\rangle = f(f^\dagger)^J|0\rangle$. In order to compute this action of f on $|J\rangle$, we calculate the commutator between f and f^\dagger :

$$[f, f^\dagger] = 4e \left(\frac{E^L + E^R}{2} \right) + 4 \left(\frac{1}{2} (E^L + E^R)^2 + (E^L + E^R)(2N - 1) + 2N(N - 1) \right) \quad (\text{D.3})$$

where we have defined:

$$e = \sum_{kl} E_{kl}^L E_{kl}^R \quad (\text{D.4})$$

and we recall that $E^{L/R} = \sum_i E_i^{L/R}$. In our case of interest $E^L = E^R = E$. Moreover, to compute this commutator we used the fact that on the intertwiner space ($\vec{J}^L = \vec{J}^R = 0$), the F and F^\dagger operators satisfy additional quadratic constraints:

$$\sum_k \left(F_{ki}^{L/R} \right)^\dagger F_{kj}^{L/R} = E_{ij}^{L/R} \left(\frac{E^{L/R}}{2} + 1 \right), \quad \sum_k F_{kj}^{L/R} \left(F_{ki}^{L/R} \right)^\dagger = (E_{ij}^{L/R} + 2\delta_{ij}) \left(\frac{E^{L/R}}{2} + N - 1 \right). \quad (\text{D.5})$$

We also need to compute the commutator between e and f^\dagger . We use the fact that the E and F^\dagger also satisfy quadratic constraints on the intertwiner space:

$$\sum_k \left(F_{ik}^{L/R} \right)^\dagger E_{jk}^{L/R} = \left(F_{ij}^{L/R} \right)^\dagger \frac{E^{L/R}}{2}, \quad \sum_k E_{jk}^{L/R} \left(F_{ik}^{L/R} \right)^\dagger = \left(F_{ij}^{L/R} \right)^\dagger \left(\frac{E^{L/R}}{2} + N - 1 \right), \quad (\text{D.6})$$

then,

$$[e, f^\dagger] = 2f^\dagger \left(\frac{E^L + E^R}{2} + N - 1 \right) \quad (\text{D.7})$$

where once again, E^L and E^R can be replaced by E . Moreover, this total area operator is clearly diagonal in the basis $|J\rangle$:

$$E|J\rangle = 2J|J\rangle \quad (\text{D.8})$$

We can then deduce the action of f on $|J\rangle$:

$$f(f^\dagger)^J|0\rangle = \sum_{k=0}^{J-1} \{ 4(2(J-1-k) + N)(f^\dagger)^k e (f^\dagger)^{J-1-k}|0\rangle + 16(2(J-1-k)^2 + (J-1-k)(2N-1))(f^\dagger)^{J-1}|0\rangle \}$$

$$\begin{aligned}
& +8(J-1)N(N-1)(f^\dagger)^{J-1}|0\rangle \\
= & \left[\sum_{k=0}^{J-1} \{8(2(J-1-k) + N)(J-1-k)(J+N-k-3) + 16(2(J-1-k)^2 + (J-1-k)(2N-1))\} \right. \\
& \left. +8(J-1)N(N-1)|J-1\rangle \right] \\
= & 4J(J+1)(N+J-1)(N+J-2)|J-1\rangle
\end{aligned} \tag{D.9}$$

Using this action, we compute the norm of the state $|J\rangle$ by recursion:

$$\langle J|J\rangle = \langle 0|f^{J-1}f|J\rangle = 4J(J+1)(N+J-1)(N+J-2)\langle J-1|J-1\rangle \tag{D.10}$$

which leads us to the scalar product:

$$\langle J|J\rangle = 2^{2J} J!(J+1)! \frac{(N+J-1)!(N+J-2)!}{(N-1)!(N-2)!} \tag{D.11}$$

Appendix E

The $\{6j\}$ -symbol - recoupling theory

The $\{6j\}$ -symbol is a real number and it is obtained by combining four normalized Clebsh-Gordan coefficients along the six edges of a tetrahedron, with edge lengths given by $j_{IJ} + \frac{1}{2} = \frac{d_{j_{IJ}}}{2}$ ($0 \leq I < J \leq 3$). We usually

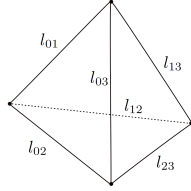


Figure E.1: Tetrahedron: edge lengths are given by $l_{IJ} = \frac{d_{j_{IJ}}}{2}$

express the $6j$ -symbol in term of the Wigner $3j$ -symbols :

$$\left\{ \begin{matrix} j_{01} & j_{02} & j_{03} \\ j_{23} & j_{13} & j_{12} \end{matrix} \right\} = \sum_{\alpha} (-1)^{j_{01}+j_{03}+j_{01}-\alpha_{01}-\alpha_{03}-\alpha_{01}} \begin{pmatrix} j_{01} & j_{12} & j_{13} \\ \alpha_{01} & \alpha_{12} & -\alpha_{13} \end{pmatrix} \begin{pmatrix} j_{13} & j_{23} & j_{03} \\ \alpha_{13} & \alpha_{23} & \alpha_{03} \end{pmatrix} \begin{pmatrix} j_{03} & j_{02} & j_{01} \\ \alpha_{03} & \alpha_{02} & -\alpha_{01} \end{pmatrix} \begin{pmatrix} j_{02} & j_{23} & j_{12} \\ \alpha_{02} & \alpha_{23} & \alpha_{12} \end{pmatrix}. \quad (\text{E.1})$$

The Wigner $3j$ symbols are very simply related to the Clebsh-Gordan coefficients $\langle j_{01}j_{12}\alpha_{01}\alpha_{12}|j_{13}\alpha_{13} \rangle$ by:

$$\langle j_{01}j_{12}\alpha_{01}\alpha_{12}|j_{13}\alpha_{13} \rangle = (-1)^{j_{01}-j_{12}+\alpha_{13}} (2j_{13} + 1/2)^{1/2} \begin{pmatrix} j_{01} & j_{12} & j_{13} \\ \alpha_{01} & \alpha_{12} & -\alpha_{13} \end{pmatrix},$$

And Racah gave a general formulae for the Clebsh-Gordan coefficient:

$$\begin{aligned} \langle j_{01}j_{12}\alpha_{01}\alpha_{12}|j_{13}\alpha_{13} \rangle &= \delta(\alpha_{01} + \alpha_{12}, \alpha_{13}) \Delta(j_{01}j_{12}j_{13}) \\ &\quad \sqrt{(2j_{13} + 1)(j_{01} + \alpha_{01})!(j_{01} - \alpha_{01})!(j_{12} + \alpha_{12})!(j_{12} - \alpha_{12})!(j_{13} + \alpha_{13})!(j_{13} - \alpha_{13})!} \\ &\quad \sum_{\mu} \frac{(-1)^{\mu}}{(j_{01}-\alpha_{01}-\mu)!(j_{13}-j_{12}+\alpha_{01}+\alpha)(j_{12}+\alpha_{12}-\mu)!(j_{13}-j_{01}-\alpha_{12}+\alpha)! \mu! (j_{01}+j_{12}-j_{13}-\mu)!} \end{aligned}$$

where $\Delta(j_{01}, j_{12}, j_{13}) = \frac{(j_{01}+j_{12}-j_{13})!(j_{01}-j_{12}+j_{13})!(-j_{01}+j_{12}+j_{13})!}{(j_{01}+j_{12}+j_{13}+1)!}$ From these, Racah gave a tensorial formulae for the $6j$ -symbol, the Racah's single sum formulae:

$$\left\{ \begin{matrix} j_{01} & j_{02} & j_{03} \\ j_{23} & j_{13} & j_{12} \end{matrix} \right\} = \frac{\sqrt{\Delta(j_{01}, j_{02}, j_{03})\Delta(j_{23}, j_{02}, j_{12})\Delta(j_{23}, j_{13}, j_{03})\Delta(j_{01}, j_{13}, j_{12})}}{\sum_{\substack{\min p_j \\ \max v_I}} (-1)^t \frac{(t+1)!}{\prod_i (t-v_I)! \prod_j (p_j-t)!}} \quad (\text{E.2})$$

with $v_K = \sum_{I \neq K} j_{IK} \forall K \in \{0, \dots, 3\}$ and $p_k = \sum_{i \neq 0, k} (j_{0i} + j_{ki}) \forall k \in \{1 \dots 3\}$.

Appendix F

Factorials

The factorial $n!$ is defined for a positive integer n as:

$$n! \equiv n(n-1) \cdots 2 \cdot 1 = \Gamma(n+1),$$

where $\Gamma(n)$ is the gamma function for integers n . This definition is generalized to non-integer values. Using the identities for the Γ function, we write explicitly the values for half-integers:

$$\left(-\frac{1}{2}\right)! = \sqrt{\pi}, \quad \left(\frac{1}{2}\right)! = \frac{\sqrt{\pi}}{2}, \quad \left(n-\frac{1}{2}\right)! = \frac{\sqrt{\pi}}{2^n} (2n-1)!! = \frac{\sqrt{\pi}(2n)!}{2^{2n}n!}, \quad \left(n+\frac{1}{2}\right)! = \frac{\sqrt{\pi}}{2^{n+1}} (2n+1)!! = \frac{\sqrt{\pi}(2n+1)!}{2^{2n+1}n!},$$

where $n!!$ is the double factorial :

$$n!! \equiv \begin{cases} n \cdot (n-2) \cdots 5 \cdot 3 \cdot 1 & \text{if } n > 0 \text{ odd,} \\ n \cdot (n-2) \cdots 6 \cdot 4 \cdot 2 & \text{if } n > 0 \text{ even,} \\ 1 & \text{if } n = -1 \text{ or } 0. \end{cases}$$

Using the asymptotic expansion of a large factorial $n! \sim \sqrt{2\pi n} \left(\frac{n}{e}\right)^n \left(1 + \frac{1}{12n} = \frac{1}{288n^3} - \frac{139}{51840n^3} - \frac{571}{2488320n^4} \cdots\right)$, we can get an asymptotic expansion for:

$$\begin{aligned} (n+1/2)! &\sim \sqrt{2\pi} e^{(n+1)\ln(n)-n} \left(1 + \frac{1}{2n}\right) \left(1 + \frac{11}{12(2n)} + \frac{1}{288(2n)^2} - \frac{139}{51840(2n)^3} - \frac{571}{2488320(2n)^4} + \cdots\right) \\ &\quad \left(1 - \frac{1}{12n} - \frac{1}{288n^2} + \frac{139}{51840n^3} + \frac{571}{2488320n^4} - \cdots\right), \\ (n-1/2)! &\sim \sqrt{2\pi} e^{n\ln(n)-n} \left(1 + \frac{11}{12(2n)} + \frac{1}{288(2n)^2} - \frac{139}{51840(2n)^3} - \frac{571}{2488320(2n)^4} + \cdots\right) \\ &\quad \left(1 - \frac{1}{12n} - \frac{1}{288n^2} + \frac{139}{51840n^3} + \frac{571}{2488320n^4} - \cdots\right), \end{aligned} \tag{F.1}$$

or more simply, at the next-to-leading order:

$$\begin{aligned} n! &\sim \sqrt{2\pi n} \left(\frac{n}{e}\right)^n \left(1 + \frac{1}{12n}\right), \\ \left(n + \frac{1}{2}\right)! &\sim \sqrt{2\pi} e^{(n+1)\ln(n)-n} \left(1 + \frac{11}{24n}\right), \\ \left(n - \frac{1}{2}\right)! &\sim \sqrt{2\pi} e^{n\ln(n)-n} \left(1 - \frac{1}{24n}\right). \end{aligned} \tag{F.2}$$

Appendix G

First approximation in the "brute force" asymptotic expansion of the $\{6j\}$

The first approximation in the "brute force" asymptotic expansion of the $\{6j\}$ -symbol is to replace the factorials by the next to leading order of the Stirling formula.

In this section, all computations are done at the next-to-leading order. We replace the factorials in equation (13.2) by their respective asymptotic expansion.

- Then, a typical triangle coefficient:

$$\Delta(\lambda d_{j_{01}}, \lambda d_{j_{02}}, \lambda d_{j_{03}}) = \frac{\left(\frac{\lambda}{2}(d_{j_{01}} + d_{j_{02}} - d_{j_{03}}) - \frac{1}{2}\right)! \left(\frac{\lambda}{2}(d_{j_{01}} - d_{j_{02}} + d_{j_{03}}) - \frac{1}{2}\right)! \left(\frac{\lambda}{2}(-d_{j_{01}} + d_{j_{02}} + d_{j_{03}}) - \frac{1}{2}\right)!}{\left(\frac{\lambda}{2}(d_{j_{01}} + d_{j_{02}} + d_{j_{03}}) - \frac{1}{2}\right)!}$$

will be

$$\begin{aligned} \Delta(\lambda d_{j_{01}}, \lambda d_{j_{02}}, \lambda d_{j_{03}}) &= 2\pi \left[e^{-\frac{\lambda}{2}(d_{j_{01}} + d_{j_{02}} + d_{j_{03}})} \ln \left[\frac{\lambda}{2}(d_{j_{01}} + d_{j_{02}} + d_{j_{03}}) \right] + \frac{\lambda}{2}(d_{j_{01}} + d_{j_{02}} + d_{j_{03}}) \left(1 + \frac{1}{12\lambda(d_{j_{01}} + d_{j_{02}} + d_{j_{03}})} \right) \right. \\ &\quad e^{\frac{\lambda}{2}(d_{j_{01}} + d_{j_{02}} - d_{j_{03}})} \ln \left[\frac{\lambda}{2}(d_{j_{01}} + d_{j_{02}} - d_{j_{03}}) \right] - \frac{\lambda}{2}(d_{j_{01}} + d_{j_{02}} - d_{j_{03}}) \left(1 - \frac{1}{12\lambda(d_{j_{01}} + d_{j_{02}} - d_{j_{03}})} \right) \\ &\quad e^{\frac{\lambda}{2}(d_{j_{01}} - d_{j_{02}} + d_{j_{03}})} \ln \left[\frac{\lambda}{2}(d_{j_{01}} - d_{j_{02}} + d_{j_{03}}) \right] - \frac{\lambda}{2}(d_{j_{01}} - d_{j_{02}} + d_{j_{03}}) \left(1 - \frac{1}{12\lambda(d_{j_{01}} - d_{j_{02}} + d_{j_{03}})} \right) \\ &\quad \left. e^{\frac{\lambda}{2}(-d_{j_{01}} + d_{j_{02}} + d_{j_{03}})} \ln \left[\frac{\lambda}{2}(-d_{j_{01}} + d_{j_{02}} + d_{j_{03}}) \right] - \frac{\lambda}{2}(-d_{j_{01}} + d_{j_{02}} + d_{j_{03}}) \left(1 - \frac{1}{12\lambda(-d_{j_{01}} + d_{j_{02}} + d_{j_{03}})} \right) \right] \end{aligned}$$

which simplifies

$$\begin{aligned} \Delta(\lambda d_{j_{01}}, \lambda d_{j_{02}}, \lambda d_{j_{03}}) &= 2\pi e^{\frac{\lambda}{2}[-(d_{j_{01}} + d_{j_{02}} + d_{j_{03}}) \ln(-d_{j_{01}} + d_{j_{02}} + d_{j_{03}}) + (d_{j_{01}} - d_{j_{02}} + d_{j_{03}}) \ln(d_{j_{01}} - d_{j_{02}} + d_{j_{03}})]} \\ &\quad e^{-\frac{\lambda}{2}[(d_{j_{01}} + d_{j_{02}} - d_{j_{03}}) \ln(d_{j_{01}} + d_{j_{02}} - d_{j_{03}}) + (d_{j_{01}} + d_{j_{02}} + d_{j_{03}}) \ln(d_{j_{01}} + d_{j_{02}} + d_{j_{03}})]} \\ &\quad \left[1 - \frac{1}{12\lambda} \left(\frac{1}{-d_{j_{01}} + d_{j_{02}} + d_{j_{03}}} + \frac{1}{d_{j_{01}} - d_{j_{02}} + d_{j_{03}}} + \frac{1}{d_{j_{01}} + d_{j_{02}} - d_{j_{03}}} - \frac{1}{d_{j_{01}} + d_{j_{02}} + d_{j_{03}}} \right) \right]. \end{aligned} \tag{G.1}$$

The factor $\sqrt{\Delta(\lambda d_{j_{01}}, \lambda d_{j_{02}}, \lambda d_{j_{03}}) \Delta(\lambda d_{j_{23}}, \lambda d_{j_{02}}, \lambda d_{j_{12}}) \Delta(\lambda d_{j_{23}}, \lambda d_{j_{13}}, \lambda d_{j_{03}}) \Delta(\lambda d_{j_{01}}, \lambda d_{j_{13}}, \lambda d_{j_{12}})}$ in equation (13.2) can then easily be put into the form:

$$(2\pi)^2 e^{\frac{\lambda}{2}h(d_{j_{IJ}})} \left(1 - \frac{1}{24\lambda} H(d_{j_{IJ}}) \right) \tag{G.2}$$

where

$$\begin{aligned}
 h(d_{jIJ}) &= \sum_{I < J} d_{jIJ} h_{d_{jIJ}} \\
 \text{with } h_{d_{jIJ}} &= \frac{1}{2} \ln \left(\frac{(d_{jIJ} - d_{jIK} + d_{jIL})(d_{jIJ} + d_{jIK} - d_{jIL})(d_{jIJ} - d_{jJK} + d_{jJL})(d_{jIJ} + d_{jJK} - d_{jJL})}{(d_{jIJ} + d_{jIK} + d_{jIL})(-d_{jIJ} + d_{jIK} + d_{jIL})(d_{jIJ} + d_{jJK} + d_{jJL})(-d_{jIJ} + d_{jJK} + d_{jJL})} \right) \\
 K &\neq L \text{ and } K, L \neq I, J \\
 H(d_{jIJ}) &= 2 \sum_{j,K} \frac{1}{\tilde{p}_j - \tilde{v}_K} - 2 \sum_K \frac{1}{\tilde{v}_K} \text{ where } K \in \{0, \dots, 3\} \text{ and } j \in \{1, \dots, 3\}
 \end{aligned} \tag{G.3}$$

$$\text{and we recall that } \tilde{v}_K = \sum_{I \neq K} \frac{d_{jIK}}{2} \quad \forall K \in \{0, \dots, 3\}, \quad \tilde{p}_k = \sum_{i \neq 0, k} \frac{(d_{joi} + d_{jki})}{2} \quad \forall k \in \{1 \dots 3\}.$$

- We now replace the factorials in the sum of (13.2) by their approximations and we change of variables:
 $t = \lambda x$:

$$\begin{aligned}
 \Sigma(\lambda d_{jIJ}) &= \sum_{x=\max_{\tilde{v}_I} \tilde{p}_j}^{\min_{\tilde{p}_j} \tilde{p}_j} (-1)^{\lambda x} \frac{(\lambda x + 1)(\lambda x)! \prod_j (\lambda(\tilde{p}_j - x)) \prod_j (\lambda(\tilde{p}_j - x) - 1)}{\prod_I (\lambda(x - \tilde{v}_I) + 3/2)(\lambda(x - \tilde{v}_I) + 1/2)! \prod_j (\lambda(\tilde{p}_j - x))!} \\
 &= \frac{1}{(2\pi)^3} \sum_{x=\max_{v_I} v_I}^{\min_{p_j} p_j} e^{G_1(x)} G_2(x)
 \end{aligned} \tag{G.4}$$

where

$$\begin{aligned}
 G_1(x) &= i\pi\lambda x + 3 \ln \lambda + \ln x + 2 \sum_j \ln(\tilde{p}_j - x) - \sum_I \ln(x - \tilde{v}_I) + (\lambda x + 1/2)(\ln x + \ln \lambda) - \lambda x + \sum_I \lambda(x - \tilde{v}_I) \\
 &\quad - \sum_I (\lambda(x - \tilde{v}_I) + 1)(\ln \lambda + \ln(x - \tilde{v}_I)) - \sum_j (\lambda(\tilde{p}_j - x) + 1/2)(\ln \lambda + \ln(\tilde{p}_j - x)) + \sum_j \lambda(\tilde{p}_j - x)
 \end{aligned} \tag{G.5}$$

which can be simplified using the fact that $\sum_I \tilde{v}_I = \sum_j \tilde{p}_j$:

$$G_1(x) = -2 \ln \lambda + \frac{1}{2} \ln \frac{x^3 \prod_j (\tilde{p}_j - x)^3}{\prod_I (x - \tilde{v}_I)^4} + \lambda \left[i\pi x + x \ln x - \sum_I (x - v_I) \ln(x - v_I) - \sum_j (p_j - x) \ln(p_j - x) \right] \tag{G.6}$$

and

$$\begin{aligned}
 G_2(x) &= \frac{1 + \frac{1}{12\lambda x}}{(1 + \frac{3}{2\lambda(x - \tilde{v}_I)}) \prod_I (1 + \frac{1}{24\lambda(x - \tilde{v}_I)}) \prod_j (1 + \frac{1}{12\lambda(p_j - x)})} \\
 &= 1 - \frac{1}{\lambda} \left(-\frac{13}{12x} + \sum_I \frac{47}{24(x - v_I)} + \sum_j \frac{13}{12(p_j - x)} + O\left(\frac{1}{\lambda}\right) \right)
 \end{aligned} \tag{G.7}$$

Moreover,

$$e^{G_1(x)} = \frac{1}{\lambda^2} e^{F(x) + \lambda f(x)} \tag{G.8}$$

where

$$\begin{aligned}
 f(x) &= i\pi x + x \ln(x) - \sum_I (x - v_K) \ln(x - v_I) - \sum_j (p_j - x) \ln(p_j - x) \\
 F(x) &= \frac{1}{2} \ln \left(\frac{x^3 \prod_j (p_j - x)^3}{\prod_I (x - v_I)^4} \right).
 \end{aligned} \tag{G.9}$$

Then the sum can be approximated by:

$$\Sigma(\lambda d_{jIJ}) = \frac{1}{(2\pi)^3 \lambda^2} \sum_{x=\max_{v_I} v_I}^{\min_{p_j} p_j} e^{\lambda f(x) + F(x)} \left(1 - \frac{1}{12\lambda} G(x) + O\left(\frac{1}{\lambda}\right) \right) e^{\lambda f(x)} \tag{G.10}$$

where

$$G(x) = -\frac{13}{x} + \sum_K \frac{47}{24(x - v_K)} + \sum_j \frac{13}{p_j - x}. \quad (\text{G.11})$$

Appendix H

Third approximation in the "brute force" asymptotic expansion of the $\{6j\}$

The third approximation in the "brute force" asymptotic expansion of the $\{6j\}$ -symbol is done using the stationary phase method.

We are interested in the $1/\lambda$ expansion of the integral:

$$I = \int_{\max \tilde{v}_I/2}^{\min \tilde{p}_j/2} dx e^{F(x)} \left(1 - \frac{1}{12\lambda} G(x) + O\left(\frac{1}{\lambda}\right) \right) e^{\lambda f(x)}.$$

We do not give here the proof of the whole expansion (equation (13.11)) because of the heavy formalism but we directly prove the next to leading order formula (equation (13.13)); the procedure is the same but the computations are easier. The asymptotic expansion of such an integral is given by contributions around the stationary points of the phase denoted x_0 . We expand the phase $f(x)$ around the stationary points x_0 at fourth order and the function $g(x) = e^{F(x)} \left(1 - \frac{1}{12\lambda} G(x) \right)$ at second order and we extend the integration to infinity.

$$I \sim \sum_{x_0} \int_{-\infty}^{+\infty} d(\delta x) \left(g(x_0) + g'(x_0)\delta x + \frac{1}{2}g''(x_0)(\delta x)^2 \right) e^{\lambda(f(x_0) + \frac{1}{2}f''(x_0)(\delta x)^2)} \left(1 + \lambda \left(\frac{1}{3!}f^{(3)}(x_0)(\delta x)^3 + \frac{1}{4!}f^{(4)}(x_0)(\delta x)^4 \right) + \frac{\lambda^2}{2} \left(\frac{1}{3!}f^{(3)}(x_0)(\delta x)^3 \right)^2 + O(\lambda^2) \right) \quad (\text{H.1})$$

where in our case, $g(x) = e^{F(x)} \left(1 - \frac{1}{12\lambda} G(x) \right)$ and then the integration are "generalized" Gaussians:

$$I \sim \sum_{x_0} e^{F(x_0) + \lambda f(x_0)} \left[\left(1 - \frac{1}{12\lambda} G(x_0) \right) \int_{-\infty}^{+\infty} d(\delta x) e^{-\lambda \left(\frac{-f''(x_0)}{2} \right) (\delta x)^2} + \frac{1}{2} \left((F'(x_0))^2 + F''(x_0) \right) \int_{-\infty}^{+\infty} d(\delta x) (\delta x)^2 e^{-\lambda \left(\frac{-f''(x_0)}{2} \right) (\delta x)^2} + \lambda \left(\frac{f^{(4)}(x_0)}{4!} + \frac{f^{(3)}(x_0)}{3!} F'(x_0) \right) \int_{-\infty}^{+\infty} d(\delta x) (\delta x)^4 e^{-\lambda \left(\frac{-f''(x_0)}{2} \right) (\delta x)^2} + \frac{\lambda^2}{2} \left(\frac{f^{(3)}(x_0)}{3!} \right)^2 \int_{-\infty}^{+\infty} d(\delta x) (\delta x)^6 e^{-\lambda \left(\frac{-f''(x_0)}{2} \right) (\delta x)^2} + O\left(\frac{1}{\lambda^{3/2}}\right) \right] \quad (\text{H.2})$$

which can easily be computed:

$$I \sim \sum_{x_0} \sqrt{\frac{2\pi}{-f''(x_0)\lambda}} e^{F(x_0) + \lambda f(x_0)} \left[1 + \frac{1}{\lambda} \left(-\frac{G(x_0)}{12} - \frac{F''(x_0) + (F'(x_0))^2}{2f''(x_0)} + \frac{f^{(4)}(x_0) + 4f^{(3)}(x_0)F'(x_0)}{8(f''(x_0))^2} - \frac{5(f^{(3)}(x_0))^2}{24(f''(x_0))^3} \right) + O\left(\frac{1}{\lambda}\right) \right] \quad (\text{H.3})$$

Appendix I

Physical States with a Real Phase

We will discuss here the case already mentioned of the Bessel-based factorized boundary state:

$$\psi_q[j_{ab}] = \prod_{a < b} \phi_B(j_{ab}) \quad (\text{I.1})$$

where

$$\phi_B(j) = \frac{I_{|d_j - d_{j_0}|}(\frac{d_{j_0}}{\alpha}) - I_{d_j + d_{j_0}}(\frac{d_{j_0}}{\alpha})}{\sqrt{I_0(\frac{2d_{j_0}}{\alpha}) - I_{2d_{j_0}+1}(\frac{2d_{j_0}}{\alpha})}} \cos(d_j \Theta) \quad (\text{I.2})$$

We are interested in the large spin limit regime and its $d_{j_0} \rightarrow \infty$ limit behaves as a Gaussian peaked around d_{j_0} :

$$\phi_B(j) \simeq \left(\frac{\alpha}{d_{j_0} \pi}\right)^{1/4} \exp\left[-\frac{\alpha}{2d_{j_0}}(d_j - d_{j_0})^2\right] \cos(d_j \Theta) \quad (\text{I.3})$$

The difference with the case studied previously of a Gaussian peaked around d_{j_0} is the phase which is real here. We recall that the factorized boundary state assumption has been made in order to perform numerical simulations and the choice of a real phase has been done in the work concerning the area correlator to turn it into an exact group integral [110] and perform exact analytical computations.

We therefore consider now a factorized Gaussian state with a real phase:

$$\psi_q[d_{j_{ab}}] \frac{1}{\mathcal{N}} \prod_{a < b} \exp(-\alpha(d_{j_{ab}} - d_{j_0})^2) \cos(d_{j_0} \Theta) \quad (\text{I.4})$$

to see if the conditions necessary to have a physical state are modified. Conditions (15.6) and (15.7) give the two following equations for \mathcal{N} and α .

$$1 = \sum_{j_{ab}} |\psi(j_{ab})|^2 = \frac{1}{(\mathcal{N}^2)^{10}} \sum_{\{j_{ab}\}} e^{-2\Re(\alpha) \sum_{a < b} (d_{j_{ab}} - d_{j_0})^2} \prod_{a < b} \left(\frac{1 + \cos(2d_{j_{ab}} \Theta)}{2}\right) \quad (\text{I.5})$$

and,

$$1 = \sum_{j_{ab}} \tilde{j} \psi(j_{ab}) \simeq \frac{1}{\mathcal{N}^{10}} \sum_{\{j_{ab}\}} \left(\prod_{a < b} d_{j_{ab}}\right)^\sigma P(d_{j_{ab}}) \sum_{\epsilon = \pm 1; \eta = \pm 1} e^{-\Re(\alpha) \sum_{a < b} (d_{j_{ab}} - d_{j_0})^2 + i \sum_{a < b} [d_{j_{ab}} (\epsilon \theta_{ab} + \eta \Theta) - \Im(\alpha) (d_{j_{ab}} - d_{j_0})^2]} \quad (\text{I.6})$$

where we have already used the asymptotic formulae of the \tilde{j} -symbol. In the large spin limit, the summation in the two previous equations can then be approximated with an integral and we can write:

$$1 \simeq \frac{1}{2\mathcal{N}^2} \int d(d_j) e^{-2\Re(\alpha)(d_j - d_{j_0})^2} \left[\frac{1}{2} + \frac{1}{4} e^{i2d_j \Theta} + \frac{1}{4} e^{-i2d_j \Theta}\right] \quad (\text{I.7})$$

and

$$1 \simeq \frac{1}{(2\mathcal{N})^{10}} \int \prod_{a<b} d[d_{j_{ab}}] \left(\prod_{a<b} d_{j_{ab}} \right)^\sigma P(d_{j_{ab}}) \sum_{\epsilon=\pm 1; \eta=\pm} e^{-\Re(\alpha) \sum_{a<b} (d_{j_{ab}} - d_{j_0})^2 + i \sum_{a<b} [d_{j_{ab}} (\epsilon\theta_{ab} + \eta\Theta) - \Im(\alpha)(d_{j_{ab}} - d_{j_0})^2]} \quad (\text{I.8})$$

The first integral (I.7) after some changes of variables is just three Gaussian integrals, which can be integrated directly:

$$\mathcal{N}^2 = \frac{1}{4} \sqrt{\frac{\pi}{2\Re(\alpha)}} \left[1 + e^{-\frac{\Theta^2}{2\Re(\alpha)}} \cos(d_{j_0} \Theta) \right] \quad (\text{I.9})$$

but we recall that $\alpha \propto \frac{1}{d_{j_0}^n}$ with $n \in]0, 2[$ from equations (15.12) and therefore in the large spin limit the second term of the right-hand side of this relation vanishes and we obtain the same relation at the leading order between \mathcal{N} and α as in the case of a Gaussian state with an imaginary phase (up to a factor $1/2$). That is:

$$\mathcal{N}^2 = \frac{1}{4} \sqrt{\frac{\pi}{2\Re(\alpha)}} \quad (\text{I.10})$$

To evaluate the second integral (I.8) in the large spin limit we expand as previously the Regge action around d_{j_0} :

$$S_R[d_{j_{ab}}] \simeq \Theta \sum_{a<b} d_{j_{ab}} + \frac{1}{2} \sum_{a<b, c<d} N_{cd}^{ab} \delta d_{j_{ab}} \delta d_{j_{cd}}. \quad (\text{I.11})$$

where

$$N_{cd}^{ab} = \frac{\partial^2 S_R}{\partial d_{j_{ab}} \partial d_{j_{cd}}} \Big|_{d_j=d_{j_0}} = \frac{\partial \theta_{ab}}{\partial d_{j_{cd}}} \Big|_{d_j=d_{j_0}} = \frac{\sqrt{3}}{4\sqrt{5}d_{j_0}} \begin{pmatrix} -4 & 7/2 & 7/2 & 7/2 & 7/2 & 7/2 & 7/2 & -9 & -9 & -9 \\ 7/2 & -4 & 7/2 & 7/2 & 7/2 & -9 & -9 & 7/2 & 7/2 & -9 \\ 7/2 & 7/2 & -4 & 7/2 & -9 & 7/2 & -9 & 7/2 & -9 & 7/2 \\ 7/2 & 7/2 & 7/2 & -4 & -9 & -9 & 7/2 & -9 & 7/2 & 7/2 \\ 7/2 & 7/2 & -9 & -9 & -4 & 7/2 & 7/2 & 7/2 & 7/2 & -9 \\ 7/2 & -9 & 7/2 & -9 & 7/2 & -4 & 7/2 & 7/2 & -9 & 7/2 \\ 7/2 & -9 & -9 & 7/2 & 7/2 & 7/2 & -4 & -9 & 7/2 & 7/2 \\ -9 & 7/2 & 7/2 & -9 & 7/2 & 7/2 & -9 & -4 & 7/2 & 7/2 \\ -9 & 7/2 & -9 & 7/2 & 7/2 & -9 & 7/2 & 7/2 & -4 & 7/2 \\ -9 & -9 & 7/2 & 7/2 & -9 & 7/2 & 7/2 & 7/2 & 7/2 & -4 \end{pmatrix}.$$

And using once again the argument that rapidly oscillating term in $d_{j_{ab}}$ will vanish when performing the integration over $d_{j_{ab}}$, we have to consider only two terms in the sum (I.8) which are two Gaussian integral:

$$1 \simeq \frac{(d_{j_0})^{(10\sigma-9/2)P}}{(2\mathcal{N})^{10}} \int \prod_{a<b} d[\delta d_{j_{ab}}] \left[e^{-\delta d_{j_{ab}} M_{cd}^{ab} \delta d_{j_{cd}}} + e^{-\delta d_{j_{ab}} Q_{cd}^{ab} \delta d_{j_{cd}}} \right] \quad (\text{I.12})$$

where M and Q are both ten by ten matrices defined by: $M_{cd}^{ab} = \alpha \delta_{cd}^{ab} - i N_{cd}^{ab}$ and $Q_{cd}^{ab} = \alpha \delta_{cd}^{ab} + i N_{cd}^{ab}$ with $a < b, c < d$ and $\delta_{cd}^{ab} = 1$ if the two couples of indices are the same and it vanishes otherwise. Therefore, M is a symmetric matrix with all its diagonal coefficients equal to $\alpha + i\sqrt{\frac{3}{5}}\frac{1}{d_{j_0}}$ and Q is a symmetric matrix with all its diagonal coefficients equal to $\alpha - i\sqrt{\frac{3}{5}}\frac{1}{d_{j_0}}$. Then the analysis is the same as the one done in the case of a Gaussian state with an imaginary phase; we have three case to consider:

1. $\alpha \gg \frac{1}{d_{j_0}}$, that is we consider here that α is proportional to $d_{j_0}^{-n}$ with $0 < n < 1$. We have then that $M \simeq \alpha Id$ and $Q \simeq \alpha Id$ and once again we write $\alpha = \frac{a}{d_{j_0}^n}$, then we get the same result as in the case of the

imaginary phase (up to some factors 2 in a) (see equations 15.21), that is:
$$\begin{cases} \alpha \in \mathbb{R} \\ \sigma = \frac{1}{4} \left(\frac{9}{5} - n \right) \text{ and } \sigma > \frac{1}{5} \\ a = 32P^4\pi \end{cases}$$

2. $\alpha \ll \frac{1}{d_{j_0}}$, that is we consider that α is proportional to $d_{j_0}^{-n}$ with $1 < n < 2$. We have to integrate $\int d[\delta d_{j_{ab}}] \exp(i \sum \delta d_{j_{ab}} N_{cd}^{ab} \delta d_{j_{cd}}) + \exp(-i \sum \delta d_{j_{ab}} N_{cd}^{ab} \delta d_{j_{cd}})$. The signature of the matrix N is equal to -2 ; therefore, $e^{i\sigma(N)\frac{\pi}{4}} = -i = -e^{i\sigma(-N)\frac{\pi}{4}}$ and then the previous integral is null so in this case we also cannot have $\alpha = \frac{a}{d_{j_0}^n}$ with $1 < n < 2$.
3. $\alpha \sim \frac{1}{d_{j_0}}$: it is the most natural case which peaks in the same way the triangle areas of the 4-simplex around the background value $A_0 = d_{j_0}$ and the dihedral angles around the background value Θ . But once again due to the fact we have chosen a factorized boundary state, this case is very complicated although the imaginary parts of the determinant of M and of the determinant of N will compensate. This confirms that a factorized boundary state is not the most natural to capture a physical state. And with a real phase it is not even possible to consider a tensorial state which could compensate iN and $-iN$ as we did in the case of the imaginary phase.

Bibliography

- [1] V. Nesvizhevsky, H. Borner, A. Petukhov, H. Abele, S. Baessler, *et al.*, “Quantum states of neutrons in the Earth’s gravitational field,” *Nature*, vol. 415, pp. 297–299, 2002.
- [2] C. Rovelli, *Quantum gravity*. Cambridge University Press, 2004.
- [3] T. Thiemann, *Modern canonical quantum general relativity*. Cambridge University Press, 2007.
- [4] J. Magnen, K. Noui, V. Rivasseau, and M. Smerlak, “Scaling behaviour of three-dimensional group field theory,” *Class. Quant. Grav.*, vol. 26, p. 185012, 2009.
- [5] M. Dupuis and E. R. Livine, “Lifting SU(2) Spin Networks to Projected Spin Networks,” 2010.
- [6] M. Dupuis and E. R. Livine, “Revisiting the Simplicity Constraints and Coherent Intertwiners,” 2010.
- [7] F. Girelli and E. R. Livine, “Reconstructing quantum geometry from quantum information: Spin networks as harmonic oscillators,” *Class. Quant. Grav.*, vol. 22, pp. 3295–3314, 2005.
- [8] L. Freidel and E. R. Livine, “The Fine Structure of SU(2) Intertwiners from U(N) Representations,” 2009.
- [9] L. Freidel and E. R. Livine, “U(N) Coherent States for Loop Quantum Gravity,” 2010.
- [10] C. Rovelli, “Graviton propagator from background-independent quantum gravity,” *Phys. Rev. Lett.*, vol. 97, p. 151301, 2006.
- [11] E. Bianchi, L. Modesto, C. Rovelli, and S. Speziale, “Graviton propagator in loop quantum gravity,” *Class. Quant. Grav.*, vol. 23, pp. 6989–7028, 2006.
- [12] M. Dupuis and E. R. Livine, “Pushing Further the Asymptotics of the 6j-symbol,” *Phys. Rev.*, vol. D80, p. 024035, 2009.
- [13] M. Dupuis and E. R. Livine, “The 6j-symbol: Recursion, Correlations and Asymptotics,” *Class. Quant. Grav.*, vol. 27, p. 135003, 2010.
- [14] E. R. Livine and S. Speziale, “Physical boundary state for the quantum tetrahedron,” *Class. Quant. Grav.*, vol. 25, p. 085003, 2008.
- [15] M. Dupuis and E. R. Livine, “Physical Boundary State for the Quantum 4-Simplex,”
- [16] R. M. Wald, “The thermodynamics of black holes,” *Living Rev. Rel.*, vol. 4, p. 6, 2001.
- [17] R. Wald, *General Relativity*. The University of Chicago Press, 1984.
- [18] S. M. Carroll, “Lecture notes on general relativity,” 1997.
- [19] L. Modesto, “Disappearance of black hole singularity in quantum gravity,” *Phys. Rev.*, vol. D70, p. 124009, 2004.
- [20] G. Amelino-Camelia and L. Smolin, “Prospects for constraining quantum gravity dispersion with near term observations,” *Phys. Rev.*, vol. D80, p. 084017, 2009.

- [21] G. Ponzano and T. Regge, “Semiclassical limit of Racah coefficients,” in *Spectroscopic and group theoretical methods in physics*.
- [22] C. W. Misner, K. S. Thorne, and J. A. Wheeler, *Gravitation*. San Francisco, 1973.
- [23] P. Dirac, *Principles of Quantum Mechanics*. Oxford University Press, 1982.
- [24] M. Henneaux and C. Teitelboim, *Quantization of gauge systems*. Princeton University Press, 1992.
- [25] H.-J. Matschull, “Dirac’s canonical quantization programme,” 1996.
- [26] P. G. Bergmann, “Conservation Laws in General Relativity as the Generators of Coordinate Transformations,” *Phys. Rev.*, vol. 112, pp. 287–289, 1958.
- [27] P. G. Bergmann, “Observables in General Relativity,” *Rev. Mod. Phys.*, vol. 33, pp. 510–514, 1961.
- [28] P. G. Bergmann and A. Komar, “The phase space formulation of general relativity and approaches toward its canonical quantization,” In *Held, A.(Ed.): General Relativity and Gravitation, Vol.1*, 227–254.
- [29] A. Komar, “General-relativistic observables via hamilton-jacobi functionals,” *Phys. Rev.*, vol. D4, pp. 923–927, 1971.
- [30] P. A. M. Dirac, “The Theory of gravitation in Hamiltonian form,” *Proc. Roy. Soc. Lond.*, vol. A246, pp. 333–343, 1958.
- [31] A. Ashtekar, *Lectures on nonperturbative canonical gravity*. Singapore: World Scientific, 1991.
- [32] A. Perez, “Introduction to loop quantum gravity and spin foams,” 2004.
- [33] P. Dona and S. Speziale, “Introductory lectures to loop quantum gravity,” 2010.
- [34] J. F. Barbero G., “From Euclidean to Lorentzian general relativity: The Real way,” *Phys. Rev.*, vol. D54, pp. 1492–1499, 1996.
- [35] J. F. Barbero G., “Real Ashtekar variables for Lorentzian signature space times,” *Phys. Rev.*, vol. D51, pp. 5507–5510, 1995.
- [36] J. F. Barbero G., “A Real polynomial formulation of general relativity in terms of connections,” *Phys. Rev.*, vol. D49, pp. 6935–6938, 1994.
- [37] G. Immirzi, “Real and complex connections for canonical gravity,” *Class. Quant. Grav.*, vol. 14, pp. L177–L181, 1997.
- [38] L. Smolin, “Recent developments in nonperturbative quantum gravity,” 1992.
- [39] C. Rovelli and L. Smolin, “Discreteness of area and volume in quantum gravity,” *Nucl. Phys.*, vol. B442, pp. 593–622, 1995.
- [40] A. Ashtekar and J. Lewandowski, “Quantum theory of geometry. I: Area operators,” *Class. Quant. Grav.*, vol. 14, pp. A55–A82, 1997.
- [41] A. Ashtekar and B. Krishnan, “Isolated and dynamical horizons and their applications,” *Living Rev. Rel.*, vol. 7, p. 10, 2004.
- [42] M. Domagala and J. Lewandowski, “Black hole entropy from quantum geometry,” *Class. Quant. Grav.*, vol. 21, pp. 5233–5244, 2004.
- [43] K. A. Meissner, “Black hole entropy in loop quantum gravity,” *Class. Quant. Grav.*, vol. 21, pp. 5245–5252, 2004.

- [44] C. Rovelli, “Black hole entropy from loop quantum gravity,” *Phys. Rev. Lett.*, vol. 77, pp. 3288–3291, 1996.
- [45] K. V. Krasnov, “On statistical mechanics of gravitational systems,” *Gen. Rel. Grav.*, vol. 30, pp. 53–68, 1998.
- [46] A. Ashtekar, J. Baez, A. Corichi, and K. Krasnov, “Quantum geometry and black hole entropy,” *Phys. Rev. Lett.*, vol. 80, pp. 904–907, 1998.
- [47] A. Ashtekar, J. C. Baez, and K. Krasnov, “Quantum geometry of isolated horizons and black hole entropy,” *Adv. Theor. Math. Phys.*, vol. 4, pp. 1–94, 2000.
- [48] A. Ashtekar, A. Corichi, and K. Krasnov, “Isolated horizons: The classical phase space,” *Adv. Theor. Math. Phys.*, vol. 3, pp. 419–478, 2000.
- [49] J. Samuel, “Is Barbero’s Hamiltonian formulation a gauge theory of Lorentzian gravity?,” *Class. Quant. Grav.*, vol. 17, pp. L141–L148, 2000.
- [50] S. Alexandrov, “SO(4,C)-covariant Ashtekar-Barbero gravity and the Immirzi parameter,” *Class. Quant. Grav.*, vol. 17, pp. 4255–4268, 2000.
- [51] S. Holst, “Barbero’s Hamiltonian derived from a generalized Hilbert- Palatini action,” *Phys. Rev.*, vol. D53, pp. 5966–5969, 1996.
- [52] N. Barros e Sa, “Hamiltonian analysis of general relativity with the Immirzi parameter,” *Int. J. Mod. Phys.*, vol. D10, pp. 261–272, 2001.
- [53] S. Alexandrov and Z. Kadar, “Timelike surfaces in Lorentz covariant loop gravity and spin foam models,” *Class. Quant. Grav.*, vol. 22, pp. 3491–3510, 2005.
- [54] E. R. Livine, “Towards a covariant loop quantum gravity,” 2006.
- [55] S. Alexandrov and D. Vassilevich, “Area spectrum in Lorentz covariant loop gravity,” *Phys. Rev.*, vol. D64, p. 044023, 2001.
- [56] S. Alexandrov, “Choice of connection in loop quantum gravity,” *Phys. Rev.*, vol. D65, p. 024011, 2002.
- [57] S. Alexandrov and E. R. Livine, “SU(2) loop quantum gravity seen from covariant theory,” *Phys. Rev.*, vol. D67, p. 044009, 2003.
- [58] A. Ashtekar and J. Lewandowski, “Projective techniques and functional integration for gauge theories,” *J. Math. Phys.*, vol. 36, pp. 2170–2191, 1995.
- [59] R. Penrose, *Quantum Theory and Beyond*, vol. D52, ch. Angular momentum: an approach to combinatorial space-time. Cambridge University Press, Cambridge, 1971.
- [60] M. P. Reisenberger, “World sheet formulations of gauge theories and gravity,” 1994.
- [61] C. Rovelli and L. Smolin, “Spin networks and quantum gravity,” *Phys. Rev.*, vol. D52, pp. 5743–5759, 1995.
- [62] J. C. Baez, “Spin network states in gauge theory,” *Adv. Math.*, vol. 117, pp. 253–272, 1996.
- [63] L. Smolin, “The Future of spin networks,” 1997.
- [64] M. Gaul and C. Rovelli, “Loop quantum gravity and the meaning of diffeomorphism invariance,” *Lect. Notes Phys.*, vol. 541, pp. 277–324, 2000.
- [65] R. Loll, “Simplifying the spectral analysis of the volume operator,” *Nucl. Phys.*, vol. B500, pp. 405–420, 1997.

- [66] A. Ashtekar and J. Lewandowski, “Quantum theory of geometry. 2. Volume operators,” *Adv.Theor.Math.Phys.*, vol. 1, pp. 388–429, 1998.
- [67] R. Loll, “Spectrum of the volume operator in quantum gravity,” *Nucl.Phys.*, vol. B460, pp. 143–154, 1996.
- [68] R. Loll, “The Volume operator in discretized quantum gravity,” *Phys.Rev.Lett.*, vol. 75, pp. 3048–3051, 1995.
- [69] T. Thiemann, “Closed formula for the matrix elements of the volume operator in canonical quantum gravity,” *J.Math.Phys.*, vol. 39, pp. 3347–3371, 1998.
- [70] J. Brunnemann and T. Thiemann, “Simplification of the spectral analysis of the volume operator in loop quantum gravity,” *Class.Quant.Grav.*, vol. 23, pp. 1289–1346, 2006.
- [71] W. Fairbairn and C. Rovelli, “Separable Hilbert space in loop quantum gravity,” *J. Math. Phys.*, vol. 45, pp. 2802–2814, 2004.
- [72] T. Thiemann, “Anomaly - free formulation of nonperturbative, four-dimensional Lorentzian quantum gravity,” *Phys.Lett.*, vol. B380, pp. 257–264, 1996.
- [73] T. Thiemann, “Quantum spin dynamics (QSD),” *Class. Quant. Grav.*, vol. 15, pp. 839–873, 1998.
- [74] T. Thiemann, “Gauge field theory coherent states (GCS): 1. General properties,” *Class.Quant.Grav.*, vol. 18, pp. 2025–2064, 2001.
- [75] R. Borissov, R. De Pietri, and C. Rovelli, “Matrix elements of Thiemann’s Hamiltonian constraint in loop quantum gravity,” *Class.Quant.Grav.*, vol. 14, pp. 2793–2823, 1997.
- [76] L. Smolin, “The classical limit and the form of the Hamiltonian constraint in non-perturbative quantum general relativity,” 1996.
- [77] T. Thiemann, “Quantum spin dynamics. VIII. The Master constraint,” *Class.Quant.Grav.*, vol. 23, pp. 2249–2266, 2006.
- [78] C. Rovelli, “A new look at loop quantum gravity,” 2010.
- [79] C. Rovelli and T. Thiemann, “The Immirzi parameter in quantum general relativity,” *Phys.Rev.*, vol. D57, pp. 1009–1014, 1998.
- [80] E. R. Livine, “Projected spin networks for Lorentz connection: Linking spin foams and loop gravity,” *Class. Quant. Grav.*, vol. 19, pp. 5525–5542, 2002.
- [81] J. C. Baez, “Spin foam models,” *Class. Quant. Grav.*, vol. 15, pp. 1827–1858, 1998.
- [82] J. C. Baez, “An introduction to spin foam models of BF theory and quantum gravity,” *Lect. Notes Phys.*, vol. 543, pp. 25–94, 2000.
- [83] J. J. Halliwell and J. B. Hartle, “Wave functions constructed from an invariant sum over histories satisfy constraints,” *Phys.Rev.*, vol. D43, pp. 1170–1194, 1991.
- [84] M. Reisenberger and C. Rovelli, “Space-time states and covariant quantum theory,” *Phys.Rev.*, vol. D65, p. 125016, 2002.
- [85] L. Freidel, “Group field theory: An overview,” *Int. J. Theor. Phys.*, vol. 44, pp. 1769–1783, 2005.
- [86] D. Oriti, “The group field theory approach to quantum gravity,” 2006.
- [87] L. Freidel and A. Starodubtsev, “Quantum gravity in terms of topological observables,” 2005.

- [88] D. Louapre, *Modèles de mousses de spin pour la gravité quantique en 3 dimensions*. PhD thesis, Ecole Normale Supérieure de Lyon, 2004.
- [89] L. Freidel and D. Louapre, “Ponzano-Regge model revisited. I: Gauge fixing, observables and interacting spinning particles,” *Class. Quant. Grav.*, vol. 21, pp. 5685–5726, 2004.
- [90] L. Freidel and K. Krasnov, “Spin foam models and the classical action principle,” *Adv. Theor. Math. Phys.*, vol. 2, pp. 1183–1247, 1999.
- [91] E. R. Livine and J. P. Ryan, “A Note on B-observables in Ponzano-Regge 3d Quantum Gravity,” *Class. Quant. Grav.*, vol. 26, p. 035013, 2009.
- [92] J. W. Barrett and I. Naish-Guzman, “The Ponzano-Regge model,” *Class. Quant. Grav.*, vol. 26, p. 155014, 2009.
- [93] R. E. Livine and D. Oriti, “Barrett-Crane spin foam model from generalized BF-type action for gravity,” *Phys. Rev.*, vol. D65, p. 044025, 2002.
- [94] J. Engle, R. Pereira, and C. Rovelli, “The loop-quantum-gravity vertex-amplitude,” *Phys. Rev. Lett.*, vol. 99, p. 161301, 2007.
- [95] J. Engle, R. Pereira, and C. Rovelli, “Flipped spinfoam vertex and loop gravity,” *Nucl. Phys.*, vol. B798, pp. 251–290, 2008.
- [96] L. Freidel and K. Krasnov, “A New Spin Foam Model for 4d Gravity,” *Class. Quant. Grav.*, vol. 25, p. 125018, 2008.
- [97] E. R. Livine and S. Speziale, “Consistently Solving the Simplicity Constraints for Spinfoam Quantum Gravity,” *Europhys. Lett.*, vol. 81, p. 50004, 2008.
- [98] J. Engle, E. Livine, R. Pereira, and C. Rovelli, “LQG vertex with finite Immirzi parameter,” *Nucl. Phys.*, vol. B799, pp. 136–149, 2008.
- [99] B. Dittrich and J. P. Ryan, “Simplicity in simplicial phase space,” 2010.
- [100] S. Alexandrov and P. Roche, “Critical Overview of Loops and Foams,” 2010. * Temporary entry *.
- [101] V. Bonzom and E. R. Livine, “A Lagrangian approach to the Barrett-Crane spin foam model,” *Phys. Rev.*, vol. D79, p. 064034, 2009.
- [102] S. Alexandrov, “Spin foam model from canonical quantization,” *Phys. Rev.*, vol. D77, p. 024009, 2008.
- [103] J. W. Barrett and L. Crane, “Relativistic spin networks and quantum gravity,” *J. Math. Phys.*, vol. 39, pp. 3296–3302, 1998.
- [104] J. W. Barrett and L. Crane, “A Lorentzian signature model for quantum general relativity,” *Class. Quant. Grav.*, vol. 17, pp. 3101–3118, 2000.
- [105] M. P. Reisenberger, “On relativistic spin network vertices,” *J. Math. Phys.*, vol. 40, pp. 2046–2054, 1999.
- [106] E. R. Livine and S. Speziale, “A new spinfoam vertex for quantum gravity,” *Phys. Rev.*, vol. D76, p. 084028, 2007.
- [107] J. Engle and R. Pereira, “Coherent states, constraint classes, and area operators in the new spin-foam models,” *Class. Quant. Grav.*, vol. 25, p. 105010, 2008.
- [108] J. C. Baez and J. W. Barrett, “The Quantum tetrahedron in three-dimensions and four-dimensions,” *Adv. Theor. Math. Phys.*, vol. 3, pp. 815–850, 1999.

- [109] J. W. Barrett, “The Classical evaluation of relativistic spin networks,” *Adv. Theor. Math. Phys.*, vol. 2, pp. 593–600, 1998.
- [110] E. R. Livine and S. Speziale, “Group Integral Techniques for the Spinfoam Graviton Propagator,” *JHEP*, vol. 11, p. 092, 2006.
- [111] L. Freidel and D. Louapre, “Asymptotics of 6j and 10j symbols,” *Class. Quant. Grav.*, vol. 20, pp. 1267–1294, 2003.
- [112] T. Regge, “General relativity without coordinates,” *Nuovo Cim.*, vol. 19, pp. 558–571, 1961.
- [113] J. W. Barrett and C. M. Steele, “Asymptotics of relativistic spin networks,” *Class. Quant. Grav.*, vol. 20, pp. 1341–1362, 2003.
- [114] J. D. Christensen, I. Khavkine, E. R. Livine, and S. Speziale, “Sub-leading asymptotic behaviour of area correlations in the Barrett-Crane model,” *Class. Quant. Grav.*, vol. 27, p. 035012, 2010.
- [115] A. Perez and C. Rovelli, “Spin foam model for Lorentzian general relativity,” *Phys. Rev.*, vol. D63, p. 041501, 2001.
- [116] A. Perez and C. Rovelli, “3+1 spinfoam model of quantum gravity with spacelike and timelike components,” *Phys. Rev.*, vol. D64, p. 064002, 2001.
- [117] J. W. Barrett and C. M. Steele, “Asymptotics of relativistic spin networks,” *Class. Quant. Grav.*, vol. 20, pp. 1341–1362, 2003.
- [118] W. Kaminski, M. Kisielowski, and J. Lewandowski, “The EPRL intertwiners and corrected partition function,” *Class. Quant. Grav.*, vol. 27, p. 165020, 2010.
- [119] J. Engle and R. Pereira, “Coherent states, constraint classes, and area operators in the new spin-foam models,” *Class. Quant. Grav.*, vol. 25, p. 105010, 2008.
- [120] T. Thiemann, “The Phoenix project: Master constraint program for loop quantum gravity,” *Class. Quant. Grav.*, vol. 23, pp. 2211–2248, 2006.
- [121] B. Dittrich and T. Thiemann, “Testing the master constraint programme for loop quantum gravity. I. General framework,” *Class. Quant. Grav.*, vol. 23, pp. 1025–1066, 2006.
- [122] B. Dittrich and T. Thiemann, “Testing the master constraint programme for loop quantum gravity. II. Finite dimensional systems,” *Class. Quant. Grav.*, vol. 23, pp. 1067–1088, 2006.
- [123] Y. Ding and C. Rovelli, “The Volume operator in covariant quantum gravity,” *Class. Quant. Grav.*, vol. 27, p. 165003, 2010.
- [124] Y. Ding and C. Rovelli, “Physical boundary Hilbert space and volume operator in the Lorentzian new spin-foam theory,” 2010.
- [125] T. Thiemann, “Complexifier coherent states for quantum general relativity,” *Class. Quant. Grav.*, vol. 23, pp. 2063–2118, 2006.
- [126] B. Bahr and T. Thiemann, “Gauge-invariant coherent states for Loop Quantum Gravity. I. Abelian gauge groups,” *Class. Quant. Grav.*, vol. 26, p. 045011, 2009.
- [127] B. Bahr and T. Thiemann, “Gauge-invariant coherent states for loop quantum gravity. II. Non-Abelian gauge groups,” *Class. Quant. Grav.*, vol. 26, p. 045012, 2009.
- [128] C. Flori and T. Thiemann, “Semiclassical analysis of the Loop Quantum Gravity volume operator. I. Flux Coherent States,” 2008.

- [129] L. Freidel and S. Speziale, “Twisted geometries: A geometric parametrisation of $SU(2)$ phase space,” 2010.
- [130] L. Freidel and S. Speziale, “From twistors to twisted geometries,” 2010.
- [131] F. Conrady and L. Freidel, “Quantum geometry from phase space reduction,” *J. Math. Phys.*, vol. 50, p. 123510, 2009.
- [132] L. Freidel, K. Krasnov, and E. R. Livine, “Holomorphic Factorization for a Quantum Tetrahedron,” *Commun. Math. Phys.*, vol. 297, pp. 45–93, 2010.
- [133] S. Alexandrov, “Hilbert space structure of covariant loop quantum gravity,” *Phys. Rev.*, vol. D66, p. 024028, 2002.
- [134] E. R. Livine and D. Oriti, “Coupling of spacetime atoms and spin foam renormalisation from group field theory,” *JHEP*, vol. 02, p. 092, 2007.
- [135] J. W. Barrett, R. J. Dowdall, W. J. Fairbairn, F. Hellmann, and R. Pereira, “Lorentzian spin foam amplitudes: graphical calculus and asymptotics,” *Class. Quant. Grav.*, vol. 27, p. 165009, 2010.
- [136] E. F. Borja, J. Diaz-Polo, I. Garay, and E. R. Livine, “Dynamics for a 2-vertex Quantum Gravity Model,” 2010.
- [137] J. Louck, “Recent progress toward a theory of tensor operators in the unitary groups,” *Am.J.Phys.*, vol. 38, pp. 3–42, 1970.
- [138] E. Alesci and C. Rovelli, “The complete LQG propagator: I. Difficulties with the Barrett-Crane vertex,” *Phys. Rev.*, vol. D76, p. 104012, 2007.
- [139] J. D. Christensen, E. R. Livine, and S. Speziale, “Numerical evidence of regularized correlations in spin foam gravity,” *Phys. Lett.*, vol. B670, pp. 403–406, 2009.
- [140] S. Speziale, “Towards the graviton from spinfoams: The 3d toy model,” *JHEP*, vol. 05, p. 039, 2006.
- [141] E. R. Livine, S. Speziale, and J. L. Willis, “Towards the graviton from spinfoams: higher order corrections in the 3d toy model,” *Phys. Rev.*, vol. D75, p. 024038, 2007.
- [142] B. Dittrich and S. Speziale, “Area-angle variables for general relativity,” *New J.Phys.*, vol. 10, p. 083006, 2008.
- [143] A. Perez and C. Rovelli, “A spin foam model without bubble divergences,” *Nucl. Phys.*, vol. B599, pp. 255–282, 2001.
- [144] W. Kaminski, M. Kisielowski, and J. Lewandowski, “Spin-Foams for All Loop Quantum Gravity,” *Class.Quant.Grav.*, vol. 27, p. 095006, 2010.
- [145] V. Bonzom, E. R. Livine, M. Smerlak, and S. Speziale, “Towards the graviton from spinfoams: the complete perturbative expansion of the 3d toy model,” *Nucl. Phys.*, vol. B804, pp. 507–526, 2008.
- [146] E. R. Livine and S. Speziale, “Group Integral Techniques for the Spinfoam Graviton Propagator,” *JHEP*, vol. 11, p. 092, 2006.
- [147] S. Deser, R. Jackiw, and G. ’t Hooft, “Three-Dimensional Einstein Gravity: Dynamics of Flat Space,” *Annals Phys.*, vol. 152, p. 220, 1984.
- [148] J. Roberts, “Classical 6j-symbols and the tetrahedron,” *Geom. Topol.*, vol. 20, pp. 21–66, 1999.
- [149] K. Schulten and R. G. Gordon, “Exact Recursive Evaluation of 3J and 6J Coefficients for Quantum Mechanical Coupling of Angular Momenta,” *J. Math. Phys.*, vol. 16, pp. 1961–1970, 1975.

- [150] K. Schulten and R. G. Gordon, “Semiclassical approximations to $3j$ and $\{6j\}$ coefficients for quantum mechanical coupling of angular momenta,” *J. Math. Phys.*, vol. 16, pp. 1971–1988, 1975.
- [151] L. Freidel and D. Louapre, “Asymptotics of $6j$ and $10j$ symbols,” *Class. Quant. Grav.*, vol. 20, pp. 1267–1294, 2003.
- [152] R. Gurau, “The Ponzano-Regge asymptotic of the $6j$ symbol: an elementary proof,” *Annales Henri Poincaré*, vol. 9, pp. 1413–1424, 2008.
- [153] E. R. Livine, S. Speziale, and J. L. Willis, “Towards the graviton from spinfoams: higher order corrections in the 3d toy model,” *Phys. Rev.*, vol. D75, p. 024038, 2007.
- [154] V. Bonzom, E. R. Livine, and S. Speziale, “Recurrence relations for spin foam vertices,” *Class. Quant. Grav.*, vol. 27, p. 125002, 2010.
- [155] L. Freidel and K. Krasnov, “Discrete space-time volume for 3-dimensional BF theory and quantum gravity,” *Class. Quant. Grav.*, vol. 16, pp. 351–362, 1999.
- [156] K. Noui and A. Perez, “Three-dimensional loop quantum gravity: physical scalar product and spin foam models,” *Class. Quant. Grav.*, vol. 22, pp. 1739–1762, 2005.
- [157] E. Bianchi, E. Magliaro, and C. Perini, “Spinfoams in the holomorphic representation,” 2010.
- [158] E. Bianchi, E. Magliaro, and C. Perini, “Coherent spin-networks,” *Phys. Rev.*, vol. D82, p. 024012, 2010.
- [159] L. Freidel and E. R. Livine, “Spin networks for non-compact groups,” *J. Math. Phys.*, vol. 44, pp. 1322–1356, 2003.